



**University of
Nottingham**

UK | CHINA | MALAYSIA

**Advanced Lung Imaging and Lung Function Testing in Ataxia-
Telangiectasia**

By

Saleh Alenazi

ID 4290214

The Final Report Submitted to the University of Nottingham for the
Degree of Doctor of Philosophy

January 2022

ABSTRACT

Although a CT scan provides high-resolution images for lung, it involves use of ionising radiation, which in some patient groups might increase risk of cancer, for example, it increases the chances of malignancy in patients with ataxia telangiectasia (AT). Therefore, it is necessary to identify an alternative imaging modality for patients with AT and other patient groups with similar risks. Magnetic resonance imaging (MRI) is a potential alternative, but there are various obstacles to its use. MRI cannot produce high-resolution images of the lungs due to the lack of strong proton signals. However, over the last few decades, various developments in MRI have given glimmers of hope for high-quality lung imaging. Currently, there are three potential ways to image the lung using MRI: hyperpolarised noble gas MRI (^{129}Xe), oxygen enhanced MR ventilation imaging (OE) and ultra-short echo time (UTE) proton imaging. Each of these methods has disadvantages and advantages but their use, either singly or in combination, has considerable potential. In this thesis, the potential to use OE-MRI has been assessed in patients with AT, because it is more readily available and inexpensive compared to hyperpolarised noble gas MRI. Moreover, it can provide temporal and spatial information compared to UTE technique,

which provides only an anatomical image. Lung function can also be assessed using physiological measurements including spirometry and lung clearance index (LCI). In this thesis, spirometry, LCI and OE-MRI were assessed for their potential to provide useful information on lung function abnormalities in children with and without AT. The main conclusions were that children with AT find it difficult to perform spirometry and LCI to adequate standards, especially in the children aged over 11. Moreover, with further optimisation, oxygen-enhanced MRI might provide an alternative way of assessing lung abnormalities in this group of patients.

Keywords: Spirometry, Lung Clearance Index (LCI), oxygen-enhanced MRI (OE-MRI), Ataxia telangiectasia.

ACKNOWLEDGEMENTS

I am grateful to the God (Allah), the Almighty, who said in the Holy Quran [Allah is the Light of the heavens and the earth. The example of His light is like a niche within which is a lamp; the lamp within glass, the glass as if it were a pearly [white] star lit from the oil of a blessed olive tree, neither of the East nor of the West, whose oil would almost glow even if untouched by fire. light upon light. Allah guides to His light whom He wills. And Allah presents examples for the people, and Allah is Knowing of all things] (Chapter 24, Verses 35). May Allah guide everyone in this life to his light. And who granted me this opportunity and provided me the strength and patience to complete this long journey.

Then, I would like to offer my utmost respect and gratitude to my parents for their endless support and sincere prayers throughout my life. I cannot forget the two beacons who lit up my path over the past four years, I have been privileged to study in the Respiratory Department and Radiology Department, University of Nottingham, under the guidance and supervision of Professor Ian Hall and Clinical Assistant Professor Andrew Prayle. I offer them my utmost respect and gratitude for their endless support with my PhD journey. Their guidance has helped me greatly during my research and thesis writing. Also, I would like to thank the beating heart of the respiratory department, Helen.

Finally, my heartfelt appreciation goes to my sponsors in the Kingdom of Saudi Arabia (The Ministry of Health) and the Saudi Arabian Cultural Bureau in the United Kingdom, for their financial support during this period.

DEDICATION

Thanks, are also extended to all my family members, especially to my wife, who did her best to provide a suitable study environment for me and for my superheroes, Turki and Naif (my sons), and for my little queen, Alkadi (my daughter).

I would like also to dedicate this to my brothers, sisters, neighbours (in Riyadh and Nottingham), friends everywhere headed by (Ahmed Al-Anazi, Qulayl Al-Dosari, and Yousif Kariri), and all Ph.D. study friends headed by (Shahida and Jonathan).

ABBREVIATIONS

A	
Approx.	Approximately
ALSPAC	Avon Longitudinal Study of Parents and Children
ASSET	Array coil Spatial Sensitivity Encoding
AT	Ataxia-Telangiectasia
ATM	Ataxia telangiectasia mutated
ATS	American Thoracic Society
B	
B_0	External magnetic field
BMI	Body Mass Index
BOLD	Blood-oxygen-level-dependent
bSSFP	Balanced Steady State Free Precession
BTFE	Balanced turbo field echo
BTPS	Body temperature and ambient pressure saturated
C	
C_{end}	Ending tracer fraction
C_{init}	Initial tracer fraction
CEV	Cumulative expired volume
CF	Cystic Fibrosis
CHU9D	Child health utility instrument - A standardized children quality of life score
Cm	Centimetre
CNR	Contrast to noise ratio
COPD	Chronic Obstructive Pulmonary Disease
COVID-19	Coronavirus disease of 2019
CPAM	Congenital pulmonary airway malformation
CT	Computed tomography scan
CTEPH	Chronic thromboembolic pulmonary hypertension
CV%	Coefficient of variation
D	
Deg	Degree
De-oxy	Deoxygenated
DL	Diffusing capacity of the lung
DLCO	Diffusing capacity of the lungs for carbon monoxide
DNA	Deoxyribonucleic Acid
DTPA	Diethylenetriaminepentaacetic Acid
E	
ECCS	European Community for Coal and Steel
ECG	Electrocardiogram
ECFS-CTN	European Cystic Fibrosis Society-Clinical Trials Network
EF	Enhancing fraction
ERJ	European Respiratory Journal

ERS	European Respiratory Society
ESJ	European Scientific Journal

F

F	Female
FEF	Forced Expiratory Flow
FEV	Forced Expiratory Volume
FEV ₁	Forced Expiratory Volume in one second
FEV ₁ /FVC	The ratio of the forced expiratory volume in the first one second to the forced vital capacity of the lungs
FLORET	Fermat looped, orthogonally encoded trajectories
FID	Free Induction Decay
fMRI	Functional Magnetic Resonance Imaging
FOAP	Fraction of oxygen-activated pixels
FRC	Functional Residual Capacity
FSPGR	Fast Spoiled Gradient-echo
FVC	Forced Vital Capacity
FoV	Field of View

H

HASTE	Half-Fourier acquisition single-shot turbo spin-echo
HRCT	High-resolution chest computed tomography
Hb	Haemoglobin
HRA	Health Research Authority
HV	Healthy Volunteer

I

i.e.,	The Latin phrase id est, meaning "that is."
ILD	Interstitial lung disease
IQR	Interquartile Range
IR-HASTE	Inversion recovery half-Fourier single-shot turbo spin-echo
IgG	Immunoglobulin G
IgG2	Immunoglobulin G2
IgA	Immunoglobulin A
IgE	Immunoglobulin E

K

kg	Kilogram
Kr ^{81m}	Krypton-81m

L

L/min	Liter Per Minute
LAV%	Percent Low Attenuation Volume
LCI	Lung Clearance Index
LLN	Lower Limit of Normal
LTD	Limited
LU	Lung Ultrasound

M

M	Male
Max	Maximum

MBW	Multiple breath nitrogen washout
mCCC	The mean cross-correlation coefficient
Min	Minimum
mm	Millimetres
mmHg	Millimetres of mercury
MRER	Mean relative enhancement ratio
MRI	Magnetic Resonance Imaging
ms	Millisecond
msec	Millisecond

N

NHS	National Health Service
N	Sample number
N ₂	Nitrogen
NCFB	Non-cystic fibrosis bronchiectasis
NIV	Non-invasive ventilation
NMD	Neuromuscular disease
NMR	Nuclear magnetic resonance
NO.	Number
NRES	National Research Ethics Service

O

O ₂	Oxygen
OE-MRI	Oxygen Enhancement Magnetic Resonance Imaging
OPSE	Optical pumping and spin exchange
Oxy-R	lack of positive the change in longitudinal relaxation rate

P

PaO ₂	Partial pressure of oxygen in arterial blood
PCD	Primary ciliary dyskinesia
PC-QOL-8	Paediatric chronic cough for a quality-of-life questionnaire
PedsQL	Paediatric Quality of Life inventory - A standardized children quality of life score
PEF	Peak Expiratory Flow
PREFUL	Phase-Resolved Functional Lung
PEFR	Peak Expiratory Flow Rate
PFT	Pulmonary function test
PIKK	Phosphatidylinositol 3-kinase like protein kinase
PO ₂	Partial pressure of oxygen

Q

QMC	Queen's Medical Centre
-----	------------------------

R

RBC	Red blood cell
R1	Longitudinal relaxation rate
RARE	Rapid acquisition with relaxation enhancement
RERs	Relative enhancement Ratio of oxygen
RF	Radiofrequency
RSE	Relative signal enhancement

S

S	Second
SBW	Single-breath washout
SD	Standard Deviation
SD-RER	Standard deviation of relative enhancement Ratio of oxygen
SDs	The standard deviations
sec	Second
SENSE	SENSitivity Encoding
SF ₆	Sulfur Hexafluoride
SI	Signal intensity
SMA	Spinal muscular atrophy
SNR	Signal to noise
SPGR	Spoiled gradient recalled
SE	Spin-echo
SPMIC	Sir Peter Mansfield Imaging Centre
SPSS	Statistical Package for Social Sciences
STIR	Short tau inversion recovery

T

T	Tesla
T1	Longitudinal relaxation time
T1 PG	T1-fat saturated post gadolinium
T2	Transverse relaxation time
T2 MVXD	T2-weighted MultiVane-XD
T2*	Transverse relaxation time
T4	Fourth thoracic vertebra (T star)
TC- ^{99m}	Technetium-99m
TE	Echo time
TI	Inversion time
TR/TE	Repetition time on echo time
TV	Tidal breath

U

UTE	Ultrashort Echo Time
UTE/ZTE	Ultrashort Echo Time and Zero Echo Time

V

V ^{tracer}	Total volume of tracer gas exhaled
V/Q	Ventilation/ Perfusion scan
VC	Vital capacity
VD	Dead space volume
V(D)J	Variable (V), diversity (D), and joining (J) gene segments in a process
VDP	Ventilation Defect Percent
VVF	Fraction of the region presenting with oxygen enhancement

X

X ²	Chi square
¹³³ Xe	Xenon 133

XTC Xenon polarisation transfer imaging

Z

Z Acoustic impedance

ΔPO_{2max_l} The maximal change in the partial pressure of oxygen in lung tissue

$\Delta R1$ The change in longitudinal relaxation rate
% Percentage

ΔPO_2 The maximal change in the partial pressure of oxygen
°C Celsius

$1/T1$ Reciprocal of relaxation time which equal longitudinal relaxation rate (R1)

^{129}Xe Xenon 129 (hyperpolarised noble gas)

2D Two-dimensional

3D Three dimensional

^3He Helium 3 (hyperpolarised gas)

TABLE OF CONTENT

ABSTRACT	I
ACKNOWLEDGEMENTS	III
ABBREVIATIONS	V
TABLE OF CONTENT	X
LIST OF TABLES	XV
LIST OF FIGURES	XIX
LIST OF EQUATIONS	XXII
Chapter 1	XXIII
1.1 Introduction.....	1
1.1.1 Hypothesis	4
1.1.2 Overall Aim	4
1.1.3 The Respiratory System	6
1.2 Lung Pathology	12
1.2.1 Chronic Obstructive Pulmonary Disease (COPD)	12
1.2.2 Non cystic fibrosis bronchiectasis	16
1.2.3 Cystic Fibrosis (CF)	17
1.2.4 Asthma	19
1.3 Lung Imaging Modalities.....	21
1.3.1 X-Ray of the Lungs (Chest X-ray).....	21
1.3.2 CT scan of the Lungs	22
1.3.3 Nuclear Medicine of the Lungs	23
1.3.4 Ultrasound of the Lungs	23
1.3.4 MRI of the Lungs.....	24
1.4 Lung Function Tests.....	26
1.4.1 Spirometry Technique.....	26
1.4.11 Some Artefacts in Spirometry Patterns Observed in Children.	47
1.4.12 Advantages and Disadvantages of Spirometry	48
1.4.13 Spirometry in Children	50
1.4.14 Spirometry in Ataxia Telangiectasia	51
1.4.2 Lung Clearance Index (LCI).....	54

1.5 Ataxia Telangiectasia (AT)	54
1.5.1 Introduction and History	54
1.5.2 Pathophysiology	56
1.5.3 Neurologic Disorders	57
1.5.4 Malignancy	59
1.5.5 Immune Deficiency, Recurrent Infections, and pulmonary disease	60
1.6 Magnetic Resonance Imaging (MRI)	61
1.6.1 Hyperpolarised Noble Gas MR Imaging using Xenon 129 (¹²⁹ Xe)	65
1.6.2 Molecular Oxygen-Enhanced (OE) MR Ventilation Imaging	69
1.6.3 Ultra-short Echo Time MR Imaging (UTE)	95
1.7 Safety Concerns with the use of Newer MR techniques	99
1.7.1 Xenon 129	99
1.7.2 Oxygen-Enhanced MRI.....	100
1.8 Literature Review	101
1.8.1 Previous Studies of the Spirometry in Children with AT	101
1.8.2 OE-MRI and LCI	106
1.9 Overview of the Thesis Plan	106
Chapter 2	107
2.1 Introduction.....	108
2.1.1 Aim and Objectives	111
2.2 Method and Material	112
2.2.1 Study Inclusion Criteria / Exclusion Criteria	116
2.2.2. The criteria of Assessing the Ability of Children with AT to Complete Spirometry.	118
2.3 Results.....	120
2.3.1 Study Recruitment and Study Population Characteristics	120
2.3.2 The Ability to Complete Spirometry between Children with AT and the Control Group.....	125
2.3.3 Spirometry Patterns of Children with AT	127
2.3.4 The Relationship between Age and Compliance with Performing Spirometry	131

2.3.5 The Correlation between the Ability to Achieve the FEV ₁ and FVC vs Age in AT and Control Groups	133
2.4 Discussion	141
2.4.1 Findings of the Study in the Context of the Literature	141
2.4.2 Strengths and Limitations of the Study	144
2.5 Conclusion	147
Chapter 3	148
3.1 Introduction.....	149
3.1.1 Overall Aim	149
3.1.2 Hypothesis	150
3.1.3 Objectives.....	150
3.2 Method and Materials.....	151
3.2.1 LCI Testing Procedure.....	151
3.2.2 Study Inclusion Criteria/ Exclusion Criteria	155
3.3 Results.....	158
3.3.1 Study Recruitment and Study Population Characteristics	158
3.3.2 The Ability of Children with AT to Undertake LCI	164
3.3.3 The Relationship between the Age and the Ability to Apply LCI Technique.....	166
3.3.4 The Relationship between Age and LCI2.5, LCI5, and FRC	170
3.3.5 The Relationship between Height against LCI2.5, LCI5, and FRC	173
3.3.6 The Relationship among Weight against LCI2.5, LCI5, and FRC	176
3.4 Discussion	180
3.5 Conclusion.....	190
Chapter 4	191
4.1 Introduction.....	192
4.1.1 OE-MRI in Ataxia Telangiectasia	195
4.1.2 Hypothesis, Aim, and Objectives	197
4.2 Material and method	199
4.2.1 Study Overview	199
4.2.2 Ethics Approval, Sponsorship, and Research Partners	200

4.2.3 My Role in the Research.....	201
4.2.4 Study Inclusion Criteria / Exclusion Criteria	202
4.2.5 Preparation for the Scan	204
4.2.6 Scanning Protocols	205
4.2.7 Statistical Analysis	210
4.3 Results.....	213
4.3.1 Study Recruitment and Study Population Characteristics	213
4.3.2 Image Acquisition and Artefact	218
4.3.3 Example Processed Data	220
4.3.4 Histogram and Normality Test.....	221
4.3.5 Boxplot	226
4.3.6 The Difference in OE-MRI Parameters (Delta-PO ₂ Whole Lung, Wash-in-Time, Delta-PO ₂ Aorta and VVF) between Both Groups	230
4.3.7 The Relationship between OE-MRI Parameters and Height in the AT Group and Control	232
4.3.8 The relationship among OE-MRI Parameters versus Age with the AT group and control group	237
4.3.9 The relationship among OE-MRI Parameters versus Gender in the AT group and control group.....	242
4.4 Discussion	245
4.5 Conclusion.....	250
Chapter 5	251
5.1 Background	252
5.2 Hypothesis and Aims of the Study	252
5.3 Key Findings of the Study	253
5.3.1 Assessing Reliability of Spirometry Measurements Patients with Ataxia Telangiectasia	253
5.3.2 Assessing Reliability of LCI Measurements Patients with Ataxia Telangiectasia	256
5.3.3 Assessing Reliability of OE-MRI Measurements Patients with Ataxia Telangiectasia	259
5.4 Strength and Limitation.....	266
5.4.1 Potential Strength	266

5.4.2 Potential Limitation	267
5.5 Future Work.....	267
5.6 Conclusion.....	268
References	269
Appendix	305
Paediatric chronic cough for a quality-of-life questionnaire	305
Paediatric Quality of Life inventory - A standardized children quality of life score.....	307
LCI Results of AT Group.....	320
Spirometry Results of AT Group	333
Spirometry Results of Control group 1	346
Spirometry Results of Control group 2	363

LIST OF TABLES

Table 1-1: Shows the main spirometric measures	28
Table 1-2: Manoeuvre criteria for acceptable spirograms.	30
Table 1-3: Severity of airflow obstruction based on percentage (%) predicted forced expiratory volume in 1 second (FEV ₁).	33
Table 1-4: Selected LCI studies to illustrate its use in several pulmonary diseases.	64
Table 1-5: Shows some of OE-MRI advantages with some pulmonary diseases.	94
Table 1-6: Shows and summarises the advantages and disadvantages of three types of lung MRI method.	98
Table 1-7: Demonstrates list of all the previous studies of spirometry have been conducted on patients with AT.	101
Table 2-1: Demonstrates the control group with different type of diseases.	120
Table 2-2: Characteristics for the AT group and Control group.	122
Table 2-3: Descriptive characteristics of individuals in the AT group and the control group of children with pulmonary diseases	123
Table 2-4: Shows the number of AT subjects (n=34) able to comply with ERS criteria for spirometry.	125
Table 2-5: Shows the ability of control subjects (n=68) to comply with ERS criteria.	126
Table 2-6: Shows the ability of the two groups to comply with spirometry criteria.	126
Table 2-7: Ability of the children with AT to achieve spirometry criteria which divided based on the age.	132
Table 2-8: Ability of the control group to achieve spirometry criteria which divided based on the age.	133
Table 2-9: Demonstrates the correlation between the best FEV ₁ and age for children with AT.	135
Table 2-10: Numbers of children with AT who can achieve predicted and lower limit of normal (LLN) values of FEV ₁ and FVC.	135
Table 2-11: Demonstrates the correlation between the best FVC and age for the children with AT.	137
Table 2-12: Demonstrates numbers of the children in control group who achieved predicted and lower limit of normal (LLN) values of FEV ₁ and FVC.	138
Table 2-13: Shows the correlation between the best FEV ₁ and age for the participants in the control group.	138

Table 2-14: Correlation between the best FVC and age for the participants in the control group.	140
Table 3-1: Statistical Analysis of the descriptive characteristics for the AT group.....	159
Table 3-2: Descriptive characteristics of individuals in the AT group. ..	161
Table 3-3: This table shows the LCI parameters for all of the participants.	162
Table 3-4: Shows the overall summary of the LCI data.	162
Table 3-5: This table demonstrates and summarises the ability of participants to comply with criteria for LCI for all the participants in this study (13 children with AT).....	163
Table 3-6: Demonstrates the potential of comply with LCI's criteria for children with AT.	165
Table 3-7: Demonstrates the LCI's parameters for the first group those aged over 9 years.....	166
Table 3-8: Demonstrates the LCI's parameters for the first group, those aged ≤ 9 years.	168
Table 3-9: Descriptive characteristics of both AT groups those were divided based on the age (>9 and ≤ 9 years).	168
Table 3-10: Shows the result of the chi square test used to determine the ability to comply with LCI's criteria for both groups of children with AT	168
Table 3-11: Shows the LCI's criteria and the potential of complying with them for both groups of children with AT (>9 years and ≤ 9 years).	169
Table 3-12: This table demonstrates and summarises the selected results of LCI studies as well as the LCI result of this study.....	185
Table 4-1: The names and the positions of the work's team.	201
Table 4-2: Shows settings for protocol 1 and 2 for dynamic oxygen enhanced acquisition.....	208
Table 4-3: Shows a protocol for Multi-slice HASTE with respiratory triggering.	210
Table 4-4: Description of the OE-MRI's parameters.....	212
Table 4-5: Descriptive characteristics of individuals in the AT group....	215
Table 4-6: Characteristics for the AT group.....	215
Table 4-7: Descriptive characteristics of individuals in the control group	217
Table 4-8: Characteristics for the AT group and control group.	217
Table 4-9: Shows the OE-MRI parameters and its region for AT group.	218
Table 4-10: Shows the OE-MRI parameters and its region for healthy volunteer.....	218
Table 4-11: Shows the normality test of delta- PO_2 in whole lung for AT group and healthy volunteer group.	221

Table 4-12: Shows the normality test of wash in time in whole lung for AT group and healthy volunteer group.	223
Table 4-13: Shows the normality test of delta-PO ₂ in aorta for AT group and healthy volunteer group.	224
Table 4-14: Shows the normality test of VVF for AT group and healthy volunteer group.....	225
Table 4-15: Demonstrates the results of the Mann-Whitney test of delta-PO ₂ in whole for AT group and healthy volunteers.....	230
Table 4-16: Demonstrates the Mann-Whitney test of the wash-in-time in whole lung for the AT group and healthy volunteers.....	231
Table 4-17: Demonstrates the Mann-Whitney test of delta-PO ₂ in aorta for AT group and healthy volunteers.	232
Table 4-18: Demonstrates the Mann-Whitney test result of VVF for the AT group and healthy volunteers.....	232
Table 4-19: Demonstrates the linear regression model of the delta-PO ₂ in whole lung versus height as covariable in healthy volunteer group and AT group.....	234
Table 4-20: Demonstrates the linear regression model of the wash-in-time in whole lung versus height as covariable in healthy volunteer group and AT group.	235
Table 4-21: Demonstrates the linear regression model of the delta-PO ₂ in the aorta versus height as covariable in healthy volunteer group and AT group.....	236
Table 4-22: Demonstrates the linear regression model of the VVF versus height as covariable in healthy volunteer group and AT group.	237
Table 4-23: Demonstrates the linear regression model of the delta-PO ₂ in whole lung versus age as covariable in the healthy volunteer group and AT group.....	239
Table 4-24: Demonstrates the linear regression model of the wash-in-time in the whole lung versus age as covariable in the healthy volunteer group and AT group.	240
Table 4-25: Demonstrates the linear regression model of the delta-PO ₂ in aorta versus age as covariable in the healthy volunteer group and AT group.	241
Table 4-26: Demonstrates the linear regression model of the VVF in whole lung versus age as covariable in the healthy volunteer group and AT group.	241
Table 4-27: Demonstrates the linear regression model of the delta-PO ₂ in whole lung versus gender as covariable in the healthy volunteer group and AT group.	243

Table 4-28: Demonstrates the linear regression model of the wash-in-time in whole lung versus gender as covariable in the healthy volunteer group and AT group. 243

Table 4-29: Demonstrates the linear regression model of the delta-PO₂ in the aorta versus gender as covariable in the healthy volunteer group and AT group. 244

Table 4-30: Demonstrates the linear regression model of the VVF versus gender as covariable in the healthy volunteer group and AT group..... 244

Table 5-1: This table summarises selected results of LCI studies, as well as the LCI result of this study..... 259

LIST OF FIGURES

Figure 1-1: Shows the first X-ray image (taken in 1895) of William Röntgen wife's hand	1
Figure 1-2: Shows an electromagnetic spectrum.	3
Figure 1-3: Shows that the respiratory system splits into 24 different pulmonary generations.....	8
Figure 1-4: Transport of oxygen (O ₂) and carbon dioxide (CO ₂) in the lung and bloodstream	11
Figure 1-5: Shows the relationship PO ₂ and haemoglobin saturation as oxyhaemoglobin dissociation curve (sigmoid-shaped).....	11
Figure 1-6: Shows the normal and abnormal (COPD) bronchioles and alveoli	16
Figure 1-7: Displays normal (in the left image) and abnormal (pneumonia) (in the right) chest x ray.	22
Figure 1-8: Depicts (A) T2 MVXD, (B) STIR, (C) BTFE, (D) T1, and (E) T1 PG.	25
Figure 1-9: Demonstrates the normal (Flow/ Volume loops) in spirometry.	27
Figure 1-10: Demonstrates the obstructive lung disorder flow/ volume loops in spirometry.	32
Figure 1-11: Demonstrates the restrictive lung disorder flow/ volume loops in spirometry	34
Figure 1-12: Examples (a) and (b) show obstructive pulmonary defects. Example (c) shows a restrictive defect. Example (d) shows a mixed defect.	35
Figure 1-13: Shows spirogram for a normal valid test.	40
Figure 1-14: Shows spirograms for common test errors.	40
Figure 1-15: Spirograms for common test errors.	44
Figure 1-16: Spirometry in Children; (a) poor effort by patient (b) patient with cough; (c) premature start and end.	48
Figure 1-17: Shows a multiple-breath washout setup of N ₂ and SF ₆	54
Figure 1-18: Shows the wash-out tracing curve of a 14-year-old female child with AT (participant 4).	57
Figure 1-19: The figure shows the device set up for the patient. This equipment is the Exhalyzer D. This figure illustrates the components of the LCI system	58
Figure 1-20: Shows T1 (on the right) and T2 weighted (on the left) MRI of the brain.	64
Figure 1-21: Hp ¹²⁹ Xe slice selective coronal MR images (in red) overlaid onto corresponding proton thoracic images from healthy volunteers and	

subjects with asthma, chronic obstructive pulmonary disease (COPD), cystic fibrosis (CF)	68
Figure 1-22: The relationship between the SNR and inter-echo spacing .	77
Figure 1-23: Images of a healthy, 36-year-old male volunteer captured using the centrally and sequentially reordered of IR-HASTE sequences.	78
Figure 1-24: Shows an assessment of regional ventilation in a normal healthy volunteer.	84
Figure 1-25: The map of the OE-MRI shows a healthy, 58-year-old male volunteer.....	86
Figure 1-26: A 68-year-old male with pulmonary emphysema and lung cancer.....	87
Figure 1-27: Shows a comparison of MRERs between COPD patients and healthy volunteers.....	90
Figure 1-28: The images above, obtained by the OE-MRI and CT, show the lungs of a COPD patient.	91
Figure 1-29: Dynamic maps of OE-MRI parameter for a severe asthmatic patient.....	93
Figure 1-30: UTE MRI in cystic fibrosis	98
Figure 2-1: ndd EasyOne Pro Lab Spirometer.	116
Figure 2-2: Ethnicity distribution for the AT participants.	121
Figure 2-3: Ethnicity distribution for the control group	121
Figure 2-4: Shows the flow/volume loop on the left side and the volume/ time graph on the right side.....	128
Figure 2-5: shows the time/volume graph for a 16-year-old male child with AT.	128
Figure 2-6: Shows the flow/volume loop on the left side and the volume/ time graph on the right side.....	129
Figure 2-7 Shows the flow/volume loop on the left side and the volume/ time graph on the right side.....	130
Figure 2-8: Shows the flow/volume loop on the left side and the volume/ time graph on the right side.....	130
Figure 2-9: Shows the best values of FEV ₁ and FVC for AT group and two control groups versus age.....	134
Figure 2-10: Shows the best FEV ₁ values of 34 children with AT versus age.	136
Figure 2-11: Shows the best FVC values of 34 children with AT versus age.	137
Figure 2-12: Shows the best FEV ₁ values of the control group versus age.	139

Figure 2-13: Shows the best of FVC values versus age for the control group.	140
Figure 3-1: Shows the ndd EasyOne Pro Lab Spirometer which was used in the study.....	155
Figure 3-2: Gender distribution for AT participants.....	158
Figure 3-3: Ethnicity distribution for the AT participants	159
Figure 3-4: Displays the final consort diagram of this study.	160
Figure 3-5: Demonstrates the ability of AT subjects (13 patients) to comply with European respiratory criteria.....	165
Figure 3-6: Ethnicity distribution for the AT participants in group1.....	167
Figure 3-7: Ethnicity distribution for the AT participants in group2.....	167
Figure 3-8: Demonstrates the ability of children with AT >9 years (6 patients) to comply with European respiratory criteria.....	169
Figure 3-9: Demonstrates the ability of children with AT \leq 9 years (7 patients) to comply with European respiratory criteria.....	170
Figure 3-10: Shows the relationship between the age and LCI2.5 values for 13 children with AT using scatter plot with linear regression in SPSS...	171
Figure 3-11: Shows the relationship between the age and LCI5 values for 13 children with AT.....	172
Figure 3-12: Shows the relationship between the age and the FRC values for 13 children with AT.	173
Figure 3-13: Shows the relationship between the height and the LCI2.5 values for 13 children with AT	174
Figure 3-14: Shows the relationship between the height and the LCI5 values for 13 children with AT	175
Figure 3-15: Shows the relationship between the height and the FRC values for 13 children with AT.	176
Figure 3-16: Shows the relationship between the weight and the LCI2.5 values for 13 children with AT.	177
Figure 3-17: Shows the relationship between the weight and the LCI5 values for 13 children with AT	178
Figure 3-18: Shows the relationship between the weight and the FRC values for 13 children with AT	179
Figure 3-19: Displays the location and volume of dead space (pre, post and total).	188
Figure 4-1: The differentiation between normoxia and hypoxia using OE-MRI	193
Figure 4-2: Diagram of the setup of the patient in the scanner.....	205
Figure 4-3: Diagram to illustrate the timing of delivery of air and oxygen to participants during protocol 1.....	207
Figure 4-4: Shows the different between two protocols.	208

Figure 4-5: Displays the consort diagram of the children with AT who participated in this study.	214
Figure 4-6: Displays the consort diagram of the healthy volunteers who participated in this study.	216
Figure 4-7: Shows an axial lung MR image which captured by protocol 1 with an artefact of horizontal lines.	219
Figure 4-8: Shows an axial lung MR image which captured by protocol 2 with an artefact horizontal line	219
Figure 4-9: Shows an area of ventilation defect in the lungs.	220
Figure 4-10: Shows the distribution of delta-PO ₂ data in whole lung for AT group and healthy volunteer group.	222
Figure 4-11: Shows the distribution of wash in time data in whole lung for AT group and healthy volunteer group.	223
Figure 4-12: Shows the distribution of delta-PO ₂ data in aorta for AT group and healthy volunteer group.	224
Figure 4-13 Shows the distribution of VVF data in whole lung for AT group and healthy volunteer group.	225
Figure 4-14: Shows the distribution of delta-PO ₂ data in the whole lung for AT group and the healthy volunteer group	226
Figure 4-15: Shows the distribution of wash-in-time data in the whole lung for AT group and the healthy volunteer group.	227
Figure 4-16: Shows the distribution of delta-PO ₂ data in aorta for AT group and the healthy volunteer's group.	228
Figure 4-17: Shows the distribution of VVF data in whole lung for AT group and healthy volunteer group.	229
Figure 4-18: Shows the OE-MRI parameters versus height for 12 children with AT and 8 healthy volunteers.....	233
Figure 4-19: Shows the OE-MRI parameters versus age for 12 children with AT and 8 healthy volunteers.	238

LIST OF EQUATIONS

Equation 1: Shows how is FRC calculated	59
Equation 2: Demonstrates how is LCI calculated.....	60

Chapter 1

Introduction

1.1 Introduction

Since the X-ray was discovered and applied in the medical field in 1895 by the German scientist, William Röntgen, who took the first X-ray image of his wife's hand (see Figure 1-1), medical imaging technologies have been improving constantly (Panchbhai, 2015). It is now possible to image any part of the human body, including vascular and neural components, with high precision. Moreover, research has made it possible to use radiographic principles for complex therapeutic purposes as well.



Figure 1-1: Shows the first X-ray image (taken in 1895) of William Röntgen wife's hand (Panchbhai, 2015).

These imaging medical technologies have been divided into two types, according to the type of radiation that they employ: those involving ionising radiation and those that do not use ionising radiation. For instance, X-ray, computed tomography scan (CT), and nuclear medicine are ionising

radiation-based imaging approaches because both X-rays and CT scan use X-rays waves, and nuclear medicine uses gamma rays or other approaches.

Both X-rays and gamma rays have a very short wavelength (see Figure 1-2) (Zamanian et al., 2005), which can damage normal cells. On the other hand, ultrasound and magnetic resonance image (MRI) are non-ionising radiation-based imaging methods. Ultrasound uses mechanical waves, whereas MRI uses radio waves, both of which are long wavelengths that do not have sufficient energy to change the structure of the cell (see Figure 1-2) (Zamanian et al., 2005).

Although the non-ionising methods provide potential advantages, these approaches may provide lower resolution compared with ionising imaging. For example, pulmonary CT imaging scans can provide images with superior quality resolution than a conventional MRI scan can achieve. Moreover, nuclear medicine techniques that use ionising radiation can deliver information on the physiological function of the lungs; for example, using isotope scanning it is possible to image ventilation/perfusion.

However, there are specific disease conditions, such as ataxia telangiectasia (AT), where exposing the patient to ionising radiation imaging techniques, such as CT and nuclear medicine imaging, could promote their risk of developing cancer due to the patients heightened sensitivity to ionising radiation.

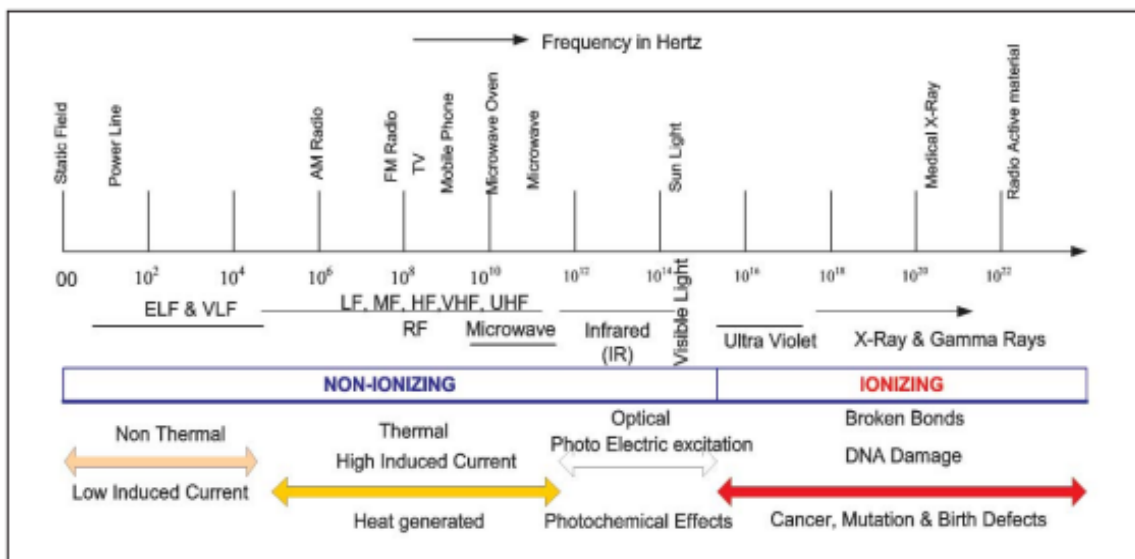


Figure 1-2: Shows an electromagnetic spectrum (Zamanian et al., 2005).

However, because pulmonary infection is a leading cause of death for patients with AT, there is a need for screening procedures to be developed that allow the early detection of lung disease in these patients. At present, there is no effective and safe way to provide physiological and anatomical lung information about these patients.

The main aim of the studies described in this thesis, was to evaluate potential ways of acquiring pulmonary function information about AT patients using effective and safe techniques. In this introduction chapter, I summarise the respiratory system, describe some common lung diseases and the approaches to lung imaging and lung function tests. Greater detail of spirometry, lung clearance index (LCI), and oxygen-enhanced magnetic resonance imaging (OE-MRI) is provided in the relevant chapters.

1.1.1 Hypothesis

The main hypothesis underlying the work described in this thesis is that in patients with ataxia telangiectasia (AT), OE-MRI could be a suitable technique for lung imaging in children and may in addition provide useful physiological information about lung disease when compared to Lung clearance index (LCI) and spirometry. To date OE-MRI and LCI have not been studied in these patients.

1.1.2 Overall Aim

To assess the feasibility of OE-MRI, LCI and spirometry in children and young adults with AT. In addition, to monitor trends in parameters derived from OE-MRI, LCI and spirometry and assess their suitability as clinical trial endpoints.

The main aim of this study was to determine the feasibility to comply with spirometry, LCI, and OE-MRI techniques in patients with AT. AT is a complex neuro-respiratory disorder, and at the outset of this study it was not known if children with AT could undertake these procedures, as they have a neurological disability. This thesis uses the following definitions of validity, reliability and feasibility below:

Validity and reliability are closely related. A test cannot be considered valid unless the measurements resulting from it are reliable. Likewise result from a test can be reliable and not necessarily valid (Phillips et al., 2021).

Validity is the ability of a measure to accurately reflect the construct it is designed to measure (Phillips et al., 2021). Types of validity are:

- 1- Content Validity (Sample Validity): The extent to which a measure covers all aspects of the intended domains or dimensions that it claims to measure.
- 2- Construct Validity: The extent to which the measurement tool actually tests the hypothesis or theory they are measuring.
- 3- Criterion-related Validity: The output of a measure produces similar results.
- 4- In this context, a valid respiratory measurement would accurately measure at least one important component of the respiratory system, and it could be used to test hypotheses about the respiratory system in the future.

Reliability is the extent to which a tool gives measurements that are consistent, stable, and repeatable (Phillips et al., 2021). Types of validity are:

- 1- Test-retest reliability: The extent to which a measure can obtain similar results in repeated trials, keeping as many external factors or conditions as stable as possible.
- 2- Internal consistency: The extent to which items among a measurement tool that propose to measure the same construct are interrelated.

Feasibility is the extent to which a measurement tool is suitable for the target population; can be successfully delivered in the target population which means the state of being possible (Phillips et al., 2021). In the context of this thesis, feasibility relates to the ability of people with AT to tolerate the procedure, specifically with reference to the progressive neurological difficulties which people with AT develop. The rest of this thesis is concerned with the feasibility (in this sense) of undertaking spirometry, lung clearance index, and lung MRI in children with AT.

1.1.3 The Respiratory System

A number of separate elements form the human respiratory system. These are namely the nose, the throat (pharynx), the voice box (larynx), the trachea, bronchi, and the lungs' parenchyma. The system is categorised into two main regions: the upper and lower respiratory systems. The nose, pharynx, and related elements form part of the upper respiratory system, while the larynx, trachea, bronchi, and lungs form the lower. Similarly, the function of the system can be divided into two, known as the conducting zone and the respiratory zone. Interconnecting cavities and tubes both outside and inside are in the former zone, where air is filtered, warmed and moistened on its way to the lungs. Gas exchange takes place in the respiratory zone, specifically in the alveoli.

1.1.3.1 Anatomy

In humans, there are two lungs which are conical and are located in the thoracic cavity. The heart is situated between the lungs, along with other intervening structures in the mediastinum. The lungs are separated into lobes by fissures, with each one containing an oblique fissure; the right lung is different to the left lobe, as it has a horizontal fissure. Each lung is therefore further separated as 'upper' and 'lower' lobes, and with a middle lobe only found in the right lung. The trachea divides into two parts, the right and left primary (main) bronchi. This division occurs at the level of the fifth vertebra of the thorax. Once in the lungs, the primary bronchi divide yet again, this time into secondary bronchi which are much smaller. Each one of these then has a host lobe within the lung. The division continues to form tertiary bronchi, arising from the secondary bronchi, which then divide into smaller bronchioles. This tree-like process continues whereby the bronchioles decrease in size until the terminal bronchioles are reached which end in sacs called alveolar. Around each alveolar duct, there are many alveolar sacs and alveoli. There are approximately twenty-three steps in subdivision between the trachea and the alveolar. These steps, or 'branches', are referred to as 'generations' (Figure 1-3). From the respiratory bronchioles, the following seven generations form a pulmonary acinus. Whilst the airway of each generation is smaller than the previous one (Figure 1-3), as there is an increasing number of airways over a larger area at each generation, the surface area of the airway increases as one moves towards the alveoli. It is thought that there are approximately 300

million alveoli in the lungs, which offer 70 m² of surface area for gas exchange.

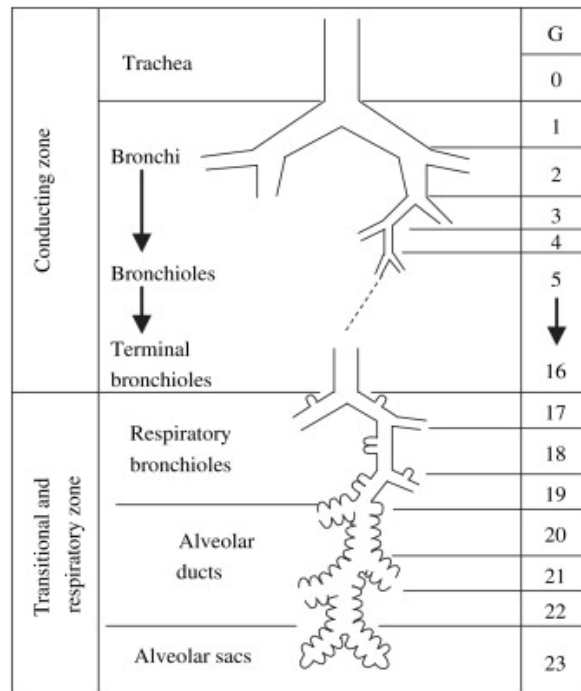


Figure 1-3: Shows that the respiratory system splits into 24 different pulmonary generations. The conducting zone is represented from 0 to 16 by the generation indexes, and the transitional and respiratory zone is represented from 17 to 23 by generation index (Feher, 2017).

1.1.3.2 Lung Physiology

1.1.3.2.1 Pulmonary Ventilation

Pulmonary ventilation describes the flow of air in and out of the lungs between the atmosphere and the alveoli. When we breathe, the muscles in the chest wall and the diaphragm contract and relax, resulting in airflow in and out of the lungs. Airflow, and subsequently ventilation, can be affected by three factors, namely the surface tension of the alveolar fluid, airway

resistance and the compliance of the lungs. When any of these factors are disrupted, ventilation may be impaired, resulting in reduced gas exchange.

1.1.3.2.2 Basic Respiratory Physiology

The respiratory system works through a simple mechanism, whereby atmospheric air containing a mixture of gases, including oxygen, enters the lungs through the trachea. The air enters the bronchus and then the bronchioles to reach the end alveolar complex, where the gaseous exchange into the circulatory system takes place. In the alveoli, oxygen from inhaled air is transfused into the blood cells through the capillaries into the systemic circulation. Carbon dioxide is expelled into the exhaled air. The freshly oxygenated blood travels to the heart through the main pulmonary veins, and deoxygenated blood is transported to the lungs via the pulmonary arteries to release CO_2 and absorb O_2 . In most patients, respiratory drive is dependent upon the partial pressure of arterial carbon dioxide (PaCO_2).

Normal respiration is dependent on the carbon dioxide levels in the blood which are sensed continuously by the central chemoreceptors, which are present in the medulla oblongata, and peripheral chemoreceptors present in carotid and aortic bodies. When the levels of carbon dioxide increase in the blood, respiratory drive is increased, and the ventilation rate and tidal volume will increase, thereby flushing out the excess carbon dioxide and oxygenating the blood adequately. In certain conditions, such as chronic

obstructive pulmonary disease (COPD), where there is low PaO_2 , this response of stimulus to increased carbon dioxide becomes blunt, leaving low oxygen levels as the primary stimulus of the respiratory cycle. This phenomenon is called a hypoxic drive.

1.1.3.2.3 Gas Exchange

Dalton's law and Henry's law both help to describe the principles of gas exchange between alveolar air and blood across the alveolar-capillary membrane in the lungs. Dalton's law explains how pressure differences between alveoli and capillary blood impacts the rate of diffusion through a liquid. Meanwhile, Henry's law considers how the diffusion of a gas through liquid impacts its solubility. The process of exchanging gas is comprised of two actions. Firstly, oxygen enters into capillary blood and then carbon dioxide moves from the blood into the alveolar air and is thus released when the lung exhales (see Figure 1-4) (Komoda & Matsunaga, 2015). Carbon dioxide is highly soluble, being 24-times more soluble than oxygen.

Having diffused through the alveolar membrane, oxygen binds to haemoglobin in erythrocytes in the blood that is travelling through the pulmonary capillaries. Oxyhaemoglobin describes haemoglobin that has picked up reversibly bound oxygen. A single haemoglobin molecule can simultaneously carry four oxygen molecules. The globin chains of the haemoglobin molecule undergo a conformational change when one oxygen molecule becomes bound, which initiates a global alteration to the

haemoglobin' quaternary structure. This in turn enables the other three oxygen molecules to bind, with each oxygen molecule binding with greater affinity than the previous. This relationship is best described by the sigmoid-shaped oxyhaemoglobin dissociation curve (see Figure 1-5) (Dunn et al., 2016).

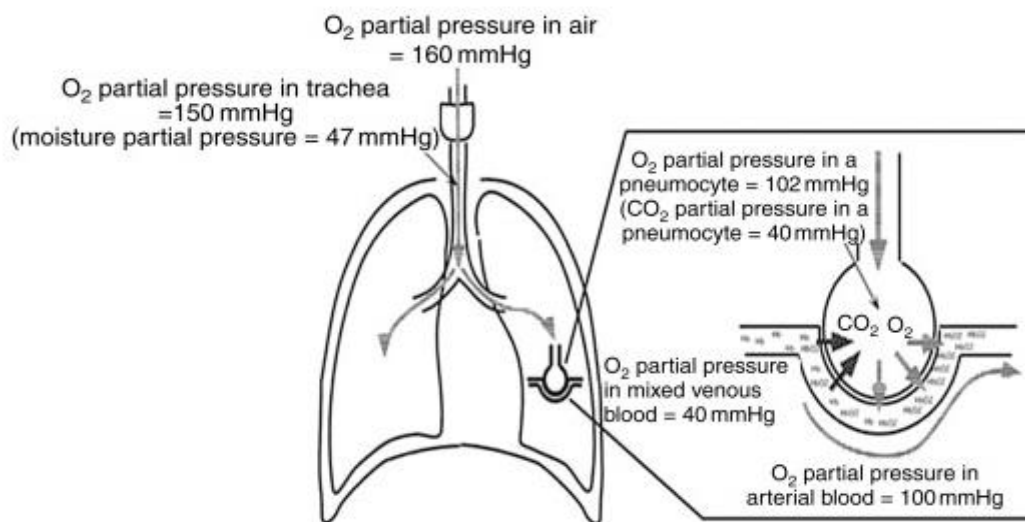


Figure 1-4: Transport of oxygen (O_2) and carbon dioxide (CO_2) in the lung and bloodstream (Komoda & Matsunaga 2015).

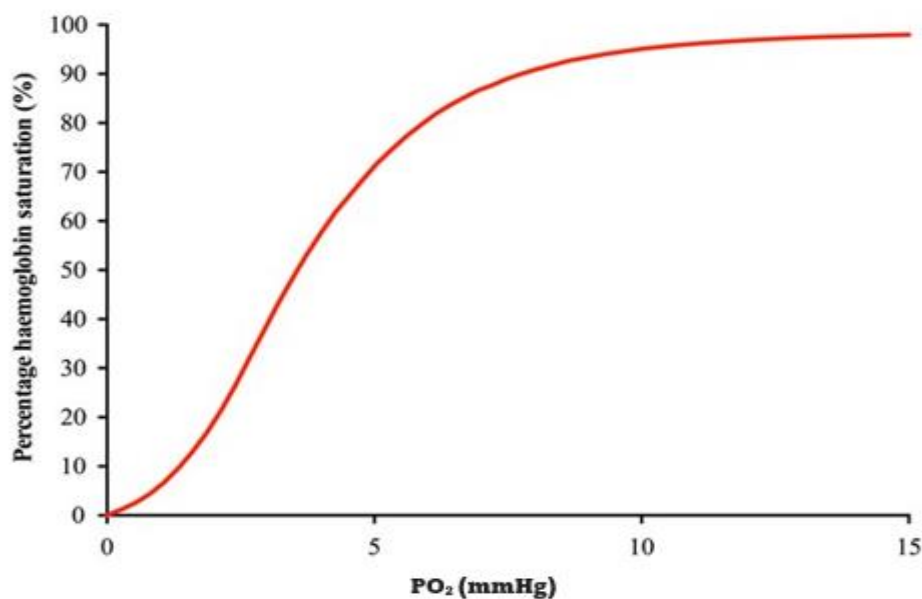


Figure 1-5: Shows the relationship PO_2 and haemoglobin saturation as oxyhaemoglobin dissociation curve (sigmoid-shaped) (Dunn et al., 2016).

1.2 Lung Pathology

Lung pathology can alter the ability of the lungs to transport oxygen and carbon dioxide. This can happen because of changes in ventilation or changes in diffusion across the alveolar-capillary membrane arising from destruction of lung tissue or thickened alveolar walls caused by, for example, interstitial fibrosis. In the next section, I will describe some common lung diseases to explain how gas transfer can be affected by pathology. The precise nature of the respiratory disease in AT is not fully known, and likely varies between patient to patient. However, there are likely parallels with chronic obstructive lung disease (specifically hyperinflation), asthma, non-cystic fibrosis bronchiectasis and cystic fibrosis. These are therefore described below.

1.2.1 Chronic Obstructive Pulmonary Disease (COPD)

Chronic obstructive pulmonary disease (COPD) is caused by inhalation of potentially hazardous chemicals (e.g., from smoking or air pollutants) in individuals predisposed to lung damage. Major symptoms include persistent coughing, shortness of breath with effort, expectoration, and wheezing due to obstructed airflow (Agustí and Hogg, 2019). These symptoms are associated with airway hyperresponsiveness, which in some circumstances may be partly reversible. COPD includes patients who have either or both chronic bronchitis, and emphysema (see Figure 1-6).

Damage to the alveolar wall causes an enlargement of the air pockets distal to the terminal bronchioles, which is the medical condition known as emphysema. When airspaces are enlarged, the quantity of oxygen diffusing across the injured alveolar-capillary membrane decreases. This causes a reduction in gas exchange. Loss of elastic fibres over time reduces the lung's elastic rebound, which increases as alveolar wall degeneration advances. Loss of elastic fibres reduces the lung's elasticity. Additionally, the final few seconds of an exhalation are the most advantageous for air retention. Tobacco use, air pollution, and prolonged exposure to industrial dust in the workplace are three of the most significant causes of emphysema.

In simple terms, chronic bronchitis is characterised by persistent inflammation of the airways. This inflammation limits airflow across the airways, making it more difficult to breathe. Since inflammation is the main cause of mucus production, the quantity of mucus generated is often excessive (McCarthy et al., 2015). The intake of harmful substances, such as those present in cigarette smoke and other kinds of air pollution, are again known risk factors. In addition to avoiding tobacco products, one of the most essential things that can be done to treat this disease is to eliminate air pollution.

The American Thoracic Society (ATS) defines COPD as a disease characterised by limitation of airflow because of emphysema or chronic bronchitis; the obstruction of airflow is generally progressive, may be

accompanied by airway hyperreactivity, and may be partially reversible (Celli and Wedzicha, 2019). Reduced maximum expiratory flow worsens over time and, in most instances, is irreversible with available medical treatment. The European Respiratory Society (ERS) has a similar definition (Iheanacho et al., 2020). In the majority of instances, airflow limitation worsens with time and is associated with an aberrant inflammatory response of the lungs to toxic particles or gases (Iheanacho et al., 2020). There is variation in how COPD affects a person's ability to breathe, whether or not the condition is completely irreversible, and the severity of symptoms.

Patients with airflow limitation have an unusually low FEV₁ and an abnormally low forced expiratory volume to forced vital capacity FEV₁/FVC ratio. In a prior ATS publication, a ratio of FEV₁/FVC less than the 5th percentile was cited as evidence of airway limitation; however, this criterion was omitted from the 1995 ATS definition of COPD (Pranata et al., 2020). The ERS defined airflow limitation in 1995 as a ratio of FEV₁ to FVC that was less than 88% of the predicted value for the ration in males and 89% of the expected value for females. In other words, the ratio for both genders were below 88% of the projected number (McCarthy et al., 2015). A ratio of FEV₁/FVC less than 70% is the gold standard for detecting airflow limitation (Iheanacho et al., 2020).

In patients with airflow limitation inhaled bronchodilators and corticosteroids may produce a degree of reversibility (Celli and Wedzicha, 2019). A recent ATS statement defined reversibility as an increase in FEV₁ of 200 mL and 12% over baseline FEV₁ for patients using inhaled bronchodilators (Severiche et al., 2019). The European Respiratory Society (ERS) defines COPD reversibility as an increase in predicted FEV₁ of more than 10% following bronchodilator treatment (Iheanacho et al., 2020). GOLD defines COPD reversibility as an increase in FEV₁ of 200 mL and a 12% improvement from baseline following therapy with inhaled corticosteroids or bronchodilators (Severiche et al., 2019).

Whilst some reversibility may be present in patients with COPD, reversibility is a key feature of asthma (see below). Lung function impairment has also been used to assess COPD severity. The ATS classifies COPD into three stages: Stage 1 (FEV₁, greater than 50%), Stage 2 (35-49%), and Stage 3 (35%) (Iheanacho, et al., 2020). The ERS defines COPD as mild (FEV₁, 70%), moderate (50-50% of anticipated), or severe (50%) based on these factors. (Agustí and Hogg, 2019). The GOLD criteria divide COPD into three stages: Stage 1 (FEV₁, 80% of expected), Stage 2 (30 to 80% of projected), and Stage 3 (30%). Stage 1 is the worst (Pranata et al., 2020).

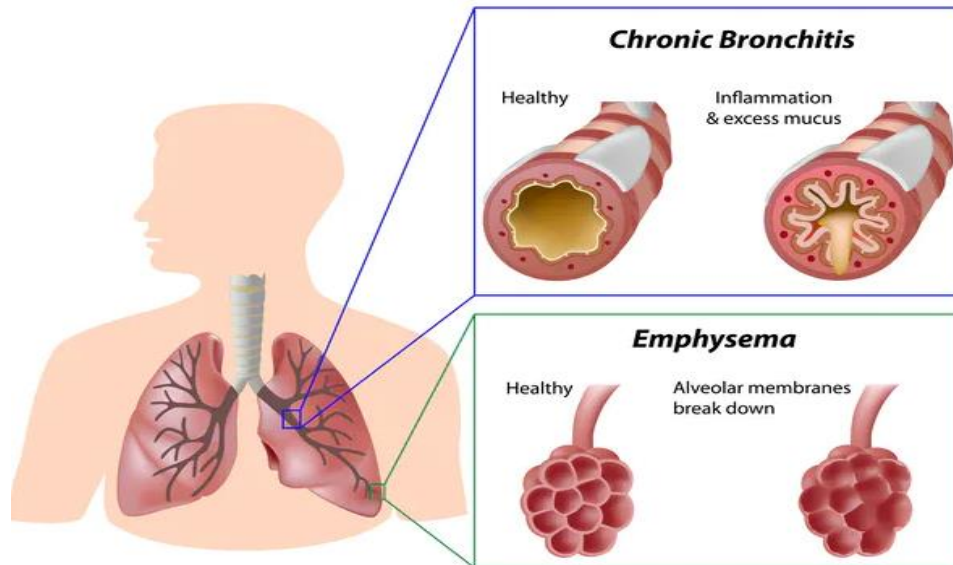


Figure 1-6: Shows the normal and abnormal (COPD) bronchioles and alveoli (Blog, 2021).

1.2.2 Non cystic fibrosis bronchiectasis

Non-cystic fibrosis bronchiectasis, also known as NCFB, has attracted the attention of scientists throughout the world because to its rising frequency, financial burden on healthcare systems, and morbidity and death it causes (Woo et al., 2019). There has been a significant surge in interest in NCFB over the last two decades, leading to the treatment of NCFB patients utilising novel medications, and a different perspective on the condition, and recognition of different endophenotypes (King et al., 2021). NCFB affects between 2 and 5 people per 1,000 years, with the majority of its victims being old (Wang et al., 2021). Importantly, if you do not look for bronchiectasis you do not find it – approximately $\frac{1}{4}$ of children in a severe asthma clinic had evidence of bronchiectasis on CT scan (Maniyar et al., 2019). In the vast majority of cases, NCFB is regarded to be idiopathic, despite the fact that a variety of factors may contribute to the illness's

development (Woo et al., 2019). Unfortunately, neither a cure nor any FDA-approved treatments are available for NCFB at this time (Chorepsima et al., 2018). The frequency of exacerbations, the many of which are caused by *Pseudomonas aeruginosa*, is the most important factor in evaluating where a patient is on the continuum of NCFB (Wang et al., 2021). As a result, it is still crucial in the therapeutic context to investigate various techniques to avoid *Pseudomonas aeruginosa* colonisation and to develop therapies for acute exacerbations.

Endophenotypes are being analysed in order to find common traits that may be tailored for particular treatments and interventions in NCFB patients. This is comparable to a large number of different medical disorders (King et al., 2021). In 2017, the European Respiratory Society issued recommendations for the diagnosis and management of NCFB in adults. These recommendations were established for the diagnosis and management of adult patients with NCFB; nevertheless, as the authors of this guideline and other professionals emphasise, there are still a number of unanswered questions (Woo et al., 2019).

1.2.3 Cystic Fibrosis (CF)

Cystic fibrosis is an autosomal recessive genetic disorder which affects 1 in 2500 new-borns in the United Kingdom. This condition simultaneously affects several systems, including organs and tissues. Mutations in the cystic fibrosis transmembrane conductance regulator (CFTR) protein cause

the disease. CFTR is expressed on the cell surface of mucus-producing cells in every mucus-producing tissue of the body. The flow of chloride ions across the plasma membrane of epithelial cells is mediated by CFTR, a kind of transporter protein. NaCl levels in perspiration can indicate malfunctioning sweat glands and may be used to identify cystic fibrosis.

It is possible to get a diagnosis at any age, even as an adult; nevertheless, new-born screening is the most prevalent method in the United Kingdom (Chorepsima et al., 2018). At the time doctors establish the diagnosis, the typical patient is merely 2 months old (Schlüter et al., 2020). Adults with cystic fibrosis were rare in the past, when the risk of dying early was higher, but this is no longer the case in more industrialised nations due to advances in treatment. However, low-income nations continue to struggle with high child mortality rates. Sixty percent or more of patients now listed on the UK cystic fibrosis registry are beyond the age of sixteen (Chorepsima et al., 2018).

This mutation impacts other organs because it causes the ducts of other organs to get clogged with thick mucus discharges. As a result of the secretions, the injured area develops a condition marked by increased inflammation and fibrosis. The majority of people with cystic fibrosis die from lung disease. The most severe types of bronchiectasis may result in lung tissue loss due to infection, inflammation, and airway obstruction (Zhou-Suckow et al., 2017).

1.2.4 Asthma

Asthma symptoms are caused by mechanisms including airway wall remodelling, mucus overproduction, bronchial hyper-reactivity, and airway constriction. The underlying pathology involves interactions between epithelial cells and a wide variety of immune cell types. These immune cell types include both innate immune cells and adaptive immune cells. This illness may manifest itself in a variety of ways, including coughing, wheezing, anxiety, trouble breathing, chest tightness, tachycardia, and overall tiredness.

Asthma is characterised by reversible airway obstruction, inflammation, and airway hyperresponsiveness. 5-10% of patients are resistant to treatment with corticosteroids. Inhaled corticosteroids diminish inflammation, whereas short- or long-acting beta2-adrenergic agonists relax the bronchial smooth muscle to reduce symptoms.

Asthmatics are more likely to have exacerbations when exposed to stimuli including pollen, mould, dust mites, and in some individual's different food types. Smoking, cold air, aspirin, sulfiting agents, and mental stress may also trigger asthma attacks. Acute asthma causes bronchiolar smooth muscle spasm and mucus congestion, whereas chronic asthma causes continual inflammation, bronchial epithelial cell loss, fibrosis, and oedema.

A range of mediators have been identified which promote airway constriction and inflammation including histamine, prostaglandins,

leukotrienes, and thromboxane (Carpaij et al., 2019). In an acute attack, asthmatics have irregular gas exchange due to a mismatch between ventilation and perfusion rates. Hypoxia and hypercapnia ensue (elevated PaCO₂).

Researchers have distinguished two asthma types. Allergic asthma affects most children and half of adults. Inhaled or ingested allergens such as home dust mites, pollen, and peanuts cause this disorder. A positive skin-prick test or serum IgE antibodies indicate sensitivity. In children, allergic sensitization may or may not be followed by eczema in the first year. These children will develop allergic rhinitis and maybe asthma.

The 'atopic march' describes this steady symptom progression. To be more precise, children with multiple allergies at a young age are at a higher risk of developing asthma (Wang et al., 2018), and studies have shown that half of atopic eczema patients develop asthma (Daugherty et al., 2018). Eighty percent of allergic asthmatics also have allergic rhinitis.

Intrinsic asthma, also known as nonallergic asthma, lacks IgE sensitivity to allergens and engages adaptive immune cells such as type 2 helper T cells covertly. This asthma usually appears in adulthood. Obesity, chronic rhinosinusitis, and nasal polyps make this version of the disease more difficult to manage and some patients require long-term systemic steroid treatment. It is commoner in females.

1.3 Lung Imaging Modalities

To assess lung pathology and function, a number of different lung imaging modalities have been developed.

1.3.1 X-Ray of the Lungs (Chest X-ray)

Chest radiography is a common imaging technique for pulmonary and cardiothoracic medical conditions; it is used for early diagnosis or disease progression monitoring in particular. With advances in computer-aided diagnosis, the capabilities of X-ray can be further enhanced. The appearance of the lungs in a paediatric patient is different from an adult because the ongoing lung development (Candemir & Antani, 2019). Although it requires a low radiation dose compared to the CT scan, a chest X-ray provides less information than a CT scan.

A standard chest X ray is associated with radiation exposure of around 0.1 millisievert (Kroft et al., 2019). When radiation penetrates the body, X-rays are stopped by tissue, so the denser the tissue, the less X-ray passes through. Therefore, a physician can assess tissue changes inferred by different patterns that reveal pneumonia or lung cancer, for example (Bhandary et al., 2020). However, X-rays cannot provide any information about lung function, only structural changes (see Figure 1-7) (Bhandary et al., 2020).

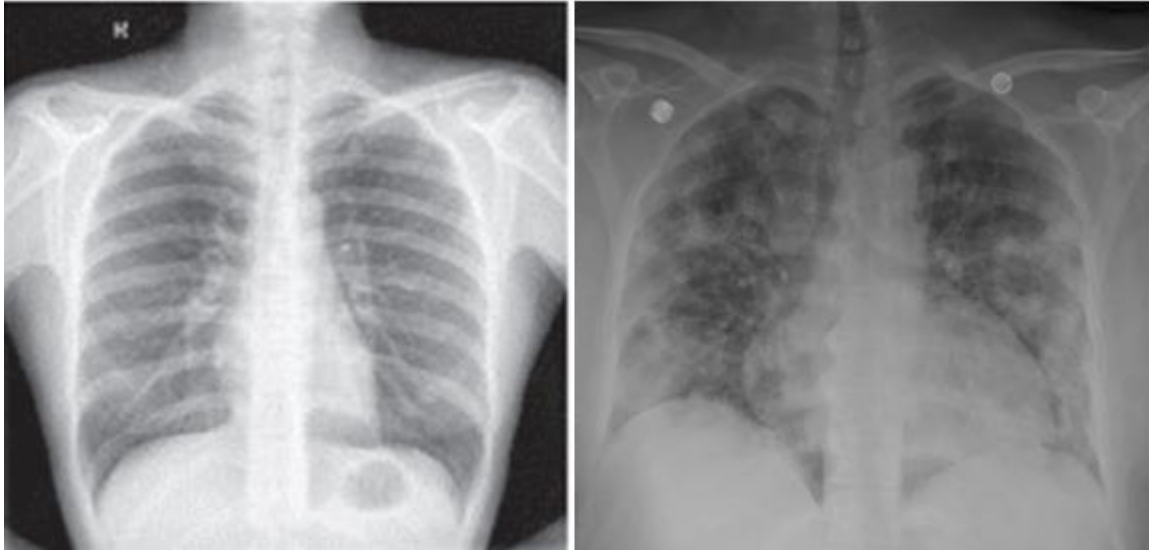


Figure 1-7: Displays normal (in the left image) and abnormal (pneumonia) (in the right) chest x ray (Bhandary et al., 2020).

1.3.2 CT scan of the Lungs

Computed Tomography (CT) scans are a non-invasive procedure that can be used to screen all body organs. For this reason, the use of CT has increased for pulmonary diseases. It is more sensitive than standard methods such as chest X-ray for lung screening. CT yields images of internal organs, blood vessels and soft tissues, and based on the same principles as standard chest X-rays but the spatial resolution is much higher. Therefore, CT is capable of detecting early-stage pulmonary diseases such as pneumonia, tuberculosis and inflammation of pleura (Makaju et al., 2018). Although a CT scan provides quick, high quality structural images of the lungs, it does not provide any functional details and it requires a higher dose of ionising radiation (around 5.5 millisievert)

(Kroft et al., 2019). There is significant variability in the dose of radiation when comparing scanners and centres through Europe (Kuo et al., 2016).

1.3.3 Nuclear Medicine of the Lungs

Some information about regional lung function can be obtained using nuclear medicine scans, which can assess both ventilation and perfusion, in a process called V/Q scanning. These tests may be undertaken together or separately. During the perfusion scan, albumin tagged with a radioactive tracer is injected into a patient's vein. Then the lungs are scanned by gamma camera to identify the location of the radioactive particles. This test is done to measure the blood supply to the entire lung. During the ventilation scan, a radioactive gas is inhaled via a mask. This test is done to detect lung ventilation. Clinically, the V/Q scan is used to detect a pulmonary embolism. The technique has relatively poor spatial resolution and requires both specialised equipment and radioactive tracers, which makes it less easy to undertake than standard X-rays.

1.3.4 Ultrasound of the Lungs

Lung Ultrasound (LU) potentially allows for the direct visualisation of the lung structure through a curvilinear probe. The resultant image of the LU is dependent upon the amount of fluid and air in the lungs. The technique relies on acoustic impedance (Z), which is the resistance of the particles to

mechanical vibration, which increases in line with the density of the medium. Therefore, the greater the difference in Z , the higher the contrast will be. When there is a fluid-filled lung, imaging can be obtained directly (Miller, 2016). However, ultrasound examination of the lungs is challenging due to poor acoustic impedance, which provides poor image quality. Moreover, performing this technique is vulnerable to misinterpretation (Touw et al., 2015). Clinically, the technique is used mainly to look for pleural fluid collections (effusions). This technique does not provide functional information.

1.3.4 MRI of the Lungs

The main advantage of MRI over other modalities is that it is non-invasive, and it does not require ionising radiation, which makes it an attractive option when trying to avoid exposure to radiation. Amongst the challenges of imaging MRI is the uncontrolled motion of artefacts due to regular cardiac and respiratory motion. Lung images obtained by conventional MRI also have much lower resolution than CT scans. Adequate lung imaging by MRI is a challenge because lungs have a very low density of protons and motion artefacts further degrade image quality. Respiratory motion can be overcome by using breath holds, but it is difficult with children and patients who have diseases that either affect their lungs or are neurodegenerative in nature.

However, attempts have been made recently to improve the resolution of lung images. According to Zeng et al. (2019), using lung MRI in conjunction with the MultiVane technique can produce high resolution, motion-suppressed images that allow the characterisation of different pulmonary diseases (for example TB). It produces results consistent with CT scans (see Figure 1-8).

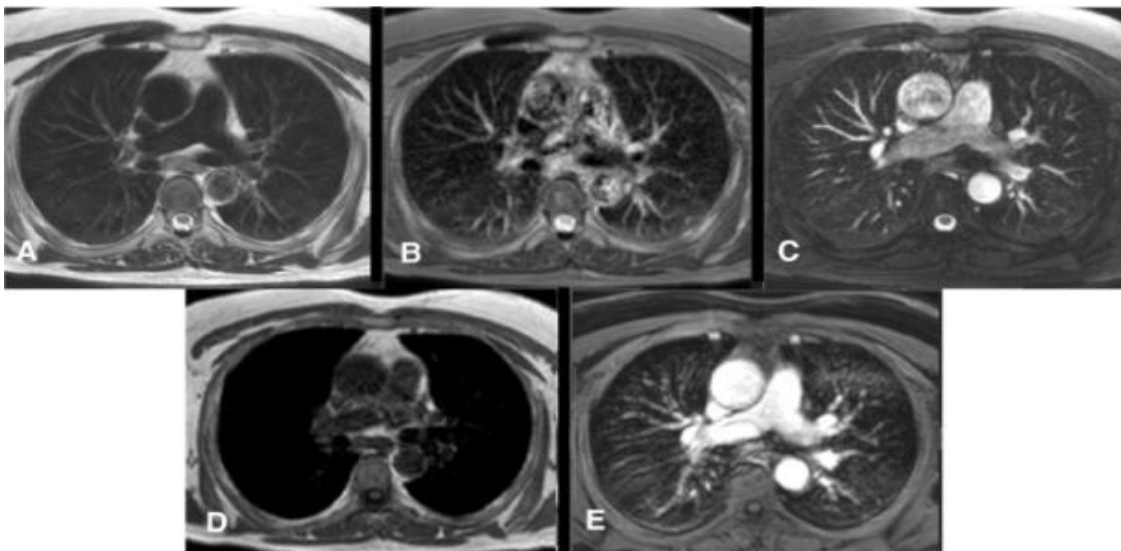


Figure 1-8: Depicts (A) T2 MVXD, (B) STIR, (C) BTFE, (D) T1, and (E) T1 PG. Major airways (arrows), ascending aorta, descending aorta, right and left pulmonary arteries are clearly visible in the T2 MVXD images. The mediastinal vessels in the middle third are obscured by artefacts, particularly in the STIR sequence. The definition of the intrapulmonary vessels is superior in (C), but the technique is associated with poor visualisation of the airways (Delineation of the intrapulmonary vessels but poor in visualisation of the airways) (Zeng et al., 2019).

The MultiVane technique involves a beam of several parallel lines, which are collected in a multi-echo instead of a single radial line. Lung parenchyma has different properties compared to liver or brain tissues due

to the low proton density in the lung. The density of healthy lung tissue is 0.1g/cm^3 , which is ten times lower than tissues in the other parts of the body. MR signal is directly related to tissue proton density. This can be catered for through the balanced steady state free precession (bSSFP) method, which has a higher signal-to-noise (SNR) ratio. The method offers high signal efficiency with relative motion insensitivity.

Moreover, there are some relatively novel techniques to depict the lungs using MRI such as, hyperpolarised inert gas, oxygen-enhanced MRI (OE-MRI), and ultrashort echo time (UTE). These methods are addressed in detail in the MRI section.

1.4 Lung Function Tests

In this section two types of the lung function tests spirometry and lung clearance index (LCI) are discussed. These techniques were selected because they were assessed in children with ataxia telangiectasia in this thesis as well as OE-MRI. A more detailed explanation of methodological issues is given in the relevant results chapters.

1.4.1 Spirometry Technique

Spirometry is a basic lung function test that measures the flow of expelled air against volume, time, and flow. It is a straightforward, non-invasive, non-ionising, inexpensive and fast test to perform, in which the patient is asked to take a maximal inhalation and then to forcefully exhale for as long

and as fast as possible (a forced vital capacity manoeuvre- Figure 1-9). Spirometry measurements are forced expiratory volume in one second (FEV_1), forced vital capacity (FVC), and the ratio of both volumes (FEV_1/FVC) (Ranu et al., 2011). Moreover, FEF25-75% is the most sensitive measure of airflow in peripheral airways where primary airflow obstruction originates, and it is reduced in early bronchial impairment, which is associated with small airway disease (Choi and Rhee, 2020).

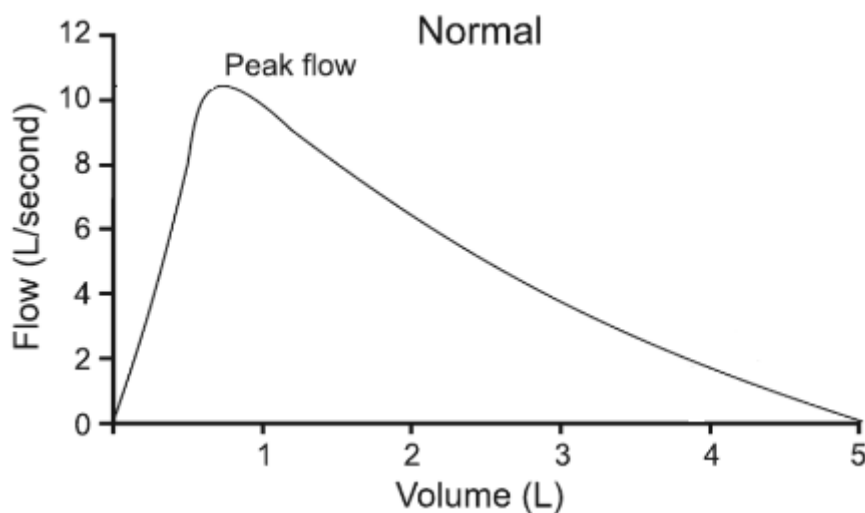


Figure 1-9: Demonstrates the normal (Flow/ Volume loops) in spirometry (Ranu et al., 2011).

The technique is easy to understand for health workers, but there are some challenges in implementing it as a routine testing technique in medical facilities. The patient needs to take a full breath and undertake a forced exhalation until residual volume is reached.

Spirometry is useful as a marker of disease progression and assessing the extent of structural changes due to respiratory conditions. The procedure

is usually straightforward but there are certain complications in real-life application. To ensure useful results, reproducibility is key, otherwise the results may be interpreted incorrectly (Wheatley, 2017). Reversibility of airway obstruction can be assessed by administering an inhaled bronchodilator drug such as salbutamol (a β_2 agonist). This can be useful in the diagnosis of patients with reversible airflow obstruction such as frequently occurs in patients with asthma (Matteo et al., 2018).

1.4.1.1 Spirometric Measurements

Table 1-1: Shows the main measurements that can be obtained by spirometry using a forced expiratory volume following a maximal inhalation.

Spirometric Measures	
FEV ₁	Forced Expiratory Volume in 1s, maximal amount of air exhaled in one second whilst blowing as fast as possible
FVC	Forced Vital Capacity, maximum volume of air exhaled while blowing as fast as possible
FEV ₁ /FVC	The ratio of exhaled air in first second and the total air exhaled
PEF	Peak expiratory flow, maximal flow of air exhaled while blowing out at a steady rate
Forced Expiratory Flow	Mid-expiratory flow or flow rate at 25%, 50% and 75% of FVC
IVC	Inspiratory vital capacity, maximum air inhaled after a full expiration

1.4.1.2 Standards of Spirometry

According to the latest European and American standards, spirometry is the test used to measure the maximal volume of air inspired and expired using maximal effort (Graham et al., 2019). The standard terms used for spirometry are:

Operator: an expert who is given the authority to conduct the spirometry test.

Patient: the person who undergoes the test, a general understanding here is that not all people undergoing breathing tests are patients.

Manoeuvre: refers to the vital capacity (VC) excursions during air inspiration and expiration. Items referred to as 'must' are the minimum criteria to meet the requirements of the standards, while the 'should' items reflect important items that may not be necessary but are important to consider if possible.

In 2005, the American Thoracic Society (ATS) and ERS developed agreed standards for spirometry, which are the basis for current standards. These standards are continuously updated as necessary. Table 1-2 focuses on how the patient and expert can jointly make an effort to achieve acceptable spirograms by using set criteria.

Table 1-2: Manoeuvre criteria for acceptable spiromograms. The table is divided into two parts: the first part demonstrates some errors which may affect the spirometry manoeuvre (these will be mentioned in detail in the next section). The second part shows the criteria between the accepted spirometry manoeuvres that are applied after obtaining the three accepted trials. All these criteria are derived from the ATS/ERS standards (Graham et al., 2019).

Within-manoevrue criteria
<p>Individual spiromograms are “acceptable” if:</p> <p>1- They are free from artefacts:</p> <ul style="list-style-type: none"> ▪ Coughing within first second of the exhalation ▪ Glottis closure that influences the measurement ▪ Early termination or cut-off ▪ Effort that is not maximal throughout ▪ Leak ▪ Obstructed mouthpiece <p>2- They have good starts:</p> <ul style="list-style-type: none"> ▪ Extrapolated volume <5% of FVC or 0.15 L, whichever is greater. <p>3- They show satisfactory exhalation:</p> <ul style="list-style-type: none"> ▪ Duration of 6s (3s for children) ▪ a plateau in the volume–time curve ▪ may still be acceptable if the subject patient should not or cannot continue exhaling
Between-manoevrue criteria
<p>Once three acceptable spiromograms are obtained, the following tests should be applied:</p> <p>1- The two highest values of FVC should be within 0.15 L of one another.</p> <p>2- The two highest values of FEV₁ should be within 0.15 L of one another.</p> <ul style="list-style-type: none"> ▪ If above two criteria are met, the testing session can be concluded. ▪ If above two criteria are not met, continue the testing session until both are met upon analysis of acceptable spiromograms from additional testing or ▪ Total eight tests are performed (optional) or the subject patient should not continue for other reasons

1.4.1.3 Applications

1.4.1.3.1 Interpreting Spirometry - Normal lung function

Spirometry results are compared against reference or control test results (i.e., normally functioning lungs). Confusingly, a number of reference ranges exist, each one of them use a slightly different equation to define values for comparison (Backman et al., 2015). The equation derived by the European Community for Coal and Steel (ECCS) is often used for reference values, as it is based on the survey of a large population made up of different age groups, physiques and fitness, ethnic origin, and occupational environment. ECCS values are derived from an equation which is linear in nature; however, this may be an oversimplification, because the distribution of lung function is non-linear at the population level (Marek et al., 2009). To address this issue, the Global Lung Function Initiative was formed as an international consortium.

The Global Lung Function Initiative (GLI) was the reference in this study. GLI was established in Berlin in September 2008, acquiring ERS Task Force status in April 2010. This initiative has developed new reference ranges for lung function on an international basis. The objectives of the GLI are to establish improved international spirometry reference equations which based on individual lung function data collected under standardised measurement conditions with documented equipment and software are modelled using modern statistical techniques to allow continuous equations

across the entire age range from early childhood to old age (Quanjer et al., 2012).

1.4.1.3.2 Interpreting Spirometry – Obstruction

Obstructive and restrictive pulmonary disorders can be identified through changes in the FEV₁/FVC ratio. Spirometry of patients with obstruction show reduced FEV₁, reduced (or normal) VC and FVC (Figure 1-10). Reduced FEV₁/FVC ratio is <70% and a concave flow-volume loop (Johns et al., 2014). Obstruction leads to a limitation in airflow to the lungs due to a decrease in the diameter of the airway; This can be the result of inflammation, mucus plugging or in the case of emphysema, collapsed airway such as asthma and COPD. The reduction in FEV₁ can be used to classify the severity of impairment in conditions such as COPD (see Table 1-3) (Johns et al., 2014).

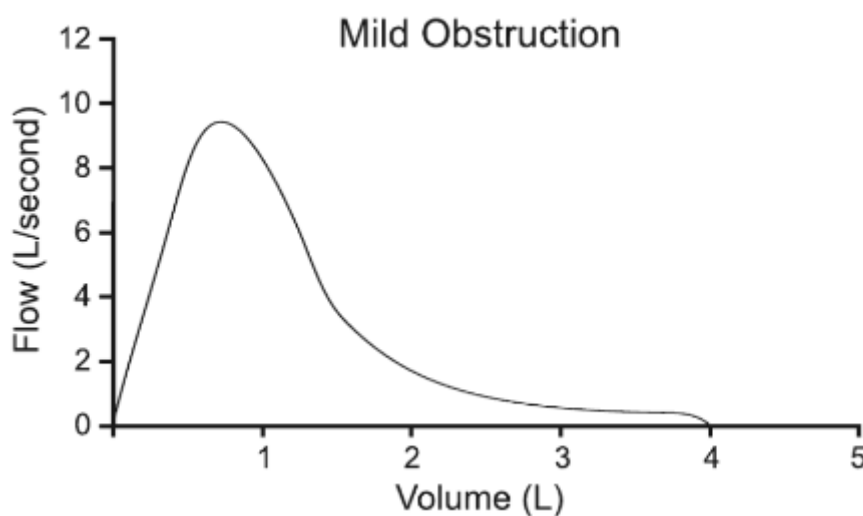


Figure 1-10: Demonstrates the obstructive lung disorder flow/ volume loops in spirometry (Ranu et al., 2011).

Asthma lies in the reversible classification of spirometry, although the results may appear normal if the subject is not experiencing exacerbation. In contrast, COPD causes irreversible airflow obstruction, although small degrees of reversibility may be present in some patients (Johns et al., 2014) (see Figure 1-12).

Table 1-3: Severity of airflow obstruction based on percentage (%) predicted forced expiratory volume in 1 second (FEV₁).

FEV ₁ % predicted	Result
80% or greater	Normal
60-69%	Mildly abnormal
50-59%	Moderate abnormal
30-49%	Severely abnormal
<30%	Very severe abnormal

1.4.1.3.3 Interpreting Spirometry – Restriction

Restrictive disorders are accompanied by loss in the lung volume where the FEV₁/FVC is >70%, the FVC is lower than FEV₁ (see Figure 1-11); Pulmonary fibrosis, kyphoscoliosis (chest wall disorders), neuromuscular disorders, pulmonary oedema, obesity, pneumonectomy and interstitial lung diseases (ILD) are some of the diseases that fall in this category (Ranu et al., 2011 and Martinez-Pitre et al., 2020). The evidence of restrictive flow in spirometry is a reduced FVC value. The FEV₁/FVC ratio increases

(normal to high) but there is often a relatively higher PEF (Martinez-Pitre et al., 2020) (see Figure 1-12).

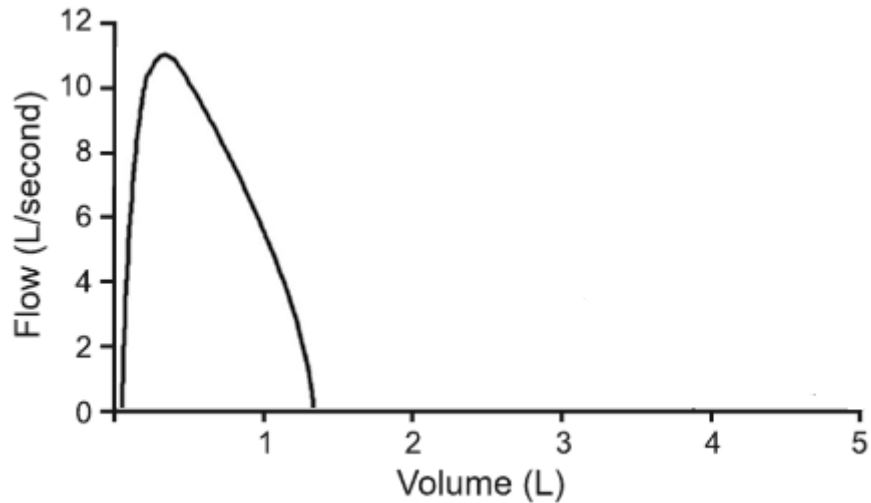


Figure 1-11: Demonstrates the restrictive lung disorder flow/ volume loops in spirometry (Ranu et al., 2011).

1.4.1.3.4 Interpreting Spirometry - Mixed Pattern

For some subjects, the spirometry pattern is not as straightforward to interpret. For example, in sarcoidosis, which is restrictive disease, half of the patients may have a mixture of restriction and obstruction present (Obi and Baughman, 2020). In such scenarios, it is clinically advised to analyse static lung volume and gas transfer in conjunction with spirometry (Obi and Baughman, 2020) (see Figure 1-12).

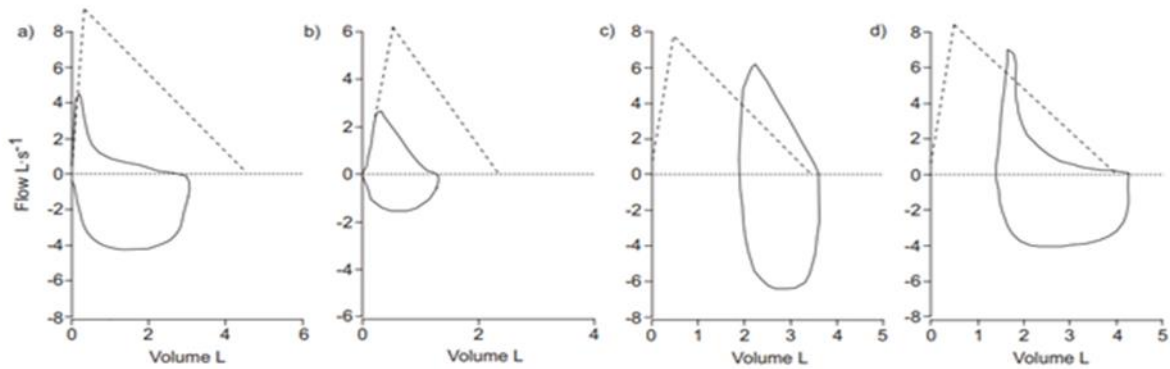


Figure 1-12: Examples (a) and (b) show obstructive pulmonary defects in both cases where TLC is normal, and flows are less than expected over the entire volume range. Example (c) shows a restrictive defect where TLC is low, and flow is higher than expected at a given lung volume. Example (d) shows a mixed defect where TLC is low and a low FEV₁/VC ratio (Pellegrino et al., 2005).

1.4.1.4 The Technique

Spirometry is usually performed by inhaling to FVC and then undertaking a forced expiration to residual volume. This yields FVC and FEV₁. PEF is obtained from manoeuvring the FVC and FEV₁ values, which can also be measured separately using a peak flow meter. To prevent air leakage from the nostrils, nose clips are essential (Moore, 2012). It is important that the patient keeps blowing until the lungs are emptied to obtain an accurate FVC measurement (Miller, 2005). Patients with obstructive disease may find it difficult; however, relaxing patients can produce better results.

The ATS and ERS have formulated guidelines for the acceptable quality of spirometry. It is suggested that there should be at least three acceptable manoeuvres for a test to qualify as valid. An acceptable manoeuvre is defined as the forced exhalation that back-extrapolates to a volume of less

than 150 ml. The manoeuvre is performed with maximum blow force; the subject does not cough during the test or has cessation of airflow. In adults, the manoeuvre should end with a 6s exhalation, in which less than 50 ml of air is exhaled in the final 2s. For the two best measurements of FEV₁ and FVC, the values should be 150 ml or $\pm 5\%$ of each other unless FVC is <1.0 l; in that case, the values should be within 100 ml. It must be noted that maximum FEV₁ and FVC can be used from different manoeuvres (Moore, 2012). Moreover, the spirometry test should be corrected for body temperature and ambient pressure saturation. This corrects for the difference in volume measured by the spirometer at room air temperature and the volume of air in the lungs at body temperature (37° C).

1.4.1.5 Types of Spirometers

The availability of portable spirometers has increased the use of this technique to a great extent (Milazi et al., 2019). The type of spirometer used depends upon the environment in which the test is being performed. PC spirometers compute measurements based on a software application, taking the signal from the breathing equipment that is externally integrated. Desktop spirometers have built-in data displays, and the results are printed on thermal and electronic displays. Hand-held spirometers are pocket-sized devices that are integrated with a real-time graphical display for the spirometry report.

Some of the portable devices can also be synchronised with PCs (Carpenter et al., 2018). These devices are often used in primary care settings, as they are portable, inexpensive and are capable of measuring FEV. Peak flow meters are not true spirometers, because they comply with different standards than regular spirometers, and only measure peak expiratory flow rate (PEFR).

1.4.1.6 Equipment

Spirometers range from portable desktop devices to large clinical versions available in hospital facilities only. Most devices measure air flow directly using pneumotachographs and turbines and then use it to calculate volume. Only a wedge below spirometer measures volume and then calculates flow based on the measurement. Larger equipment is more stable as compared to hand-held devices and they have built in controls to measure spirometry indices. The portable ones store flow-volume loops and require a computer to be attached to it (Moore, 2012).

1.4.1.7 Calibration

Prior to testing spirometry, the equipment needs to be calibrated at the beginning of every session. The procedure varies slightly according to the type of equipment. Either a 3-liter syringe is pumped through to check the meter reading, or a 1 litre syringe is pumped at repeatably up to 7-litre (Moore, 2012). The rationale behind the procedure is to verify the linearity and the midpoint of volume measurement. For most of the spirometers, if

the calibration is out, the equipment cannot be calibrated in-house and needs to be returned to the manufacturer. It is recommended to verify the spirometry values weekly using a healthy person (as biological control).

1.4.1.8 Additional Information and Contraindications

Preliminary information required for spirometry includes the age, sex, height and weight of the subject, along with prescribed medications the patient is taking so that the effect of medications and therapies can be accounted for when analysing spirometry results. In particular, inhaled bronchodilators may affect the measurements of the spirometry test. In the event that a reversible airflow obstruction is present, post-bronchodilator spirometry will be greater than pre-bronchodilator measures. There are contraindications for spirometry, including when a patient has recently experienced haemoptysis, abdominal or cerebral aneurysms, eye surgery or pneumothorax, thoracic or abdominal surgical procedures or has acute disorders that can affect the test performance such as vomiting or nausea (Moore, 2012). Patient positioning plays an important role in obtaining correct measurements. The patient should be sitting upright and there should be no restriction to exhalation and inhalation. The feet should be flat, and legs uncrossed, so that abdominal muscles are not in use. Bacterial-viral filters should be thrown away at the end of each session and the equipment should be stripped down and sterilised if the test is performed on infectious patients (Moore, 2012).

1.4.1.9 Valid Normal Test

Figure 1-13 shows the pattern of a valid normal test with three repetition traces. All the spirometry criteria mentioned above can be derived from these three manoeuvres. The exhalation course time is shown at the left of the figure. The volume/ time curve starts from the zero (baseline), rises rapidly, before plateauing at the end of expiration.

According to the ATS and ESJ recommendations, the exhalation time should be at least 6s for adults and 2 or 3s for children. A healthy adult, however, may have completed exhalation before this 6s. The manoeuvre should not be deleted just due to exhalation time, because the FEV₁ result may be still acceptable.

The flow/ volume curve shown on the right side of the figure shows the flow rate at different stages of exhalation. This curve demonstrates three characteristics: an immediate steep rise in flow rate, a sharp peak and smooth descending line which returns to the zero as flow reduces later in a forced expiratory manoeuvre. The following paragraphs address common spirometry test errors, their effects, and possible solutions.

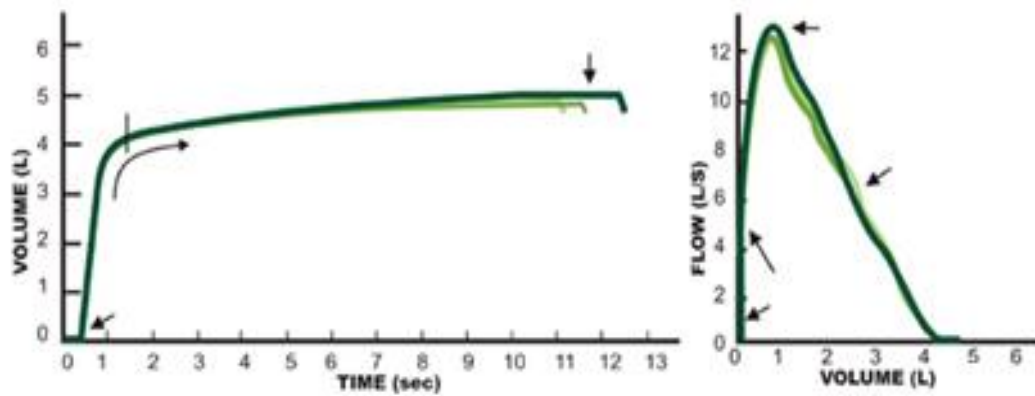


Figure 1-13: Shows spirogram for a normal valid test (Beeckman-Wangner and Freeland, 2012).

1.4.1.10 Spirometry Test Errors

This section addresses twelve types of spirometry errors. Spirometry graphs of the errors are presented in Figures 1-14 and 1-15.

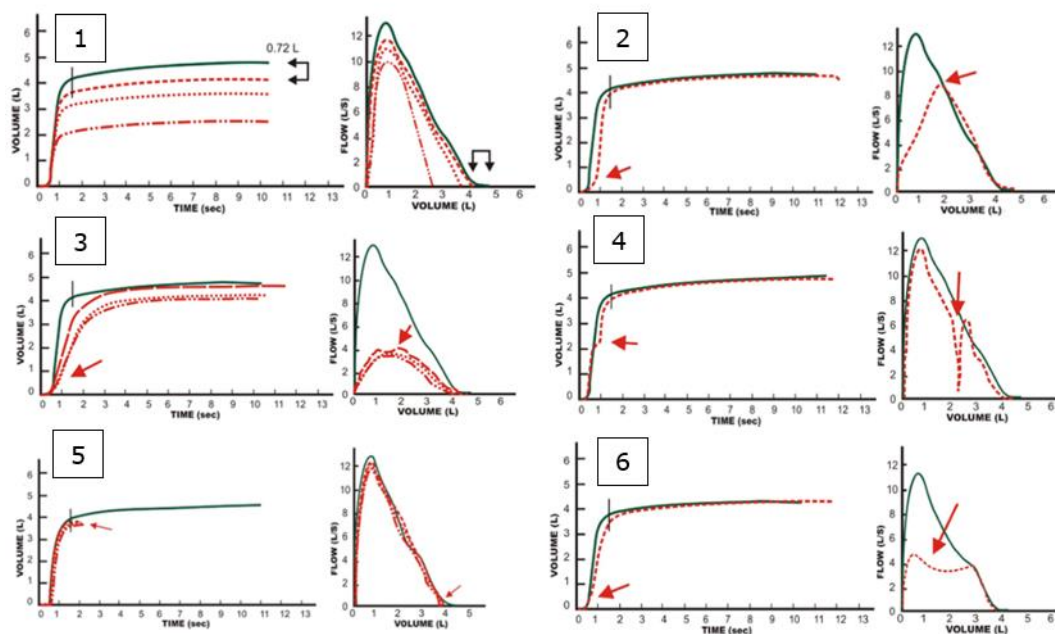


Figure 1-14: Shows spirometry graphs for common test errors (Beeckman-Wangner and Freeland, 2012).

1.4.1.10.1 Sub-maximal Inhalation

This error is considered an important and frequent issue that leads to the misinterpretation of spirometry results. The error is clearly seen in the volume/ time curves as the gap between the curves (see Figure 1-14, left figure 1). It is also seen in the flow/ volume curves as a space between the end points (Figure 1-14, right Figure No.1). Sub-maximal inhalation results in a reduced FVC value, which can wrongly be interpreted as evidence of a restrictive disorder. Moreover, false results will affect the repeatability of the test. The solution to this is coaching the patient to take the deepest possible expiration before starting the test.

1.4.1.10.2 Excessive Extrapolated Volume

This is a problem in which a patient starts exhalation faster initially. This error can affect the FEV₁ measure. However, if the plateau is reached, the trace may still be used to provide a valid FVC. It can be seen from Figure 1-14 right panel 2 that the peak flow point is shifted to the right in the flow/ volume curve. In this case, the spirometer automatically establishes an extrapolated volume. The extrapolated volume is rejected when it exceeds 5% of the FVC or 0.15 l. A large extrapolated volume can erroneously cause an increase in FEV₁ and sometimes the opposite can happen to. The issue can be resolved when the coach instructs the patients to blast immediately.

1.4.1.10.3 Sub-maximal Expiration

The error takes place because of reduced effort at the beginning of the test which affects the results. It is seen to reduce the PEF in the flow/volume curve (in the left of Figure 1-14 panel 3). The volume/time curve is also affected, and this error produces a slower rise in the curve from the zero point. Both FEV_1 and FVE_1/FVC ratio decline. If all curves are the same (because of reduced effort in all tests), it may be falsely interpreted as showing an obstructive impairment. The coach should instruct the patient to exhale harder, which should resolve the issue.

1.4.1.10.4 Cough in First Second

This error will affect the FEV_1 . Normally, the FVC measurement will also be reduced and inconsistent with other accepted curves. Coughing is seen in the flow-volume curve as a wavy interruption (Figure 1-14 panel 4), but it may be difficult to see on the volume/ time curve. Although the example shown has a single cough, sometimes multiple coughs occur in a single trial as well. Depending upon its strength, a cough can affect FEV_1 by either falsely increasing or decreasing the value obtained. Moreover, a strong cough may also falsely reduce the FVC measurement, thereby altering the observed FEV_1/FVC ratio. Controlling coughing is very difficult but offering water to the patient before starting the manoeuvre can help resolve the problem.

1.4.1.10.5 Early Termination

This happens when a patient stops exhaling before reaching FVC. It is seen on the volume/ time curve as a lack of horizontal straight line (plateau) (Figure 1-14 panel 5). It is also seen on the flow/ volume curve as a sharp descent. Although most healthy adults are able to exhale for more than six seconds, which is long enough to reach plateau, some will achieve a plateau within three to five seconds, which may mean the tests are still to be acceptable. A decreased FVC due to early termination might be wrongly interpreted as evidence of a restrictive impairment. The apparent increase in the FEV₁/FVC ratio may actually mean a true "obstructive impairment" is missed. Coaching the patient to continue blowing is the solution.

1.4.1.10.6 Variable Effort

This can be a problem especially during the first two and three seconds when there is significant irregular exhalation. This error is seen in the flow/ volume curve (in the right Figure 1-14 panel 6) as a concave line, and not as a variable line as seen in cough error. The reduction in the height of the curve increases with reduced effort. Since this error causes a false decrease in the apparent FEV₁ and FEV₁/FVC ratio, these results may be misinterpreted as an obstructive impairment. However, the reduced PEF and altered shape of the curve should be enough evidence to indicate poor effort. The solution is to coach the patient to take a full inspiration and exhale as hard and fast as possible, and also to keep blowing out until the end of expiration is reached.

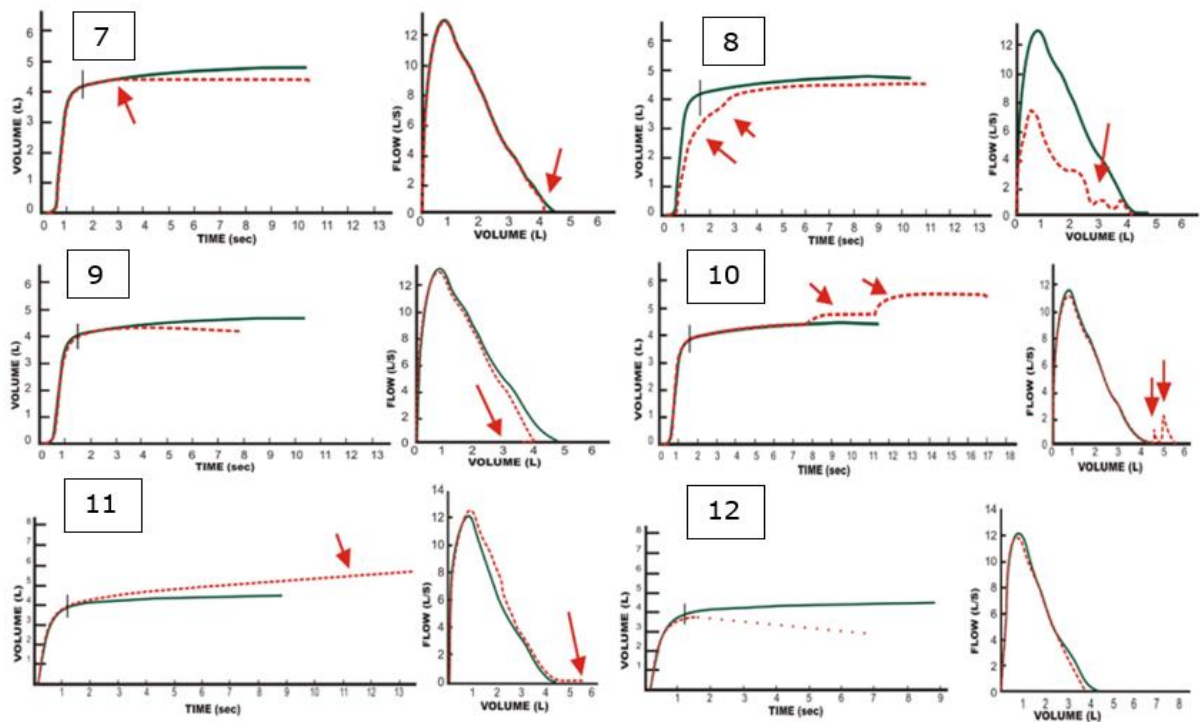


Figure 1-15: Spirograms for common test errors (Beeckman-Wangner and Freeland, 2012).

1.4.1.10.7 Cessation of Airflow – Glottis Closure or Breath Holding

This error occurs when the subject's exhalation suddenly ceases before emptying of the lungs is complete. This abrupt cessation is seen as a sudden horizontal trace in the volume/ time curve (left Figure 1-15 panel 7) and as a sharp drop line in the flow/ volume (right Figure 1-15 panel 7). It may be falsely interpreted as a restrictive impairment due to the apparent reduction in FVC. Moreover, this leads to a false increase in FEV_1/FVC ratio, which could also suggest normal results even when a mild obstructive impairment is present. This error may occur when the glottis closure happens involuntarily. The solution is to encourage the patient to make a full expiration.

1.4.1.10.8 Partially Obstructed Mouthpiece

The exhalation speed can be reduced due to a partial blockage of the mouthpiece, for example by the patient's teeth, tongue, loose dentures or due to biting strongly on the mouthpiece. This blockage can affect both the curves' shape (volume/ time and flow/ volume) and result in the trace being deformed in a variety of ways. For example, the flow/ volume curve (right Figure 1-15 panel 8) might reduce the peak flow rate, which will flatten the curve. Flattening also appears after the rising volume/ time curve (left Figure 1-15 panel 8). The more that the mouthpiece is blocked, the higher the degree of flattening. The apparent FVC can also be reduced with increasing pressure on the mouthpiece.

Therefore, the falsely reduced FEV_1 and FEV_1/FVC ratio might be misinterpreted as an obstructive impairment. The solution is to check that the mouthpiece is properly situated (i.e., on the top of the tongue and between the teeth). Some subjects may have dentures. Dentures help the patient to maintain the anatomical shape of the mouth; therefore, the subject is informed to lightly bite the mouthpiece and seal it tightly with the lips. However, ill-fitting dentures should be removed.

1.4.1.10.9 Leak

Spirometer leaks predominately occur around the patient's mouthpiece or the hose. The greater the leakage, the more the line descends after

reaching a plateau. This is seen in the volume/ time curve (left Figure 1-15 panel 9). The flow/ volume curve is also affected with an increased rate of decline at the end of the trial (right Figure 1-15 panel 9). The effect appears on both graphs. The FVC may be significantly affected, whereas the FEV₁ is usually less affected, thereby causing a false rise in the FEV₁/FVC ratio. The consequences are that there may be a failure to detect obstructive diseases, or the results may be falsely interpreted as showing the presence of restrictive disease.

To resolve this issue, the correct protocol must be used to prevent leakage from the hose, mouthpiece or spirometer. After making sure that the spirometer parts are properly connected, any leak can be detected during calibration using a syringe filled with a fixed volume of air. The commonest site of leakage is from the mouthpiece, and to prevent this the patients' lips should be tightly sealed around it.

1.4.1.10.10 Extra Breath(s)

This can happen near or at the end of the trial when an extra breath is taken via the nose or around the mouthpiece. This error is easily seen in the volume/ time curve as another plateau (left Figure 1-15 panel 10) and as a small curve after the main curve in the flow/ volume curve (right Figure 1-15 panel 10). Despite FEV₁ not being affected, the FVC is falsely increased, which reduces the apparent FEV₁/FVC ratio, thereby leading to possible misinterpretation as an obstructive case.

1.4.1.10.11 Positive Zero-Flow Error

This fault is due to software error from the flow sensor and arises from the incorrect setting of the zero point. It is clearly seen in the volume/ time curve (left Figure 1-15 panel 11) as a rising curve, which does not achieve a plateau and the rise angle is increased depend on the error severity. This can be seen in the figure (flow/ volume curve (right Figure 1-15 panel 11)) at the end of exhalation as a long tail. The FVC in this error is affected more than the FEV₁, which can lead to a falsely reduced FEV₁/FVC ratio. This can be misinterpreted as indicating the presence of obstructive lung disease. Many spirometry machines are prone to this error. The solution is to block the sensor outlet, preventing the flow of air through the sensor and keeping it in the vertical position during the manoeuvre.

1.4.1.10.12 Negative Zero-Flow Error

This is seen as a sudden or gradual drop at the end of the curve, which looks like a large leak, or in the volume/ time curve (left Figure 1-15 panel 12). This error leads to the under-recording of results. The greater the severity of the error, the greater the slope. It also occurs due to the incorrect setting of the zero point. The FVC here is influenced more than the FEV₁, which might be falsely interpreted as indicating restrictive disease or obscure true obstructive lung disease because of the false reduction in the FEV₁/FVC ratio.

1.4.11 Some Artefacts in Spirometry Patterns Observed in Children

Although spirometry is a safe technique and widely available, its application may pose difficulties for some adult patients and children, in particular can face some difficulties applying this technique. The main difficulty is the continued exhalation., The period of exhalation required is different for adults (6 seconds) and children (2 to 3 seconds). Some children are able to apply the necessary exhalation duration after receiving clear explanation and encouragement to keep blowing. However, not all children are able to comply with spirometry criteria. Figure 1-16 shows some children spirometry errors.

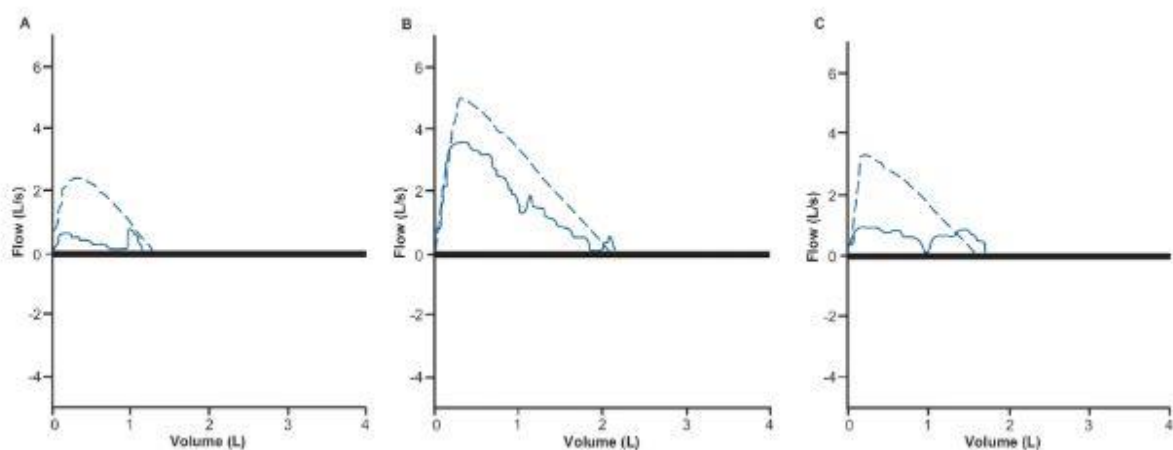


Figure 1-16: Spirometry in Children; (a) poor effort by patient (b) patient with cough; (c) premature start and end (Jat, 2013).

1.4.12 Advantages and Disadvantages of Spirometry

Spirometry provides lung function measurements, which are valuable for diagnosing and monitoring of lung disease. Spirometry is simple to perform; spirometers are portable and are inexpensive. It is easy to undertake repeated measurements. The non-invasiveness of this technique

is a key feature, making it advantageous for use by patients with AT. However, the need to hold and manoeuvre breath can prove to be difficult for some AT patients. Moreover, spirometry was considered an aerosol-generating procedure during the COVID-19 pandemic. Therefore, it may contribute to the transmission of infection between patients (especially, during this pandemic), and use of it was limited in the pandemic.

There are mild risks associated with undertaking this procedure. The patients can feel dizzy and lightheaded after continuous forceful inhalation and exhalation. There have been cases of spirometry tests being conducted on patients suffering from lymphangiomyomatosis, resulting in them to have a pneumothorax (Taveira et al., 2016). Indeed, after spirometry or exercise testing, pneumothorax cases have been reported in patients with lung disease. This retrospective study run between 1995 and 2015, reported on 691 in-patients in the National Institutes of Health Clinical Research Centre. In this study three patients developed pneumothorax after pulmonary function tests and/or exercise tests. The incidence of pneumothorax associated with lung function testing was 0.14–0.29 per 100 patients, or 0.02–0.04 per 100 tests. The incidence of pneumothorax in patients undergoing exercise testing was 0.14–0.28 per 100 patients or 0.05–0.10 per 100 tests (Taveira et al., 2016). Similarly, patients with neuromuscular diseases may also find it difficult to fulfil all the criteria for spirometry, which can in turn hinder achieving accurate results. According to Chiang (2018), both FEV₁ and FVC are particularly pertinent to

individuals with neuromuscular disease (NMD). Compared to healthy controls, FEV₁ and FVC are often reduced in children with NMD, because they are determined by inspiratory and expiratory muscle strength, as well as by chest wall and lung compliance. Total lung capacity itself is reduced because of reduced muscle strength, and as a result, there is a reduction in the exhalation airflow despite structurally normal airways. The FEV₁ is reduced in proportion to FVC; therefore, the FEV₁/FVC ratio generally remains in the normal range (i.e., 80%–100%) (Panitch, 2009). This constellation of spirometry findings is categorised as being consistent with restrictive lung disease. Despite FEV₁ and FVC both being consistently reduced in NMD patients, the severity of any spirometric abnormality, whether restrictive or obstructive in nature, is still based on FEV₁ alone. The FEV₁-categorisation of severity is as follows: mild is >70% of predicted, moderate is 60%–69% of predicted, moderately severe is 50%–59% of predicted, severe is 35%–49% of predicted and very severe is <35% of predicted (Chiang et al., 2018).

1.4.13 Spirometry in Children

Respiratory disorders are responsible for mortality and morbidity in children. Promoting the use of spirometry to help diagnose paediatric respiratory diseases could bring rates down. Jat (2013) states that currently, spirometry is underused by primary care physicians for diagnosing respiratory conditions in children. It can prove to be useful in the diagnosis of asthma, cystic fibrosis and congenital/ acquired airway

malformations. The reason for its under use is linked with the presumption that spirometry is difficult for children to perform, as it requires patients' cooperation in performing breathing manoeuvres.

Therefore, healthcare practitioners historically have found it convenient to use other techniques, such as tidal breathing or forced oscillation to assess lung function in paediatric patients. In a survey conducted to assess the uptake of spirometry, it was revealed that only half of the paediatricians use spirometry for managing children with respiratory diseases. Half admitted that they did not know how to interpret spirograms (Aurora et al., 2004). According to research, spirometry is safe to use for children and adults with cardiac arrhythmias, cystic fibrosis, chronic cough and cystic fibrosis (Sanders et al., 2008).

Spirometry also has a role to play in assessing lung function in other paediatric diseases, which can affect the lungs, including transfusion-dependent β -thalassaemia major or sickle cell anaemia, ataxia telangiectasia, haemato-oncology conditions, or connective tissue disorder. There is no absolute contradiction to spirometry apart from a new pneumothorax. However, it is recommended the technique be avoided when the patient is suffering from respiratory tract infection/ influenza, uncontrolled hypertension, vomiting or pain, abdominal or eye surgery, or dementia (Roberts et al., 2018).

1.4.14 Spirometry in Ataxia Telangiectasia

Ataxia Telangiectasia is a genetic disorder which is characterised by neurodegeneration, genomic instability, immunodeficiency, and radio-sensitivity, the latter increasing the susceptibility of the patient to cancer. Progressive cerebellar ataxia occurs in the severest form of the disorder (Schoenaker et al., 2016). As of now, there are no therapies available to cure this disorder or to prevent it from developing. It is only possible to suppress some of the symptoms associated with immunodeficiency and deteriorating lung functioning through medical interventions such as aggressive treatment of infection.

However, the neurodegeneration and predisposition to cancer are incurable. The immunodeficiency results in many of these patients developing lung disease. In other patient groups, CT scan is the standard method for anatomical lung imaging; but it is an unsafe solution in AT due to sensitivity of patients to ionising radiation.

Spirometry is a potentially safer solution to look for underlying lung disease in AT patients, but if patients are unable to comply with the technique the results will be inaccurate and might lead to false diagnosis (Vilozni et.al, 2010). The rate of deterioration in the condition of AT patients with lung disease is directly related to the degree of airway obstruction (Vilozni et.al, 2010).

Vilozni et al. (2010) suggested that patients with AT are able to conclude the test successfully and deliver reproducible results. In their study, the

researchers explored the feasibility of forced spirometry in patients with AT. They performed spirometry on 28 patients, age ranging between 3 and 19 years. The parameters of the spirometry traces were evaluated to look for pulmonary illness. The results showed that the rise time to peak flow increased by 16.2 ± 12.5 ms/year. Expiration time was significantly lower (i.e., 1.21 ± 0.47 sec) and it ended abruptly in 57% of the patients. Only 12 of the 20 patients were able to establish a reliable FEV₁. It was concluded that forced spirometry could be undertaken and was to some extent reproducible and that lung function showed deterioration over time.

In another study (McGrath-Morrow et al., 2008), lung volume measurements in adolescent AT patients were undertaken by performing spirometry tests on 15 patients and measuring lung volumes using the helium dilution technique. Measurements were taken on three separate occasions; the test was also repeated in another group of 10 AT patients. The objective of the study was to assess the reliability of pulmonary testing in this patient group. Most of the subjects had a residual volume greater than predicted.

Lung volume measurements from AT adolescents revealed near normal TLC values with increased RV and decreased VC values. These findings indicate a decreased ability to expire to residual volume, rather than a restrictive defect. Spirometry was also found to be reproducible in AT adolescents, suggesting that spirometry testing may be useful for tracking changes in pulmonary function over time in this population.

1.4.2 Lung Clearance Index (LCI)

Lung clearance index (LCI) measured by multiple breath washout (MBW) is a sensitive measure of ventilation inhomogeneity. Whereas FEV₁ in health and early disease mostly reflects proximal airways, LCI is considered to reflect abnormalities of the smaller airways which are considered the site of early lung injury in CF and some other diseases. LCI is a measure of the number of times the volume of gas in the lung at the start of the washout (the FRC) must be turned over in order to wash out the tracer gas to the pre-defined endpoint (1/40th of the tracer gas starting concentration). With increasing disease severity, LCI increases (Horsley, 2009). The washout technique can be of one of two types depending on the tracer gases used – that is either nitrogen (N₂) or sulphur hexafluoride (SF₆). Figure 1-17 below shows the two setups. For this thesis, I used the multiple breath N₂ setup.

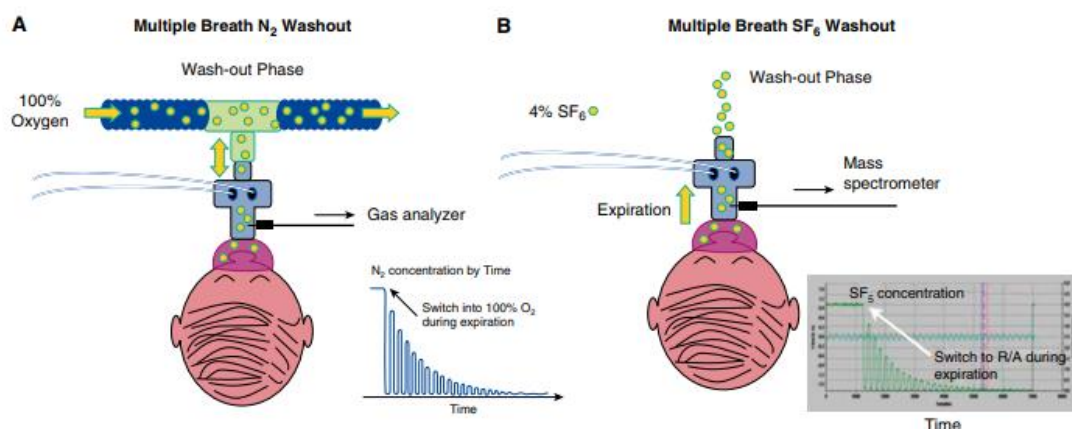


Figure 1-17: Shows a multiple-breath washout setup of N₂ and SF₆ (Subbarao et al., 2015).

1.4.2.1 Background History of Lung Function Testing with Reference to Lung Clearance Index

Historically, spirometry is the most commonly used technique to monitor the respiratory health of patients (spirometry in AT is considered in Chapter 2 of this thesis). However, this is challenging for children under the age of 6-years old. Over the past 15 years or so, interest in gas dilution techniques, particularly the MBW technique, has increased (Fretzayas et al., 2019). It is often considered to be more sensitive and accurate than spirometry (Fretzayas et al., 2019), particularly in detecting the onset of milder lung disease. It is also useful, as it can be used for all of the patients regardless of their age.

In 1952, the MBW test was introduced by Fowler (Fretzayas et al., 2019). He developed a method that could measure the extent of uneven ventilation. He represented it by pulmonary nitrogen clearance curves of a single-breath wash-out from some healthy people and patients who were suffering from cardiorespiratory diseases. This set the basis for more technological advancements and improvements in the application of this method. According to Subbarao (2015), this method has been in used since 1985.

Working of LCI

LCI is derived from MBW. The basic principles behind MBW are quite simple. Most of these principles date back more than 50 years but remain valid

(Fretzayas et al., 2019). The test involves the wash-out of an inert tracer gas from the lungs during relaxed tidal breathing. Generally, the tracer gas is nitrogen, which is always present in a person's lung, as it forms a major portion (79%) of air.

Other tracer gases in commercial use include sulphur hexafluoride (SF_6). It must be noted that the tracer gas should be inert, and it should not be absorbed or lost by the body. During every successive breath of the wash-out, the concentration of the exhaled tracer gas declines.

The MBW consists of two phases, which are the wash-in phase and wash-out phase (Fretzayas et al., 2019). The wash-in phase only applies to the techniques using an exogenous inert tracer gas, such as SF_6 . In the wash-in phase, the subject breathes a mix of the tracer gas and oxygen (Stahl et al., 2018). This gas is usually SF_6 of known concentration. The subject breathes until the concentration of expired gases reaches the concentration of the delivered gas. This marks the beginning of wash-out phase. During this phase, the subject in an exogenous tracer gas study is allowed to inhale the surrounding room air, or 100% oxygen for nitrogen wash-out studies.

The wash-out phase of the procedure and the underlying theoretical basis is the same. Specifically, the volume of each breath and the tracer gas concentration are measured on a breath-by-breath basis. In the work presented in this thesis, nitrogen is used for the children with AT. Figure 1-18 shows an example of the MBW test.

MBW is performed with specialised equipment. Currently, there are three commercially available systems competing in the United Kingdom (Eco Medics AG Exhalyzer D, Innovision Innocor and ndd EasyOne Pro Lab) (Nuttall et al., 2019). The basic requirements include an analyser for the tracer gas, a mean to measure the inspired and expired volumes of gases and a system that delivers the gas mixture. If the tracer gas is nitrogen, the gas delivered during wash-out is oxygen, though mixtures of oxygen and argon gas can also be used. An example setup of equipment for MBW testing is shown in Figure 1-19.

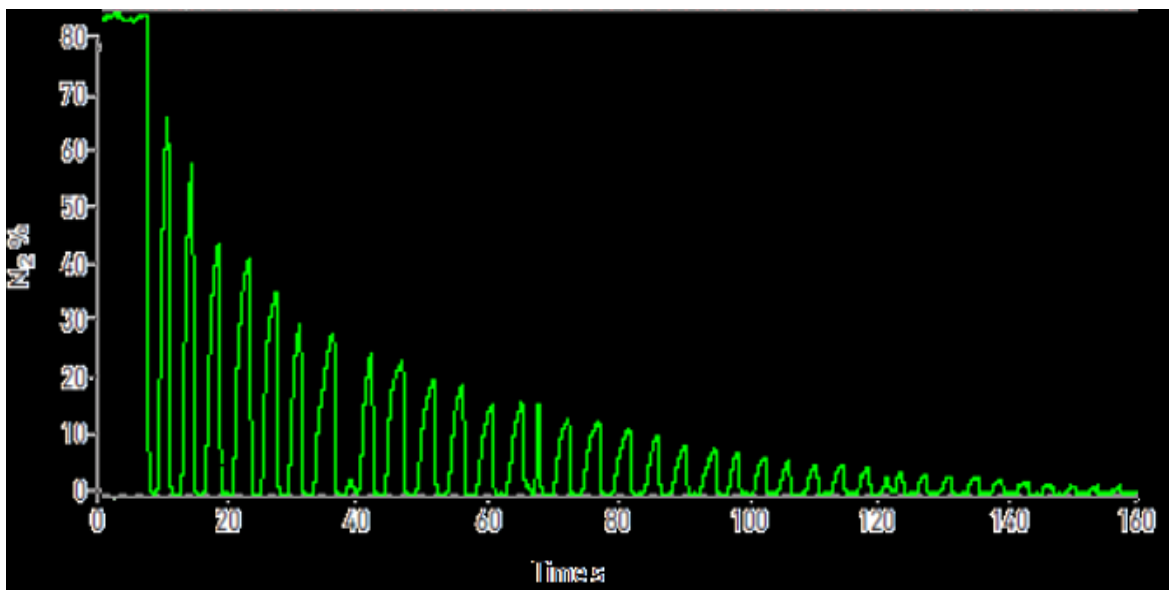


Figure 1-18: Shows the wash-out tracing curve of a 14-year-old female child with AT (participant 4), who twice underwent LCI. The second trial was selected, and an exam's duration was 158.1 sec, which involved 49 breaths. The EE_N₂'s value before administering pure O₂ was 78.05. The Y-axis represents the scale of N₂ concentration and X-axis represents the time. With each successive breath, the nitrogen concentration decreases, as it is "washed out".

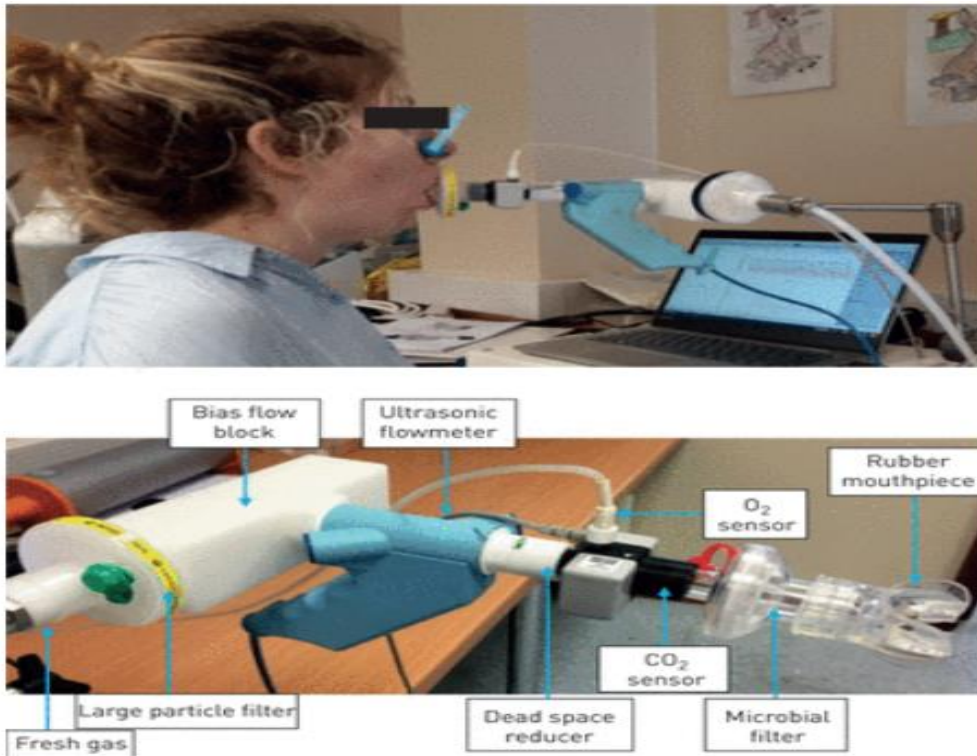


Figure 1-19: The figure shows the device set up for the patient. This equipment is the Exhalyzer D. This figure illustrates the components of the LCI system (Nuttall et al., 2019).

As described above, many respiratory diseases share the common pathophysiology of limited or obstructed airflow. Airway diseases cause constriction of air passages due to multiple factors such as inflammation, clogged mucus, and structural damage in the walls of the airways that might tend to collapse (malacic airways). Due to these factors, affected people experience uneven ventilation, which is termed heterogeneity of alveolar ventilation. This ventilation heterogeneity affects the overall gas mixing efficiency of the lungs. This trait can be used to measure the variation in wash-out of a tracer gas during tidal breathing. A LCI is calculated from an MBW, and it increases with increased heterogeneity of alveolar ventilation.

LCI is calculated once the wash-out process is completed. In a MBW test, the tracer gas is washed until there is almost no tracer gas remaining in the lungs, whilst measuring the volume of gas, which is inhaled and exhaled on a breath-to-breath basis. By convention, the wash-out is considered complete when end-tidal tracer gas concentration becomes less than 1/40th of the initial concentration (Robinson, 2013). LCI is basically the number of lung turnovers that are required to reduce inert gas concentration to 1/40th of the initial concentration.

To calculate LCI, the functional residual capacity and cumulative expired volume (CEV) is required (see Equation 1). To calculate functional residual capacity, the initial and final end-tidal fractions of tracer gas are used and are denoted by C_{init} and C_{end} respectively (see Equation 2). We divide the difference of the two values and divide total volume of the exhaled tracer gas by this difference.

$$FRC = \frac{V_{tracer}}{C_{init} - C_{end}} \quad (1)$$

Equation 1: Shows how the functional residual capacity (FRC) is calculated. V_{tracer} is the total volume of tracer gas exhaled, C_{init} is the initial tracer fraction and C_{end} is the ending tracer fraction.

$$LCI = \frac{CEV}{FRC} \quad (2)$$

Equation 2: Demonstrates how LCI is calculated. CEV is the cumulative expired volume and FRC is functional residual capacity.

LCI is somewhat easy to calculate and understand. Therefore, this calculated value is used for medical or clinical requirements. For children where spirometry may be normal, or difficult to undertake, it is considered by some workers to be the preferred outcome parameter of ventilation inhomogeneity in studies related to CF (Robinson, 2010).

1.4.2.2 Applications of LCI

LCI is capable of early detection of airways diseases in children (Bhatt, 2013). Overall, it is sensitive, appropriate for children and moderately straightforward to perform. Compared to spirometry, LCI is easier for the patient, but harder for the person interpreting the test.

LCI is known for its feasibility in children and is used in an outcome measure in respiratory research, such as in cystic fibrosis. The MBW test for derivation of LCI requires simple relaxed tidal breathing. Therefore, it is easy for children as well as adults. The success rate of the test in the clinical setting is impressively high. Children older than five years rarely face any difficulty during the test, even under unsedated conditions (Stahl et al., 2018). The success rate is between 75% and 100% (Stahl et al., 2018). However, the test seems less feasible for unsedated children younger than

five years, but the success rate for sedated infants ranges between 78.9% and 100% (Stahl et al., 2018).

Although, LCI is an age-independent index for healthy people, it was proved that LCI varied from person-to-person based upon each person's body size (Lum, 2013). It was observed that LCI seemed to be significantly reduced in children younger than six years, though this was not the case for children older than six years (Stahl et al., 2018).

Therefore, it is necessary use an appropriate reference equation to monitor LCI reference values throughout the childhood of an individual who might be suffering from respiratory health conditions (Fretzayas et al., 2019). Patients with AT have a neurodegenerative condition which affects control of breathing, and which might affect their regular breathing (tidal volume). Therefore, it is likely that there need to be normal ranges for specific conditions, such as AT.

Nowadays, LCI has become increasingly popular. It is used in extensively in research, and also has been adopted in medical practice. A combination of well-developed modern analyser technology and data analysis software, along with generally increasing interests in development of lung function techniques for infants, have been seen as the major factors in the further development of the concept of LCI and its associated test technique.

This is vital, as this helps doctors in the optimisation of management of patients suffering from lung diseases, such as CF. Moreover, it involves simple, relaxed breathing. The subject needs to perform quiet breathing

through a facemask or mouthpiece depending upon his age. Since, it is not too difficult, this test is most suitable for children. A number of studies have been carried out.

1.4.2.3 Previous Clinical Work with LCI

A comprehensive systematic review of every study undertaking LCI in children is outside the scope of this thesis. However, in this section key references will be summarised to provide context for later chapters on the usefulness of LCI in a variety of settings.

In 2003, a Swedish group described the use of a mass spectrometer to perform washouts using 4% SF₆ as the inert tracer gas. They reported that compared to 28 healthy controls, LCI was elevated in 43 children with CF, aged 3–18 years (Gustafsson et al., 2003). LCI has been studied most in the field of CF.

Recently, research has explored the use of LCI with Non-CF Bronchiectasis (NCFB). It aimed to identify the clinical utility of LCI in NCFB and assess MBW parameters for the purpose of distinguishing between the increases in LCI due to specific ventilation inequality and increased respiratory dead space.

According to Gonem et al. (2014), LCI is repeatable, discriminatory and is associated with spirometric airflow obstruction in patients with NCFB. LCI vent and LCI ds are a practical and repeatable alternative to phase III slope analysis. The latter is an advanced method for the study of ventilation

distribution in the lung, where each expiratory N₂ trace registered during the multi-breath N₂ wash-out is analysed. The analysis may allow a further level of mechanistic information to be extracted from the MBW test of patients with severe ventilation heterogeneity.

Horsley (2009) found that non-bronchodilator responsive residual airways disease was not detected by spirometry, but the LCI was able to identify it. LCI is also thought to act as an alternative method for assessing airway physiology among the population (Horsley, 2009).

Studies have been carried out to discover the usefulness and importance of LCI. Its clinical purposes have been studied thoroughly. Table 1-4 summarises important studies and research regarding LCI.

Chapter 1

Table 1-4: Selected LCI studies to illustrate its use in several pulmonary diseases.

Clinical condition	Aim	Result
Asthma	The study aim was to evaluate the impact of salbutamol on the LCI in asthmatic children and compare LCI results between asthmatic children and controls.	In the study, 32 asthmatic children (ages 4.7 to 17.4 years) and 42 control children (ages 5.3 to 20.8 years). Patients and controls differed in mean LCI, (patient mean= 6.48 (SD is 0.48); control mean =6.21 (SD is 0.38) (P=0.008). In the asthmatic group, LCI is not significantly affected by using salbutamol. Both stable asthmatic and healthy individuals having a normal range of LCI. In asthmatics, however, the LCI value is significantly increased, suggesting that in asthmatic patients, MBW may be important to assess small airway disorders (Zwitzerloot et al., 2014).
Asthma	The study aimed to investigate the presence of ventilation heterogeneity in asthmatic children using MBW, with assessing LCI and asthma disease severity.	Increased ventilation heterogeneity is present in some children with asthma. Spirometry is not sensitive enough to detect small airway involvement in asthma. LCI is abnormal in a significant subgroup of children with severe asthma, but rarely in children with mild-moderate asthma. The data suggests that LCI monitoring should be considered in children with severe asthma. (Nuttall et al., 2021).
Non-cystic fibrosis bronchiectasis	The aim of this study was to determine the LCI's clinical utility in NCFB.	NCFB patients had LCI values that were significantly higher than those of healthy controls were (9.99 versus 7.28; p<0.01). Repeatability of LCI was observed with a significant correlation between LCI and spirometry airflow measurements in obstruction diseases (Gonem, 2014).
Cystic fibrosis	The study aimed to compare sensitivity, repeatability, and test time of the LCI 1/10, 1/20 and 1/30, to 1/40.	In this study, repeatability of the coefficient of variation (CV%) in all concentrations was not significantly different to controls. Sensitivity of LCI 1/40, LCI1/30 and LCI1/20 to presence of CF equal (67%). Sensitivity of LCI 1/ 10 and FEV ₁ % pred. lower (53% and 47%). Test duration of LCI 1/30, 1/20 and 1/10 significantly shorter than 1/40. LCI1/20 shorter and may make research and clinical measurements more feasible (Hannon et al., 2014).
Cystic fibrosis	The purpose of this study was to detect lung disease and to evaluate the relationship between LCI and per cent of ventilation defect.	Significant differences were observed between the CF and healthy groups for LCI (P = 0.004) and VDP (P = 0.011). A significant and strong correlation was observed between VDP and LCI for all subjects (coefficient of multiple correlation, R ² = 0.88, P < 0.0001). For all participants, there was a weak correlation between FEV ₁ and both VDP (R ² = 0.31, P = 0.03) and LCI (R ² = 0.48, P = 0.004) (Kanhare et al., 2017).
Primary ciliary dyskinesia (PCD)	The primary objective of this study was to assess the association of LCI and pulmonary exacerbation within the context of long-term global variability of LCI.	LCI increases during pulmonary exacerbation and LCI decrease indicates potential recovery after pulmonary exacerbation. Therefore, LCI could serve as an adjunct to clinical and spirometric assessment of individuals with PCD (Singer et al., 2021).
Spinal muscular atrophy (SMA)	To describe RF in childhood SMA and assess differences between those using and not using non-invasive ventilation (NIV).	NIV is common in SMA. Normal respiratory function does not exclude sleep disordered breathing. Children with more abnormal FVC and LCI should be considered at risk of starting NIV during/following a lower respiratory tract infection (Kapur et al., 2019).

1.4.2.4 Advantages of LCI

Spirometry is considered insensitive for detecting small airway diseases. The small airways (i.e., those with a diameter of less than 2 mm) have greater surface area to volume ratio; hence, the flow rate through these passages is low. As the resistance through the airways is low, spirometry is not well suited to assessing small airway dysfunction (McNulty & Usmani, 2014). LCI serves as a suitable alternative (Nuttall et al., 2019). LCI also comes in use in place of FEV_1 , which is considered insensitive to disturbances in ventilation distribution (McNulty & Usmani, 2014). In simple words, LCI fills an important gap by being able to track airway diseases non-invasively. Moreover, single breath wash-out tests are feasible and a reproducible method for evaluating small airway disease. However, on the other hand, LCI is known for its good reproducibility (Nuttall et al., 2019).

Another advantage of using LCI is that unlike spirometry, LCI is independent of height and gender. Since it is derived using FRC, differences due to physical size are already considered. This trait of LCI is useful for longitudinal studies. As spirometry varies with height, age, and gender, FEV_1 is usually expressed as percentage or Z score, but this is not completely satisfactory, as there are wide ranges of FEV_1 values that are considered "normal". Therefore, the absolute values of FEV_1 and FVC increase over time as a child grows (Quanjer et al., 2010). In contrast, LCI is intuitive to use, as it remains independent of the age and height of the

patient (Hatziagorou et al., 2015); therefore, abnormal results are easy to identify.

1.4.2.5 Disadvantages of LCI

LCI is more time consuming to conduct than spirometry. It is even more time consuming when an exogenous gas is used, as this process requires both wash-in and wash-out phase to be conducted (Horsley et al., 2020). For children with mild symptoms, it takes around 5 minutes. However, as the test is repeated thrice, the complete process requires around 30 minutes, as there is a rest phase between each measurement. As far as adults are concerned, this time span is even greater, as their lungs generally have increased heterogeneity of alveolar ventilation. Every phase of MBW takes approximately twice as much time as it takes in children. The test requires a specific mouthpiece or facemask, which adds to the cost of test. Also, the patients undergoing the test require good mouthpiece seal, which is quite difficult to sustain for a prolonged time.

As already discussed about the sensitivity of LCI, it is also pertinent to note that its improved sensitivity makes it much less informative and more protracted in those with significant airflow obstruction. In people with mild CF the reduced information may not be significant, but in those showing severe symptoms of CF, they may be at a great risk. This can lead to an increase in the heterogeneity between good and poorly ventilated units, hence making things adverse. In this context, spirometry may be

considered the better option. If the symptoms of CF seem to be severe, spirometry is preferred to LCI.

The LCI equipment is complex and has multiple components. This device has sensors (gas-composition, flow, and pressure) located at various sites, depending upon the manufacturer. When the sensors are placed directly in the flow of inhaled and exhaled gas, the sensors are termed mainstream. Typically, these sensors are in a hand-held unit, into which the patient breathes. When gas is aspirated out of the device and analysed by the machine that is around a metre away (for example), the setup is termed a side-stream sensor. Some devices have a mix of both. For example, in the Exhalyzer D, the carbon dioxide is a mainstream sensor, but oxygen is a side-stream sensor. The importance of this is that side-stream sensors have a time lag; therefore, there needs to be calibration of the device signals. The flow rate gas (approximately 9 ml/s) is moved via a sampling tube from the location of mainstream sensor to the side-stream sensor; the transport delay between two locations is about 1s.

For the present study, the ndd EasyOne Pro Lab was used, which uses side-stream sensors. This device was selected for this study because it is able to conduct both spirometry and LCI. Moreover, it is portable, which allowed for its routine transport to the MRI facility.

1.5 Ataxia Telangiectasia (AT)

1.5.1 Introduction and History

AT is an autosomal recessive neurodegenerative disorder. The disease is characterised by cerebellar atrophy (leading to ataxia), immunodeficiency, radiosensitivity and the development of malignancies, especially of the lymphoreticular system (Raslan et al., 2021). It is a rare disorder with a prevalence as low as 1:100 000, but it is more common in some populations, due to the frequency of the underlying gene mutation (Amirifar et al., 2019). As an autosomal recessive cause of ataxia, it is second only to Friedreich's ataxia in frequency and is actually more frequent in children, revealing its symptoms within the first few years of their life.

The cerebellar disease progression means that people with AT are usually wheelchair users by their mid-teens, and the survival rate of AT patients beyond the age of 20 is only 50% (Raslan et al., 2021). The earliest patient reported to have AT dates back to 1926. A clear description of a patient with this disease was provided later in 1958, after which it was named 'ataxia telangiectasia' for cerebellar ataxia and conjunctival telangiectasia. Louis-Bar syndrome is a common alternate name for it (Teive et al., 2015). Later in 1995, the responsible gene was successfully identified and sequenced; it was named ataxia telangiectasia mutated or ATM (Savitsky et al., 1995 and Rothblum et al., 2016). This revealed that the ATM gene has a vital role in DNA repair. Since then, the research has concentrated on understanding the mechanism through which the gene product works (Choy & Watters, 2018).

1.5.2 Pathophysiology

The ATM gene codes for the ATM serine/ threonine kinase, which is in the super-family of phosphatidylinositol 3-kinase like protein kinases (PIKK). ATM is one of several proteins that are responsible for DNA repair. (Bryan et.al, 2018). It is a 350-kDa protein and has three functional domains, which are critical to the phosphorylation of substrates responsible for repairing DNA double strand breaks (Bryan et.al, 2018). The process of continuous replication damages DNA, which in turn can cause damage to tumour suppressor genes. When ATM is mutated, it results inefficient repair of double stranded DNA breaks (Ambrose and Gatti, 2013).

ATM also impacts the tumour suppressor genes, p53, ChK2 and DNA repair kinases. ATM inhibits the cells from reaching S and M1 phases of the cell cycle. This prevents the replication of damaged DNA, and it simultaneously activates kinases which rectify damage to the DNA (Ge & Blow, 2010). The cells are pushed to apoptosis whenever the DNA cannot be repaired.

However, when ATM is absent, a cell with damaged DNA is driven towards malignant transformation. The inability to repair DNA damage in AT causes the patient to become radiosensitive, increasing their risk of developing malignancies, compounded by severe immune deficiency (Taylor et al., 2019). Neurodegeneration is associated with oxidative stress. ATM protects against damage from reactive oxygen species (Taylor et al., 2019), so when ATM is absent or mutated, high levels of oxidative damage occur, as seen

in ATM mice and AT patients (Kamsler et al., 2001). The neurodegenerative process is linked to two anti-oxidation processes, which are adversely affected by ATM deficiency (Taylor et al., 2019). Most studies have only focused on the pathology of neurons. However, the lack of ATM is also shown to affect the functioning of astrocyte morphology, which further adds to the possibility of inducing toxicity in neurons (Taylor et al., 2019).

Newer evidence also suggests that ATM plays a significant role in the intrauterine stage of neurogenesis and cell migration. Ectopic Purkinje cells found in the brains of ATM mice results in the cerebellum developing abnormally. Mild microcephaly is common amongst patients with AT, especially in children, and it is a further indicator of abnormal neurodevelopment (Nissenkorn et al., 2011). Therefore, AT is often perceived as primarily a neurodevelopmental disorder. ATM also has roles in synaptic vesicle transmission (Li et al., 2009) and pathway regulation of mTOR. It also contributes to development of insulin resistance, hence has a causal relationship to metabolic syndrome (Lie et al., 2009).

1.5.3 Neurologic Disorders

Neurodegeneration in AT patients is revealed through dysarthria, dysmetria, extrapyramidal movements and oculomotor apraxia. Even though the symptoms are progressive, the effect can vary from person to person. Ataxia is present in 87%–100% of AT patients and in all individuals with the classic phenotype. The onset symptoms of ataxia start at the age

of 1 year and usually appear by 5 years of age (Nissenkorn et al., 2011). Often, the children who reveal symptoms of AT later than this also present with chorea or myoclonus. These symptoms are usually evidenced through unstable walking (Nissenkorn et al., 2011). Twenty per cent of children with AT start walking at 4 years of age. Children with AT walk on their toes, and instead of having a wide gait base, they continue to walk on a narrow base. However, they become more stable while running, so the children prefer to run instead.

Dysarthria is a common symptom too, and it often presents along with the cerebellar symptom in AT patients. Often when dysarthria appears, the child is in nursery and begins to have unclear speech, with words that are jumbled and short sentences, or the child refrains from engaging in conversation.

Eye movement especially oculomotor apraxia is one of the main symptoms of AT in patients (Federighi et al., 2017). Severe eye movement abnormalities are found in 80% of patients and they generally appear after 5 years of age (Nissenkorn et al., 2011). The symptoms are initially intermittent, but with age, they become constant and eventually lead to ophthalmoplegia. AT patients are also observed to have upward gaze limitation and an inability to fix their gaze (Nissenkorn et al., 2011).

The cerebellar abnormalities also have an effect on cognition, which is linked with attention, language, recognition, and even memory (Federighi

et al., 2017). Patients with AT show a gradual decline in cognition; although initially it is very mild, it starts to become evident at the age of 10 years. The involvement of cognition in AT has not yet been studied deeply; however, below average intelligence was identified in one of the studies (McFarlin et al., 1972). Patients were reported to have speech impairment, and experience difficulty with solving problems, which is associated with cognition. Cognitive decline is rather slow, and as such non-progressive. Meanwhile progressive decline of limbs in the form of dysmetria, bradykinesia and other medical conditions, affect the graphomotor abilities; with age, the child loses their ability to write and read. AT patients have special needs and require special schooling due to these motor disabilities.

1.5.4 Malignancy

ATM is of essential importance in cell cycle checkpoint signalling, as most of its substrates are genes that inhibit tumour suppressor genes, such as BRCA1 (Cremona and Behrens, 2014). ATM dysfunction is one of the key pathophysiological mechanisms in many tumours (Taylor et al., 2019). Because of abnormal ATM function, malignancy affects approximately 30% of patients with AT and is an important cause of death (Suarez et al., 2015). The following malignant diseases are the most common in patients with AT: acute T-cell lymphoid leukaemia, haematopoietic lymphoid and non-Hodgkin lymphomas (B- cell), acute myeloid leukaemia and Hodgkin lymphoma (Suarez et al., 2015). Radiosensitivity makes the treatment of

these tumours more complicated; therefore, radiotherapy dosages need to be reduced, and chemotherapy protocols should be employed to reduce toxicity and maintain efficacy (Sandlund et al., 2014). Solid tumours, such as breast cancer, gastric adenocarcinoma, melanoma and ovarian tumour are more common in adults and older children with AT (Suarez et al., 2015). Nervous system cancers are generally not characteristic of AT.

1.5.5 Immune Deficiency, Recurrent Infections, and pulmonary disease

Recurrent sinopulmonary infection and immune deficiency are key symptoms of patients with AT. This is in part due to ATM's function in combining non-homologous ends and recombination of V(D)J domains essential to immune response diversity (Amirifar et al., 2019). Low immunoglobulin levels, in particular the immunoglobulins A, E and G2, are common in these patients and the antibody response to vaccination with pneumococcal polysaccharide is very low (Staples et al., 2008). About a third of AT subjects suffer from a defect in the immune system, specifically in the cellular arm, with moderate lymphopenia, and a reduced number of CD4 cells (Schubert et al., 2005). Immunoglobulin replacement therapy decreases the likelihood of recurrent infections (Condino-Neto et al., 2014). However, pulmonary diseases remain common and are a major cause of mortality (McGrath-Morrow et al., 2014). The inability to cough properly and aspiration, together with immune deficiency cause recurrent infections,

which ultimately lead to bronchiectasis (McGrath-Morrow et al., 2014). Furthermore, those patients are more prone to interstitial pulmonary disease (McGrath-Morrow et al., 2010).

Patients with AT may need to undergo radiological imaging investigation, especially lung imaging, as chronic pulmonary infections and other lung pathologies are common. However, there is a unique problem associated with imaging in this condition. As described above, the cells of AT patients after exposure to ionising radiation, show marked a reduction in cell division and replication, and this change occurs at all phases in the cell cycle in AT lymphoblastoid cells (Beamish and Lavin, 1994). These result in an increased sensitivity to ionising radiation and elevated risk of developing malignancies as a consequence of the irregularities in cell division. Hence, using ionising radiation in patients with AT is contraindicated. There exists a strong need for imaging techniques that do not use ionising radiation, but which have high precision in diagnosing lung pathology. MRI could be a safer alternative for these patients.

1.6 Magnetic Resonance Imaging (MRI)

As the name implies, MRI uses the technique of magnetic resonance to image the human anatomy. Standard MRI depends on detecting proton signals in the human body. The design of an MRI machine is relatively straightforward, in principle. The major components are briefly described here. The strength of the main magnet is measured in Tesla units. Different

type of coils can be used depending on the organ to be imaged, in addition to the shim coils located in the MRI machine which are used for adjusting the homogeneity of the magnetic field. Three gradients are used: slice selection, phase encoding gradient and frequency encoding gradient; these are perpendicular to each other inside the MRI machine in three different axes (x,y,z), through which different type of images are obtained. A radiofrequency (RF) system excites the sample and also detects the nuclear magnetic resonance (NMR) signal, which is produced by the RF system. All these systems are controlled and coordinated by one or more computers in the control panel (Westbrook and Roth, 2011).

The origin of the signal in MR is used to generate all clinical images originating from hydrogen nuclei, which consists of one proton that has a single positive charge. The proton spins continually, and so the positive electrical charge also spins. This causes the generation of a current, which generates a magnetic field. Protons generate their own magnetic field, so they act like small bar magnets. When an external magnetic field (B_0) is applied over these protons, the protons are aligned in one of two ways - either they are parallel to the field applied, or they are against the applied external field (Currie et al., 2013). The parallel to B_0 alignment is preferred, as this alignment has the lowest energy requirement. When the field is applied to protons, the process is called precession. The speed of precession is the number of times a proton precesses in a second. In this process, when a patient moves within the coils, it becomes a magnet whose

magnetic field is in the same direction as of B_0 . This magnetisation in the patient is known as longitudinal magnetisation. This magnetisation in the patient develops shifts of RF pulses.

These pulses switch between on and off to create disturbance in proton alignment to generate resonance. This resonance develops only when RF pulses are generating through the same frequency as the frequency of precession protons. This generates two effects: it shifts protons to a higher energy state and secondly, it enables protons to remain in phase. The term 'in phase' means the protons are in same direction at the same time instead of being in random directions. The moving magnetic field is known as the transverse magnetisation vector; if a conductive receiver coil is located in the vicinity, then an alternating voltage is generated around it. This causes the formation of an electrical current, which is detected by an antenna and produces signals of MR. When the RF pulses are turned off, the electrons move out of the phase and fall back to a lower energy state; this is known as the relaxation phase. These relaxations are occurring in two different ways, either longitudinal magnetisation or transverse magnetisation. The relaxation, in which the disappearance of transverse magnetisation, occurs is called transverse relaxation, while the one in which longitudinal magnetisation disappearance occurs is called longitudinal relaxation. Transverse relaxation is also known as T2 relaxation, while longitudinal relaxation is also known as T1 relaxation (Currie et al., 2013).

The T1-weighted imaging is most commonly helpful in obtaining morphological information and in post-contrast imaging. It is most widely employed in imaging subacute haemorrhage, independent fatty tissue, the cerebral cortex and focal liver lesions. T2-weighted imaging is helpful in detecting water content in conditions such as oedema, inflammation and in visualising organs and zonal anatomy (Westbrook and Roth, 2011). In T2 images, water is white, and fat is darker (see Figure 1-20).

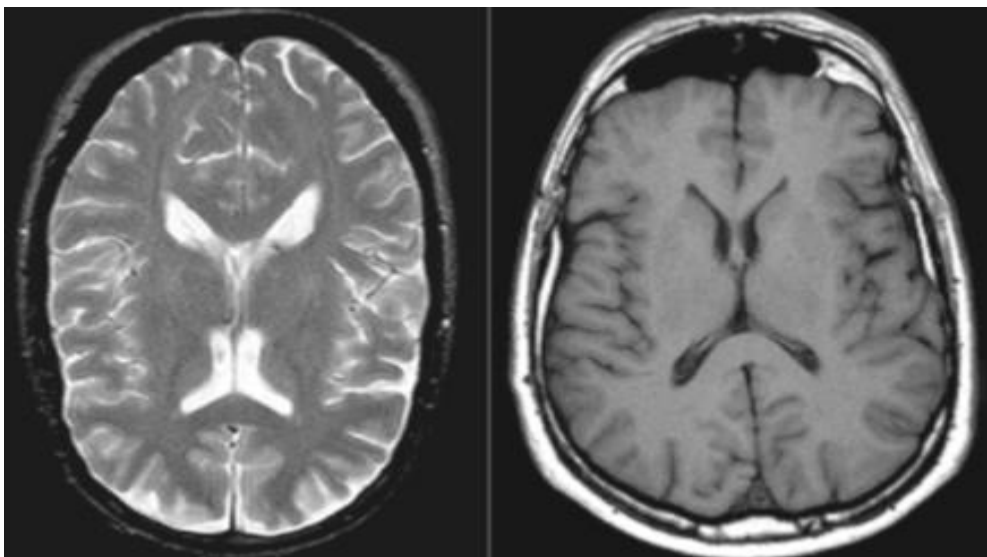


Figure 1-20: Shows T1 (on the right) and T2 weighted (on the left) MRI of the brain (Westbrook and Roth, 2011).

Unlike nuclear medicine and CT scanning which uses ionising radiation, MRI should provide a safer alternative for AT patients, as it does not involve the use of ionising radiation. Therefore, MRI can potentially play a crucial role if it provides high-resolution imaging of the lung. However, the quality of images produced by MR imaging technique depends on the hydrogen proton signal and because the lungs have low proton density, conventional

proton-based imaging results in a very poor MRI signal and ultimately poor quality of images.

This weakness together with the potential risk of radiation has inspired research in this area and has led to improvements in MR imaging. I briefly discuss the possibility of imaging the lung with magnetic resonance using three techniques that can deliver higher resolution lung images. These techniques are hyperpolarised noble gas MR imaging using xenon 129 (^{129}Xe), molecular oxygen-enhanced MR imaging (OE-MRI) and ultra-short echo-time MR imaging (UTE-MRI).

1.6.1 Hyperpolarised Noble Gas MR Imaging using Xenon 129 (^{129}Xe)

Hyperpolarised noble gas MR imaging is a relatively novel technology that has been used for around 20 years. It is used to produce lung images and provide anatomical and physiological information using MRI (Salerno et al., 2001). ^{129}Xe and helium 3 (^3He) are employed in this technique belong to the group of noble inert gases. They are administered to the patient through the inhalational route during the MRI scan. Although this method has proven to be useful in providing quality lung images, there are many challenges in using these approaches. Although ^3He yields high signals in the MRI due to strong magnetic moment, it is not available in abundance. It is both expensive and difficult to obtain. Furthermore, recently, its sale has been banned for security reasons (Driehuys et al., 2009). These

obstacles have made the usage of ^3He in hyperpolarised imaging techniques more troublesome and have resulted in the need to find an appropriate alternative.

^{129}Xe is increasingly being used as a successful replacement for ^3He in hyperpolarising noble gas imaging techniques. The signal-to-noise ratio is worse for ^{129}Xe than ^3He , and ^3He provides a stronger MR signal, due to its larger nuclear magnetic moment. However, ^{129}Xe is potentially a better alternative due to various other reasons. Levels of polarisation depend on the type of polariser that is used. Historically, polarisation levels of ^{129}Xe have been around 10% while for a similar quantity of ^3He they are greater than 30%, making ^3He superior. But the evolution of polarising systems has made it possible to produce larger quantities of more polarised ^{129}Xe (Hersman et al., 2008), which can enhance the quality of the images. Also, ^{129}Xe is cheaper and is readily available in the Earth's atmosphere (Mugler and Atles, 2013).

Unlike ^3He , ^{129}Xe is particularly attractive for finding specific lung function characteristics, such as gas exchange and uptake/ventilation parameters. It can be used to measure ventilation/perfusion matching by assessing the diffusion and gas exchange by measuring the signal from tissue and the bloodstream (Driehuys et al., 2009). Once inhaled, ^{129}Xe will readily dissolve into the blood and reach all tissues of the lung parenchyma with the residual undissolved ^{129}Xe remaining in the airspace.

Multiple MRI spectral peaks will be produced, and each one is associated with a different compartment. The single large peak produced after inhalation is due to the residual ^{129}Xe in the lung airspaces, while around 1%-2% is dissolved in the lung parenchyma and blood and resulting in smaller gas peaks (Ruppert et al., 2000; Sakai et al., 1996). These smaller peaks play a pivotal role in ^{129}Xe technique, as they allow ventilation, tissue uptake and gas transfer into blood to be measured separately (Mugler et al., 2010). The variation between residual and dissolved peaks of the ^{129}Xe in the lung arising in this dynamic equilibrium process provides potentially important information about lung function (Sun et al., 2011).

Recent studies have demonstrated that both ^3He and ^{129}Xe imaging are safe to use in paediatric and adult populations and can help evaluate the lung function in pulmonary diseases that affect children such as CF (Ebner et al., 2017), as well as adult conditions such as COPD. While ventilation images with hyperpolarised ^3He remain the gold standard (Kirby et al., 2013), significant improvements in hyperpolarised ^{129}Xe makes it a strong competitor in MR ventilation imaging (Mugler and Atles, 2013). There are studies supporting this, which show that hyperpolarised ^{129}Xe can provide acceptable resolution for functional lung imaging and alveolar airspace structure comparable to hyperpolarised ^3He (Mugler and Atles, 2013) (See figure 1-21). All these factors mean that currently ^{129}Xe is a better option than ^3He for hyperpolarised noble gas MR imaging.

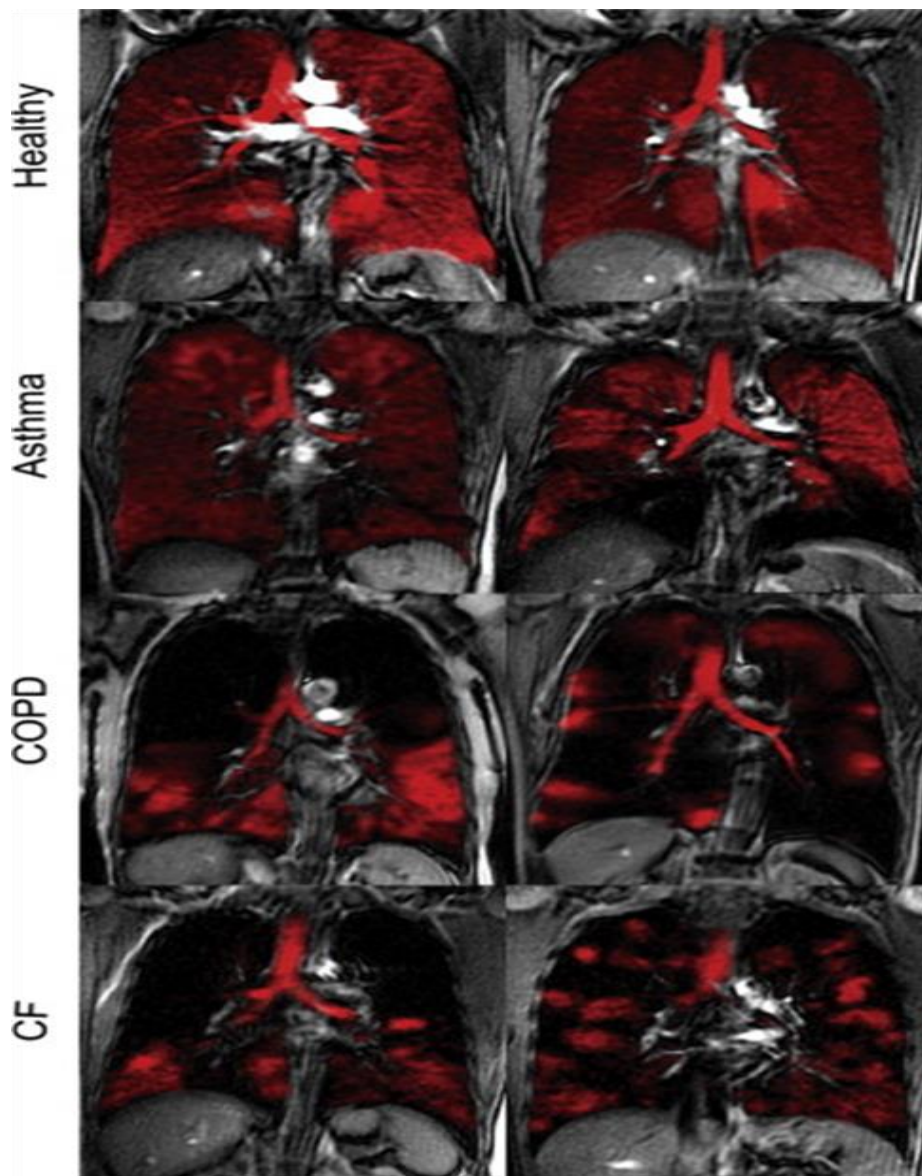


Figure 1-21: Hp ^{129}Xe slice selective coronal MR images (in red) overlaid onto corresponding proton thoracic images from healthy volunteers and subjects with asthma, chronic obstructive pulmonary disease (COPD), cystic fibrosis (CF) (Lilburn et al., 2013).

One disadvantage of the hyperpolarised lung imaging technique is the dependency of this imaging modality on a laser-based polarisation device combined with MR techniques. The essential requirement in a hyperpolarised noble gas MRI is the presence of polarised ^{129}Xe or ^3He , and to generate this polarised inert gas, a laser-based polarisation device is

essential. According to Kern and Vogel-Claussen (2018) this can be achieved by using a method called optical pumping and spin exchange. This process uses laser photons to flip the electron spin in rubidium atoms by absorbing spins from laser photons in order to polarise its outer orbital electron.

After the nuclei of ^{129}Xe collides with rubidium, spin exchange occurs, which transfers the polarisation from the outer orbital electrons of rubidium to the nuclear spin of the noble gas atom (Kern and Vogel-Claussen, 2018). Therefore, compared with a conventional proton MRI, several additional items of hardware are necessary to perform hyperpolarised noble gas MR imaging (Mugler and Atles, 2013).

An additional disadvantage of hyperpolarised noble gas MRI requires the patient or research participant to inhale and hold their breath on command. This therefore makes this challenging for children with a neurological disease such as AT.

1.6.2 Molecular Oxygen-Enhanced (OE) MR Ventilation Imaging

Molecular oxygen-enhanced MR ventilation imaging (OE-MRI) is potentially an effective method of lung imaging and is a readily available solution to depict the lung. The potential to image the process of ventilation with the application of this MRI techniques has significant value in diagnosing and evaluating numerous pulmonary disease states, including but not limited to

pulmonary embolism, emphysema, lung cancer and diffuse pulmonary disease.

This method depends on molecular oxygen and does not require administration of any agents other than oxygen. It avoids the need to generate hyperpolarised noble gases and the attendant risks of hypoxia associated with having to inhale a relatively large volume of inert gas.

1.6.2.1 Physiology of the Lung with reference to oxygen transfer and OE-MRI

In order to understand OE-MRI, a brief discussion of pulmonary physiology is required. The fundamental processes that result in exchange of gas, or the absorption of O₂ and the expulsion of CO₂, are typically divided into four functional subdivisions. The first process is ventilation, which is the movement of air from outside into the body, and the distribution of air within the tracheobronchial system to units of exchanging lung gas. The second process is diffusion, where the transport of gas occurs through the alveolar-capillary membranes from the blood to the gas in the alveoli or vice versa. The third process is perfusion, which is the transmission of mixed venous blood from the heart via the pulmonary artery and, its distribution to units of exchanging gas and capillaries, and its return of this blood from the lungs to the heart through the pulmonary veins. The fourth process is breathing control, which is ventilation control; normally it is modulated in line with changing metabolic requirements.

Among pulmonary disorders, the key cause of hypoxia in many respiratory disorders are changes in V/Q ratios and the deficient diffusion of O₂ from the alveoli into the capillaries. This means that a wide range of pathophysiological conditions may affect the respiration process. Alveolar ventilation supplies oxygen to the alveoli and is expelled by blood circulation. Likewise, CO₂ in mixed venous blood moves into the alveoli through diffusion from the capillaries and is then expelled from the alveoli by ventilation. Therefore, the relationship between perfusion and alveolar ventilation determines the alveolar PO₂ and PCO₂. Changes in the ventilation-perfusion ratio can lead to changes in the alveolar PCO₂ and PO₂, and in the gas supply to or from the lungs (Powers and Dhamoon, 2020). Alveolar ventilation in adults is usually 4–6 l/min, and pulmonary blood flow has the same range; therefore, the ventilation ratio is between 0.8 and 1.2 for the entire lungs (Powers and Dhamoon, 2020). However, V/Q should be matched at the level of the alveolar capillary, and the V/Q ratio for the entire lung is only a rough estimate of all the units of the alveolar capillary in the pulmonary ventilation-perfusion ratio (Powers and Dhamoon, 2020).

Pulmonary diffusion capacity (DL) is the amount of gas transferred through alveolar capillaries. The alveolar-capillary membrane acts as a diffusive barrier in the lungs, separating blood from gas, absorbing O₂ and expelling CO₂. There has not been confirmation of the presence of unique O₂ and CO carrier pathways allowing their transfer through the barrier of tissue (Hsia

et al., 2011). In light of the identical sizes molecular of carbon monoxide and oxygen, the diffusing capacity for carbon monoxide (DLCO) can be replaced with the DL of oxygen. The diffusing capacity of the lungs measures the transfer of gas from the air in the lungs to the red blood cells in lung blood vessels. The diffusing capacity for carbon monoxide measures the conductance or ease by which carbon monoxide molecules move through the alveoli and into the haemoglobin in erythrocytes in the pulmonary circulation. According to the diffusion law, the surface area of the barrier membrane is proportional to the DL and inverse proportional to the membrane thickness (Hsia et al., 2011).

OE-MRI can detect both lack of alveolar ventilation, and also diffusing capacity of oxygen on a regional basis within the lungs, and therefore it is useful a test of overall lung function, rather than as a lung structural modality.

1.6.2.2 Mechanism Underpinning OE-MRI

In OE-MR imaging, the paramagnetic oxygen molecules dissolve in the tissue fluid and plasma within the lung parenchyma, increasing the lung T1 relaxation rate in proportion to the dissolved oxygen concentration and the local oxygen partial pressure (Ohno et al., 2001). The MRI longitudinal relaxation rate is sensitive to changes in the molecular oxygen dissolved in interstitial tissue fluid or plasma (O'Connor et al., 2019). When gas with a

high oxygen concentration is inhaled, excess oxygen is carried in the plasma to tissues with adequate perfusion. Since adequately oxygenated tissue is similar to the saturation of haemoglobin molecules (Pittman et al., 2011), the excess oxygen that is delivered will remain dissolved in blood plasma and interstitial tissue fluid. When subjected to magnetic resonance, these oxygen molecules have an increased R1 value (T1 relaxation rate), thereby producing different images to those of parenchymal cells that are adequately perfused with molecular oxygen.

Although this distinguishes it from healthy it doesn't show structural abnormalities (i.e., bronchiectasis) which is what CT scans show. Therefore, although it provides clinical information it is not a replacement for CT. Rather, OE-MRI gives regional functional information regarding ventilation and diffusion. It is in this context that free breathing OE-MRI could have a place in assessing lung health in AT. This is the motivation for the primary aim of this study, specifically to determine the feasibility of OE-MRI in AT.

1.6.2.3 The Theory behind OE-MRI and its Relationship to the Physiology of the Respiratory System

The MRI signals of blood and other fluids are modulated by oxygen through the exploitation of the paramagnetic property of both the oxygen molecule itself and deoxyhaemoglobin (Buxton, 2013). Due to a compartmentalisation of deoxyhaemoglobin in erythrocytes, protons of

water tissue cannot enter to coordinating sites, which is needed for the longitudinal interactions that cause T1 shortening (Ohno and Hatabu, 2007). Therefore, T2* is shortened by deoxyhaemoglobin in red blood cells with only a slight effect on T1 shortening (Ohno and Hatabu, 2007).

This effect of deoxyhaemoglobin provides a key contrast in blood-oxygen-level-dependent imaging and is widely used to assess tissue oxygenation and regional blood flow (Loued-Khenissi et al., 2019). During the exchange of oxygen between the blood and air in the capillaries in the alveoli, O₂ not only combines with haemoglobin but also readily dissolves into the bloodstream (Molnar and Gair, 2013). Due to the paramagnetic property of O₂, the T1 of pulmonary vein blood is shortened by dissolved molecular oxygen.

Pure oxygen inhalation is visualised as an increase in signal intensity (SI) due to its ability to shorten the T1 relaxation time. Although the time spent breathing pure oxygen is very short, the proportion of oxygen binding to haemoglobin is high enough to cause an effect on T1. This is because the concentration of dissolved oxygen in arterial blood rises much more than the concentration of haemoglobin-bound oxygen. The blood oxygen concentration is dependent on the oxygen partial pressure (PaO₂) in the alveoli. During the breathing of pure oxygen, the concentration of oxygen rises around fivefold (Hsia et al., 2013).

Moreover, PO_2 in normal air is around 100 mm Hg inside the alveoli, but it can be as high as 663 mm after administering 100% oxygen (Cruickshank and Hirschauer, 2004). An increased concentration of oxygen in the blood also prolongs $T2^*$, but since it is less than 10 ms, this only has a small effect on SI (Buxton, 2013). Blood oxygen concentration is dependent on the PaO_2 in the alveoli.

It has been reported that the $T1$ effect during oxygen inhalation reduced $T1$ time in the lungs by about 9% (Ohno and Hatabu, 2007). This can only be calculated by making a clear comparison between atmospheric and pure oxygen because the amount of difference between them is significant. Therefore, OE-MRI may provide accurate information on physiological states such as oxygen supply, oxygen solubility and blood volume.

1.6.2.4 Design of an OE-MRI Ventilation sequence

The lung parenchyma has multiple air interfaces/tissues, which generate very short $T2^*$; therefore, using conventional sequences provides images with very low signal intensity (Ma et al., 2015). However, a sufficient signal from the pulmonary parenchyma and small pulmonary vessels can be obtained with a very short echo time (TE) (Ma et al., 2015). Therefore, to obtain the anatomical and physiological information of the lung parenchyma via oxygen enhancement, a specific OE-MRI sequence must be designed. The following factors should be present in this design.

Firstly, one of the following sequences must be installed in the MRI: half-Fourier single-shot turbo spin-echo (HASTE) or single-shot rapid acquisition with relaxation enhancement (RARE). Secondly, a short TE should be used as often as possible. Thirdly, there should be a centricly reordered phase encoding scheme on the HASTE sequence.

Finally, to minimise motion artefacts or respiratory gating the duration of data acquisition must be shorter than the breathing process. Although a FLASH sequence with a short TE and TR has sometimes been used to generate a T1 map of oxygen enhanced with a short acquisition time (Taylor et al., 2016), more commonly OE-MR sequences are designed using rapid acquisition with relaxation enhancement (RARE) and HASTE single-shot sequences.

Oxygen enhancement is evaluated by using a map of T1 changes, a relative enhancement map or a cross-correlation map (Kindvall et al., 2017). Both single shots of the HASTE and RARE sequences are optimised with a short TE to increase the short T2* signal from the entire lung. In addition, the diffusion and perfusion effects are minimised through the use of short inter-echo space; field inhomogeneities of lung tissue sensitivity can be minimised by combining these sequences with the acquisition window. The signal of pulmonary parenchyma and SNR of the lung are markedly improved when ultra-short TE is adopted for 3s or less (see Figure 1-22).

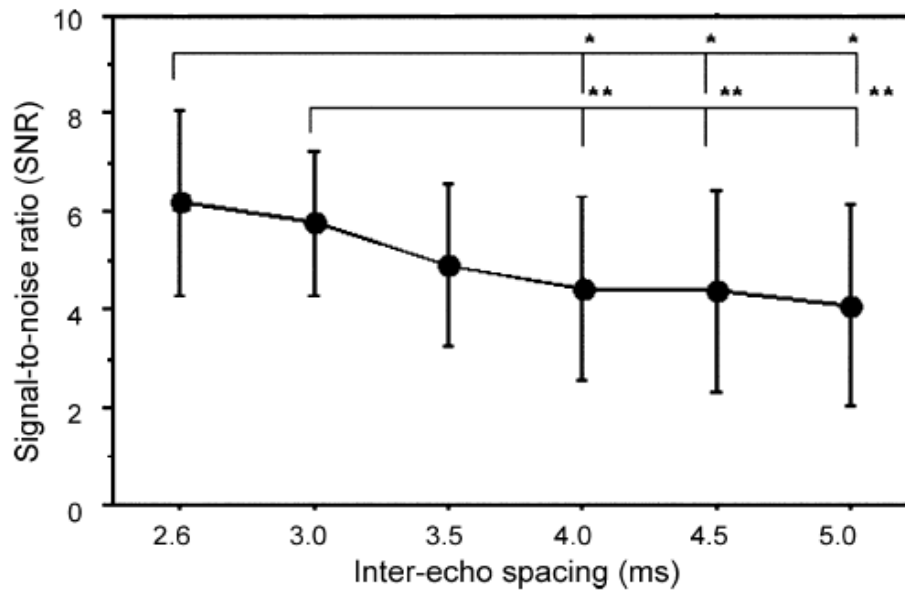


Figure 1-22: The relationship between the SNR and inter-echo spacing. The SNR increases, as the inter-echo spacing decreases. The star (*) denotes significantly ($p < .05$) less than 2.5 ms and the two stars (**) denotes significantly ($p < .05$) less than 3.0 ms (Ohno and Hatabu, 2007).

Maps of spatial frequency in k-space describe all MR images. The lines surrounding the k-space's centre determine the image's contrast, whilst the lines coming out from the centre provide the image's details (Moratal et al., 2008). During the first part of the readout interval, the centre of the k-space is centrally collected by a reordered encoding phase scheme. Tissue with a short T2 and T2* provides the SNR of the source image because of the effectiveness of the short TE compared to images obtained from the reordered encoding phase (Ohno and Hatabu, 2007).

The centrally reordered phase encoding scheme's T2 decay is not smooth, as the phase encoding direction is taken as steps (Ohno and Hatabu, 2007). This technique leads to the overlapping of the smooth decay, thereby causing blurring as well as a ghost artefact, which arises due to a periodic

deviation of the smooth decay. This improvement of both standard deviations also results in the signal intensity of the tissue with a short T2 and T2* (Ohno and Hatabu, 2007).

A study conducted by Ohno et al. (2004) sought to determine the effect of the phase encoding scheme on OE-MRI using an IR-HASTE series reordered centrally and sequentially. The study results are as follows. The contrast-to-noise ratio of the sequentially reordered IR-HASTE image (2.9 ± 0.9) was significantly lower than that of the centrally reordered IR-HASTE image (4.2 ± 0.8) (see Figure 1-23). This improvement is a consequence of the improvements in the standard deviations and signal intensities before and after the OE-MRI images (Ohno and Hatabu, 2007).

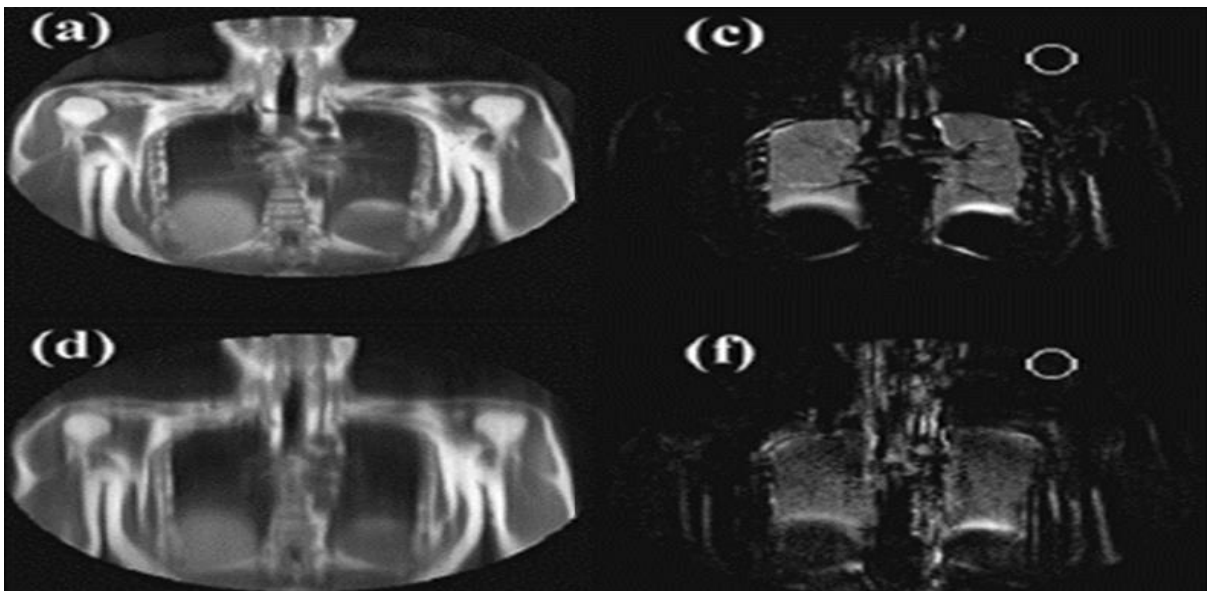


Figure 1-23: Images of a healthy, 36-year-old male volunteer captured using the centrally and sequentially reordered of IR-HASTE sequences. Image A was captured before the inhalation of pure O₂, and image B is an enhanced image taken after the inhalation of pure O₂, captured by the centrally reordered IR-HASTE sequence. D and F represent matching images captured by the sequentially reordered IR-HASTE sequence. The first sequence provides images with a higher oxygen enhancement, and the blurring and ghost artefacts are improved (Ohno and Hatabu, 2007).

Oxygen molecules are used as a T1 contrast agent in the OE-MRI. In Ohno et al.'s study (2004), T1 weighted images were obtained using a sequence of fast spin-echo pulse or an IR single-shot turbo or IR-HASTE sequence without or with synchronisation of respiration or/and ECG, whilst the subject was alternately ventilated with pure oxygen and with normal air. The IR-HASTE sequence with breath-holding and ECG synchronisation has been adapted by a few researchers to minimise mis-registration for cross-correlation analysis (Ohno et al., 2004). Despite the fact that breath holding positively affects OE-MRI parameter maps by reducing spatial mis-registration, it also affects pulmonary physiopathology and the physiology of both normal and abnormal subjects with lung diseases.

Therefore, it is preferable to use the synchronisation technique with the OE-MRI sequence. Moreover, respiratory synchronisation was suggested to be more useful than ECG synchronisation, as it achieves results of ventilation maps in MR ventilation studies that are statistically more relevant. Moreover, the single-shot feature is likely to keep the data collection time shorter than the duration of respiration (Krishnamurthy et al., 2015).

1.6.2.5 Comparison of Oxygen Enhancement and MR Ventilation Imaging Using Hyperpolarised Noble Gas

The use of ^{129}Xe and ^3He as hyperpolarised noble inert gases in MRI is a recently development and a superior approach to functional lung imaging

(Ebner et al., 2017). In this technique, air spaces and airways are visualised by using the gas itself. Many researchers have reported using hyperpolarised ^3He lung imaging in clinical conditions such as emphysema, asthma and CF (Ebner et al., 2017). Additionally, the xenon polarisation transfer contrast (XTC) technique has been employed to evaluate perfusion and pulmonary parenchyma by assessing pulmonary ventilation from gas phase images (Ebner et al., 2017).

This approach only images the ^{129}Xe gas phase, resulting in a significant SNR advantage over imaging dissolved ^{129}Xe (directly). The image contrast is obtained by magnetisation of the dissolved gas phase saturation or selective inversion by using a number of radiofrequency (RF) pulses with a narrow bandwidth. The exchange of xenon atoms between the compartments of the gas- and dissolved-phase between each of the two RF pulses results in an exchange-dependent reduction in magnetisation of the gas phase (Dregely et al., 2012). Hyperpolarised gases, such as ^{129}Xe and ^3He , are different in their molecular weight to oxygen, which is why they might have different gravity effects. ^3He provides high-resolution anatomical pulmonary images, whereas the ability to dissolve into plasma and blood means that ^{129}Xe provides anatomical and physiological images with a good resolution (Ebner et al., 2017). The high cost of these gases and the need for special equipment, such as laser equipment are regarded as the main drawbacks of these imaging modalities.

Conversely, oxygen molecules are a safe, cost-effective, and easily available contrast agent that can be used with a conventional MRI scan. The underlying physiological mechanism of the OE-MRI technique may differ from that of hyperpolarised noble gas, in particular ^3He , because the transmitted oxygen molecules from the alveoli to the capillary bed provide regional information on the transfer of oxygen, ventilation and perfusion (Ohno and Hatabu, 2007).

1.6.2.6 Advantages and Disadvantages of the OE-MRI

MRI has an important role in clinical diagnosis and biomedical research. MRI techniques have gone through rapid development, and they have been used for numerous applications over the past few years. This development has been accompanied by the optimisation and improvement of conventional MRI techniques (Dong et al., 2015). OE-MRI is a safe method of estimating environmental ventilation and the alveolar diffusion of oxygen into lung capillaries.

There are several disadvantages of OE-MRI. Firstly, compared to ^{129}Xe or ^3He , OE-MRI has a relatively low SNR. Secondly, molecular oxygen is used as a contrast agent, but this itself cannot be seen prior to being dissolved in blood or other fluids. Thirdly, oxygen administration may cause changes to lung pathophysiology. Finally, since the respiration process is dependent on the carbon dioxide ratio, excessive administration of pure oxygen may cause hypoxic drive. OE-MRI can be applied in any hospital that has the

necessary analysis software and in which the OE-MRI sequence is available. Thus, this approach has the potential to expand in the clinical practice of pulmonary functional imaging in future (Ohno and Hatabu, 2007).

1.6.2.7 Basic Study of OE-MRI

1.6.2.7.1 Animal Studies

In a pig model, an arterial line was placed in the right femoral artery to monitor gas and blood pressure; the connection between T1 and the concentration of oxygen was examined. Arterial blood gas analyses with T1 measurements were performed for each of following oxygen concentrations: 25%, 50%, 75% and 100%. This study demonstrated a strong relationship between the T1 of lung parenchyma and arterial blood oxygen pressure ($R^2 = 0.99$) (Ohno and Hatabu, 2007).

Since there is a close relationship between the blood oxygen pressure of the arteries and the oxygen pressure of the pulmonary veins, there is also the same relationship for the oxygen pressure in the pulmonary capillary blood. Despite the fact that the linear correlation between PaO_2 and $1/T1$ indicates that the probability of oxygen transfer and regional pulmonary ventilation can be quantitatively measured, further theoretical work and experimentation are needed (Ohno and Hatabu, 2007). In the pig model of airway obstruction, the capability of OE-MRI to detect regional air ventilation defects was examined. In the secondary right bronchus, a 4-Fr catheter was placed and inflated by the balloon to block the airway

supplying the lower right lobe (Ohno and Hatabu, 2007). Although no anatomical abnormality was observed in the lower right lobe using a T1-weighted turbo spin-echo, a deficiency in ventilation to the occluded bronchus was revealed through the use of OE-MRI (Ohno and Hatabu, 2007).

Moreover, a pig model of pulmonary embolism has been tested to assess the capacity of OE-MRI to detect regional defects of V/Q (Ohno and Hatabu, 2007). Perfusion defects were seen in the lower lobe of the left and right lung using contrast-enhanced MR perfusion imaging. However, the OE-MRI sequence for the same animal did not display any defects. The mismatch was caused by a pulmonary embolism between V/Q. Thus, the results of the two studies show the ability of OE-MR imaging to evaluate pulmonary embolisms and obstructive lung diseases.

1.6.2.7.2 In vivo Study

Showing similar findings as the first oxygen-enhanced MRI study published by Edelman in 1996, analysis of the relevant region in a dynamic OE-MR image of a healthy subject is illustrated in Figure 1-24. The graph shows the change in the signal in the lung relative to the time. After using pure oxygen, the signal intensity rose rapidly to about 50%, and T1 relaxation time was also shortened. After switching to normal oxygen, the signal intensity dropped rapidly and eventually reached the baseline level. Pulmonary ventilation dynamic measurement with OE-MRI was used for the

direct evaluation of the signal intensity–time of the oxygen enhancement course curve (Bauman and Eichinger, 2012).

This technique provides temporal and spatial images that have good resolution. The difference in decay constants between the wash-in and the wash-out was small and not statistically significant (Ohno and Hatabu, 2007). This slight difference might occur due to the flow of pulmonary blood, which contributes to removing oxygen from the lung tissue, consequently enhancing wash-out and working against wash-in (Bauman and Eichinger, 2012).

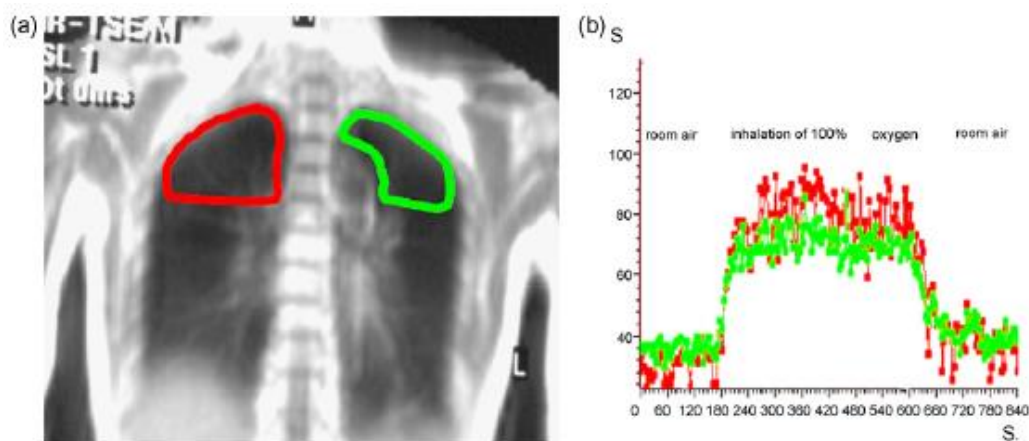


Figure 1-24: Shows an assessment of regional ventilation in a normal healthy volunteer. Figure (a) is of the IR-HASTE sequence for an area of interest and shows the pulmonary anatomy. Figure (b) shows the pulmonary parenchyma signal intensity over time. The signal intensity correlated with the inhalation of pure O_2 . When pure O_2 was switched on, there was an increase and when it was switched off, there was a decrease. (Ohno and Hatabu, 2007).

Another potential use of OE-MRI is the creation of V/Q images and the V/Q signal ratio from the data of OE-MRI combined with perfusion data of non-

contrast-enhanced MRI derived from arterial spin labelling (Bauman and Eichinger, 2012).

Several studies have shown that ventilation-perfusion and its signal intensity ratio images have been successfully obtained through the use of OE-MRI. The average ratio of the signal intensity for VQ and VQ was for the left lung (0.355 ± 0.073) and for the right lung (0.371 ± 0.093), in line with the theoretical signal intensity ratio of V/Q (Ohno and Hatabu, 2007).

Moreover, the signal intensity of VQ plots was close to the normal logarithmic distribution achieved by several elimination techniques of inert gas with many ratios that matched ventilation and perfusion (Ohno and Hatabu, 2007). The combination of arterial spin labelling with the OE-MRI allows for the provision of non-invasive assessment of perfusion, ventilation or the VQ ratio without ionised radiation.

Mai and his team conducted a study to measure the effectiveness of using oxygen flow rates to evaluate T1 changes in OE-MRI in six healthy subjects, in which the following flow rates of oxygen were administered: 5, 10, 15, 20, and 25 l/min (Mai et al., 2002). The results demonstrated that 15 l/min with a non-rebreathing ventilation mask was the optimum flow rate for OE-MRI using a 1.5 Tesla MRI scanner. Moreover, the average signal intensity pattern and T1 measured at diverse rates of oxygen flow are potentially associated with the dissolved oxygen concentration or saturation in blood plasma, thus indicating a limited ventilation mechanism is present (Mai et al., 2002).

1.6.2.7.3 Clinical Studies of OE-MRI

Recently, some researchers have published promising results regarding the use of OE-MRI scans for the assessment of normal and abnormal ventilation (Halaweish and Charles, 2014). The modality can also be used to evaluate pulmonary function parameters, enabling comparison between patients with CF, lung cancer, pulmonary emphysema, interstitial pneumonia and pulmonary thromboembolism (Ohno and Hatabu, 2007).

In these clinical studies, the quantitative or semi-quantitative results of regional OE-MRI were assessed and compared to pulmonary function test parameters. Regional anatomical and physiological abnormalities were evaluated using density-masked CT, thin-section CT and ventilation and/or perfusion scintigraphy. A reference map of OE-MRI of a healthy volunteer is shown in Figure 1-25.

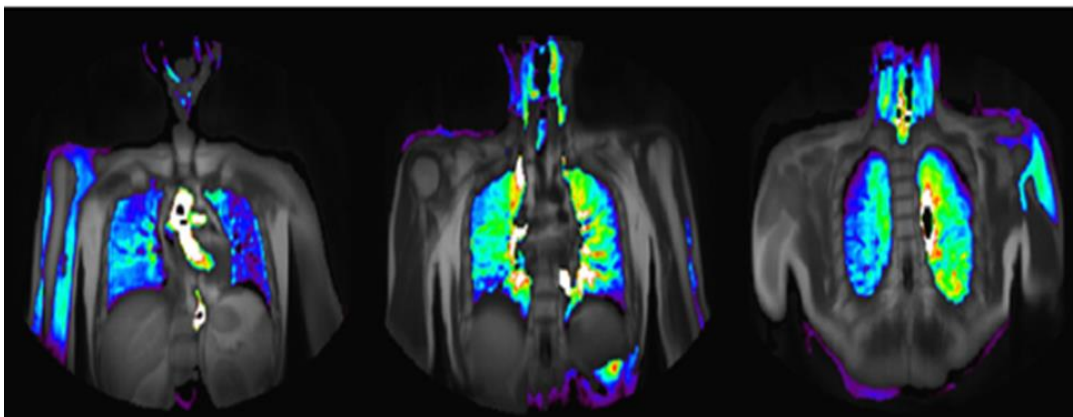


Figure 1-25: The map of the OE-MRI shows a healthy, 58-year-old male volunteer, whose lungs are both homogenous with a high signal of oxygen enhancement (from left to right) (Ohno and Hatabu, 2007).

Figure 1-26 shows an OEMR image of a subject with pulmonary emphysema and lung cancer. Oxygen enhancement is shown in the coloured map, with blue representing relatively poor enhancement and red relatively high enhancement. Both lungs of the healthy volunteer are homogenous and significantly improved on the relative enhanced maps.

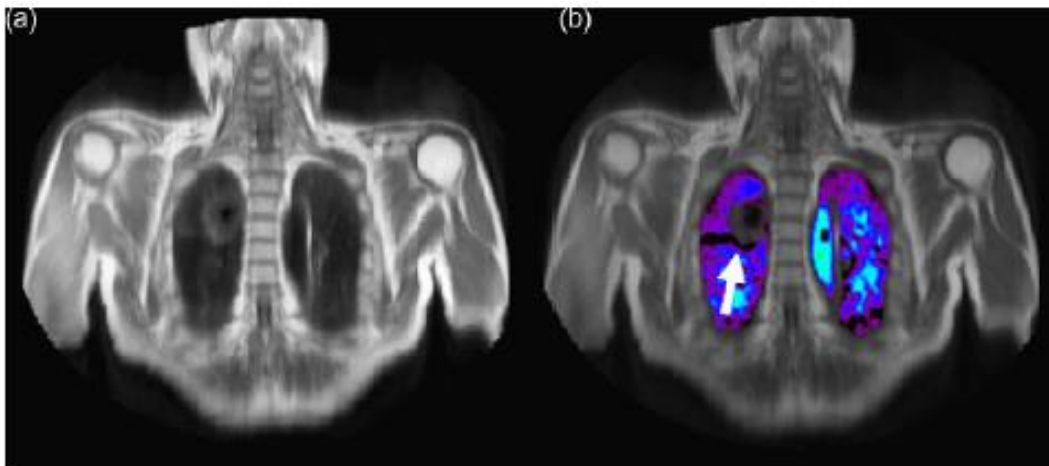


Figure 1-26: A 68-year-old male with pulmonary emphysema and lung cancer is depicted above. Figure (a) shows the MRI lung image which was captured by a T1 weighted IR-HASTE image and shows the tumour in the right side of the lung. Figure (b) is the relative map of the OE-MRI. The pulmonary parenchyma, with the exception of lung tumour (arrow); a heterogeneous and poor relative enhancement is shown owing to lung emphysema (Ohno and Hatabu, 2007).

This poor oxygen enhancement occurred as a result of the lung's functional defects, considering the comparison findings between the lung function test and the OE-MRI parameters (Ohno and Hatabu, 2007). These outcomes show that the OE-MRI and OE-MRI slope reflect DLCO and FEV₁ (Ohno and Hatabu, 2007). These results are regarded as compatible with the aforementioned oxygen enhancement theory and respiratory physiology. The preliminary outcomes of other studies have reported the use of MR ventilation and perfusion imaging for subjects with lung diseases (Ohno and

Hatabu, 2007), using OE-MR imaging and perfusion imaging of MR contrast enhancement.

These findings demonstrate the potential to substitute nuclear medicine ventilation-perfusion scans with a physio-pathological evaluation of lung diseases by combining contrast-enhanced MR perfusion imaging with OE-MR imaging. However, further basic studies and clinical trials of patients with different lung diseases are needed before nuclear medicine VQ scans can be substituted. Other comparative research on thin-section CT, density-masked CT and the scintigraphy of ventilation and perfusion has been carried out in an effort to use the OE-MRI technique for clinical routine practice (Ohno and Hatabu, 2007).

The study compared the predictive capability of the lung function of patients with pulmonary cancer using the OE-MRI technique and other modalities, such as perfusion scintigraphy and quantitative (density-masked) and qualitative CT following the surgical removal of entire segments of the lung. Although the correlation between predictions and results for each of these techniques was significant, the prediction of OE-MRI was more accurate than that of qualitative CT or perfusion scintigraphy, and virtually equal to that of quantitative CT (Ohno and Hatabu, 2007). Thus, the findings of this study indicate that the OE-MRI technique is more valuable than qualitative CT or perfusion scintigraphy, and it is as valuable as quantitative CT in patients with lung cancer. Further studies, however, are needed to assess its effectiveness in routine clinical practice in pulmonary medicine.

OE-MRI is a subject of interest in medical science; many researchers are evaluating the feasibility of this technique for conditions like COPD, chronic thromboembolic pulmonary hypertension (CTEPH), bronchial carcinomas, asthma, and many other respiratory and cancer-related medical conditions. Traditionally, HRCT is used to evaluate the heterogeneous distribution of emphysema in COPD patients. However, OE-MRI is a superior method for obtaining information related to perfusion, ventilation and diffusion in the lungs, because it does not expose the patient to radiation. As yet, the method has not been clinically implemented, and it is still in the process of undergoing clinical trials (Fuseya et al., 2018). The aim of the studies is to compare the validity of HRCT and OE-MRI by demonstrating reproducibility. Forty COPD patients underwent a quantitative comparison; they were tested using OE-MRI, HCRT, a pulmonary function test and arterial blood gas analysis.

In addition to these patients, nine healthy subjects were tested as well, as controls. The severity of emphysema was evaluated according to the percentage of low attenuation volume (LAV%) of the whole lung and the standard deviation in the value of LAV% for ten isovolumetric partitions as an index for heterogeneity. From the OE-MRI test, the oxygen relative enhancement ratios (RERs) and standard deviation (SD-RER) were analysed.

COPD patients showed a significantly lower mean RER (12.6%) than control subjects (22%). RER and LAV% were both related to the diffusion capacity,

whilst the partial pressure of O₂ in arterial blood was only related to RER. Nevertheless, OE-MRI parameters showed a direct association with oxygen uptake in COPD lungs (see Figure 1-27). Therefore, it can be concluded that functional OE-MRI can provide insights into COPD pathophysiology that were not known before, and also without the risk of radiation exposure (Fuseya et al., 2018).

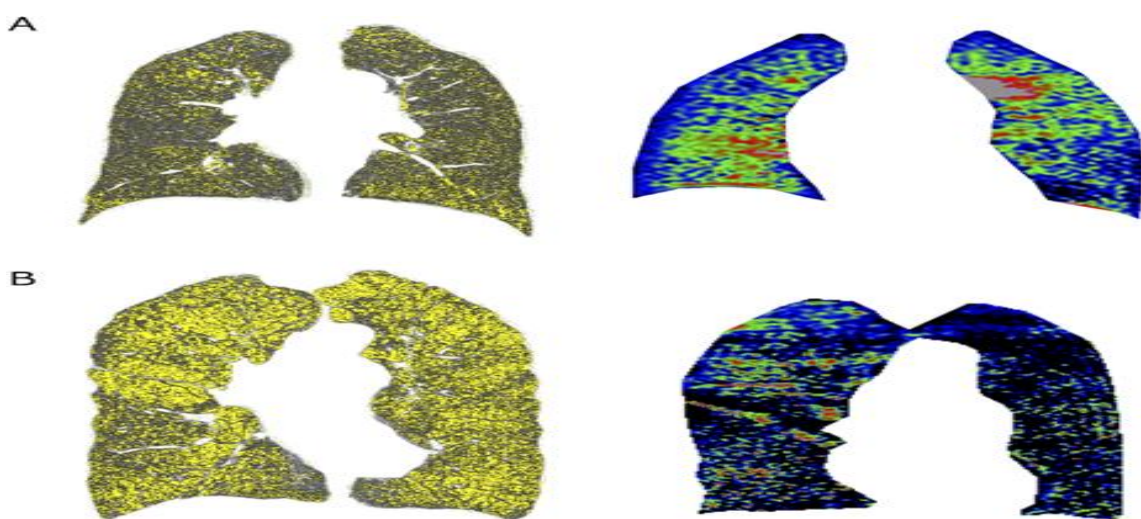


Figure 1-27: Shows a comparison of MRERs between COPD patients and healthy volunteers. The mean relative enhancement ratio (MRER) is the average of the relative enhancement oxygen ratios (RER) which measured the area of interest drawn over both lungs (Fuseya et al., 2018).

The imaging of regional ventilation is essential information for evaluating a variety of pathological conditions besides emphysema, such as pulmonary embolism and pneumonia. For patients with these conditions, there is a mismatch in ventilation-perfusion, and ventilation defects are shown (see Figure 1-28) (Zhang et al., 2015).

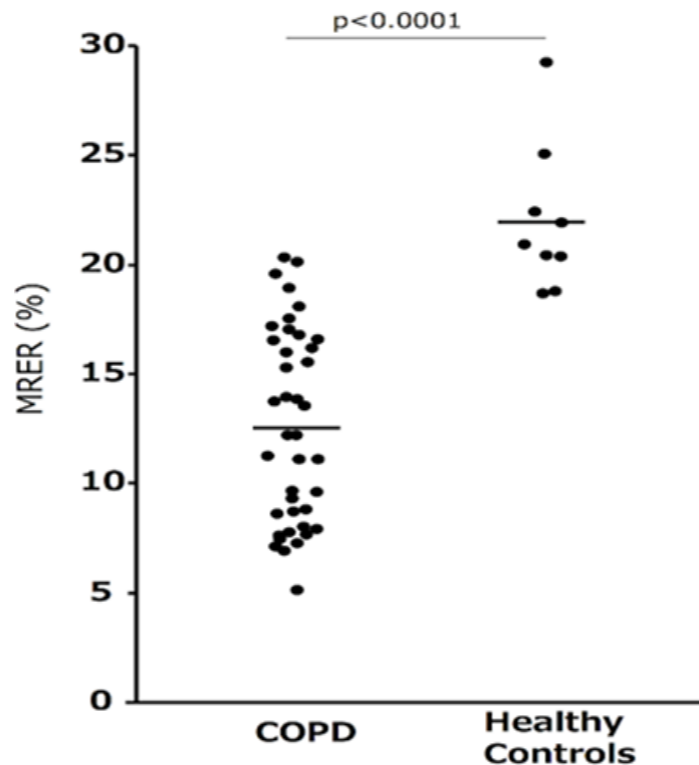


Figure 1-28: The images above, obtained by the OE-MRI and CT, show the lungs of a COPD patient. The yellow dots in the CT scan indicate LAV. The CT image showed clear emphysematous lung changes in the lower left lobe. Additionally, the OE-MRI demonstrated poor oxygen dissolve in the same area. Image B is of a patient with severe emphysema, the CT image demonstrated that both upper lungs have changes of an emphysematous nature. Despite this, the OE-MRI revealed less oxygen absorption in the upper left lung lobe. In the OE-MRI, the low RER regions do not necessarily correspond to the LAR of the CT images (Fuseya et al., 2018).

One of the common causes of pulmonary hypertension is chronic thromboembolic pulmonary hypertension (CTEPH). Quantitative parameters that relate to the severity of CTEPH can be determined by OE-

MRI. Ten patients with CTEPH underwent computed tomography, ventilation/perfusion scintigraphy and OE-MRI to determine the cross-correlation coefficient (mCCC) to calculate the mean cross-correlation coefficient (mCCC) and a fraction of oxygen-activated pixels (fOAP). Based on the results, it was concluded that OE-MRI is a feasible method for the diagnosis of CTEPH. It provides functional and morphological information and the quantitative parameters to help assess the severity of CTEPH (Maxien et al., 2012). The reproducibility of dynamic OE-MRI applies to asthmatic lungs as well (Zhang et al., 2015).

According to a study approved by the National Research Ethics Committee, ten asthmatic patients between the ages of 18 and 53 were tested with OE-MRI. Six severely asthmatic patients had a smaller mean enhancing fraction (EF) and mean maximum O₂ partial pressure ($\Delta PO_2\text{max}_I$) in lung tissues and a higher interquartile range compared to the four mildly asthmatic patients. The study concluded that OE-MRI is a feasible method for testing the sensitivity and severity of asthma.

A recent study established OE-MRI's feasibility in asthma (see the next figure 1-29). It proves that OE-MR imaging can provide reliable indices related to regional oxygen delivery, oxygen uptake and washout in asthma (Zhang et al., 2015).

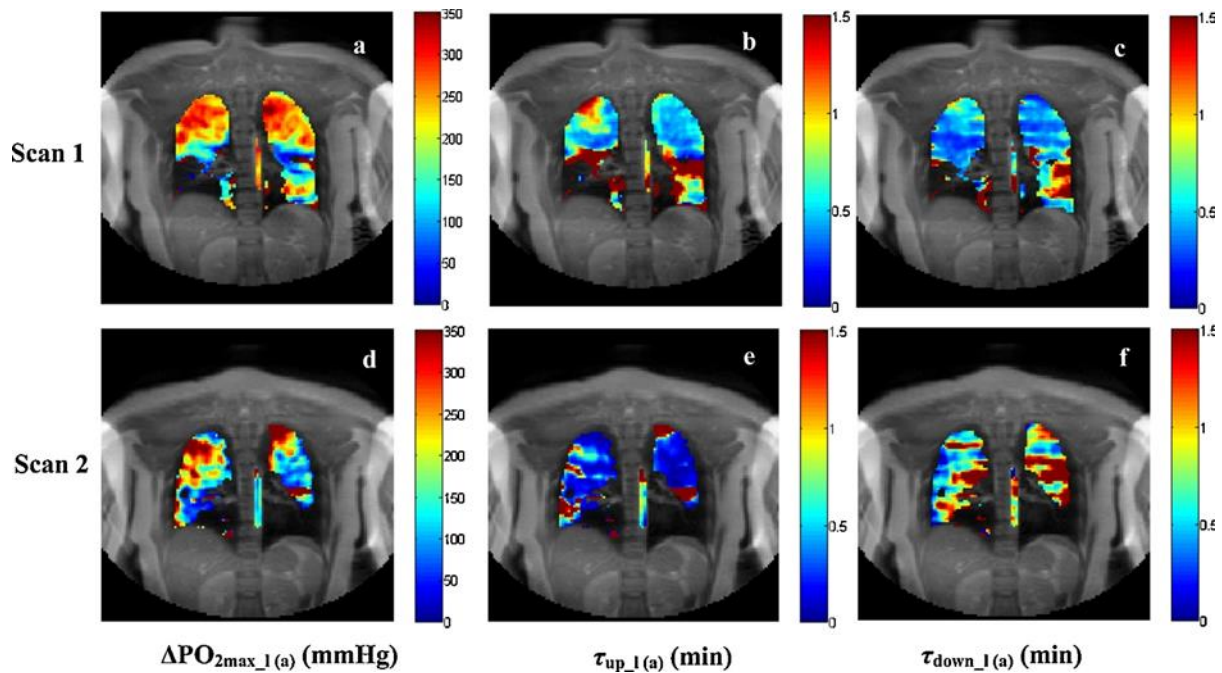


Figure 1-29: Dynamic maps of OE-MRI parameter for a severe asthmatic patient (female, 19 years old, FEV₁% predicted= 64%). The enhancing fraction in the first is 82% scan and in the second scan is 67%. EF is the enhancing fraction, $\Delta\text{PO}_{2\text{max_l}}$ is the maximal change in the partial pressure of oxygen in lung tissue and arterial blood of the aorta ($\Delta\text{PO}_{2\text{max_a}}$), ($\tau_{\text{up_l}}$, $\tau_{\text{up_a}}$) is the oxygen wash-in, and ($\tau_{\text{down_l}}$, $\tau_{\text{down_a}}$) is wash-out (Zhang et al., 2015).

Young et al. (1981) were the first group to use oxygen as a paramagnetic contrast agent (Edelman et al., 1996). Recently, regional ventilation has also been demonstrated using OE-MRI. Table 1-5 summarises the benefits obtained using OE-MRI in clinical conditions as indicated by a review of recent literature:

Table 1-5: Shows some of OE-MRI advantages with some pulmonary diseases.

Clinical Condition	Benefits in using OE-MRI
Chronic Obstructive Pulmonary Disease (COPD)	Assesses loss of pulmonary function and classifies clinical stage (Ohno et al., 2002) (see figure 1-27).
Bronchial Asthma	OE-MRI is as effective as CT for evaluating loss of pulmonary function and classification, while avoiding radiation exposure that a CT delivers (Ohno et al., 2011) (see figure 1-29).
Cystic Fibrosis	Important functional information in CF could be measured using OE-MRI techniques, which is comparatively safe compared to CT (Jakob et al., 2004).
Interstitial Lung Diseases (ILD)	Signal intensities from OE-MRI helps in spatially resolved assessment of the pulmonary diffusion capacity in ILD (Molinari et al., 2007).
Malignancies	Changes in tumour oxygen concentration can be studied using OE-MRI which will help in identifying tumour regions which are hypoxic and will enable spatial mapping of tumour oxygen concentration changes and helping in treatment planning (O'Connor et al., 2009) (see figure 1-26).

OE-MRI is highly applicable in the detection of tumour masses (Maxien et al., 2012). One study of this involved the use of OE-MRI on 10 patients with bronchial carcinomas. Relative signal enhancement (RSE) was used to locate the tumour masses. There was an increase in the signal in the centre of the tumour compared to the peripheral area.

This OE-MRI technique can be used to evaluate changes in tissue oxygenation in the case of tumours (Colliez et al., 2015). Oxygen enhancement MRI is an emerging technique for quantifying the extent of oxygen delivery by determining the change in longitudinal relaxation rate ($\Delta R1$) and molecular oxygen in plasma. Oxy-R fraction determines and

quantifies hypoxia accurately; therefore, it is a technique immediately translatable to the clinical setting for tumour detection as it is accurate and non-invasive (O'Connor et al., 2016).

Hypoxia prevails in human tumours and its resistance to chemotherapy and radiotherapy increases the likelihood of developing metastasis; this can worsen the overall prognosis. However, OE-MRI can serve to quantify spatial variation by a change in R_1 . The same correlation is valid for a brain tumour as well.

1.6.3 Ultra-short Echo Time MR Imaging (UTE)

Ultra-short echo-time MR imaging (UTE) is the final of the three methods used to visualise the lung using MRI discussed here. Bergin et al. (1991) were the first to report acquiring an effective MRI lung image obtained by using a gradient echo sequence which has short TE (less than 1 ms) to visualise pulmonary tissues. This method works by generating ultrashort pulse sequences, thereby minimising the echo time. UTE pulse sequences use customised and special reconstruction and acquisition techniques to enable detection of the ultrashort- T_2 components *in vivo*. This sequence permits the direct visualisation of tendons ($T_2^* = 1$ ms) (Deligianni, 2013), cortical bone ($T_2^* = 0.4$ ms) (Reichert et al., 2005), and lung parenchyma ($T_2^* = 0.5\text{--}3$ ms). Reducing TE to less than 100 μsec is achieved by using free inducting decay with UTE, which provides more detail from tissues have short T_2^* (Bergin et al., 1991).

This approach is helpful in imaging tissues that have a short T2 signal and which exhibit small or null signal when a traditional MRI technique is used (Fabich et al., 2014). A few examples of such tissues are the knee meniscus, cartilage, tendon and cortical bone (O'Brien et al., 2009). Early-stage symptoms of various lung diseases, such as mucus plugging, consolidation, air trapping and bronchial wall thickening, can be identified easily using this technique, which is not possible using conventional MR imaging techniques (Roach et al., 2016).

UTE can be acquired in either two-dimensional or three-dimensional modes, with the two-dimensional mode requiring the use of half-pulse excitations. When using two-dimensional UTE breath holding sequences, there is a limitation in the spatial coverage (Chandra et al., 2011). However, three-dimensional UTE can provide solutions to many issues, such as minimising motion sensitivity of repeating k-space and providing isotropic high spatial resolution (Bannas et al., 2016).

Although motion minimises image sharpness, UTE can provide clear imaging (Tibiletti et al., 2016). However, using respiratory and cardiac gating, produces higher quality UTE images. Breath holding can also be avoided by using respiratory gating. Improved images can be obtained with the three-dimensional UTE normal breathing sequence, and this has enabled the visualisation of pulmonary parenchyma covering all the chest areas. This along with a high SNR signal gives an isotropically high spatial resolution (Johnson et al., 2013).

Although the UTE is more sensitive to gradient fidelity plus higher levels of acoustic noise, it provides further flexibility in volume selection and image contrast (Larson et al. 2016). Furthermore, by using variable density readout gradients with UTE, which have led to an increase in SNR of up to 67%, this method can produce high quality images of microvasculature (1 mm isotropic) and also provides high quality imaging of the pulmonary parenchyma (<0.1 msec) (Johnson et al., 2013). This increase in SNR allows for better differentiation between small vessels, bronchi and pulmonary tissue compared to MR angiography (Bannas et al., 2016). UTE provides a higher CNR allowing better imaging of pulmonary embolism and the pulmonary vasculature than MR angiography does (Bannas et al., 2016).

The advantages of this method are the lack of a need for breath holds, which cause problems for some patients, such as those in the paediatric age group and dyspnoeic patients (Johnson et al., 2013). In addition, three-dimensional UTE can provide high quality images of the pulmonary parenchyma (Johnson et al., 2013). Parenchymal imaging becomes essential in the early detection of some lung pathologies. Free breathing UTE can produce accurate images showing emphysema or fibrosis early in the development of the condition, which cannot be depicted with standard MR angiography (Johnson et al., 2013) (See figure 1-30). The next table summarises the advantages and disadvantages of all previous MRI techniques.

Table 1-6: Shows and summarises the advantages and disadvantages of three types of lung MRI method which was mentioned before.

Types of MRI technique	Advantage	Disadvantage
Hyperpolarised noble gas MR (^3He)	1. Yielding high signals in the MRI which provides quality lung images. 2. Safe	1. An expensive and difficult to obtain. 2. A depend on a laser-based polarisation device
Hyperpolarised noble gas MR (Xenon)	1. Safe 2. Providing anatomical and physiological information	1. Low quality image compared to ^3He 2. a dependency on a laser-based polarisation device combined with MR techniques
Oxygen enhanced MRI	1. Inexpensive, safe, and relatively accessible 2. Providing reliable data on regional oxygen delivery, uptake and the ability to visualise regional functional abnormalities.	1. a low-quality image 2. the gas itself is invisible in an MRI
Ultra-short echo time MR	1. providing high quality imaging. 2. Free breathing technique	1. it has high levels of acoustic noise, 2. it doesn't provide physiological information

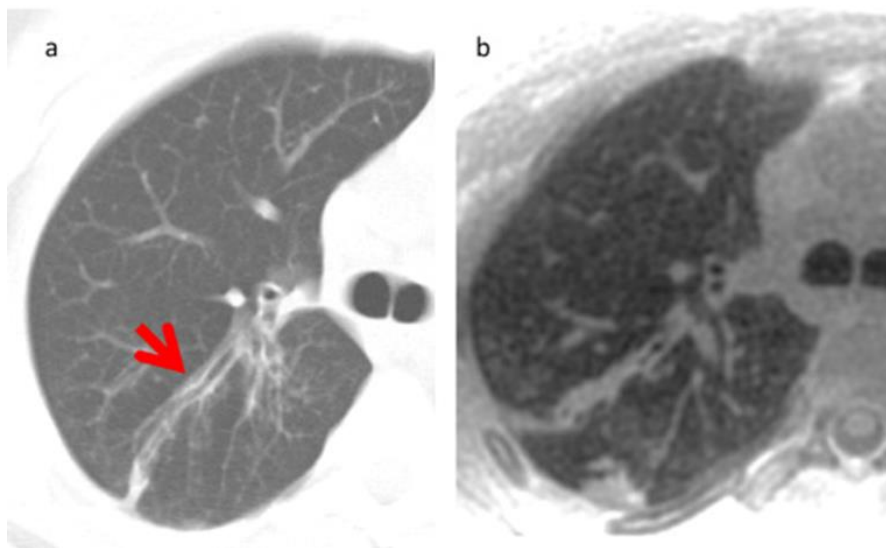


Figure 1-30: UTE MRI in cystic fibrosis. High-resolution computed tomography (HRCT) images (a) acquired 14 months prior to UTE MRI (b) in a 17-year-old with CF. Arrow indicates a region of bronchiectasis and mucus plugging well visualized on both HRCT and UTE MRI. Images were acquired using 3D radial UTE (Torres et al., 2019).

1.7 Safety Concerns with the use of Newer MR techniques

Though there are innumerable advantages offered by hyperpolarised inert gas-assisted methods, and other MR imaging provides compared to conventional techniques, the health and safety of the patient is the top priority in the selection of the imaging method to use. Doing harm to a patient while trying to diagnose the disease condition is unacceptable and defeats the purpose of imaging. Out of the three methods discussed above, imaging using ^{129}Xe and oxygen-enhanced imaging have a few safety issues, which are noteworthy to highlight separately.

1.7.1 Xenon 129

There are proven mild side effects of inhaled ^{129}Xe , such as dizziness, headache and nausea. These automatically disappear after inhaling natural air, as ^{129}Xe is rapidly eliminated (Driehuys et al., 2012). However, the ^{129}Xe that is dissolved before flushing out by normal atmospheric air may cause moderate to severe effects on the nervous system according to alveolar concentrations (Sanders et al., 2003). For example, low alveolar concentrations of ^{129}Xe may cause dizziness and euphoria, and high alveolar concentrations may even result in anaesthesia (Sanders et al., 2003). However, since ^{129}Xe is an inert gas, no major biochemical changes take place in the human system.

According to Salerno et al. (2003) this safety issue could be partially resolved by using spiral k-space trajectories. K-space is the distribution of data collected from MRI signals on an image. Spiral k-space fills from the centre towards the edges, which facilitate faster imaging and minimises the breath-holding time needed for ^{129}Xe due to its short readout duration. It should also be noted that mixing oxygen (T1 relaxation) with ^{129}Xe would alleviate this issue (Mugler et al., 2010).

1.7.2 Oxygen-Enhanced MRI

Unlike ^{129}Xe MRI, the OE technique does not result in any oxygen displacement in the alveoli, since the gas used itself is oxygen, thereby avoiding many of the side effects that happen with the ^{129}Xe method. However, a significant drawback of OE-MR imaging may occur in a small number of patients with conditions such as COPD, who are dependent on hypoxic drive to maintain respiration. In such cases, administering more oxygen for the MR technique may result in a negative hypoxic drive, thereby causing respiratory depression.

Extreme caution must be taken while selecting patients for this procedure and also while performing the technique. Furthermore, the disadvantages of MRI vs CT from the child's point of view are that:

1. Time for the scan - typically several minutes in which the child needs to lie still.

2. Claustrophobia - difficult to tolerate the scan
3. Noise - and specifically that children with AT have an exaggerated startle reflex - so they struggle to remain still when the scan initiates.
4. Boredom during the scan - some scanners have TV equipment etc - but this one doesn't.

1.8 Literature Review

1.8.1 Previous Studies of the Spirometry in Children with AT

To date, the number of clinical studies exploring spirometry in AT patients total only five, and the results reported vary quite markedly (Table 1-7). Some of the studies apparently obtained reproducible spirometric values, whilst others found it difficult to obtain spirometry results that satisfy standard criteria.

Table 1-7: The table listing all the previous studies of spirometry have been conducted on patients with AT.

Author	Title	Year & Country	Sample size	Age
McGrath-Morrow	Pulmonary function in adolescents with AT	2008 USA	10	12-20
Berkun Y	Reversible airway obstruction in children with AT	2010 Israel	27	3.7-19.3
Vilozni D	The feasibility and validity of forced spirometry in AT	2010 Israel	28	3.7-19.3
McGrath-Morrow	Pulmonary function in children and young adults with AT	2014 USA	100	6-29
Vilozni D	FVC deterioration, airway obstruction determination, and life span in AT	2015 Israel	37	4-21

Ataxia telangiectasia patients have considerable morbidity and death from pulmonary illness, according to the first article by McGrath-Morrow et al. (2014). Using pulmonary function tests on 100 consecutive AT patients, McGrath-Morrow et al. (2014) examined the relationship between age and lung function in young adults and children as well as the causes of decreasing lung function. Pulmonary function tests were performed on children and adults with the diagnosis of AT, ranging in age from 6 to 29. In this study, the population's mean forced vital capacity percentage (FVC%) was $56.6 \pm 20.0\%$. Between the ages of 6 and 10, both boys and girls exhibited comparable lung function abnormalities. In comparison to younger females and men of the same age, younger females had higher FVCs% (about 13% difference). Older and younger men had relatively the same FVCs% (about 1% variation). However, younger females had substantially higher FVCs% compared to older females (about 36% variation). Supplemental gamma globulin usage was linked to noticeably reduced FVC (McGrath-Morrow et al., 2014). Lower FVC in men were shown to be modestly correlated with increased radiation-induced chromosomal breakage. In a sample of participants ($n = 25$) who received pulmonary function testing twice or more during an average of two years, there was no discernible change in FVC (McGrath-Morrow et al., 2014).

The second article by Berkun et al. (2010) demonstrates that respiratory illness is a key factor in the AT patients' short lifespan. This paper noted that it is challenging to quantify lung function objectively in AT. In this

study, 27 AT patients' medical and spirometry data were gathered between 2004 and 2007. The investigators evaluated test results, dietary state, treatment plans, lung conditions, and cancers. The following step was to examine each of the spirometry measurements, including forced vital capacity (FVC), forced expiratory volume in one second (FEV_1), forced expiratory volume at 0.5 seconds ($FEV_{0.5}$), mid-expiratory flow (FEF₂₅₋₇₅), peak expiratory flow (PEF), and time increase to peak flow. According to clinical symptoms and their bronchodilator reversibility, eleven individuals (or 40.7%) were deemed to have asthma. FEV_1 and $FEV_{0.5}$ were significantly decreased in comparison to healthy values. In 5 of 11 asthmatic patients, FEF₂₅₋₇₅ was considerably lower than that of control children. All 27 patients displayed FEV_1/FVC and $FEV_{0.5}/FVC$ ratios that were lower than normal. In comparison to healthy youngsters, the increased time to peak flow was three times longer.

In a third publication, Viložni et al. (2015) investigated how spirometry helped with the identification of airflow obstruction and how this related to survival time in patients with AT. During 5.4 ± 1.8 years, they retrospectively collected clinical information and the yearly best spirometry manoeuvres from 37 AT patients (196 spirometry tests) (initial age 4-21 years). Twenty-five participants were confined to wheelchairs, eight of whom were approaching end-stage lungs illness. Of the twelve patients who were walking, seven had recurring respiratory infections. The spirometry indices evaluated were FVC, FEF₂₅₋₇₅, tidal volume VT/FVC and FEF₂₅₋

75/FVC ratios. For those able to walk, the FVC values significantly decreased from the expected values and FEF₂₅₋₇₅ levels were higher ($116 \pm 23\%$ predicted). In those able to walk, the VT/FVC ratio was 0.25 ± 0.06 , rose to 0.35 in those using a wheelchair, and was even higher to 0.57 ± 0.19 in those in whom the illness was at its final stage. In end stage disease, the FEF₂₅₋₇₅/FVC ratio was 4.16 ± 0.75 , which was 2.54 ± 0.70 above normal.

A fourth publication, again by Viložni et al. (2010) examined forced spirometry's applicability and reliability in patients A–T. They conducted spirometry on 28 individuals (3.7–19.3 years old) on 47 occasions. Technical quality, relationships to expected values, and pulmonary disease were the evaluated parameters. The start of test criteria for the accurate expiratory effort was considerably delayed (183 ± 115 ms; $P= 0.001$). Children without respiratory symptoms (Group-FRS; $n= 8$) had a rise-time to peak flow that was 16.2 ± 12.5 ms/year over indicated, whereas children with recurrent infections ($n= 8$) had a rise-time to peak flow that was 30.4 ± 16.1 ms/year above recommended, $P= 0.01$ (Viložni et al., 2010). In 57% of the patients, the total expiration time (1.21 ± 0.47 sec) was reduced. In 8/20 cases, the FEV₁ could not be determined. The pre-set criteria were satisfied for intra-subject repeatability in those able to comply. Patients with hyperreactive airways (Group-HRA; $n=12$) exhibited an FVC deterioration rate of 3.6%/year, compared to the rest of the group-annual FVC decline of 2.2%. (Viložni et al., 2010). However, baseline values in the

Group-HRA were considerably lower than those in the comparison group ($P=0.029$) at similar ages, demonstrating reduced lung function at young age in Group-HRA. FEV_{0.5} deterioration rates were similar in both groups (2.2 and 2.0, respectively). The decline in FEV_{0.5} values was also linked ($P= 0.017$) with body mass index.

However, due to underlying bulbar frailty, incoordination, and difficulty coordinating voluntary respiratory manoeuvres, objective measurements of lung function may be challenging to obtain. McGrath-Morrow et al. (2008) state in a fifth article that pulmonary complications seem to be common among adolescents with AT.

McGrath-Morrow et al. (2008) made small improvements to stabilize the head and reduce leaks in the system to boost the reliability of pulmonary testing. Using the helium dilution technique to measure lung volumes, fifteen AT teenagers performed lung volume measurements. Ten AT teenagers conducted three separate spirometry tests to evaluate the test repeatability. In this study 12 out of 15 evaluated teenagers had normal or hardly diminished total lung capacity (TLC).

Functional residual capacity (FRC), a measure not reliant on patient effort, and TLC were correlated ($R^2=0.71$) The majority of people had reduced vital capacities (VC) that were less than 70% expected (9/15) and residual volumes (RV) that were larger than 120% predicted (10/15). Forced vital capacity (FVC) and forced expiratory volume in one second (FEV₁)

measurements by spirometry were repeatable in the 10 subjects tested on three consecutive occasions ($R=0.97$ and 0.96 , respectively). Seven of the ten teenagers had FEV_1/FVC ratios greater than 90%.

1.8.2 OE-MRI and LCI

OE-MRI and LCI have not yet been applied to patients with AT. Although it has been suggested that OE-MRI could be a more suitable technique for lung imaging in children, and it may provide more useful physiological and anatomical information about lung disease than LCI. Prayle et al. (2017) also suggest that OE-MRI or LCI will become useful for taking measurements in future clinical trials.

1.9 Overview of the Thesis Plan

The aims of the work presented in this thesis are to assess the potential value of spirometry, LCI and OE-MRI for the evaluation of lung function in patients attending the national clinic for AT in Nottingham, UK.

This thesis is divided into five main chapters as follows:

Chapter 1 - Introduction; providing an overview of the thesis starting by describing important aspects of lung anatomy, physiology, and pathology, and how these can be affected in patients with AT. Then with the aim of providing a general overview, the chapter explains lung imaging modalities (X-ray, CT scan, ultrasound, nuclear medicine, and MRI) and lung function tests (spirometry and LCI). MRI is addressed in detail because this

technique based on non-ionising radiation. A literature review is provided describing the previous studies of spirometry in AT patients.

Since each chapter involves a different method the material and method sections have been placed within each relevant chapter.

Chapter 2 – Spirometry in children with AT. The aim of this chapter is to assess the ability to comply with the European Respiratory Journal (ERJ) spirometry criteria to obtain satisfactory results. A control group for this test was children with pulmonary diseases. The work described in this thesis on spirometry in AT is the first study in the UK and European region. The study sample represents approximately a third of the population of AT patients in the UK.

Chapter 3 – LCI in children with AT. Although LCI is non-invasive, non-ionising and allows for free breathing, it has not been applied to AT patients previously. Therefore, the aim of the work described in this chapter is to determine the technique's effectiveness for children with AT.

Chapter 4 – Oxygen-enhanced magnetic resonance imaging (OE-MRI) in children with AT. This technique is a relatively new technique and has the same features of the LCI technique in terms of being non-invasive, does not use ionising radiation and allows free breathing; it has not been used in AT. Thus, the aim of this chapter is also to determine the effectiveness of the OE-MRI technique for this patient population.

Chapter 5 – General discussion and Conclusion. This chapter reviews the main findings from the work described in the results chapters and includes suggestions for future work.

Chapter 2

Assessing Feasibility of Spirometry measurements patients with Ataxia

Telangiectasia

2.1 Introduction

Spirometry is a fundamental test that studies lung function by applying the basic metrics of flow, volume and time (Haynes, 2018). The values of interest in a spirometry test are FEV₁, FVC and the PEF (peak expiratory flow). These are measured during a forced expiratory manoeuvre. As the measurements vary according to individual's age, sex, height and race, measures of spirometry are compared with values obtained in a control population so that abnormalities can be accurately identified (Haynes, 2018). Unlike FEV₁ in which the first part is effort dependent, FEF_{25-75%} measures airway flow rates during mid-expiration, which describes the flow in the medium-to-small airways. Therefore, impairment of FEF_{25-75%} indicates the impairment of medium-sized and small airways. FEF_{25-75%} requires the participant to fully exhale to plateau - and this is of particular importance for AT, as these children may not do this.

Today, spirometry is used by many clinicians around the world as a basic diagnostic test for respiration related health problems, such as COPD, asthma and interstitial lung disease. It is also used in monitoring the general health of the lungs (Burkhardt & Pankow, 2014). Besides serving as an early diagnosis technique, it also helps to assess the response of the body to a drug administered to a patient with a chronic lung condition.

It is suggested that patients diagnosed with any chronic respiratory diseases be regularly assessed using spirometry to see if the patient is

responding to treatment or to see if their underlying disease is deteriorating (Burkhardt & Pankow, 2014). Patients may also be requested to undergo spirometry when they are scheduled for a planned surgical procedure. The rationale for that is to determine if the patient's lungs are capable of handling the surgical procedure and any post-surgical complications (Kelkar, 2015). Besides the clinical applications of the technique, spirometry is also used in occupational health where there are regular check-ups of employees' health, and in the early detection of occupational-related disorders (Townsend, 2020).

The frequency at which spirometry is conducted is usually dependent upon the severity of the underlying breathing disorder. Obstruction is defined as difficulty expelling the air from the lungs due to narrowing in the airways that lead to trapped air in the lungs. In contrast, restriction is defined as difficulty filling the lungs with air during inhalation. In obstructive disorders the FEV_1/FVC ratio is decreased, whereas in restrictive disorders it is normal or increased, and the FVC is low. Furthermore, the degree of disorder is determined either by a reduction in FVC, indicating a reduction in lung volume (as seen in patients with restrictive disorders including those with interstitial lung disease or musculoskeletal diseases affecting the chest wall) or by a reduction in FEV_1 which indicates airflow obstruction. Airflow obstruction is seen in patients with narrowed airways, for example due to COPD or poorly controlled asthma.

As patients with AT have significant airway disease, spirometry might be an effective technique to monitor their lung function. However, little is known about the reproducibility of spirometry in this specialised group of patients (Gold & Koth, 2016). Lung infections are the leading cause of death in AT patients (Bhatt et al., 2015). The probability of viral infections and pneumonia is increased in AT patients partly due to their underlying immunocompromised systems, but also due to cough discoordination, impaired mucociliary clearance and swallow dysfunction (Bhatt et al., 2015). Spirometry can be used periodically to check the health of the lungs in order to detect lung disease at an early stage; this proactive approach could potentially minimise the risk of mortality and morbidity in AT patients. Nevertheless, only a few studies have reported on pulmonary complications in patients with AT.

One study showed that obstructive lung disease was common amongst AT patients. In the study by Viložni et al. (2015), spirometry showed high reproducibility when measuring for deterioration in pulmonary function. However, in an earlier study, it was suggested that restrictive impairment in AT patients is due to neuromuscular impairment and an element of interstitial lung disease (Viložni et al., 2010).

CT scan is the conventional method of obtaining anatomical images of lungs, but it is an unsuitable modality for AT patients, as they are sensitive to ionising radiation due to the underlying mutation that increases their risk of DNA damage. Hence, other methods are needed to assess lung function

over time in these patients. In this chapter, I describe studies that address the potential use of spirometry as an alternative solution.

2.1.1 Aim and Objectives

The primary aim of this chapter is to assess the effectiveness of spirometry in children with AT, to see whether they can comply with the European Respiratory Society (ERS) criteria in obtaining valid results or not. In addition, I explore relationships between the measures obtained and the patients' underlying characteristics including age, height, weight, and sex.

2.2 Method and Material

The results in this chapter are formed from two groups of participants. The first group of participants is all participants who were recruited to the ImaginAT study (ethics number 17/EM/0149) – a 3-year longitudinal study of lung function and physiology in AT. The second cohort was all patients in the National AT clinic who had had lung function assessed with the nDD Prolab device, matched to controls (the same device used in the ImaginAT study) as part of the ongoing service improvement project which commenced with the purchase of the Prolab device.

As this was a feasibility study, a power calculation for our study was not formally undertaken. The information about the feasibility of spirometry with the Prolab device has not previously been reported in the medical literature prior to this study. Furthermore, AT is an ultra-rare condition – only about 100 paediatric patients in the UK and considering age restrictions for Spirometry, there are approximately only 50 patients in the UK who could be expected to do spirometry for our study.

Given the limited potential number of participants we decided to utilize all existing spirometry data available including both the ImaginAT participants, and the clinical spirometry tests from the AT clinic. This approach allowed us to continue our study despite the challenging conditions and make meaningful deductions from the available data. We then matched each patient to two anonymized controls who were paediatric patients who had

not previously done Spirometry - matching with two patients (rather than one) increases the power of the study to detect a difference.

The sample size therefore is one of convenience - essentially all the children with AT who had either.

(a) been in the initial phase of the ImaginAT study or

(b) had lung function measured with the nDD Prolab (the same equipment we used in the ImaginAT study).

In most clinical trials, a power calculation is essential to ensure enough participants are included to confirm the effectiveness of one treatment over another. However, our study's primary aim was different: to ascertain whether children with AT can perform Spirometry (i.e., is it feasible) and to compare their performance to that of children without AT doing the procedure for the first time.

Unfortunately, our already limited sample was further impacted by the COVID-19 pandemic, which resulted in fewer patient visits and, therefore, fewer spirometry readings.

The ImaginAT study was originally designed as a longitudinal study for three years. We planned to recruit 25 children with AT in the UK, with an interim analysis of the data quality from OE-MRI, LCI and spirometry after the first year of recruitment. A control group was not required for the original study. However, the initial design had to be changed due to COVID-19, as we had to pause the study during 2020-2022.

During this time, we, therefore, commenced an additional sub-project to evaluate the ability of children with AT to undertake Spirometry compared to control patients from the respiratory clinic. The respiratory clinic maintains an anonymized dataset from children who have undergone lung function for internal quality control and service improvement. We used this dataset to select a control group that matched the study sample regarding height, gender, and age. However, we found it difficult to match the age and height of two groups (children with AT and the control group) because children with AT are typically short. Therefore, we focused only on age and gender. We searched the anonymized dataset from the clinic. We selected chronologically the first two anonymized patient spirometry datasets that matched our criteria for age and sex and who had had lung function done on the Prolab.

In the spirometry study, thirty-four children with AT (22 male/12 female), aged 6-16 years, were recruited from the AT clinic to perform spirometry tests. Spirometry test procedures were explained, and informed consent was obtained. A trained nurse demonstrated Spirometry. As discussed above, this study used ERS criteria as the international respiratory standard. In addition, 68 children with other pulmonary diseases (non-AT patients) (44 male/ 24 female), aged 6-16 years, were used as a comparison group. In order to increase the study power, there were two non-AT patients for each child with AT. These groups were compared to the group with AT to determine the ability of children with AT to comply with spirometry criteria compared with children with other lung diseases. In

order to try and ensure comparability, groups were matched by age and sex as closely as possible.

The two-proportion test in Minitab was used to determine if there were statistically significant differences between the ability of groups to comply with spirometry criteria, taking $p < 0.05$ as the accepted threshold for statistical implication. Additional analyses were performed using linear regression tests to look for correlations between the factors of age, height, weight, and sex and the spirometry variables, FEV₁ and FVC.

The spirometry device used was ndd EasyOne Pro Lab (Switzerland) (see Figure 2-1). The machine was calibrated daily before starting the exam using an air syringe. This device was used in this study because it allows both lung clearance index (LCI) and Spirometry to be measured; it is the only commercially available machine. A disposable mouthpiece was used for each participant. Measurements were made seated; no AT group member was confined to a wheelchair in this study. Spirometry was conducted either in the respiratory clinic or in the MRI department.

Spirometry was normally repeated three times, and the two best manoeuvres were recorded as long as the criteria were achieved on at least two manoeuvres. If the participants could not comply, the manoeuvres were repeated up to eight times to obtain acceptable results. Tests were supervised by Dr. Prayle, the head of the project, the responsible nurse, and me. Finally, I was directly involved in all of the work described in this study under the clinical supervision of Dr. Prayle, the head of the project

and the research nurse. This included direct participation in spirometry studies. Moreover, I have analysed all the spirometry data presented.



Figure 2-1: ndd EasyOne Pro Lab Spirometer.

2.2.1 Study Inclusion Criteria / Exclusion Criteria

2.2.1.1 Inclusion Criteria – for the service improvement project.

- The children who attended the clinic AT a time when we had Prolab in the clinic.
- Aged between 6 to 20 years.

- The cohort of control patients who attended the clinic with a range of pulmonary diseases matched the gender and age of children with AT a time when we had Prolab in the clinic.

2.2.1.2 Inclusion criteria – for the ImaginAT study

- Diagnosis of AT (or an AT like syndrome) attending the National Paediatric AT clinic.
- Judged by the investigator and the parents that the participant would be able to lie relatively still in an MRI scanner for 15 minutes.
- Aged less than 20 years at consent, and over 5 years.

2.2.1.3 Exclusion criteria– for the ImaginAT study

The ImaginAT study protocol included exclusion criteria pertaining to (for example) MRI exclusion criteria such as metal implants and claustrophobia.

These were as follows:

- Standard MRI exclusion criteria – a history of implanted / indwelling magnetically active material.
- Participation in another research study which excludes participation in an observational cohort study such as the ImaginAT study.
- Participant not deemed fit enough to tolerate procedure.
- Participant deemed unsuitable due to being unlikely to comply with instructions or tolerate scanning.

2.2.2. The criteria of Assessing the Ability of Children with AT to Complete Spirometry.

The following criteria are the ATS/ERS standards:

A. Within-manoeuvre criteria: Individual spirograms are "acceptable" if:

1- They are free from artefacts:

- Coughing within the first second of the exhalation.
- Glottis closure that influences the measurement.
- Early termination or cut-off.
- Effort is not maximal throughout.
- Leak.
- Obstructed mouthpiece.

2- They have good starts:

- Extrapolated volume <5% of FVC or 0.15 L, whichever is greater.

3- They show satisfactory exhalation:

- Duration of 6s (3s for children).
- a plateau in the volume–time curve.
- may still be acceptable if the subject patient should not or cannot continue exhaling.

B. Between-manoeuvre criteria: Once three acceptable spirograms are obtained, the following tests should be applied:

- 1- The two highest values of FVC should be within 0.15 L of one another.
- 2- The two highest values of FEV₁ should be within 0.15 L of one another.
- 3- If the above two criteria are met, the testing session can be concluded.
- 4- If the above two criteria are not met, continue the testing session until both are met upon analysis of acceptable spirograms from additional testing or total eight tests are performed (optional) or the subject patient should not continue for other reasons.

In addition, we included ERS criteria which have substantial overlap with the ATS criteria. Criteria used in this study were:

- 1- Cough free in the first second at least for 2 trials.
- 2- Reached a plateau in at least 2 trials.
- 3- Exhaled for 2 seconds in at least 2 trials.
- 4- Satisfactory exhalation in at least 2 trials.
- 5- Reproducibility (take the best two manoeuvres).

2.3 Results

2.3.1 Study Recruitment and Study Population Characteristics

34 children (22 males and 12 females), who had been diagnosed with AT were approached to partook part in the study. The characteristics of the study population are summarised in Table 2-2. The nature of the study was clearly explained to the child and their parents, and the potential future benefits of the research described. All the AT subjects and 68 additional children underwent spirometry testing with the nDD ProLab device for the first time. The 68 other children had a range of other pulmonary diseases see the next table and had not previously undertaken spirometry.

Table 2-1: Characteristics of the spirometry comparison group

Category	Disease	No.
Respiratory	asthma	43
	cough	3
	restrictive disorders	2
	obstruction disorders	2
	interstitial lung disease (ILD)	2
	pneumonia	1
	rhinitis	1
	adenoidal hypertrophy	1
	congenital pulmonary airway malformation (CPAM)	1
Other	scoliosis	4
	lymphoid leukaemia	4
	Lemaire's disease	1
	autism	1
	lupus	2

Each child with AT was matched with two children from the control group, by age and gender (Table 2-2). The control groups were not matched by ethnicity (Figure 2-2 and 2-3). The majority of the subjects in both groups were Caucasian and Asian.

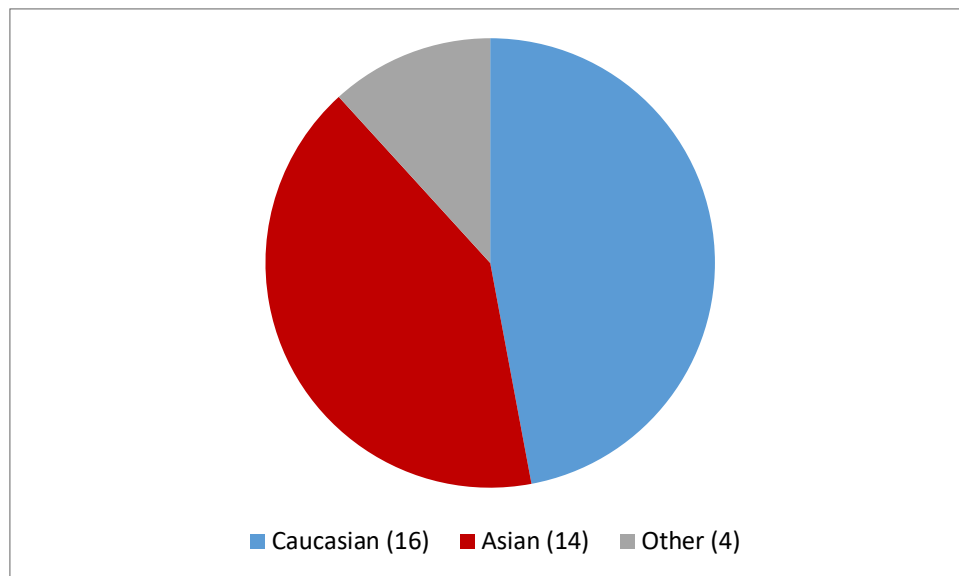


Figure 2-2: Ethnicity distribution for the AT participants. 'Others' means ethnicity not recorded in the PRO LAB device.

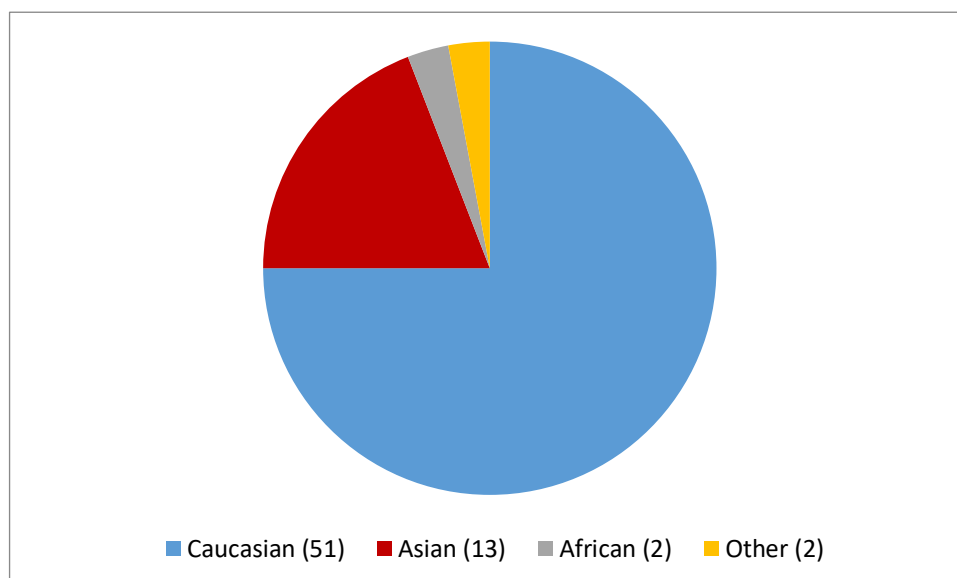


Figure 2-3: Ethnicity distribution for the control group which contains 68 participants.

Table 2-2: Characteristics for the AT group and Control group.

Descriptive Parameter		AT group	Control group
Age (Median, Range)		11 years, 6– 16 years	11 years, 6– 16 years
Sex (%)		Male= 64.70%	Male= 64.70%
		Female= 35.30%	Female= 35.30%
Ethnicity	Caucasian	16	51
	Asian	14	13
	Other	4	2
	African	0	2
Height (Median, Range)		134.9 cm, (107.8 cm / 163.6 cm)	148.5 cm, (111.6 cm / 180.8 cm)
Height Z Score (Median, Range)		-1.65 cm, (-5.47 cm / 1.31 cm)	-0.09 cm, (-3.38 cm / 2.28 cm)
Weight (Median, Rang)		30 kg, (17 kg / 54 kg)	37 kg, (19 kg / 80 kg)
Weight Z Score (Median, Range)		-1.7 kg, (-5.93kg / 1.3 kg)	0.16 kg, (-3.02 kg / 2.08 kg)
BMI (Median, Range)		16.2, (12.7 / 25.2)	17.55, (12.3 / 29.7)

Chapter 2

Table 2-3: Descriptive characteristics of individuals in the AT group and the control group of children with pulmonary diseases (68 participants) who were matched with the AT group by age and gender. Two children in this group were matched with one child in AT group. The rest of the table follows on the next page.

NO	AT group						Control 1						Control 2					
	Age	Sex	Race	Height	Weight	BMI	Age	Sex	Race	Height	Weight	BMI	Age	Sex	Race	Height	Weight	BMI
1	6	Female	Caucasian	112 cm	21 Kg	16.7	6	Female	Asian	111.6 cm	19 Kg	15.3	6	Female	Caucasian	116 cm	27 Kg	20.1
2	6	Male	Other	110.6 cm	19 Kg	15.5	6	Male	Asian	118 cm	21 Kg	15.1	6	Male	Caucasian	123.3 cm	28 Kg	18.4
3	6	Male	Caucasian	119 cm	21 Kg	14.8	6	Male	African	120.9 cm	26 Kg	17.8	6	Male	Caucasian	120 cm	23 Kg	16
4	7	Female	Asian	109 cm	17 Kg	14.3	7	Female	Caucasian	121 cm	20 Kg	13.7	7	Female	Asian	132.7 cm	29 Kg	16.5
5	7	Female	Caucasian	121 cm	23 Kg	15.7	7	Female	Caucasian	132 cm	27 Kg	15.5	7	Female	Caucasian	119 cm	23 Kg	16.2
6	8	Female	Caucasian	129 cm	35 Kg	21	8	Female	Asian	128 cm	27 Kg	16.5	8	Female	Caucasian	121.5 cm	21 Kg	14.2
7	8	Male	Other	138.1 cm	32 Kg	16.8	8	Male	Caucasian	141 cm	36 Kg	18.1	8	Male	Caucasian	127.7 cm	24 Kg	14.7
8	8	Male	Other	125 cm	27 Kg	17.3	8	Male	Asian	129 cm	30 Kg	18	8	Male	Caucasian	134 cm	34 Kg	18.9
9	9	Male	Asian	126 cm	40 Kg	25.2	9	Male	Caucasian	137 cm	35 Kg	18.6	9	Male	Caucasian	136.5 cm	33 Kg	17.7
10	9	Male	Other	145 cm	35 Kg	16.6	9	Male	Other	140 cm	31 Kg	15.8	9	Male	Caucasian	141 cm	34 Kg	17.1
11	9	Male	Caucasian	131 cm	33 Kg	19.2	9	Male	Asian	131 cm	27 Kg	15.7	9	Male	Other	131.4 cm	37 Kg	21.4
12	10	Female	Caucasian	127 cm	21 Kg	13	10	Female	Asian	136.6 cm	23 Kg	12.3	10	Female	Caucasian	143 cm	37 Kg	18.1
13	14	Male	Caucasian	151.8 cm	30 Kg	13	14	Male	Asian	171.3 cm	55 Kg	18.8	14	Male	Caucasian	153.1 cm	38 Kg	16.2
14	10	Male	Asian	134.8 cm	24 Kg	13.2	10	Male	Caucasian	141 cm	36 Kg	18.1	10	Male	Caucasian	142 cm	33 Kg	16.4
15	10	Male	Asian	136 cm	34 Kg	18.4	10	Male	Caucasian	149 cm	45 Kg	20.3	10	Male	Asian	149 cm	36 Kg	16.2
16	9	Male	Caucasian	132 cm	29 Kg	16.6	9	Male	Caucasian	131.8 cm	26 Kg	15	9	Male	Caucasian	135 cm	29 Kg	15.9
17	11	Female	Caucasian	129 cm	23 Kg	13.8	11	Female	Caucasian	137.6 cm	31 Kg	16.4	11	Female	Caucasian	159.4 cm	61 Kg	24
18	11	Male	Asian	107.8 cm	17 Kg	14.6	11	Male	Asian	154.6 cm	67 Kg	28	11	Male	African	143.7 cm	31 Kg	15

Chapter 2

No	AT group						Control 1						Control 2					
	Age	Sex	Race	Height	Weight	BMI	Age	Sex	Race	Height	Weight	BMI	Age	Sex	Race	Height	Weight	BMI
19	11	Male	Caucasian	141 cm	31 Kg	15.6	11	Male	Caucasian	163.7 cm	56 Kg	20.9	11	Male	Caucasian	151 cm	36 Kg	15.8
20	12	Male	Asian	144 cm	38 Kg	18.3	12	Male	Caucasian	166.3 cm	59 Kg	21.3	12	Male	Caucasian	159.4 cm	41 Kg	16.1
21	12	Male	Caucasian	125.6 cm	20 Kg	12.7	12	Male	Caucasian	148 cm	46 Kg	21	12	Male	Asian	148 cm	34 Kg	15.5
22	12	Male	Asian	135 cm	25 Kg	13.7	12	Male	Caucasian	151 cm	50 Kg	21.9	12	Male	Caucasian	127 cm	26 Kg	16.1
23	12	Male	Caucasian	125 cm	24 Kg	15.4	12	Male	Caucasian	157 cm	43 Kg	17.4	12	Male	Caucasian	148 cm	41 Kg	18.7
24	12	Male	Caucasian	141 cm	30 Kg	15.1	12	Male	Caucasian	152 cm	39 Kg	16.9	12	Male	Caucasian	166 cm	44 Kg	16
25	13	Male	Asian	131 cm	24 Kg	14	13	Male	Caucasian	162 cm	78 Kg	29.7	13	Male	Asian	149.5 cm	39 Kg	17.4
26	14	Female	Asian	163.6 cm	54 Kg	20.2	14	Female	Caucasian	156.5 cm	60 Kg	24.5	14	Female	Caucasian	163.5 cm	46 Kg	17.2
27	14	Female	Caucasian	139.7 cm	35 Kg	17.9	14	Female	Caucasian	159 cm	37 Kg	14.6	14	Female	Caucasian	172 cm	80 Kg	27
28	14	Female	Caucasian	143 cm	34 Kg	16.6	14	Female	Caucasian	164.7 cm	44 Kg	16.2	14	Female	Caucasian	163 cm	43 Kg	16.2
29	14	Female	Caucasian	137 cm	33 Kg	17.6	14	Female	Caucasian	151.5 cm	53 Kg	23.1	14	Female	Caucasian	165.5 cm	67 Kg	24.5
30	14	Female	Asian	151 cm	42 Kg	18.4	14	Female	Caucasian	153 cm	37 Kg	15.8	14	Female	Caucasian	161 cm	56 Kg	21.6
31	14	Female	Asian	151.3 cm	45 Kg	19.7	14	Female	Caucasian	158.8 cm	63 Kg	25	14	Female	Caucasian	161.9 cm	49 Kg	18.7
32	14	Male	Asian	147.2 cm	28 Kg	12.9	14	Male	Caucasian	173 cm	71 Kg	23.7	14	Male	Asian	180.8 cm	68 Kg	20.8
33	15	Male	Asian	149 cm	35 Kg	15.8	15	Male	Caucasian	173 cm	61 Kg	20.4	15	Male	Caucasian	164 cm	49 Kg	18.2
34	16	Male	Asian	159.5 cm	44 Kg	17.3	16	Male	Caucasian	162.7 cm	75 Kg	28.3	16	Male	Caucasian	171 cm	55 Kg	18.8

2.3.2 The Ability to Complete Spirometry between Children with AT and the Control Group

The ability of children with and without AT to complete spirometry with an acceptable technique was compared. Of 34 children in the AT group, 11 (32%) were able to complete spirometry with satisfactory technique (see Table 2-4). In contrast, 54 out of 68 (79%) of the control group were able to complete spirometry (see Table 2-5). The reasons for failing to complete adequate spirometry are detailed below. As mentioned before, the participant's result was accepted if he or she could comply with the European spirometry criteria for at least two trials.

Table 2-4: Shows the number of AT subjects (n=34) able to comply with ERS criteria for spirometry.

Criteria	Number of subjects
Cough free in the first second at least for 2 trials (%)	26/34 (76%)
Reached a plateau in at least 2 trials	17/34 (50%)
Exhaled for 2 seconds in at least 2 trials	13/34 (38%)
Satisfactory exhalation in at least 2 trials	11/34 (32%)
Reproducibility: Three reproducible curves	9/34 (26%)
Reproducibility: Two reproducible curves	9/34 (26%)
Reproducibility: Non- reproducible curves	16/34 (47%)

Table 2-5: Shows the ability of control subjects (n=68) to comply with ERS criteria.

Criteria	Number of subjects
Cough free in the first second at least for 2 trials	66/68 (97%)
Reached a plateau in at least 2 trials	58/68 (85%)
Exhaled for 2 seconds in at least 2 trials	56/68 (82%)
Satisfactory exhalation in at least 2 trials	54/68 (79%)
Reproducibility: Three reproducible curves	53/68 (78%)
Reproducibility: Two reproducible curves	14/68 (21%)
Reproducibility: Non- reproducible curves	1/68 (0.01%)

It is clear that not all of the children with AT were able to do satisfactory spirometry. However, the majority of the children who did not have AT were able to do satisfactory spirometry. The null hypothesis is that there is no difference between the proportion of children with AT who can adequately do spirometry and the proportion of children in the control population. Therefore, using GraphPad, I analysed a 2x2 contingency table to determine whether these differences were statistically significant. The result of this test showed that the AT group are significantly less able to do adequate spirometry than the control group ($p < 0.0001$) (see Table 2-6).

Table 2-6: Shows the ability of the two groups to comply with spirometry criteria. Fisher's exact test calculated with Graphpad.

	Can comply with the spirometry	Cannot comply with spirometry	Total
Children with AT	11	23	34
Control group	54	14	68
Total	65	37	102
Fisher's exact test	The two-tailed P value is less than 0.0001.		

2.3.3 Spirometry Patterns of Children with AT

Low spirometry results for children with AT could be due to one of two reasons. The first is that the patient is unable to do spirometry. The second reason is the patient's lung condition has deteriorated. According to the above results, there are many children with AT who cannot do adequate spirometry and there are many children in the control group who can do it. Therefore, some adequate and inadequate spirometry results have been further assessed.

2.3.3.1 Adequate Spirometry Patterns of Children with AT

An illustrative example of two results of adequate spirometry have been selected (Figures 2-4 and 2-5). These patients were selected because they were able to comply with spirometry criteria. Figure 2-4 shows the time/volume graph for a 6-year-old female with AT. Inspection of the time/volume graph reveals this participant was able to achieve spirometry criteria after four manoeuvres. Diagnostically, the time/volume graph seems normal because the FEV_1/FVC ratio was 0.74.

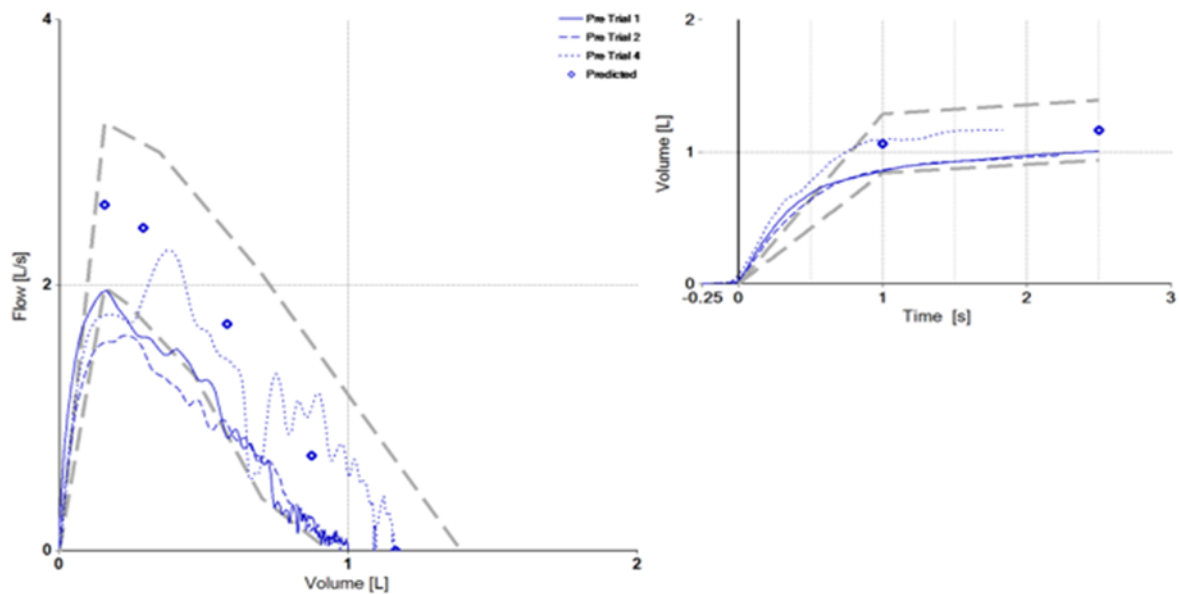


Figure 2-4: Shows the flow/volume loop on the left side and the volume/time graph on the right side. Predicted FEV_1 is 1.06 and the LLN is 0.84 and the best FEV_1 is 0.86. Predicted FVC is 1.16, the LLN is 0.93, and the best FVC is 1.16. The variation between two FEV_1 is 0.23 and between two FVC is 0.16 with two reproducible curves.

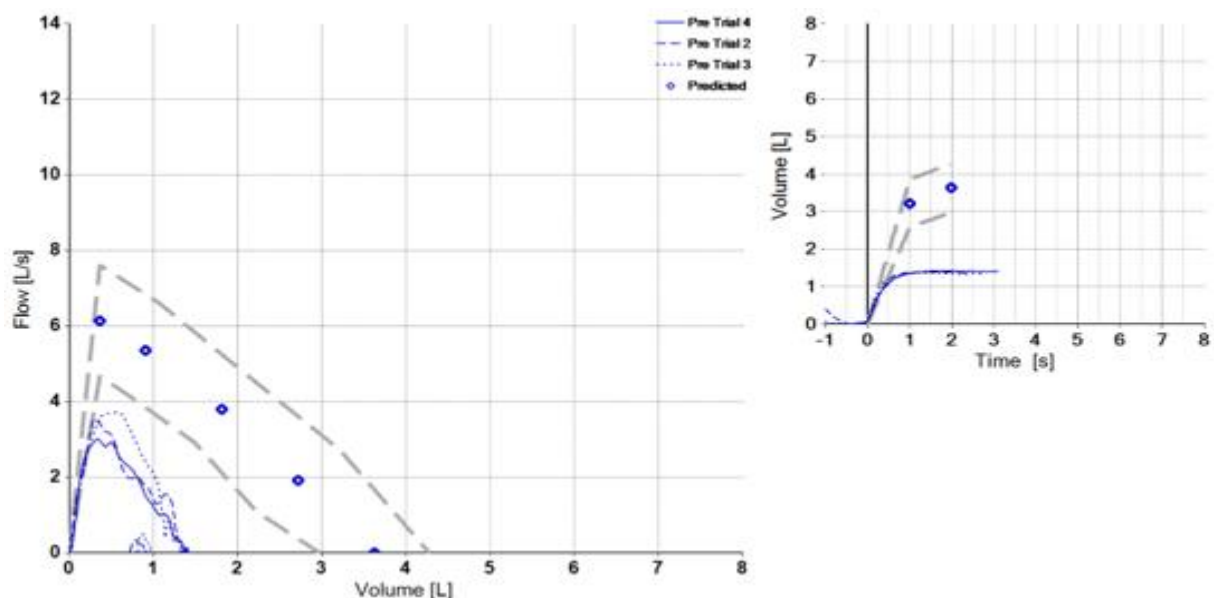


Figure 2-5: shows the time/volume graph for a 16-year-old male child with AT. The time/volume graph indicates that this participant was able to achieve spirometry criteria after four manoeuvres. Diagnostically, this patient has a restrictive lung disorder because the FEV_1/FVC ratio was 0.97.

2.3.3.2 Inadequate Spirometry Patterns of Children with AT

As described above, the majority of AT participants were unable to comply with spirometry's criteria. Twenty-three of the 34 AT patients were unable to produce any adequate spirometry. Unaccepted results were due to cough in the first second, failure to reach a plateau in at least two manoeuvres and failure to exhale continuously for 2 seconds. Representative traces are shown in Figures 2-6, 2-7 and 2-8.

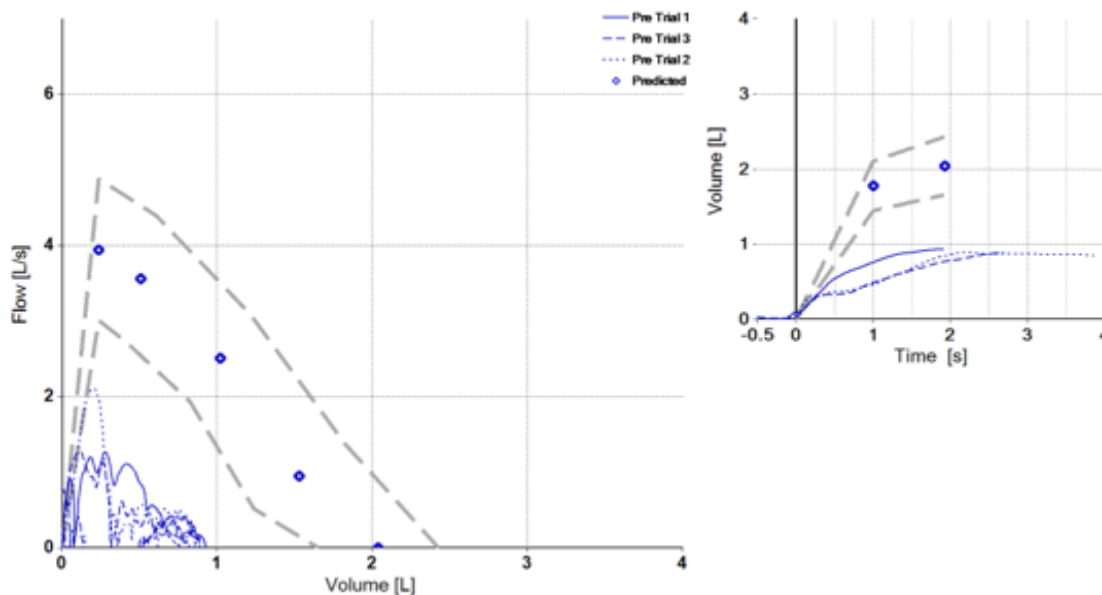


Figure 2-6: Shows the flow/volume loop on the left side and the volume/time graph on the right side. The predicted FEV₁ is 1.77 and the LLN is 1.44 and the best FEV₁ is 0.75 and the predicted FVC is 2.04, the LLN is 1.65 0.93, and the best FVC is 0.93. The variation between two FEV₁ is 0.27 and between two FVC is 0.04 with two reproducible curves. The main fault was due to cough in the second and third trials.

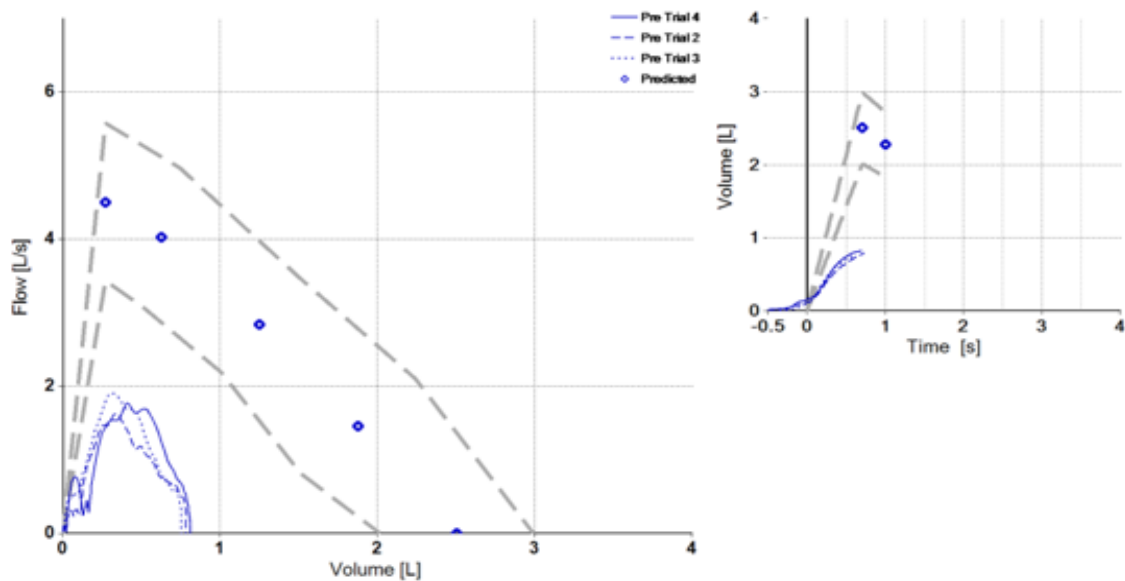


Figure 2-7 Shows the flow/volume loop on the left side and the volume/time graph on the right side. The predicted FEV_1 is 1.83 and the LLN is 1.48 and the best FEV_1 is 1.11 and the predicted FVC is 2.07, the LLN is 1.7, and the best FVC is 1.11. The variation between two FEV_1 is 0.05 and between two FVC is 0.05 with two reproducible curves. This was unacceptable due to cough in all trials and with no exhalation greater than two seconds and no plateau achieved in all trials.

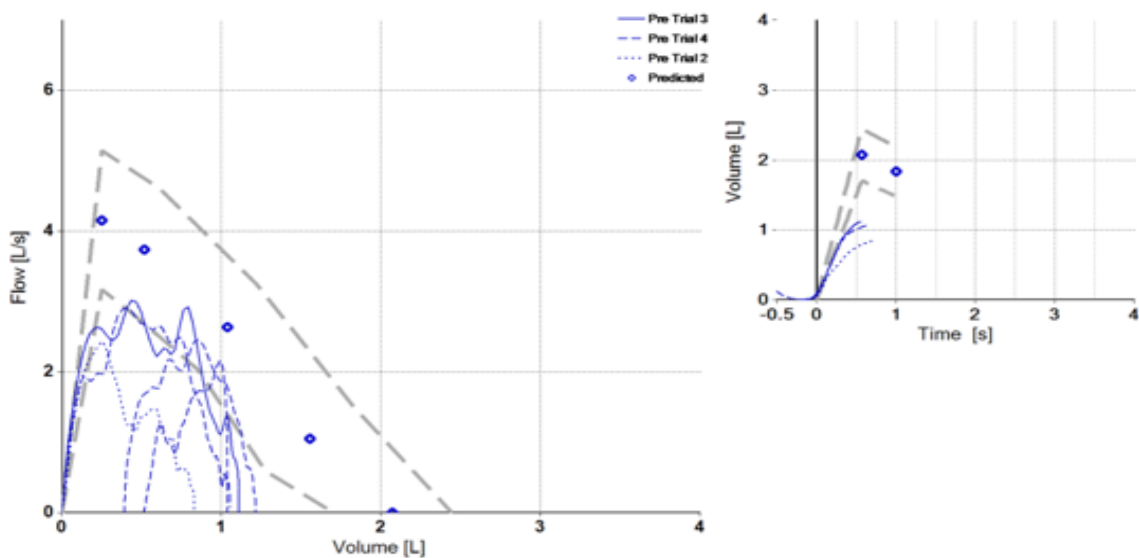


Figure 2-8: Shows the flow/volume loop on the left side and the volume/time graph on the right side. The predicted FEV_1 is 2.27 and the LLN is 1.83 and the best FEV_1 is 0.81 and the predicted FVC is 2.5, the LLN is 2.02, and the best FVC is 0.81. The variation between two FEV_1 is 0.03 and between two FVC is 0.03 with three reproducible curves. No exhalation of greater than two seconds was achieved, and a plateau was not achieved in all trials.

2.3.4 The Relationship between Age and Compliance with Performing Spirometry

After comparing two groups and finding that the children with AT are less able to comply with spirometry tests than the comparison group, a post hoc analysis of the effect of age on spirometry of the two groups. Both groups were divided into two subgroups based on age. The first group was those aged 11 or under and the second those aged 11 or over. The cut of off 11 years was decided, as this is typically the age at which ataxia progresses such that patients with AT start to require a wheelchair.

We speculated that lung function may decrease with age in the AT group because of recurrent infection; therefore, there spirometric measurements (e.g., FVC) may decrease. Furthermore, in general, older children are expected to understand the task of spirometry better, and therefore are better able to comply with spirometry. However, another potential issue for children with AT is that as they get older and ataxia symptoms worsen, it may become more difficult for the older AT subjects to comply with spirometry. This post hoc analysis therefore analysed the impact of age on both spirometry measurements and spirometry adequacy.

2.3.4.1 Children with AT: Effect of Age on Adequate Spirometry Compliance

I assessed the ability of the AT patients to comply with spirometry in those aged 11 or under with those aged over 11. Nine out of 18 (50%) of the

children with AT aged 11 or under in this study were able to perform the test whereas 2 out 16 (12.5%) participants greater than 11 years were able to complete the test. The null hypothesis is that there was not impact of age on ability to undertake spirometry. The result of this test shows that the children with AT, aged 11 or under, are significantly more able to do adequate spirometry than children with AT aged over 11 ($p= 0.0296$) (see Table 2-7).

Table 2-7: Ability of the children with AT to achieve spirometry criteria which divided based on the age. Fisher's exact test calculated with Graphpad.

	Can comply with the spirometry	Cannot comply with the spirometry	Total
Children with AT aged ≤ 11 years	9	9	18
Children with AT aged >11	2	14	16
Total	11	23	34
Fisher's exact test	The two-tailed P value is less than 0.0296.		

2.3.4.2 The Control Group: Effect of Age on Ability to Complete Spirometry

I assessed the ability of the control group to comply with spirometry. Of the 36 children in the control group aged 11 or under, 25 (69%) were able to perform the test, whereas 29 out 32 (91%) participants greater than 11 years were able to complete the test. Statistical analysis showed that children aged 11 or under are significantly less able to do adequate spirometry than the group of children aged over 11 ($p= 0.0386$) (see Table

2-8). These results contrast markedly with those of the AT group, where the ability to comply was reduced with age.

Table 2-8: Ability of the control group to achieve spirometry criteria which divided based on the age. Fisher's exact test calculated with Graphpad.

	Can comply with the spirometry	Cannot comply with the spirometry	Total
Control group aged ≤ 11 years	25	11	36
Control group aged > 11 years	29	3	32
Total	54	14	68
Fisher's exact test	The two-tailed P value is less than 0.0396.		

2.3.5 The Correlation between the Ability to Achieve the FEV₁ and FVC vs Age in AT and Control Groups

The FEV₁ and FVC are the key values obtained from spirometry, which enable the FEV₁/FVC ratio to be calculated. A restrictive defect is formally defined as a reduction in total lung capacity (TLC) below the 5th percentile. Typically, spirometry findings are reduced FVC, and normal FEV₁/FVC or increased FEV₁/FVC ratio (Stanojevic et al., 2022); and when this ratio is less than the normal ratio, it implies an obstructive disorder. As mentioned before, age plays a key role both in technique but also in determining the range of these values, which will increase as lung growth continues during childhood unless significant lung disease is present. Using Scatterplot (Minitab 17.2.1) and Pearson correlation in SPSS, I assessed the correlation between the FEV₁ and FVC values with age for both the AT group and the control group. Figure 2-9 demonstrates the best values of FEV₁ and FVC for

AT group and two control groups versus age. It was combined in one figure to facilitate the comparison among the groups. After that, each group will be separately demonstrated.

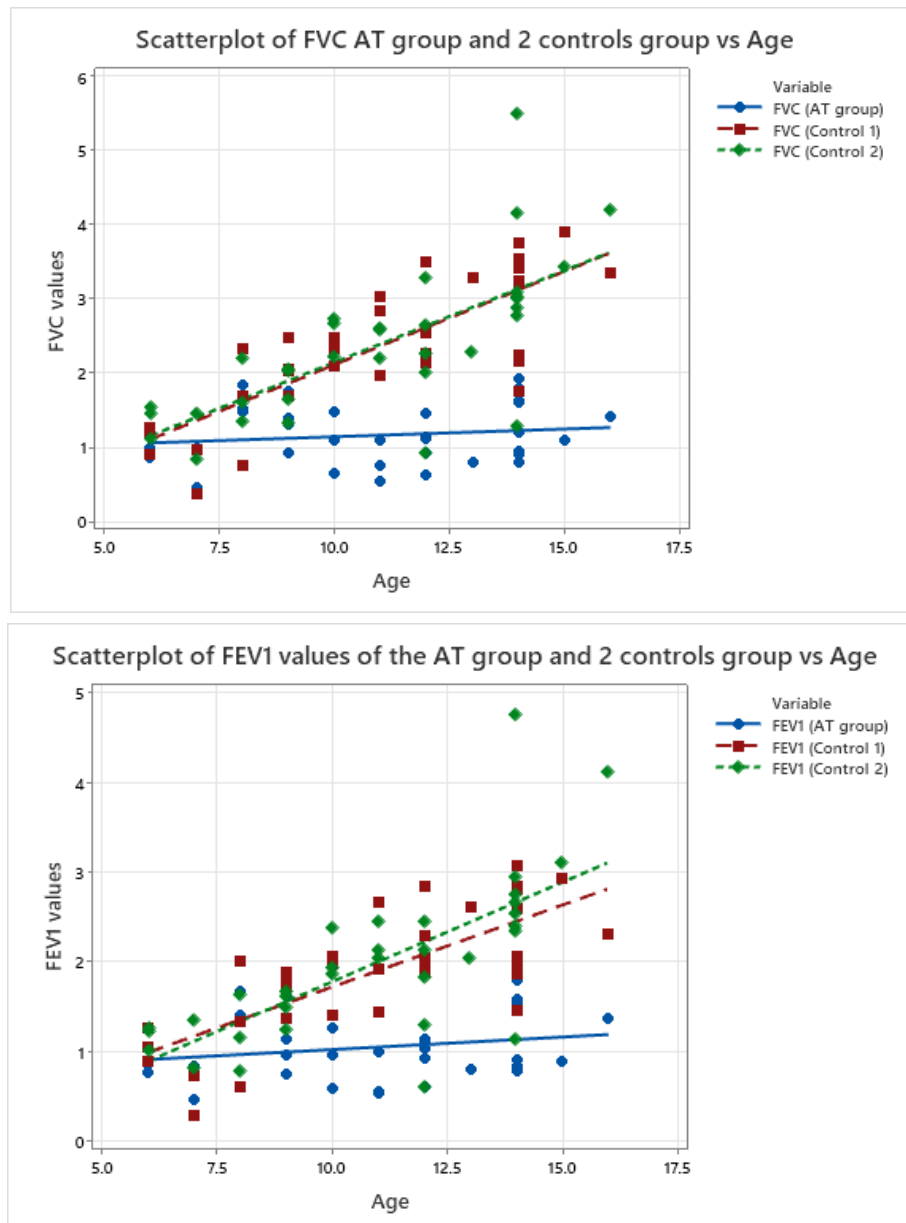


Figure 2-9: Shows the best values of FEV₁ and FVC for AT group and two control groups versus age. Each group is represented in a different colour as shown on the top right in each figure.

2.3.5.1 Lung Function in Children with AT

The correlation between FEV₁ and age was assessed (see Figure 2-10 and Table 2-9). For the purposes of these analyses, the best values obtained were used, irrespective of the ability to complete spirometry with adequate technique. Figure 2-10 shows the best FEV₁ values for 34 children with AT. Pearson's r revealed a poor correlation between the FEV₁ and age ($r=0.22$) (see the table below). Moreover, 1 out of 34 was able to achieve FEV₁ predicted value and only two patients amongst 34 children with AT were able to achieve the lower limit of normal of FEV₁ (see Table 2-10).

Table 2-9: Demonstrates the correlation between the best FEV₁ and age for children with AT.

		Age	The best FEV ₁ for AT group
Age	Pearson Correlation	1	.220**
	Sig. (2-tailed)		0
	N	371	371
The best FEV ₁ for AT group	Pearson Correlation	.220**	1
	Sig. (2-tailed)	0	
	N	371	371
**. Correlation is significant at the 0.01 level (2-tailed).			

Table 2-10: Numbers of children with AT who can achieve predicted and lower limit of normal (LLN) values of FEV₁ and FVC.

Criteria	Results
Achieved predicted FEV ₁	1 out of 34
Achieved predicted LLN of FEV ₁	2 out of 34
Achieved predicted FVC	2 out of 34
Achieved predicted LLN of FVC	3 out of 34

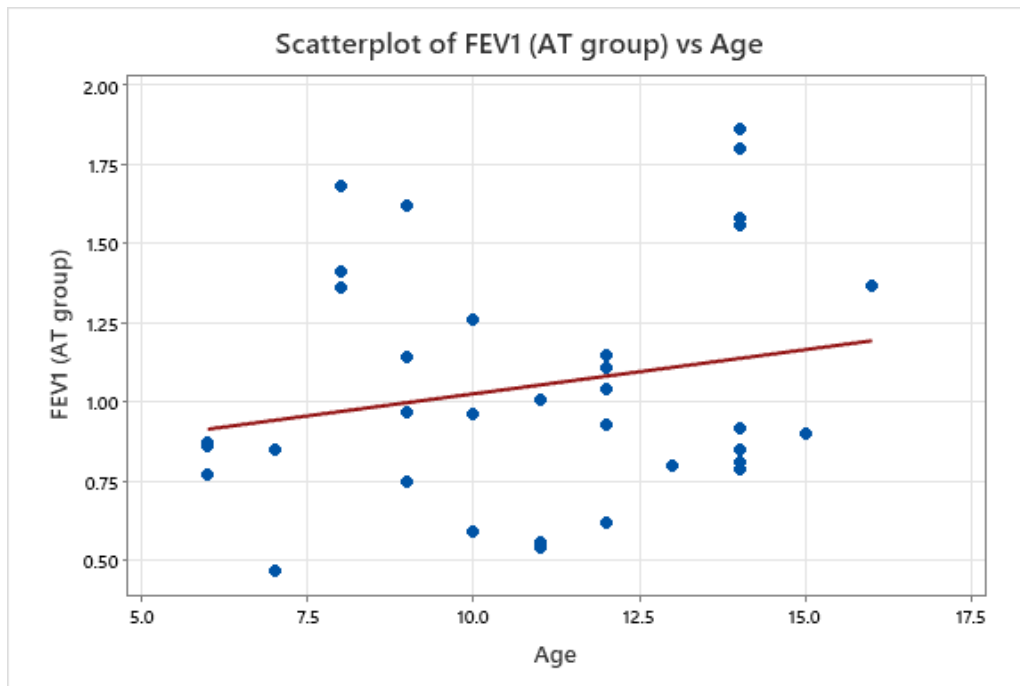


Figure 2-10: Shows the best FEV₁ values of 34 children with AT versus age.

I studied the correlation between FVC and age (see Figure 2-11 and Table 2-11). This figure shows the best FVC values for 34 children with AT. Pearson's r data revealed a weak correlation between FVC and age ($r=0.15$). Moreover, 2 out of 34 were able to achieve FVC predicted value and only three patients were able to achieve the lower limit of normal of FVC (see Table 2-10). Only 1 out of 34 children with AT has been able to achieve the FEV₁ and FVC together. Although this participant was able to achieve predicted FEV₁ and FVC, he was unable to exhale continuously to reach 2 seconds despite seven attempted manoeuvres.

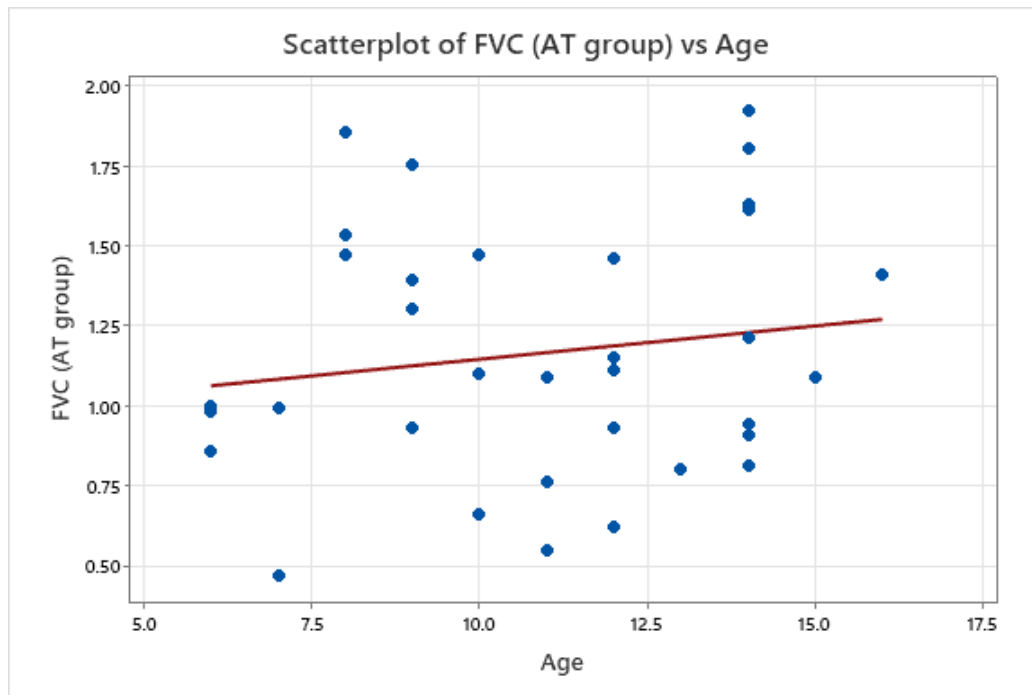


Figure 2-11: Shows the best FVC values of 34 children with AT versus age.

Table 2-11: Demonstrates the correlation between the best FVC and age for the children with AT.

		Age	The best FVC for AT group
Age	Pearson Correlation	1	.158**
	Sig. (2-tailed)		.002
	N	371	371
The best FVC for AT group	Pearson Correlation	.158**	1
	Sig. (2-tailed)	.002	
	N	371	371
**. Correlation is significant at the 0.01 level (2-tailed).			

2.3.5.2 Control Group

The correlation between FEV_1 and age was assessed by scatterplot in Minitab (see Figure 2-12) and Pearson correlation in SPSS (see Table 2-13). This figure shows the FEV_1 values for 68 children with pulmonary

diseases (the control group). Pearson's r revealed a strong positive correlation between FEV₁ and age ($r=0.68$). Moreover, 10 out of 68 achieved the FEV₁ predicted value, and 34 out of 68 were able to achieve the lower limit of normal of FEV₁ (see Table 2-12).

Table 2-12: Demonstrates numbers of the children in control group who achieved predicted and lower limit of normal (LLN) values of FEV₁ and FVC.

criteria	Results
Achieved predicted FEV ₁	10 out of 68
Achieved predicted LLN of FEV ₁	34 out of 68
Achieved predicted FVC	13 out of 68
Achieved predicted LLN of FVC	35 out of 68

Table 2-13: Shows the correlation between the best FEV₁ and age for the participants in the control group.

		Age	The best FEV ₁ for the control
Age	Pearson Correlation	1	.681**
	Sig. (2-tailed)		.000
	N	742	742
The best FEV ₁ for the control	Pearson Correlation	.681**	1
	Sig. (2-tailed)	.000	
	N	742	742
**. Correlation is significant at the 0.01 level (2-tailed).			

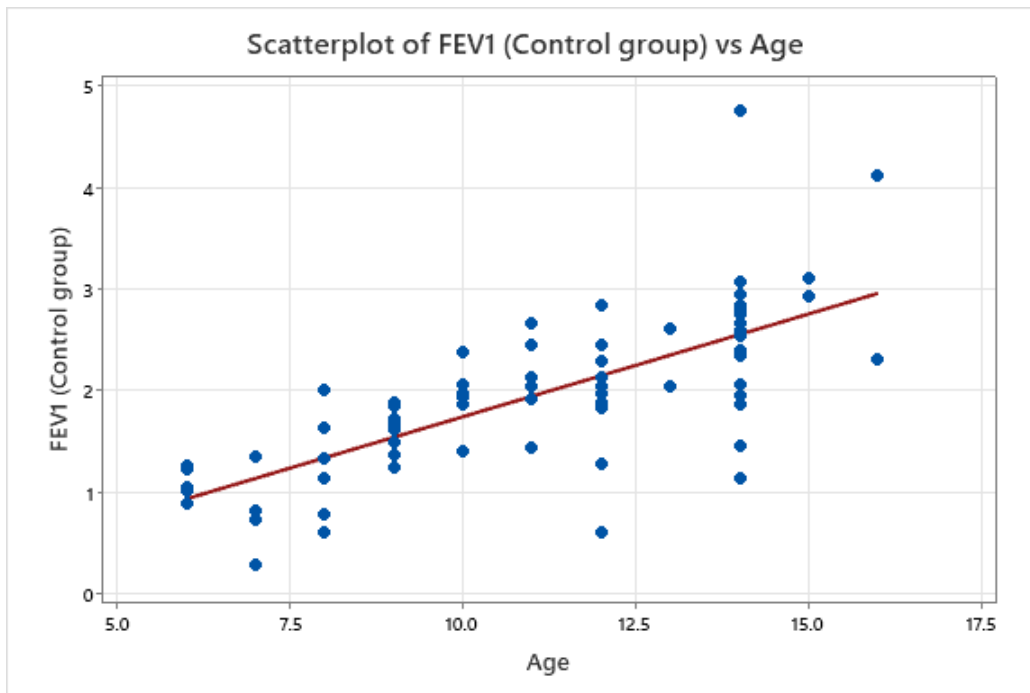


Figure 2-12: Shows the best FEV₁ values of the control group versus age.

The correlation between FVC and age was also assessed (see Figure 2-13 and see Table 2-14). This figure shows the best FVC for the control group. Pearson's r data revealed a strong positive correlation between FVC and age ($r=0.70$). Furthermore, 13 out of 68 successfully achieved the FVC predicted value and 35 out of 68 were able to achieve the LLN of FVC (see Table 2-12).

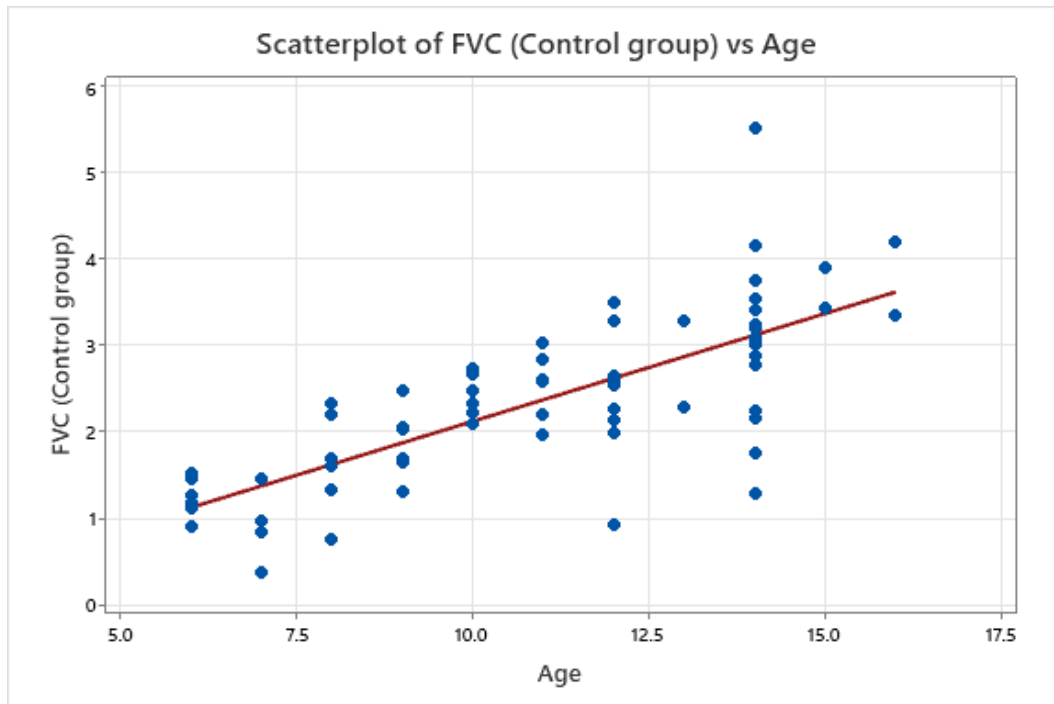


Figure 2-13: Shows the best of FVC values versus age for the control group.

Table 2-14: Correlation between the best FVC and age for the participants in the control group.

		Age	The best FVC for the control
Age	Pearson Correlation	1	.706**
	Sig. (2-tailed)		.000
	N	742	742
The best FVC for the control	Pearson Correlation	.706**	1
	Sig. (2-tailed)	.000	
	N	742	742
**. Correlation is significant at the 0.01 level (2-tailed).			

2.4 Discussion

2.4.1 Findings of the Study in the Context of the Literature

The key objective of this chapter was to assess whether or not children with AT can undertake Spirometry – i.e., is it a feasible test. The second aim was to examine any correlations between age and ability to perform Spirometry among the children. The described patients were compared with a group of children with a range of respiratory conditions acting as a control group of the research, matching controls to AT in a 2:1 ratio. This study showed that it is less feasible for children with AT to perform Spirometry than the control group children.

To explore the correlation between age and the ability to comply with spirometry criteria, children with AT were divided into two groups based on age (the median age is 11); 18 participants aged 11 or under and 16 participants over 11. This study showed that young children with AT were more able to do spirometry to adequate standards (50% were able to perform the test) than the older children with AT (only 12.5% were able to perform the test). Interestingly, the young children with AT were more able to do Spirometry than the older ones. The most likely explanation is that older children with AT increase with age, reducing their ability to coordinate respiratory effort.

The control group was also divided into two groups based on age using the same age cut off; 36 participants aged 11 or under and 32 participants over

11. This study showed that the older children in this 'control' group had a greater capacity to do Spirometry to an adequate standard (91% were able to perform the test) than the younger children did (96% were able to complete the test). This shows that in children referred to a respiratory clinic for problems other than AT, the ability to comply with Spirometry to achieve satisfactory recordings increased with age.

The results of this study were compared with a 2010 study conducted by Viložni. The study aimed to analyse the validity and feasibility of involuntary Spirometry, especially in patients with AT. The main recommendation was that additional studies were required.

In this study, Viložni studied 28 patients with AT, aged 3.7 to 19.3 years. The present study was in children with AT aged 6 to 16 years because in general slightly older children are better able to undertake spirometry; those at the age of below five may face difficulties in applying Spirometry. In the Viložni study, 19 out of 28 conducted Spirometry, and 14 out of 28 were still walking, and 14 out of 28 were destined to use a wheelchair, all at the mean age of 9.0 ± 3.2 years.

Age was also studied in Viložni's study, they found that the AT patients in the study were able to execute the test at a young age when they were given the required assistance and guided accordingly, especially in holding their hands in the right place and controlling the outflow at the mouthpiece. In the study, some curves met reproducibility criteria despite failing to meet the other criteria for Spirometry. In addition, the measures for precise

Spirometry in preschool children were also not met. Regardless of the AT patients failing to conform with all the recommended measures, especially those for tolerable curves at adult ages, the young patient's patients were seen to resemble those children with healthy patterns or those considered to be without respiratory disease (Vilozni et al., 2010).

Vilozni, in the 2010 study also showed that 8/20 patients with AT could not adequately achieve their predicted FEV₁. For instance, once the disease progressed further, the patients were observed to have lower FVC, FEV₁, FEV 0.5, and also PEF values than the ones predicted. In addition, the FEF25 was found to be restrictive in pattern. 11 out of 34 children with AT had satisfactory exhalation in at least two trials in this study.

Furthermore, FEV₁/FVC and/or FEV_{0.5}/ FVC ratios were higher than predicted (Vilozni et al., 2010). As the predicted vital capacity was lower than predicted, the findings matched those of the former findings of McGrath-Morrow et al. (2014). Patients confined to a wheelchair are more likely to deform their posture, which can affect the lungs causing a decrease in the lung's vital capacity (McGrath-Morrow et al., 2014). Comparable observations have been found especially among the patients with Duchenne spinal muscular atrophy and muscular dystrophy (McGrath-Morrow et al., 2014). In this case, it was observed that the FVC tends to depreciate quicker than the FEV₁ or the FEV_{0.5} (% projected).

Another study conducted by Vilozni showed that shared spirometry indices such as the FEV₁/FVC and the FEV₁ are not always accurate in defining the

extent of airway impediment, especially among AT patients (Vilozni et al., 2015). For instance, the FEF25-75 labelled as "mild obstruction" in terms of values identifies a group who appear to have more severe airway impediment among AT patients. FEF25/FVC ratios rose rapidly towards the end-stage of the disease. FVC volume tends to deteriorate along with the tidal volume in late-stage lung disease.

In the work presented here, children, in the control group had a moderate/high positive correlation between their FEV₁ and age ($r=0.68$) and between the FVC and age ($r=0.70$). In addition, 44 out of 68 in the control group achieved predicted FEV₁ and FVC. Furthermore, the number of children unable to reach the lower limit of normal was higher in the AT group than in the control group (see Tables 2-10 and 2-12). As expected in patients referred to a respiratory clinic, even those with adequate spirometry, there is evidence of lung disease. This could occur in AT children because of the neuromuscular disorder, which might cause restrictive lung disorders. In addition, due to immuno-compromise, AT children are more susceptible to pathogenic disease and increased pulmonary infections, which ultimately is a major cause of death in this group of patients.

2.4.2 Strengths and Limitations of the Study

The strength of our study lies in including a control group composed of children without AT but with a range of pulmonary diseases who are also

unfamiliar with spirometry. This novel comparison, absent from the Vilozni and McGrath Morrow studies, allows us to discern the impact of inexperience with spirometry on the effects of AT on lung function. Instead of merely asserting that children with AT struggle with spirometry, we have a control group without AT attempting spirometry for the first time. This enables us to compare children's AT performance against their counterparts. Given the significant role of fatigue in AT, the number of spirometry attempts we can perform with children with AT is limited. Our study design acknowledges this constraint and emphasizes the need for efficient, meaningful data collection, thereby enhancing the reliability of our findings.

A major limitation of this study is the small sample size of patients with AT, despite including half of the entire childhood UK population with AT. This is because AT is a rare disease. Secondly, the time available to perform spirometry was quite limited. Thirdly, a physiologist conducted the experiment, but in routine clinical practice, many spirometry measurements may not be done by a physiologist.

The weaknesses of the post hoc analysis of the impact of age on spirometry should also be considered. This analysis was not planned prior to the initiation of the comparison between AT and controls, and it should be viewed with caution. Additionally, the cut off of 11 years was chosen after the initial data analysis. This result should be viewed as being hypothesis generating and requires confirmation.

At the time of the analysis of the adequacy of spirometry in children with AT compared to controls, it was not possible to blind myself to the status of the child (i.e., AT or otherwise). I had undertaken many of the spirometry tests in AT myself, and these are often very recognisable from the spirogram trace. In future comparisons, the assessor of the spirometry and the person undertaking the spirometry should be different people in order to blind the assessor from the status of the child.

2.5 Conclusion

In conclusion, these results showed that the children with AT find it difficult to comply with spirometry for a range of reasons. Moreover, I found two-third of the children with AT were unable to perform spirometry to an adequate level. Since the spirometry technique needs co-ordinated effort to be used successfully, children with AT find it difficult perform. Overall, in conclusion, although spirometry is undertaken in AT, the results of spirometry are often not valid.

Therefore, in the next chapter of my thesis, I assess LCI as an alternative method of evaluating lung function, which might be more reliable in this group of patients. The main advantage of this technique over spirometry is that there is no need for any forced expiratory effort as the technique is dependent on tidal breathing. Interestingly, the LCI technique has not been applied in AT patients to date.

Chapter 3

Assessing Feasibility of performing Lung Clearance Index (LCI)

Measurements in patients with Ataxia Telangiectasia

3.1 Introduction

As an assessment technique for respiratory health, LCI is growing in importance worldwide. It is potentially a useful technique which can be used to improve diagnosis and management of respiratory issues. For example, in patients with conditions such as cystic fibrosis (CF), non-cystic fibrosis bronchiectasis (NCFB) and asthma LCI could be used as a clinical tool to provide physiological information about lung health. LCI is a measure of abnormal ventilation distribution that is derived from the multiple breath inert gas wash-out (MBW) technique.

Interestingly, although LCI is considered a safe, reproducible, and non-ionising technique, it has not been used on patients with AT. All the features of LCI have motivated me to investigate its potential use in these patients.

As discussed in previous chapters, patients with AT are more vulnerable to lung infections, which constitutes one of the main causes of death (Yeo et al., 2019). As mentioned before, AT is characterised by immunodeficiency and radiosensitivity; hence assessment techniques are required to avoid exposure to ionising radiation (Yeo et al., 2019).

To date, many of the paediatric studies assessing LCI have been performed in patients suffering from CF where it is being explored for use as an outcome measure in CF and NCFB (Bhatt, 2013).

3.1.1 Overall Aim

The main aim of the work described in this chapter was to assess the feasibility of performing LCI in children and young adults with AT. At the outset of this study, we were concerned that children with an ataxic neurological disease associated with involuntary movements may not be able to remain still enough for LCI to be feasible. The secondary aim was to obtain pilot data derived from LCI, such as LCI2.5 and LCI5, as an initial assessment of their suitability as clinical trial endpoints.

3.1.2 Hypothesis

The hypothesis underlying in this chapter is that in patients with AT, LCI could be a more suitable technique for monitoring their lung function and may provide useful physiological information about lung disease. Moreover, LCI has not applied yet on those patients. Anecdotal evidence from the National Clinic was that some children could perform advanced lung function tests. It is hypothesised that it is feasible for over half of children with AT to undertake LCI.

3.1.3 Objectives

- 1- To determine the feasibility of LCI in patients with AT.
- 2- To determine the relationship between the age and the ability to comply with LCI criteria.
- 3- To evaluate LCI parameters (LCI2.5, LCI5, and FRC) for AT patients and explore relationships between these and height, weight, and age.

3.2 Method and Materials

This study was ethically approved by the National Research Ethics Service (NRES) and the Health Research Authority (HRA) (ethics number 17/EM/0149) and designed as a longitudinal study for three years. Our original aim was for twenty-five children with AT aged 6-16 to be recruited from the AT clinic to perform LCI within the ImaginAT study, and for all the participants to have the LCI measured yearly for three years. Unfortunately, the initial design has had to be changed due COVID-19.

This study commenced in 2018, when 15 children with AT were recruited. Before the first set of follow up tests could be conducted, the COVID-19 pandemic started, and the policy of lockdown started applying globally. As mentioned before, as lung infection is the main cause of death for people with AT; therefore, the study follow up was suspended. Consequently, the method was changed; this thesis presents data on the first part of the cohort (15 children with AT). LCI test procedures were explained, and informed consent obtained.

3.2.1 LCI Testing Procedure

In the Nottingham clinic, LCI is undertaken by at least two members of staff. However, in undertaking LCI on children with neuro-disability, we ideally have 3 members of staff – one to operate the Prolab, one to hold the face mask on the participant, and one to observe for breathing irregularities and / or air leaks.

At least one member of staff is required to have the European Cystic Fibrosis Society-Clinical Trials Network (ECFS-CTN) accreditation. In the case of this study, A Prayle and C Youle are the certified members of staff, and the author assisted with the LCI.

The LCI device used was ndd EasyOne Pro Lab, (Switzerland) (see Figure 3-1). This device was used in this study because it allows both LCI and spirometry to be measured; it is the only commercially available machine that does this. Additionally, it is a portable device, which meant that the device could be moved from the lung laboratory to the physiology suite of the Sir Peter Mansfield Imaging Centre (SPMIC) and therefore the LCI could be done in the same visit as the MRI scans.

LCI was measured using a modified version of the ECFS-CTN guidelines. Rather than a mouthpiece, which children with neurodisability struggle to make a seal with an unvented single use anaesthetic face mask appropriately sized for the face was used (Economy anaesthetic face mask, Intersurgical, UK).

The patient was sat either in their wheelchair, or on a standard seat for the duration of the test. The equipment was shown to the participant, and the noise which the machine makes during washout was demonstrated (as this can cause an exaggerated startle reaction in children with AT). A MBW was commenced with the face mask held gently onto the face, with the second operator controlling the Prolab, whilst the third operator observed for leaks at the face mask and breathing consistency. When the patient had settled

into relaxed tidal breathing, the washout was manually commenced. A total of up to 4 trials were allowed but usually only two were required.

3.2.1.1 Criteria for a Successful Trial

We considered the ability to achieve a LCI5 without leakage as a successful LCI trial. These criteria were derived from European Respiratory Society (ERS) criteria: (Robinson et al., 2013) and are summarised below:

1. The similarity in the first four breaths before the wash out. The maximum and minimum variation must be $\leq 10\%$ of the mean.
2. The similarity in the first three breaths after the wash out. The maximum and minimum variation must be $\leq 10\%$ of the mean.
3. Trajectory consistency. The nitrogen concentration should decrease consistently with each breath, following an approximate exponential decay pattern.
4. Avoiding leakage. This can be seen where the leak appears as a sudden spike in N_2 concentration.
5. LCI5. Where the wash out should continue until the end-tidal marker has fallen below $1/20^{\text{th}}$ of the starting concentration over several breaths. over three subsequent breaths.
6. LCI2.5. Where the wash out should continue until the end-tidal marker has fallen below $1/40^{\text{th}}$ of the starting concentration over several breaths. over three subsequent breaths.

3.1.1.2 Test Supervision

Tests were supervised by Dr. Prayle, the head of the project, the responsible nurse, and me. I was directly involved in all of the work described in this study under the clinical supervision of Dr. Prayle, the head of the project and the research nurse. This included directly undertaking the LCI measurements under supervision. Moreover, I have analysed all the LCI data presented.

3.1.1.3 LCI Analysis

LCI traces were analysed off-line using WBreath Research Tool V3.52.3 (nDD). This software automatically calculates the LCI parameters from the washout raw data. Additionally, it allows inspection of the traces manually to identify leaks. Individual traces were inspected to identify leaks and to observe for consistency in tidal breath volume.

3.1.1.4 Statistical Analysis

The study population was divided into two groups depending upon age. We divided the 15 participants into two groups using the median age (9 years) as the cut off.

Demographic data were described narratively. The one proportional test in Minitab was used to determine whether there were statistically significant differences between the groups in their ability to comply with LCI's criteria, taking $p < 0.05$ as the pre-specified threshold for statistical significance.

The chi square test in SPSS was used to determine if there were statistically significant differences between the groups in their ability to comply with LCI's criteria, taking $p < 0.05$ as the pre-specified threshold for statistical significance. Additional analyses to look for correlations between age, height, weight and LCI variables (LCI2.5, LCI5 and FRC) were performed using linear regression. In this study, these values LCI2.5, LCI5, and FRC were derived from the ndd spirometry device (see Figure 3-1). They automatically were calculated (see Table 3-3).



Figure 3-1: Shows the ndd EasyOne Pro Lab Spirometer which was used in the study. The parts of the machine have been explained in the introduction section.

3.2.2 Study Inclusion Criteria/ Exclusion Criteria

3.2.2.1 Inclusion Criteria – for the service improvement project.

- Children who attended the AT clinic at a time when we had Prolab in the clinic.
- Aged between 6 to 20 years.
- The cohort of control patients who attended the clinic with a range of pulmonary diseases matched the gender and age of children with AT a time when we had Prolab in the clinic.

3.2.2.2 Inclusion criteria – for the ImaginAT study

Because the children studied with AT were attending as part of the ImaginAT study I have also included the inclusion/exclusion criteria for this study below:

- Diagnosis of AT (or an AT like syndrome) attending the National Paediatric AT clinic.
- Judged by the investigator and the parents that the participant would be able to lie relatively still in an MRI scanner for 15 minutes.
- Aged less than 20 years at consent, and over 5 years.

2.2.2.4 Exclusion criteria– for the ImaginAT study

The ImaginAT study protocol included exclusion criteria pertaining to (for example) MRI exclusion criteria such as metal implants and claustrophobia.

These were as follows:

- Standard MRI exclusion criteria – a history of implanted / indwelling magnetically active material.

- Participation in another research study which excludes participation in an observational cohort study such as the ImaginAT study.
- Participant not deemed fit enough to tolerate procedure.

Participant deemed unsuitable due to being unlikely to comply with instructions or tolerate scanning.

3.3 Results

3.3.1 Study Recruitment and Study Population Characteristics

Fifteen children (9 males and 6 females of different ethnicities), who had been diagnosed with AT were initially approached to take part in the study (Figures 3-2 and 3-3; Table 3-1). Their parents or legal guardians gave consent. Thirteen of the children underwent a lung clearance index test (LCI) using a Pro Lab device (Figure 3-1).

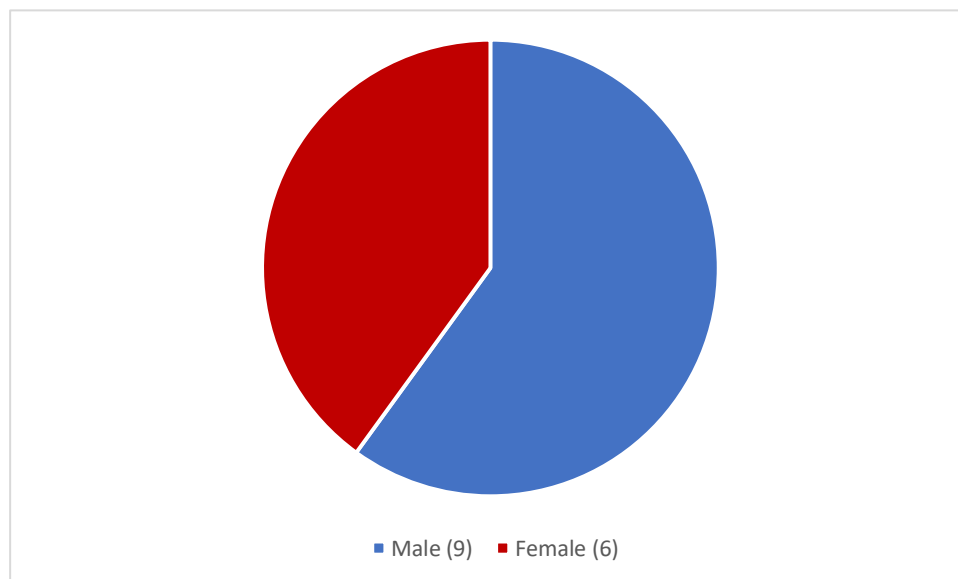


Figure 3-2: Gender distribution for AT participants.

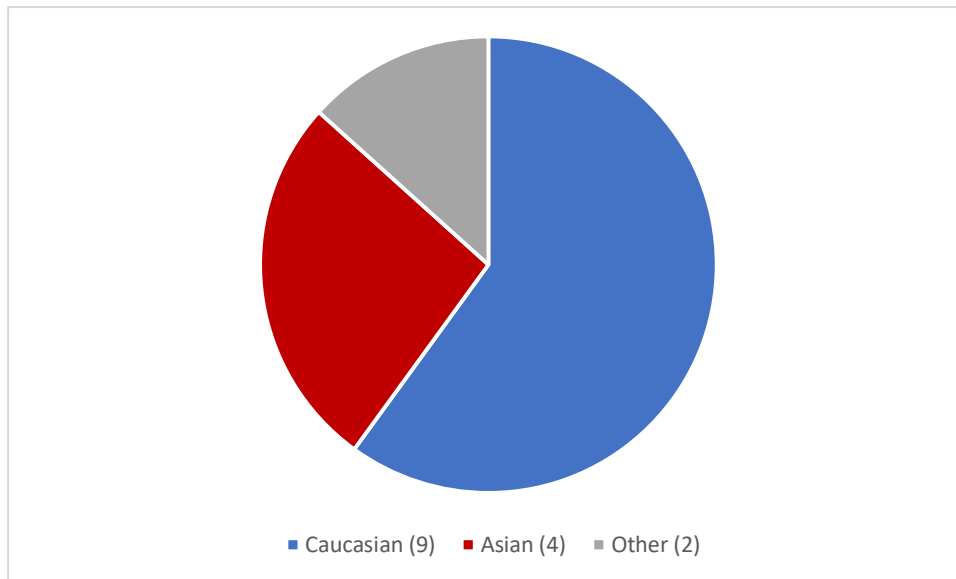


Figure 3-3: Ethnicity distribution for the AT participants. 'Others' indicates race was not recorded in the PRO LAB device.

Table 3-1: Characteristics of the AT group.

Descriptive Parameter		Statistical Results
Age (Median, Range)		9 years, 6 – 14 years
Sex (%)		Male= 60%
		Female= 40%
Ethnicity	Caucasian	9
	Asian	4
	Other	2
Height (cm) Median (Range)		131 (109 to 151.3)
Height Z Score Median (Range)		-1.15 (-3.97 / 1.31)
Weight (kg) Median (Range)		31 (17 to 45)
Weight Z Score Median (Range)		-0.55 (-4 to 1.3)
BMI (kg/m ²) Median (Range)		16.6 (14.3 to 25.2)

The study population is summarised in Table 3-1, which provides detailed data regarding the physical characteristics such as age, sex, ethnicity, height and weight.

Figure 3-4: Displays the final consort diagram of this study.

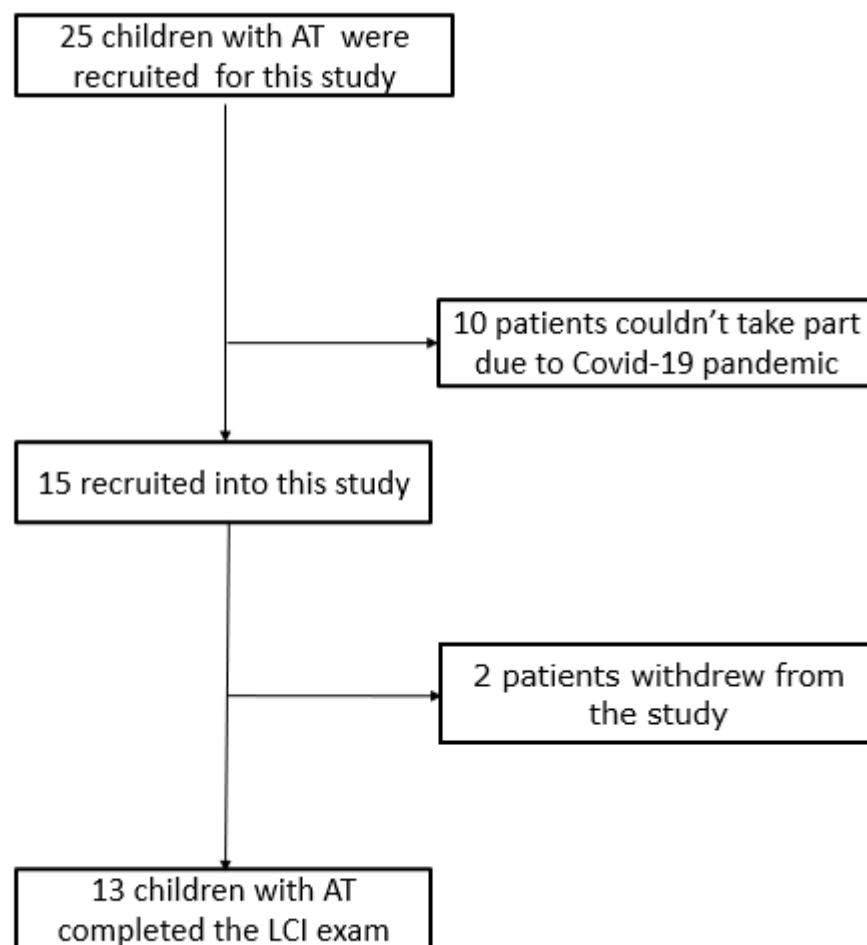


Table 3-2: Descriptive characteristics of individuals in the AT group. Ethnicity was categorised according to the per-specified groups within the nDD device, which are linked with GLI equations. Therefore, several ethnicities have to be coded as “other” (this is a limitation in this device). The Z score compares a child's weight or height to the population weight of children in the same age group and represents the number of standard deviations from the mean. The Z scores values were calculated by the first link below. BMI means the body mass index which is a measure that measures the weight and height to determine the weight mass status. Where an ideal BMI is from 18.5 to 24.9 for adults. Children and adolescents aged from 2 to 18, given the age, gender, height, and weight are all factors in calculating the BMI. Values of 18.5 to 24.9 are healthy, from 25 to 29.9 is overweight, and from 30 to 39.9 is obese. These BMI values were calculated by the NHS website which is below the second link.
¹(<https://www.bcm.edu/bodycomplab/BMIapp/BMI-calculator-kids.html>).
²(<https://www.nhs.uk/live-well/healthy-weight/bmi-calculator/>).

NO.	Age	Sex	Race	Height	Height Z score	Weight	Weight Z score	BMI
1	12	Male	Caucasian	125 cm	-3.97	24 kg	-4	15.4
2	14	Female	Caucasian	137 cm	-3.7	33 kg	-2.98	17.6
3	14	Female	Asian	151 cm	-1.6	42 kg	-1.21	18.4
4	14	Female	Asian	151.3 cm	-1.56	45 kg	-0.75	19.7
5	9	Male	Asian	126 cm	-1.71	40 kg	1.3	25.2
6	12	Male	Caucasian	141 cm	-1.35	30 kg	-1.96	15.1
7	6	Male	Caucasian	119 cm	-0.13	21 kg	-0.42	14.8
8	8	Male	Other	125 cm	-0.97	27 kg	0	17.3
9	8	Female	Caucasian	129 cm	-0.44	35 kg	1.08	21
10	9	Male	Other	145 cm	1.31	35 kg	0.74	16.6
11	11	Male	Caucasian	141 cm	-1.01	31 kg	-1.44	15.6
12	7	Female	Asian	109 cm	-2.81	17 kg	-2.52	14.3
13	7	Female	Caucasian	121 cm	-0.77	23 kg	-0.38	15.7
14	9	Male	Caucasian	132 cm	-1	29 kg	-0.55	16.6
15	9	Male	Caucasian	131 cm	-1.15	33 kg	0.2	19.2

Table 3-3: This table shows the LCI parameters for all of the participants. (*) means this participant has no data due to withdrawal. Time means the period of the test and breath's number shows the number of breaths in this period. N₂% means the nitrogen concentration before starting pure O₂. The nitrogen concentration should decrease consistently with each breath until reaches gas concentration to 1/40th of the initial concentration (LCI2.5) and to 1/20th of the initial concentration (LCI5). FRC is functional residual capacity and CEV is cumulative expired volume.

NO.	Age [year]	Time [s]	N ₂ [%]	CEV [L]	LCI2.5 [L]	LCI5 [L]	FRC [L]	Number of breaths
1	12	162.1	78.64	0.00	9.22	7.52	0.934	43
2	14	153.4	80.46	0.00	11.87	10.54	1.032	67
3	14	138.6	78.54	9.50	9.91	8.04	0.961	44
4	14	158.1	78.05	10.54	8.81	7.25	1.196	49
5	9	98.11	79.01	7.75	10.83	6.67	0.715	49
6	12	158.6	79.11	11.75	10.35	7.93	1.140	67
7	6	143.4	79.15	9.12	10.86	8.54	0.839	69
8	8	136.9	78.75	8.49	8.11	6.27	1.045	30
9	8	*	*	*	*	*	*	*
10	9	130.3	78.8	10.48	8.88	6.71	1.182	45
11	11	203.7	78.08	11.60	7.91	6.18	1.469	64
12	7	176	79.13	7.34	9.73	7.64	0.753	56
13	7	*	*	*	*	*	*	*
14	10	201	78.85	9.37	10.23	7.49	0.971	59
15	9	145.3	78.93	9.28	9.76	7.11	0.950	53

Table 3-4: Shows the overall summary of the LCI data.

LCI's parameter	All participants (n= 13)	Participants with acceptable quality control (n= 11)
LCI2.5 (Median, IQR)	9.76 (1.47)	9.76 (1.445)
LCI5 (Median, IQR)	7.49 (1.22)	7.25 (1.095)
FRC (Median, IQR)	0.971 (0.206)	1.032 (0.205)

Chapter 3

Table 3-5: This table demonstrates and summarises the ability of participants to comply with criteria for LCI for all the participants in this study (13 children with AT).

Criteria \ Participants NO.	I01	I02	I03	I04	I05	I06	I07	I08	I10	I11	I12	I14	I15
Number of attempts	2	2	2	2	4	3	3	3	4	3	3	2	3
The selected attempt number	2	1	2	2	2	2	3	3	4	3	2	2	3
The mean of the 4 breaths preceding the washout	0.266	0.218	0.272	0.291	0.142	0.187	0.393	0.491	0.325	0.185	0.248	0.252	0.208
The maximum difference from the mean in % of the first 4 breaths after washout	9.02%	41.5%	20.9%	16.4%	76.7%	25.1%	45.4%	41.7%	15%	65.9%	32.6%	99.2%	73.3%
The minimum difference from the mean in %	12%	57.5%	18.7%	13.4%	61.2%	19.2%	35.8%	40.3%	18.1%	36.7%	22.1%	69.7%	43.5%
Meet the <10% criteria from the mean	NO	NO	NO	NO	NO	NO	NO	NO	NO	NO	NO	NO	NO
The mean of the 3 breaths after washout	0.210	0.165	0.261	0.329	0.275	0.225	0.199	0.391	0.368	0.242	0.196	0.251	0.243
The maximum difference from the mean in %	20.4%	43.1%	25.4%	23.7%	24%	10.6%	63%	20.2%	14.9%	17.7%	12.2%	12.5%	29.8%
The minimum difference from the mean in %	33.3%	44.2%	29.8%	31.6%	12%	5.33%	54%	21.4%	11.1%	30.5%	16.8%	22.9%	33%
Meet the <10% criteria from the mean	NO	NO	NO	NO	NO	NO	NO	NO	NO	NO	NO	NO	NO
Trajectory	NO	NO	YES	YES	YES	YES	YES	NO	NO	NO	NO	YES	YES
Leaks	NO	NO	NO	NO	NO	NO	NO	NO	NO	NO	NO	NO	NO
LCI5	YES	YES	YES	YES	YES	YES	YES	YES	YES	YES	YES	YES	YES
LCI2.5	NO	NO	YES	YES	YES	YES	YES	YES	YES	YES	YES	YES	YES

3.3.2 The Ability of Children with AT to Undertake LCI

This was primarily a feasibility study, but as we had undertaken measurements of LCI, we undertook an exploratory analysis. We planned a statistical analysis of older vs younger participants after we found the difference in feasibility of spirometry when comparing older vs younger participant. The neurological disease can rapidly progress after the age of 9 years, which was also the median age of participants in the LCI study, and so we used this as a cut off to compare older vs younger participants. We did not use the same cut off of 11 years used for the spirometry study, as this would have led to a severe imbalance in the size of the groups. I have presented the findings of the analysis (which showed no evidence of a difference) but acknowledge the very small sample size.

Thirteen children with AT underwent the LCI technique; of these, 11 (84.6%) could satisfactorily undertake LCI. We defined the ability to undertake LCI as being able to continue tidal breathing during the washout until LCI5 was achieved without leakage diagnosed on the LCI trace (see Methods).

Next, I explored LCI quality control criteria and the ability of children with AT to meet them. It is clear from Figure 3-5 and Table 3-6, that two criteria (the first four breaths before the wash out and the first three breaths after the wash out) are considered the most difficult criteria for children with AT to comply with, as none of the children were able to fulfil them. However,

all the participants were able to achieve LCI5 and maintain no leakage. Two were unable to fulfil the LCI2.5 criterion. Finally, 11 out of 13 were able to fulfil the trajectory consistency criteria.

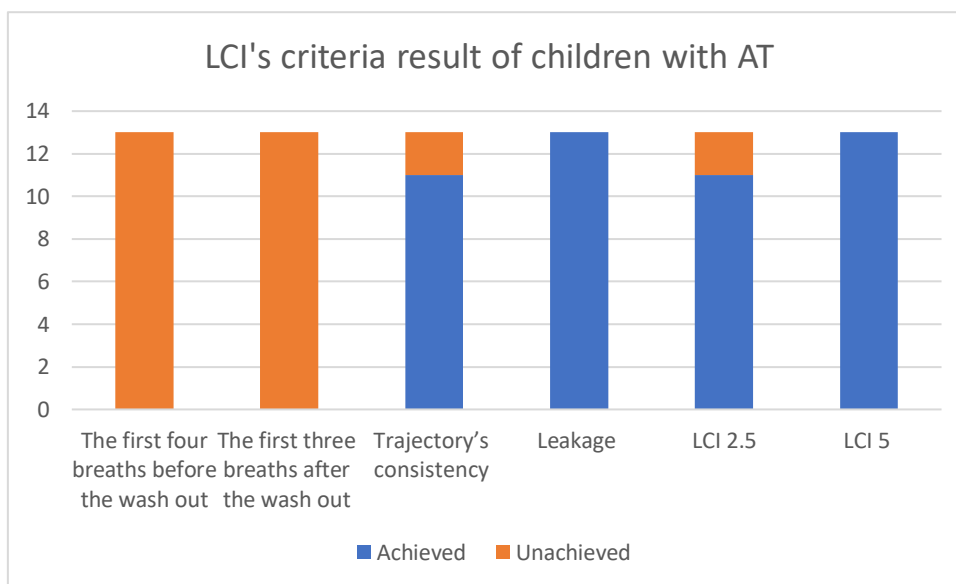


Figure 3-5: Demonstrates the ability of AT subjects (13 patients) to comply with European respiratory criteria.

Table 3-6: Demonstrates the potential of comply with LCI's criteria for children with AT.

Criteria	Achieved criteria (%)
The first four breaths before the wash out	0 / 13 (0%)
The first three breaths after the wash out	0 / 13 (0%)
Trajectory's consistency	11 / 13 (84%)
Leakage (i.e., no leakage observed)	13 / 13 (100%)
LCI5 achieved	13 / 13 (100%)
LCI2.5 achieved	11 / 13 (84%)

3.3.3 The Relationship between the Age and the Ability to Apply LCI Technique

I undertook a preliminary analysis exploring the effect of age by dividing the sample into two groups depending upon the participant's age. The first group had seven participants, whose age was less than or equal to 9 years. The second group had six participants, whose age was greater than 9 years. The chi square test was used to evaluate the two groups statistically to determine which group could comply with LCI's criteria.

The null hypothesis (H_0) was that there is no difference between the two groups in terms of ability to comply with LCI's European respiratory criteria and obtain acceptable results. H_1 : there is a difference between the two groups in terms of ability to comply with LCI's European respiratory criteria and obtain acceptable results.

Table 3-7: Demonstrates the LCI's parameters for the first group those aged over 9 years. Test status which was accepted after achieving LCI's criteria.

NO.	Age	Sex	CEV0	CEV5	FRC	LCI2.5	LCI5	Status
1 (1)	12	M	0	6.97	0.934	9.22	7.52	unaccepted
2 (2)	14	F	0	10.67	1.032	11.87	8.93	accepted
3 (3)	14	F	9.5	7.64	0.961	9.91	8.04	accepted
4 (4)	14	F	10.54	8.63	1.196	8.81	7.25	accepted
5 (6)	12	M	11.75	8.8	1.14	10.35	7.93	accepted
6 (11)	11	M	11.6	9.09	1.469	7.91	6.18	accepted

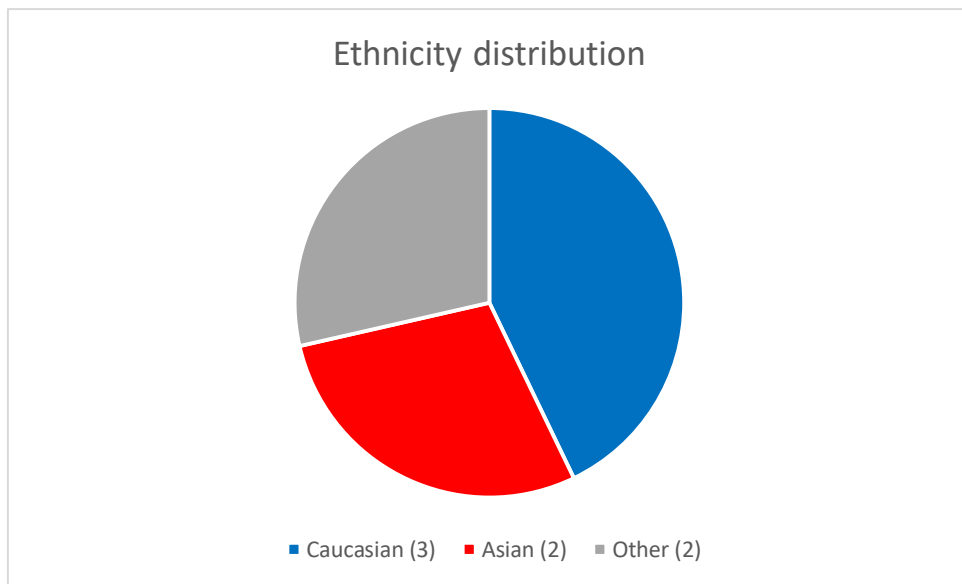


Figure 3-6: Ethnicity distribution for the AT participants in group1.

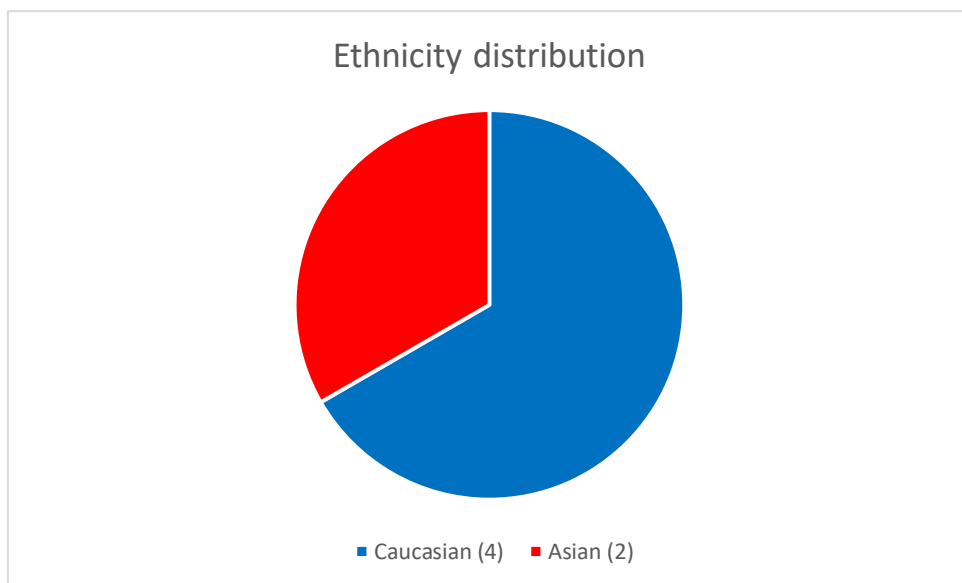


Figure 3-7: Ethnicity distribution for the AT participants in group2.

Table 3-8: Demonstrates the LCI's parameters for the first group, those aged ≤ 9 years. Test status which was accepted after achieving LCI's criteria. As noted above, none of the participants met two of the criteria (the first four breaths before the wash out and the first three breaths after the wash out).

NO.	Age	Sex	CEV0	CEV5	FRC	LCI2.5	LCI5	Status
1 (5)	9	M	7.75	4.53	0.715	10.83	6.67	accepted
2 (7)	6	M	9.12	7.01	0.839	10.86	8.54	unaccepted
3 (8)	8	M	8.49	6.41	1.045	8.11	6.27	accepted
4 (10)	9	M	10.48	8.38	1.182	8.88	7.16	accepted
5 (12)	7	F	7.34	5.62	0.753	9.73	7.64	accepted
6 (14)	9	M	9.37	6.64	0.971	10.23	7.49	accepted
7 (15)	9	M	9.28	6.55	0.95	9.76	7.11	accepted

Table 3-9: Descriptive characteristics of both AT groups those were divided based on the age (>9 and ≤ 9 years).

Criteria	>9	≤ 9
Height (Median)	126 cm	141 cm
Weight (Median)	29 kg	32 kg
Gender	6 Male/ 1 Female	3 Male/ 3 Female

Table 3-10: Shows the result of the chi square test used to determine the ability to comply with LCI's criteria for both groups of children with AT using Minitab.

Children with AT	Accepted results	Unaccepted results	p-value
Children with AT ≤ 9	6	1	0.906
Children with AT >9	5	1	

It is evident from the chi square result that there is no difference between the two groups in terms of the ability to comply with LCI's criteria and obtain acceptable results. The significance value was 0.906, and chi square statistic was 0.014 which is less than the result in chi square distribution (3.84). The reasons for failure to meet criteria for the whole population (divided by age) are shown in table 3-11 and figures 3.8 and 3.9.

Table 3-11: Shows the LCI's criteria and the potential of complying with them for both groups of children with AT (>9 years and ≤9 years).

Criteria	>9	≤9
The first four breaths before the wash out	0/6 (0%)	0/7 (0%)
The first three breaths after the wash out	0/6 (0%)	0/7 (0%)
Trajectory's consistency	5/6 (83%)	6/7 (83%)
Leakage	6/6 (100%)	7/7 (100%)
LCI2.5	4/6 (67%)	7/7 (100%)
LCI5	6/6 (100%)	7/7 (100%)

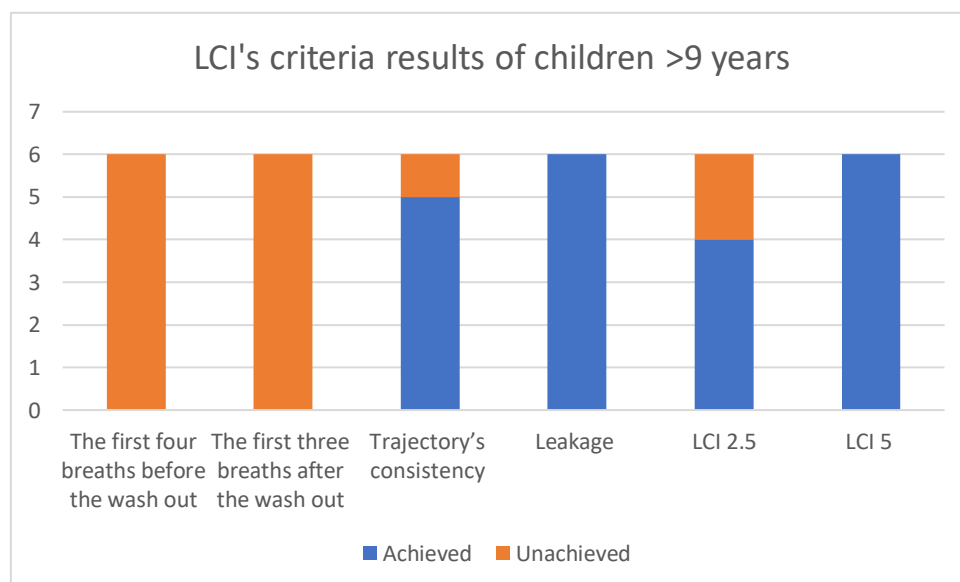


Figure 3-8: Demonstrates the ability of children with AT >9 years (6 patients) to comply with European respiratory criteria.

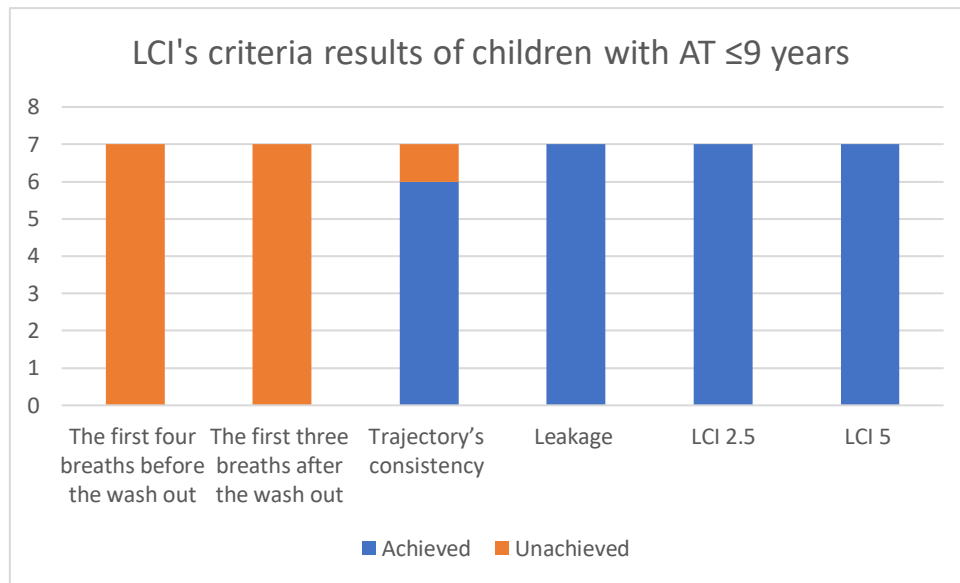


Figure 3-9: Demonstrates the ability of children with AT ≤9 years (7 patients) to comply with European respiratory criteria.

3.3.4 The Relationship between Age and LCI2.5, LCI5, and FRC

3.3.4.1 The Relationship between Age and LCI2.5 values

In addition, I studied the relationship between LCI2.5 and age using a scatterplot and regression in SPSS (see Figure 3-10). There was no relationship between LCI2.5 and the age ($R^2= 0.004$).

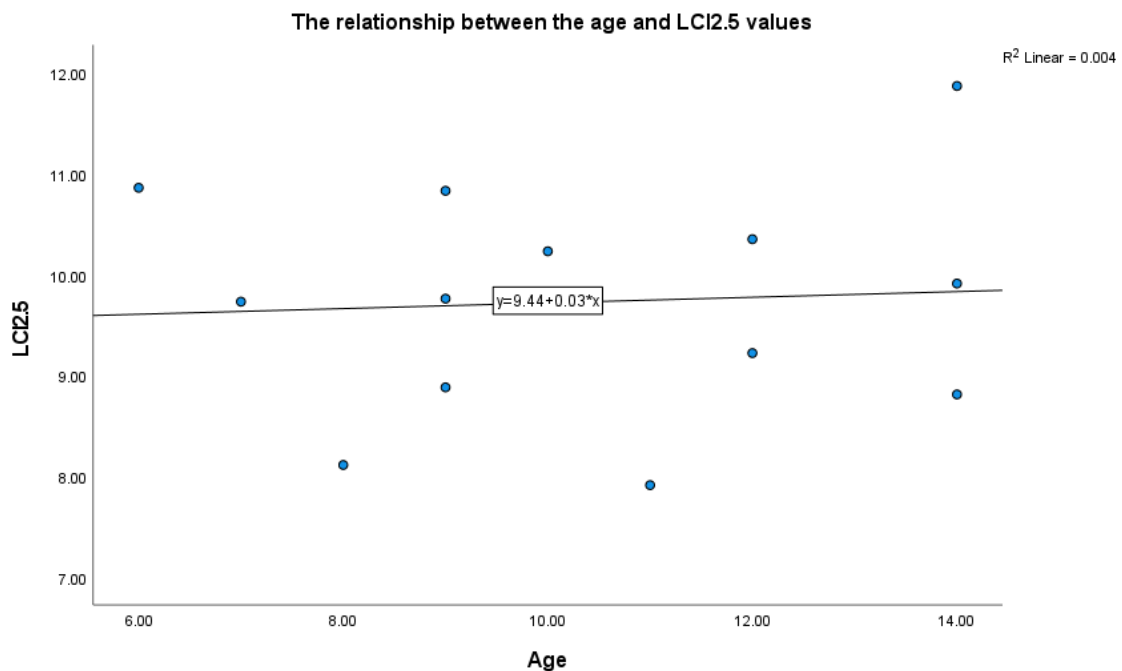


Figure 3-10: Shows the relationship between the age and LCI2.5 values for 13 children with AT using scatter plot with linear regression in SPSS.

3.3.4.2 The Relationship between Age and LCI5 values

The relationship between LCI5 and age was explored using a scatterplot and regression in SPSS (see Figure 3-11). There was a very weak relationship between LCI5 and age ($R^2 = 0.118$).

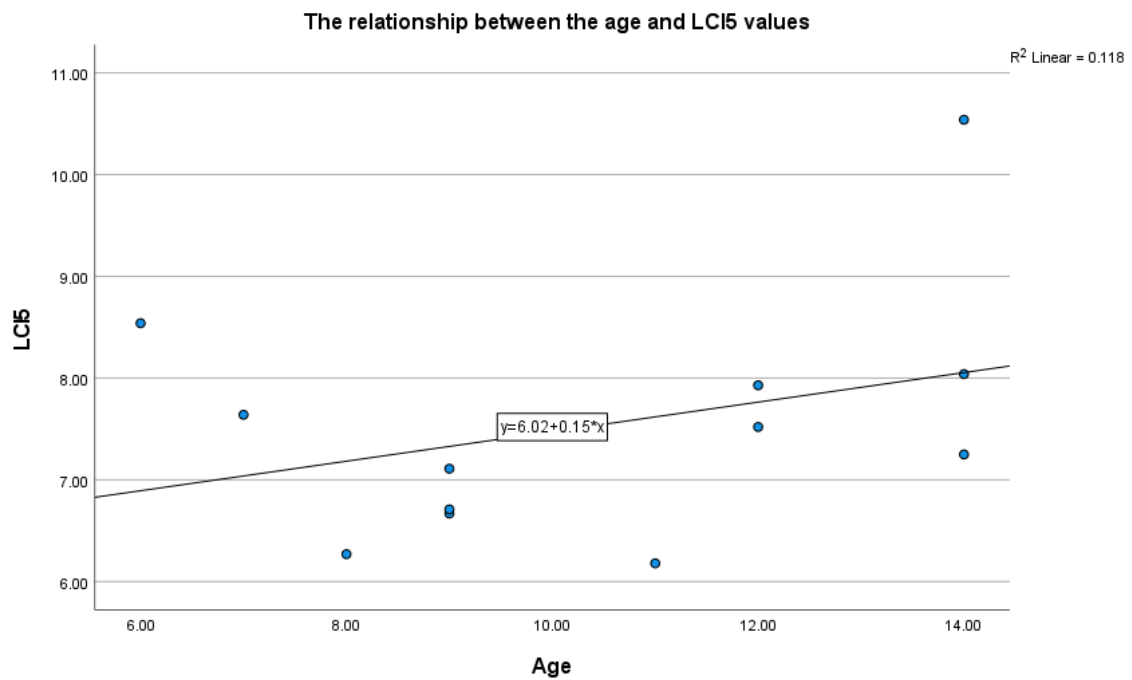


Figure 3-11: Shows the relationship between the age and LCI5 values for 13 children with AT using scatter plot with linear regression in SPSS.

3.3.4.3 The Relationship between Age and FRC values

The relationship between FRC and age was elucidated from a scatterplot and regression in SPSS (see Figure 3-12). There was a very weak relationship between FRC and age ($R^2 = 0.178$).

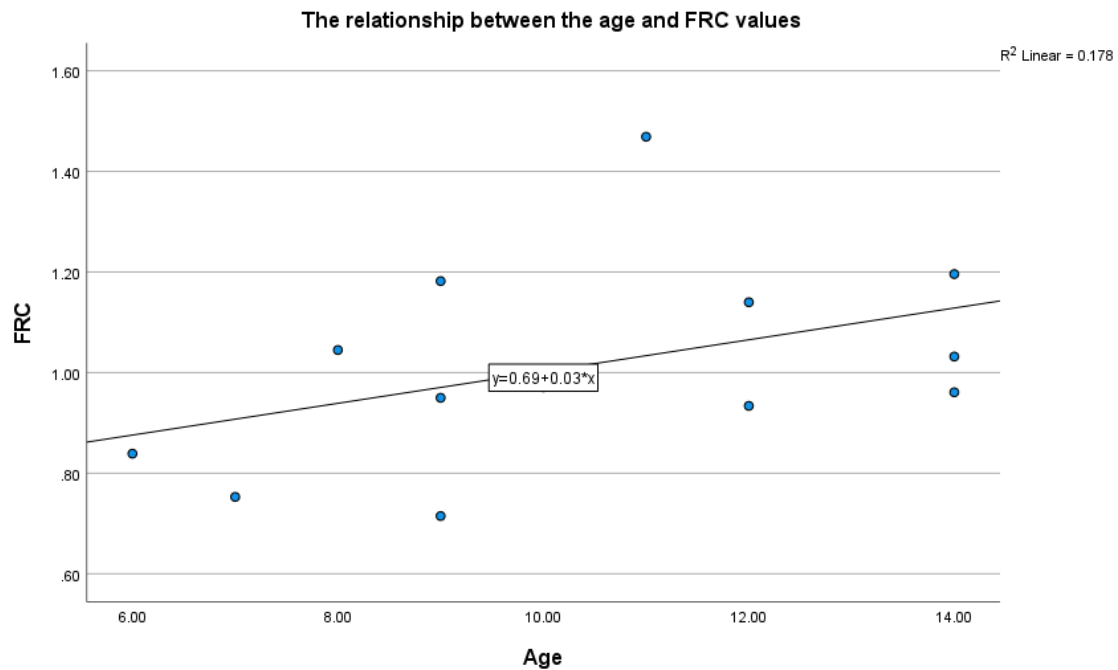


Figure 3-12: Shows the relationship between the age and the FRC values for 13 children with AT using scatter plot with linear regression in SPSS.

3.3.5 The Relationship between Height against LCI2.5, LCI5, and FRC

3.3.5.1 The Relationship between Height and LCI2.5 values

Furthermore, I studied the relationship between LCI2.5 and height by scatterplot and regression in SPSS (see Figure 3-13). There was no relationship between LCI2.5 and height ($R^2 = 0.034$).

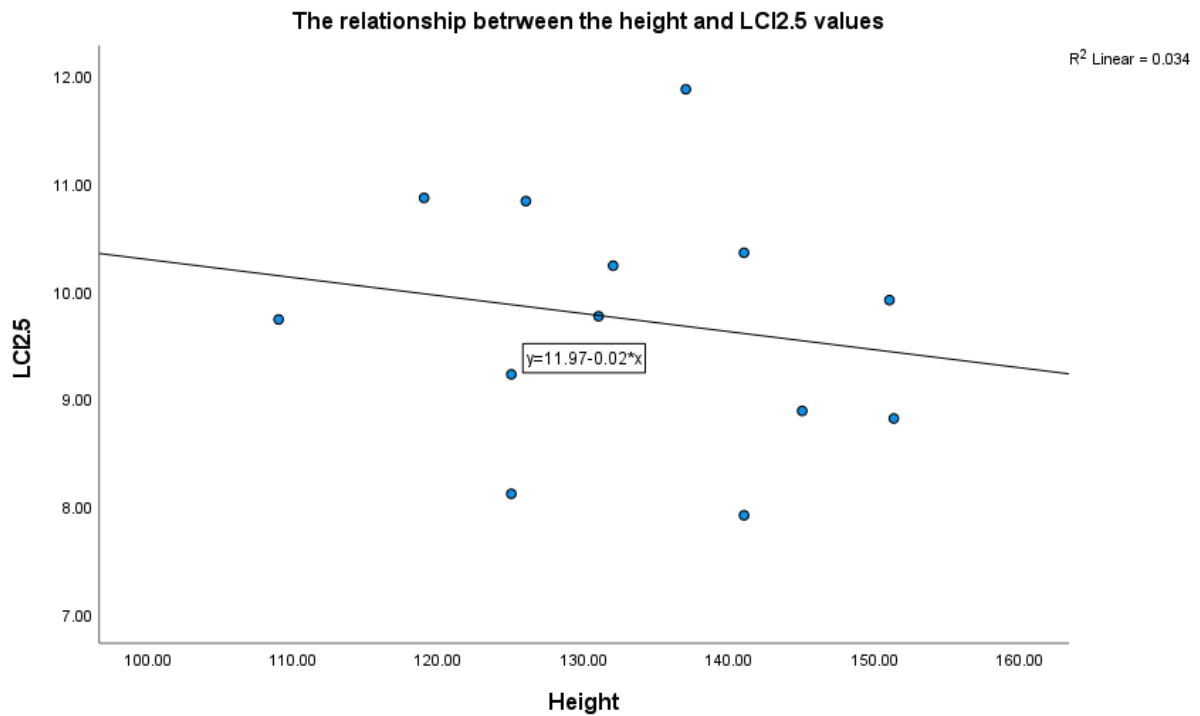


Figure 3-13: Shows the relationship between the height and the LCI2.5 values for 13 children with AT using scatter plot with linear regression in SPSS.

3.3.5.2 The Relationship between Height and LCI5 values

In addition, I studied the relationship between LCI5 and height by scatterplot and regression in SPSS (see Figure 3-14). There was no relationship between LCI5 and height ($R^2 < 0.01$).

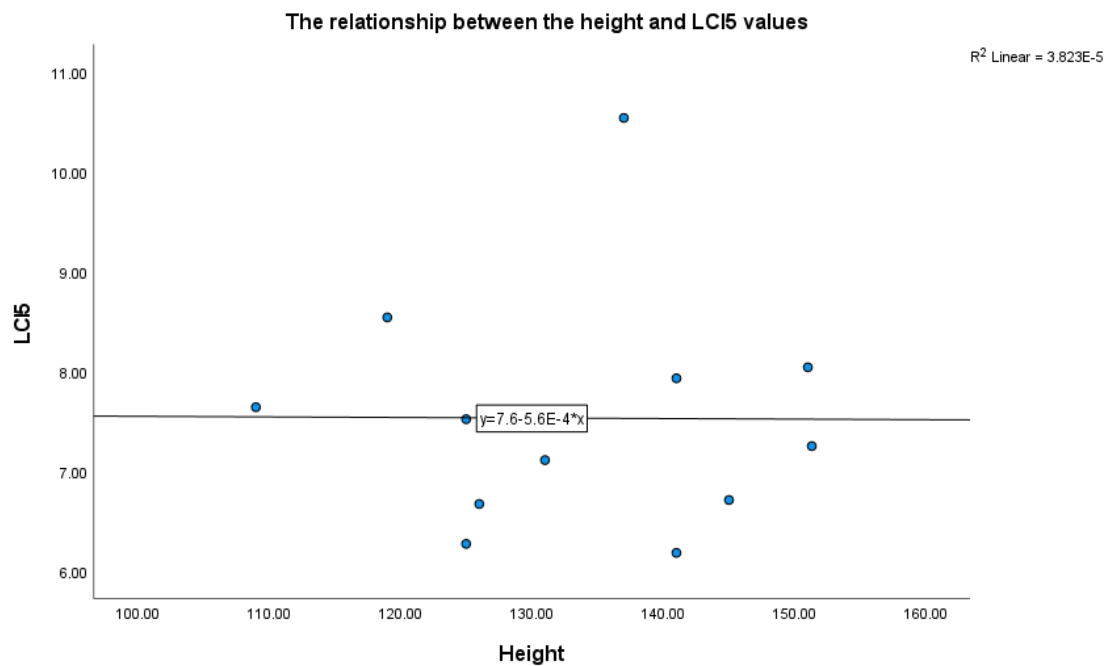


Figure 3-14: Shows the relationship between the height and the LCI5 values for 13 children with AT using scatter plot with linear regression in SPSS.

3.3.5.3 The Relationship between Height and FRC values

In normal cases, there is a positive relationship between height and FRC, but this has not been explored in patients with AT. Therefore, I studied the relationship between FRC and height by scatterplot and regression in SPSS (see Figure 3-15). There is a relationship between FRC and height ($R^2 = 0.452$).

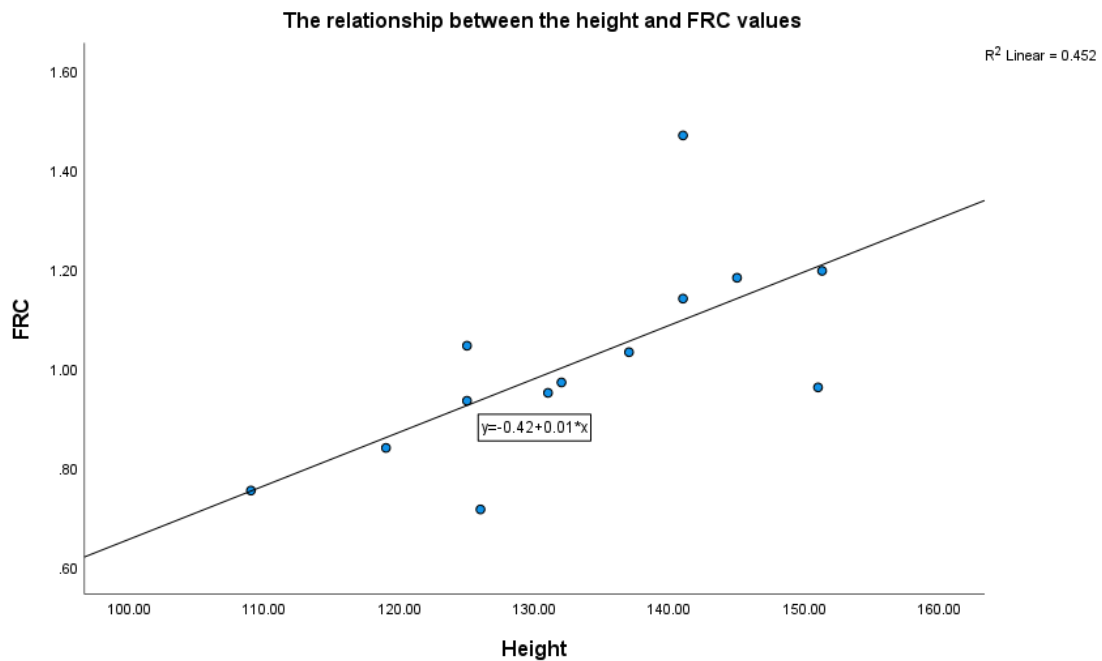


Figure 3-15: Shows the relationship between the height and the FRC values for 13 children with AT using scatter plot with linear regression in SPSS.

3.3.6 The Relationship among Weight against LCI2.5, LCI5, and FRC

3.3.6.1 The Relationship between Weight against LCI2.5

Likewise, the relationship has been conducted between LCI2.5 and weight using scatterplot and regression in SPSS (see Figure 3-16). There was no relationship between weight and LCI2.5 ($R^2 < 0.01$).

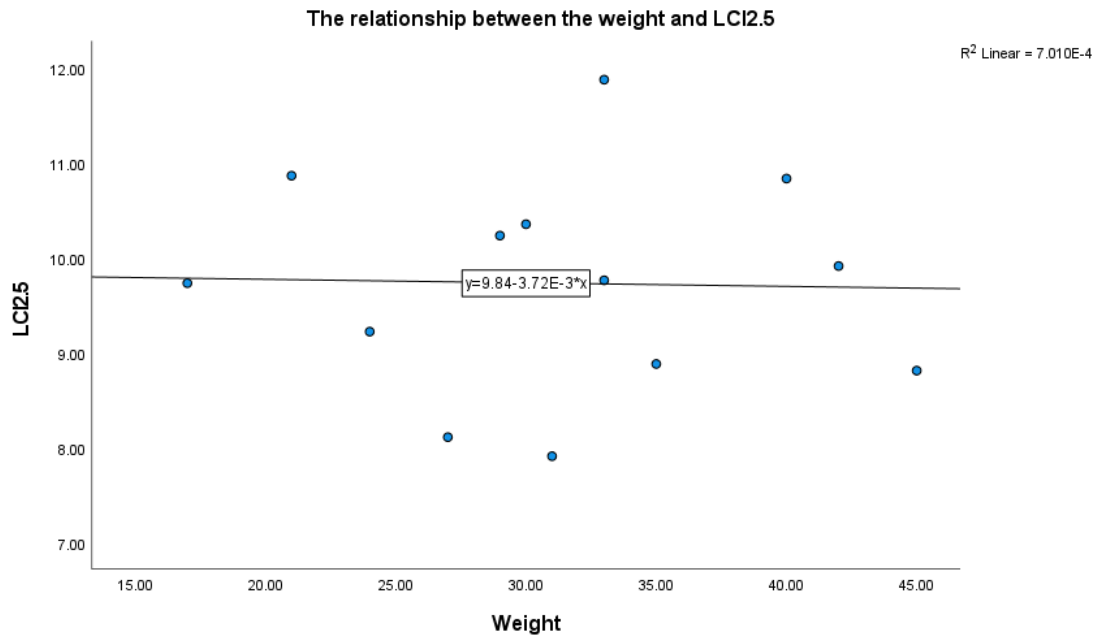


Figure 3-16: Shows the relationship between the weight and the LCI2.5 values for 13 children with AT using scatter plot with linear regression in SPSS.

3.3.6.2 The Relationship between Weight and LCI5

Additionally, the relationship has been done between LCI5 and weight by using a scatterplot and regression in SPSS (see Figure 3-17). There was no relationship between LCI5 and weight ($R^2 = 0.010$).

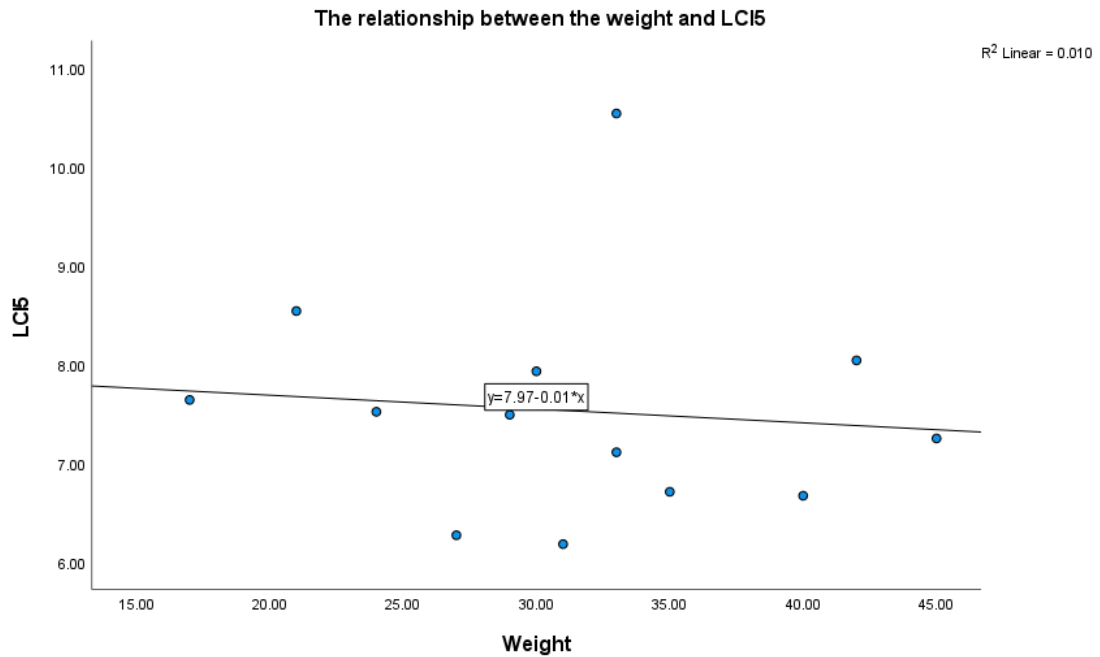


Figure 3-17: Shows the relationship between the weight and the LCI5 values for 13 children with AT using scatter plot with linear regression in SPSS.

3.3.6.3 The Relationship between Weight and FRC

In addition, I studied the relationship between FRC and weight using a scatterplot and regression in SPSS (see Figure 3-18). There was no relationship between FRC and weight ($R^2 = 0.083$).

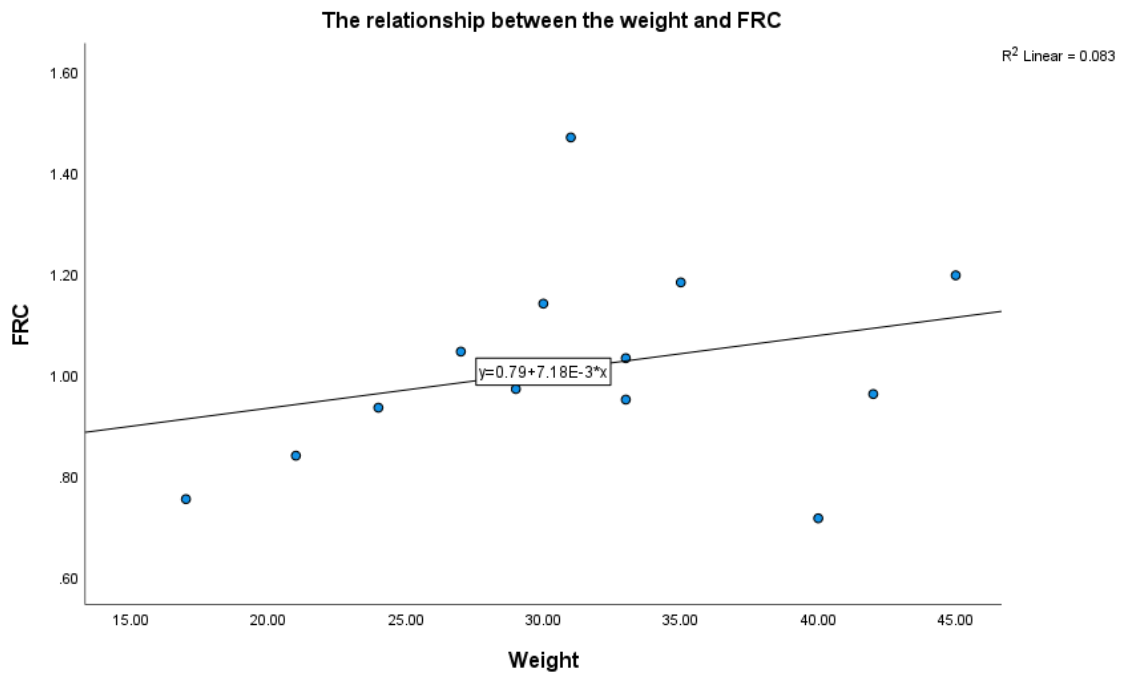


Figure 3-18: Shows the relationship between the weight and the FRC values for 13 children with AT using scatter plot with linear regression in SPSS.

3.4 Discussion

In the work described in this chapter, I set out to assess whether or not children with AT are able to undertake the lung clearance index technique. This technique is safe (non-ionising radiation), and it does not require any effort from the participants other than to breath normally. Interestingly, this technique has never yet been applied in those patients. I selected 15 children with AT to determine their ability to comply with LCI criteria. These criteria were derived from European Respiratory Society criteria. These are the similarity of the first four breaths before the wash out, the similarity of the first three breaths after the wash out, trajectory's consistency, avoiding leakage, and achieving LCI2.5 and/ or LCI5 values.

Although normal breathing does not require any additional effort, none of the participants were able to fulfil two of these criteria, the acceptance range of similarity of tidal breath (10% less or greater) in the first four breaths before the wash-out and the first three breaths after the wash-out. Whilst there shouldn't be any technical issue preventing all children from taking four breaths before wash-out or three breaths after washout, there are click sounds (like snoring) from the machine that may induce an irregular breathing pattern.

As MBW requires a consistent breath-to-breath tidal volume, this finding is somewhat concerning. However, children with AT, despite being given time to settle into a tidal breathing pattern, do not appear to have consistent breath size, especially when a face mask is applied to the face. Additionally,

the noise of the click of the valve system after the washout commenced appeared to cause further variability in the size of the tidal volume. Despite this, children were able to continue through the test and give a consistent trajectory of nitrogen washout. So it may be that with longer preparation, we will be able to undertake a washout which meets all the criteria. This issue may be solved using music via headphones to minimise the machine's clicking sound and distract subjects. In addition, we could modify how we encourage children with better an explanation before starting the test.

In contrast, all the participants were able to achieve the two criteria of wash-out to LCI5 and avoidance of leakage. Moreover, 11 out of 13 were able to fulfil the two criteria of the LCI2.5 and the trajectory's consistency (see Table 3-6). Therefore, the LCI5 may be more appropriate because of its short time, which takes half the time of the LCI2.5. According to Hannon et al. (2014), the duration of LCI1/20 is shorter and may make research and clinical measurements more feasible.

In this study, 2 of the 15 participants withdrew, but not due to the LCI. The underlying reason for this withdrawal of those participants was the LCI has been conducted after doing OE-MRI, and OE-MRI made them anxious due to claustrophobia. Therefore, 13 children with AT underwent the LCI technique. Eleven out of 13 was able to provide acceptable results. In general, children with AT are able to comply with LCI instructions, because unlike spirometry, these instructions do not require controlled effort. Moreover, in order to explore the correlation between age and the ability

to comply with LCI criteria, the group of children with AT was divided into two groups based on age (the median age being 9). The first group was composed of children aged 9 or under (7 participants) and the second group had children aged over 9 (6 participants). The result of this study showed that there is no significant difference in the ability to undertake LCI between young children with AT and older children with AT. Where 83.3% of the children with AT aged 9 or under in this study were able to perform the LCI test. Likewise, 83.3% of the children with AT greater than 9 years were able to complete the test. The most likely explanation for that this is, even though the older children were better able to understand the test, other consequences of AT increase with age, reducing their ability to co-ordinate respiratory effort.

Age and height are deemed the main factors that play a crucial role in lung size. Therefore, initial analyses of the LCI_{2.5}, LCI₅, and FRC lung function values obtained (regardless of quality) were conducted to determine the relationship between these values and these factors (age, height and weight) using scatterplot and regression in SPSS. This study revealed that for the children in the AT group, there was no relationship between LCI_{2.5} and age, ($R^2=0.004$) and very weak relationship between LCI₅ and FRC and age ($R^2= 0.118$, $R^2= 0.178$) respectively.

Moreover, the relationships between LCI_{2.5}, LCI₅ and FRC, and height were explored using scatterplot and regression in SPSS. These results reveal for those children in the AT group, there was no relationship between LCI_{2.5}

and LCI5, and height ($R^2= 0.034$, $R^2 <0.01$) respectively. However, there was a relationship between FRC and height ($R^2= 0.452$). As FRC is well known to correlate with height, this finding is reassuring as this is in keeping with what we would expect regarding FRC and height. Likewise, scatterplot and regression has been used in SPSS to determine the relationships between LCI2.5, LCI5 and FRC, and weight. This study revealed that for children in the AT group, there was no relationship between LCI2.5, LCI5 and FRC, and weight ($R^2 <0.01$, $R^2= 0.010$, and $R^2= 0.083$ respectively).

As mentioned before, the LCI technique has not previously been applied to AT patients. Therefore, the study's findings have been compared to previous data published about children with CF, asthma, PCD and neuromuscular diseases such as SMA. For the integrity of comparison, the LCI results will be presented as parametric and nonparametric data, due to the published outcomes of the selected studies.

The result of LCI2.5 (LCI) for the eleven participants with AT ($n= 11$) was (median, interquartile (IQR)) (9.76, 1.445), age (median, IQR) (10, 4). In addition, the result of LCI5 was also shown which might be more suitable for the children with AT because of its short time compared to LCI. The result of LCI5 for the eleven participants ($n= 11$) was (median, IQR) (7.25, 1.095), age (median, IQR) (10, 4).

In a study exploring LCI in patients with CF, the LCI result for 10 patients with CF was [mean \pm SD (range)] 12 ± 3 (6.7–16), age, year 13 ± 2.5 (10–

17). Furthermore, in the same study, the LCI result for 5 healthy volunteers was [mean \pm SD range] 6.7 ± 0.5 (5.9–7.2), age, year 12.4 ± 2.4 (10–17) (Kanhere et al., 2017). A recent study using LCI on asthmatic patients conducted by Nuttall et al. (2021) yielded the following results: mild/moderate asthma (n= 7), LCI median (interquartile range) 6.69 (6.11 to 6.90), age 12.5 (8.6 to 14.0). Severe asthma (n= 23), LCI median (interquartile range) 7.49 (6.63 to 7.84), age 11.8 (9.2 to 15.3). The healthy volunteers in the same study (n= 7), LCI median (interquartile range) 6.48 (6.13 to 6.78), age 13.9 (10.5 to 14.4) (see Table 3-12).

Moreover, since AT is characterised by neuromuscular involvement, I compared my results to those from a study conducted on patients with SMA, a disease that weakens the respiratory muscle. Type 2 and 3 children have varying outcomes, but most type 2 children develop respiratory failure, either chronically or intermittently due to infections of lower respiratory tract. The results of the study, which was conducted by Kapur et al. in 2019 on 15 children with SMA, were LCI (median, IQR) (8.06, 2.44), age (median, IQR) (9.30, 4.67).

A recent study using LCI was conducted on patients with PCD by Singer et al. (2021). The study's results for the 90 participants were as follows: the LCI median (interquartile range) 9.70 (8.24 to 11.74), age median (interquartile range) 12.8 (9.1 to 17.8). These results are presented in Table 3-12.

Chapter 3

Table 3-12: This table demonstrates and summarises the selected results of LCI studies as well as the LCI result of this study.

Clinical conditions		Sample size	Age Median (IQR range)	LCI's result Median (IQR range)	FRC % predicted	Equipment	Reference
Asthma	Mild/ moderate	7	12.5 (8.6 to 14.0)	6.69 (6.11 to 6.90)	NA	Exhalyzer D	Nuttall et al., 2021
	Severe	23	11.8 (9.2 to 15.3)	7.49 (6.63 to 7.84)			
	Healthy	7	13.9 (10.5 to 14.4)	6.48 (6.13 to 6.78)			
Cystic fibrosis/ healthy [Mean \pm SD range]		10	13 \pm 2.5 (10–17)	12 \pm 3 (6.7–16)	114 \pm 15 (87–153)	Exhalyzer D	Kanhere et al., 2017
		5	12.4 \pm 2.4 (10–17)	6.7 \pm 0.5 (5.9–7.2)	119 \pm 9 (107–133)		
Primary ciliary dyskinesia Median (IQR range)		90	12.8 (9.1 to 17.8)	9.70 (8.24 to 11.74)	NA	Exhalyzer D	Singer et al., 2021
Spinal muscular atrophy (Median, IQR)		15	8.06 (2.44)	9.30 (4.67)	NA	NA	Kapur et al., 2019
Ataxia Telangiectasia (Median, IQR)		11	10 (4)	9.76 (1.445)	1.032 (0.205)	Ndd EasyOne Pro Lab	This thesis

The LCI's result for children with AT was (median= 9.76), which is higher than healthy volunteers in the studies evaluating asthma (median= 6.48) and CF (mean= 6.7 \pm 0.5), which is anticipated. Also, it is higher than in children with severe and mild/ moderate asthma (median= 7.49 and 6.69) respectively.

Furthermore, it is lower than the LCI result of children with CF (mean= 12 ± 3). In contrast, the LCI result for children with AT was (median= 9.76), which is fairly similar to the LCI results for children with PCD and SMA (median= 9.70 and 9.30) respectively. Impressively, the similarity in the results of LCI between children with AT and SMA. This similarity could be due to muscle weakness between two groups, which is a common factor. Also, both groups used a facemask and there was similarity in the sample size.

Finally, the main strength of this study is that this is the first description of applying this technique in patients with AT. Although the study sample is small, it constitutes 13% of the entire paediatric AT population in the UK. In addition, this sample is an unselected group of children with AT (so should be broadly representative). This study was not specifically selecting children who had been diagnosed with lung disease for investigation.

Children with AT find it difficult to seal their mouth tightly on a mouthpiece due to neuromuscular degeneration. To allow measurement of LCI in the hospital setting, we used a modified technique with a facemask for children with AT as an alternative to a mouthpiece. To overcome interface issues, we used an anaesthetic mask which had the ability to mould to the face when held in position, as there is an inflated cushion for an interface. In all other respects, we used. European respiratory standards were applied to ensure patient safety and obtain satisfactory results. This is an innovative way to avoiding a leakage.

A key factor limiting this study was that much of the planned work was paused due to the COVID-19 pandemic. All non-essential research was paused due to the pandemic in March 2020 as it was not safe for children with immunodeficiency to come to the hospital during a lockdown or even later when restrictions were limited as they are considered a clinically extremely vulnerable group. Later LCI and spirometry were considered aerosol-generating procedures so research using them was not straightforward to undertake.

Another limitation of this study is the sample size in this study is very small to make any meaningful analysis. Therefore, we recommend increasing the number of participants in the future.

Moreover, children with AT find it difficult to comply with the similarity in regular breathing, which represents two criteria of European respiratory standards. We are not yet certain how much the inability to make the regular tidal breaths at the start of each LCI measurement impacts the LCI result. Although using a facemask is regarded to be an innovative method to avoid leakage for use by children with AT, further work needs to be conducted to see if the facemask influences the result. This raises several issues: risk of leak despite the close observation, dead space, and difficulty in an adjustment of the size of the dead space.

It is difficult to measure the size of the dead space in the mask, due to the differences in the shape of patients' faces. This makes it harder to assess the amount of dead space in a mask than the dead space in a mouthpiece,

where it is known. The use of a facemask increases the dead space, which increases LCI and FRC values compared to a mouthpiece (Robinson et al., 2018). This increase in LCI values is explained owing to the effect of dead space, which increases both CEV and wash-out time. This increase in LCI values is explained owing to the effect of dead space, which increases both CEV and wash-out time. The measurements of LCI and FRC values, however, can be corrected by equipment VD (see Figure 3-19).

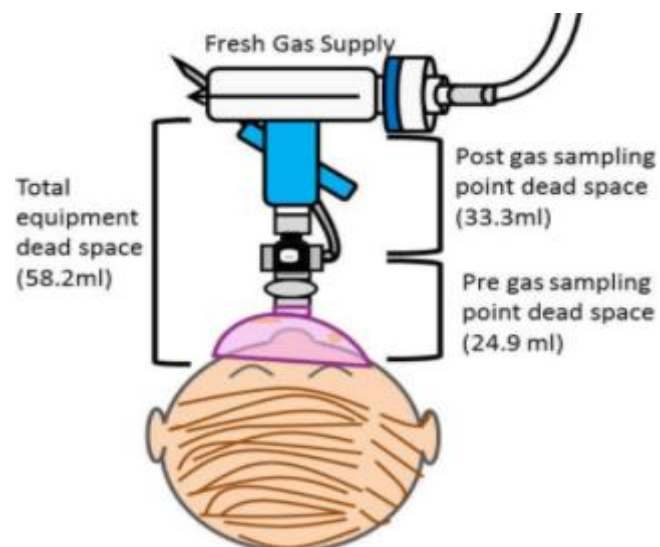


Figure 3-19: Displays the location and volume of dead space (pre, post and total) (Benseler et al., 2015).

An FRC value is corrected by deducting the entire pre-gas sampling point dead space from a measured FRC. Whilst corrected (CEV) is obtained by deducting the entire pre-gas sampling point dead space from the tidal breath (TV) of each breath. However, it is difficult to define the facemask dead space exactly because of difference in face shape and the volume

within the facemask (Robinson et al., 2018). A 3d scan of the face may be useful in correcting for this but further work is needed.

In addition, when leaks occur, the result of LCI is invalidated; therefore, it can be difficult to diagnose a leak in real time on the Pro Lab device, as the screen is small. However, this was addressed in offline analysis using WBreath (the programme for analysing scientific data collected by the nnd EasyOne Pro Lab device).

3.5 Conclusion

In conclusion, this study is regarded as the starting point for applying the LCI technique to AT patients. This may have a role in being a pulmonary outcome measure in future studies. The results of this study show that the children with AT were able to comply with the majority of the LCI's criteria. Since the LCI is a free breathing technique, there is no need for coordinated forced effort, unlike spirometry. In this technique, and in spirometry, I focused on the ability of children with AT to comply with technique's criteria, regardless of the technique results. I then presented data showing that the LCI results for children with AT are fairly similar to the LCI results for children with PCD and SMA. Whereas it is lower than the LCI result for children with CF and higher than the result for children with mild-severe asthmatic patients, as well as healthy volunteers.

The next chapter of my thesis presents data that assesses OE-MRI as another method of evaluating lung health, which might be more reliable in children with AT. Although more than half of the study cohort could undertake LCI, this still leaves a considerable number who are unable to do this technique, meaning there is still a need to identify an alternative assessment method.

Chapter 4

Assessing Feasibility of Oxygen Enhancement Magnetic Resonance
Imaging (OE-MRI) Measurements Patients with Ataxia Telangiectasia (AT)

4.1 Introduction

Oxygen-enhanced MRI (OE-MRI) is a non-invasive, ventilation imaging technique that promises significant advancements in medical practices (Ohno et al., 2003). Moreover, OE-MRI is a particularly safe technique for use in subjects with AT because it uses non-ionising radiation to provide ventilation and perfusion information. Whilst applications of OE-MRI have been explored in a range of medical fields (Fuseya et al., 2018), the full significance of the medical breakthrough made by OE-MRI has yet to be elucidated (O'Connor et al., 2016). However, extensive medical research efforts have been made to investigate the potential of OE-MRI as a reliable option for use in different fields of medicine. This imaging technique can quantify the spatial distribution of oxygen delivery to cells and can differentiate well-oxygenated tissue from oxygen-deprived tissue (O'Connor et al., 2016).

Variation in the levels of oxygen dissolved in blood plasma and interstitial tissue fluids changes their longitudinal relaxation rates in MRI (see Figure 4-1) (O'Connor et al., 2016). Investigation of oxygen enhancement is potentially useful in any organ system which is metabolically active or involved in oxygen transfer. Thus, OE-MRI can lead to detection of tumours at early stages by detecting oxygen use. It also holds promise in investigating lung disease by detecting oxygen transfer.

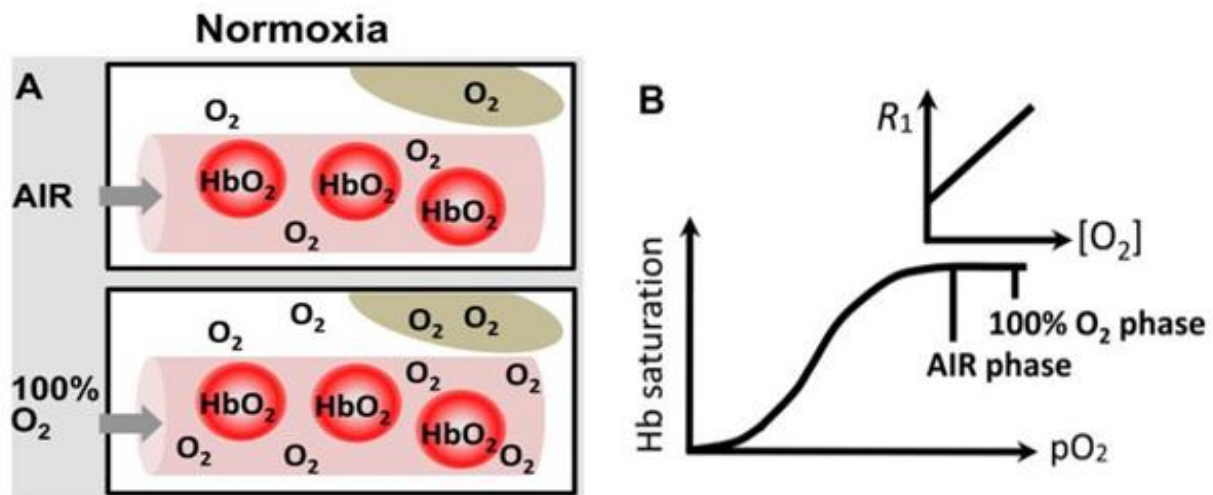


Figure 4-1: The differentiation between normoxia and hypoxia using OE-MRI. Diagrams A and B represent an imaging voxel that contains red blood cells in blood vessels (pink), tumour cells (grey), and the interstitial space surrounding them (white). (A) In the normoxic tissue, molecules of haemoglobin (Hb) in the red blood cells are saturated by oxygen to become oxyhaemoglobin. The plasma contains the dissolved dioxygen molecules. Hyperoxic gas inhalation significantly increases the dissolved plasma concentration of dioxygen, but oxyhaemoglobin concentrations have fundamentally not changed. (B) Increased PO_2 concentrations in interstitial fluid and plasma result in an increase in the longitudinal relaxation rate (R_1) of the tissue, which can be detected via MRI (O'Connor et al., 2016).

However, OE-MRI is a relatively novel method, and its full importance and scope has yet to be determined. Research is ongoing in different domains (Ohno et al., 2003). Most relevant to the work presented in this thesis, is preliminary work which has been conducted on the use of OE-MRI in the early identification of respiratory diseases. For example, researchers have suggested OE-MRI to be a complementary procedure to high-resolution chest computed tomography (HRCT) for evaluating the heterogeneous distribution of emphysema. Heterogeneous distribution of oxygen through the lung is a key feature in emphysema and COPD more generally (Fuseya

et al., 2018). Recent publications have also focused on identifying the severity of asthma by estimating oxygen delivery and wash-out in the lungs using OE-MRI (Zhang et al., 2015). Investigators are also evaluating the reliability of using OE-MRI to differentiate chronic pulmonary thromboembolic hypertension from other pulmonary hypertension causes. This has been done by qualitatively analysing OE-MRI images and studying the quantitative parameters, such as ventilation, perfusion and diffusion (Maxien et al., 2012).

Tumour masses have also been evaluated using OE-MRI. It has been observed that patients with lung parenchymal tumours produce an increase in an OE-MRI signal during oxygen inhalation (O'Connor et al., 2016). Studies suggest OE-MRI can be combined with arterial spin labelling for ventilation and perfusion (Mai et al., 2002). Upon validation of clinical trials, OE-MRI might reduce the need for using radioactive tracers in nuclear medicine V/Q scans (ventilation-perfusion).

The use of dynamic OE-MRI for the detection of ventilation defects in respiratory diseases is a trending research area. For the past few decades, the only method available for this purpose was ventilation scintigraphy, which uses a radiolabelled aerosol, such as Tc-99m-labelled DTPA (diethylenetriaminepentaacetic acid), or radioactive gases, like Kr^{81m} or Xe¹³³ (Ohno and Hatabu, 2007). However, the low spatial resolution of this method and the need for radioactive material inhalation, poses significant

limitations. Recently, hyperpolarisation of noble gas MRI became a novel tool for evaluating ventilation; positive results have been obtained using laser hyperpolarised ^{129}Xe and ^3He (Ohno and Hatabu, 2007). However, specialised RF transmitters/receivers and laser equipment are needed for the use of hyperpolarised noble gas (Ohno and Hatabu, 2007). The OE-MRI technique is especially suitable for patients with AT, as lung imaging is challenging for patients with AT because of their heightened sensitivity to ionising radiation (Prayle et al., 2018). In this chapter, I describe studies that address the potential use of OE-MRI as an alternative method of assessing lung disease in patients with AT.

4.1.1 OE-MRI in Ataxia Telangiectasia

As discussed in the Introduction to the thesis, Ataxia Telangiectasia is a genetic disorder characterised by immunodeficiency, radiosensitivity, neurodegeneration, genomic instability and a predisposition to cancer (Rothblum-Oviatt et al., 2016). Progressive cerebellar ataxia is also an aspect of the disorder. There are no therapies available at present to cure the disorder or even prevent it. It is only possible to suppress some of the symptoms associated with immunodeficiency and deteriorating lung functioning. Neurodegeneration and predisposition to cancer are incurable (Rothblum-Oviatt et al., 2016). In the current realm of medicine and technology, great amounts of research have been done on the immunology

aspect of AT, whilst finding a safe technique for the lung imaging aspect has been neglected (Sahama et al., 2014).

Many patients with AT develop serious respiratory conditions, which carry the potential to shorten their lives (Rothblum-Oviatt et al., 2016). There are limited studies on the most effective means of treating respiratory conditions in AT patients. This study used OE-MRI to investigate the lungs of AT patients because this technology does not use ionising radiation.

Moreover, unlike many other lung scanning techniques, OE-MRI does not require patients to hold their breath, making it easier for them to participate. An OE-MRI scan reveals the distribution of oxygen in the lungs, which is an added benefit to the research as it displays the functioning of the lungs in conjunction with the structural changes.

For this study, the OE-MRI was performed during a 10–20-minute test in which the children were required to lie in the scanner and breathe normally through a facemask. The procedure was painless and did not require any injections or medications.

The study aimed to assess the feasibility of conducting OE-MRI on AT patients, as it had not been done before. A feasibility study was necessary as first step to determine the ability of AT patients to comply with this technique. We had hypothesised that the children would be able to complete the OE-MRI procedure without any major difficulty, as it did not require them to hold their breath during the scan.

4.1.2 Hypothesis, Aim, and Objectives

4.1.2.1 Hypothesis

The hypothesis underlying in this chapter is that OE-MRI is a feasible technique for lung imaging in children with AT and it may provide useful physiological information about lung disease.

OE-MRI has not previously been used in this patient population. Given that lung disease is a leading cause of death, identifying a safe imaging technique would have potential value in the long-term assessment of respiratory disease in these patients.

4.1.2.2 Overall Aim

To assess the feasibility of using OE-MRI in children and young adults with AT. In addition, to monitor trends in parameters derived from OE-MRI and assess their suitability as clinical trial endpoints.

4.1.2.3 Objectives

- 1- To determine the feasibility and utility of OE-MRI in patients with AT.
- 2- To develop MRI scanning protocols to optimise MRI in respiratory disease in AT and other paediatric respiratory-neurological disease. It was anticipated at the outset that although the protocol used is known to be

feasible in healthy volunteers, the imaging protocol would require further optimisation in patients with AT.

- 3- To compare OE-MRI parameters (delta-PO₂ whole lung, wash-in-time whole lung, delta-PO₂ aorta, VVF) between AT patients and healthy volunteers.
- 4- To compare OE-MRI parameters for AT patients versus height, age, and gender.
- 5- To compare OE-MRI parameters for healthy volunteers versus height, age, and gender.

4.2 Material and method

4.2.1 Study Overview

The study commenced in 2018 and it was designed as a single-centre longitudinal study. Participants were recruited from the National AT clinic, with support from the AT Society. Twenty-five children with AT aged 6-16 years were recruited to perform OE-MRI. The study was designed in two workstreams. Workstream 1 featured OE-MRI in 25 children with AT and optimised the techniques during this period. Workstream 2 followed up with each of these children once a year for two years. Due to the recent coronavirus pandemic, this study has required adjustment. This study began in 2018, with 15 children with AT. Then, as COVID-19 developed into a global pandemic, the policy of lockdown was applied everywhere. This led to a pause in recruitment – and data from the initial work in 15 participants is presented in this thesis. After negotiation with the funder, a no-cost extension to the study has been awarded, and this will be used to increase the study recruitment to 25 and undertake follow-up scans for the whole study cohort in 2023 and 2024.

As mentioned previously, lung infection is the main cause of death in these patients. As COVID-19 affects the respiratory tract, this led to further challenges, namely, there was a need to adapt the methodology resulting in the study being conducted with a pool of 15 children with AT. The new method involved imaging this number of the participants and comparing OE-MRI outcome measures (delta-PO₂ (Δ PO₂) whole lung, delta-PO₂ aorta,

wash in time whole lung, and ventilated volume fraction (VVF) (see Table 4-4)) with healthy volunteers.

Moreover, these parameters were compared to height, age and gender. All these comparisons are described in the statistical analysis section. Regarding healthy volunteers, we aimed to recruit up to 20 healthy volunteers for imaging scanning protocol development in children.

4.2.2 Ethics Approval, Sponsorship, and Research Partners

The study protocol was approved by the East Midlands Nottingham 2 Research Ethics Committee (17/EM/0149) and it is sponsored by Nottingham University Hospitals NHS Trust. The NHS trust has arrangements in place for this study for the University of Nottingham to undertake the MRI scans, and the image analysis to be undertaken by Bioxydyn Ltd (Manchester).

The study Co-ordinator is Andrew Prayle. Key protocol contributors were Andrew Prayle, Jayesh Bhatt, Ian Hall, Michael Barlow, Rob Dineen, Andrew Bush, Matthew Hurley, Shahideh Safavi, Jan Paul and Saleh Alenazi (the author) (Table 4-1).

Table 4-1: The names and the positions of the work's team.

Jayesh Bhatt	Medical doctor and paediatric respiratory physician for the AT clinic
Ian Hall	Medical doctor – respiratory physician and clinical MRI imaging group leader
Rob Dineen	Paediatric Radiologist, and researcher of AT children's MRI
Michael Barlow	MRI physicist
Andrew Bush	Respiratory paediatrician
Jan Paul	Research radiographer
Shahideh Safavi	Respiratory doctor
Andrew Prayle	Respiratory pediatrician and MRI researcher
Mathew Hurley	Respiratory paediatrician

4.2.3 My Role in the Research

I assisted in the MRI department as PhD student with Mr Jan Alappadan Paul (Research Radiographer MRI). We used a GE Signa HDxt 1.5 T (MRI machine). Prior to the patient's arrival, we prepared the MRI room. I assembled the oxygen apparatus and connected and tested the gas mixer (Bioxydyn) using the medical air cylinder and oxygen cylinder. During dynamic scanning, it is important that the oxygen and air are delivered at precisely the right times. Whilst the MRI radiographer monitored the scan and the medical doctor monitored the patient, my role during the scan was to ensure that the oxygen was delivered at the right time per protocol. Working with the radiographer, I also positioned the participant for the scan, ensuring that the participant was comfortable.

After obtaining informed consent, we positioned the patient in an appropriate and comfortable position in the MRI scanner. Children with AT

have reduced mobility, as the ataxia causes difficulty in walking. Younger children can usually walk into the scanner unaided, but older children needed support using an MRI compatible wheelchair or they were carried in by their parents. Care was taken to position them in a comfortable position in the scanner, as they may not easily be able to move when in the scanner. I played a key role in keeping the children calm and happy whilst the scan was being setup, which was crucial to the success of the scan.

4.2.4 Study Inclusion Criteria / Exclusion Criteria

4.2.4.1 Inclusion Criteria

- Diagnosis of AT (or an AT like syndrome) attending the National Paediatric AT clinic.
- The ability to lie down for fifteen minutes in the MRI scanner as judged by the investigator and the parents.
- Aged between 5 to 20 years at consent.

4.2.4.2 Exclusion Criteria

- Participation in another research study, which excludes participation in an observational cohort study, such as the Imaging AT study.
- Participant has a magnetically active material (an MRI exclusion criterion).

- Participant unlikely to tolerate the procedure.
- Participant deemed unable to comply with instructions.

Participants attended the Sir Peter Mansfield Imaging Centre "an interdisciplinary, cross-faculty centre for innovative imaging in experimental and translational medicine" in Queen's Medical Centre (QMC) for their first study day. Written informed consent was taken from a parent, and the child provided assent. Parents received the information about the study at least 24 hours prior to the study to decide if they wanted their child to participate. However, in practice, they had several weeks, as the scan had to be scheduled, and most participants required a hotel visit for an overnight stay. A medical questionnaire was administered, followed by lung function measurements (spirometry and multiple breath washout) using an nDD Pro Lab (nDD Systems, Switzerland). Prior to the scan and afterwards, a set of observations (pulse oximetry, blood pressure and respiratory rate) was taken. The scan was conducted as per the scanning protocols (see below). The following questionnaires were administered:

1. An MRI acceptability questionnaire.
2. A PC-QOL-8 (a quality-of-life questionnaire for paediatric chronic cough).
3. A CHU9D (child health utility instrument - A standardised children quality of life score).

4. A PedsQL (Paediatric Quality of Life inventory - A standardised children quality of life score).
5. MRI safety questionnaire (administered by the radiographer).

4.2.5 Preparation for the Scan

The purpose and process of undertaking the scan was explained to each patient prior to the scan. To aid in this, a LEGO model of an MRI scanner was used, and the mock MRI scanner was used to demonstrate what an MRI scanner looks like, and how it sounds. This was individualised on a participant-to-participant basis, depending upon the age of the participant. The SPMIC has a "mock MRI scanner" which is a life-sized MRI scanner without the MR coil. Still, it can simulate a complete MRI, including giving the participant the experience of lying on a moving MRI examination couch, being moved into a scanner, and the noise of the MRI scanner. This preparatory experience allowed participants to understand what they needed to do before entering the riskier environment of the MRI scanner.

4.2.5.1 Patient Position

Patients were scanned either supine or prone, depending upon their preference. Ideally, they were scanned supine, but patients often found prone easier as they could watch a television screen in the observation room and see their parents. The patient was positioned in a supine position with feet entering the MRI scanner first (see Figure 4-2). A pillow was used

under the patient's head to make them comfortable. Knee support was also used. The respiratory trigger was used for acquisition coronal multi-slice HASTE images. A non-rebreathe facemask was used to provide air or oxygen, with a medical gas blender used to select the gas was positioned in the control room. The patient was positioned inside the scanner bore and centred on the fourth thoracic vertebrae (T4).



Figure 4-2: Diagram of the setup of the patient in the scanner. Dynamic OE-MRI scan is undertaken with the patient positioned as above (if cannot do supine). Note that T4 is the centre point of the image.

4.2.6 Scanning Protocols

4.2.6.1 Protocol 1

Imaging was conducted on a GE Signa HDxt1.5 T. An 8-channel HD Torso coil was used. Medical air and oxygen were supplied to the patient via a standard non-rebreathing facemask from cylinders outside of the scanning room. Prior to scanning, the gases were set up, and the participant was

positioned. The parameters were the acquisition matrix to 88 x 88, TR/TE (repetition time / echo time) was 4/0.73 mm, and the number of dynamic scans from 180. This led to a scanning time of 15 minutes, during which the first 2 minute is in air, then in oxygen until 8 minutes 30 seconds, followed by air until the end of the scan (see Table 4-2).

4.2.6.2 Initial Registration Images and Series of Varying Flip Angles

A three-plane localiser and field of view (FoV) positioning sequence was taken. This was followed by a series of 3D Variable Flip angle Fast Spoiled Gradient-Echo (FSPGR), with varying flip angles as follows: 5, 2, 7 and 9. The rest of the parameters for these scans are the same as the dynamic scan (table 4-2).

4.2.6.3 Dynamic Imaging

Consecutive volumetric 3D Spoiled Gradient Echo (SPGR) images were acquired over 15 minutes whilst the subject was free breathing approximately. During the scan, the patient breathed medical air followed by O₂ as shown in Figure 4-3. Transition from air to O₂ was done swiftly with a gas mixer.

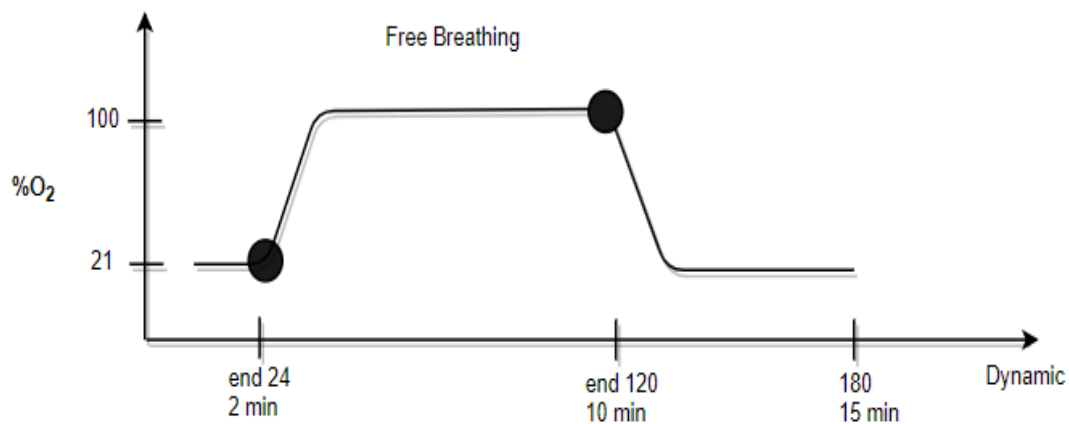


Figure 4-3: Diagram to illustrate the timing of delivery of air and oxygen to participants during protocol 1. A non-re-breath mask was connected to a medical gas blender in the control room. Initially, 15l/min of medical air is used, which was swapped to the medical oxygen and back again as above. Based on a diagram provided in the Bioxydyn imaging manual for OE-MRI (unpublished). The numbers 24, 120 & 180 on the X-axis represent the number of images.

- **Important parts of the method to ensure it worked were:**

1. Pixel, matrix, geometry, slice thickness and dimensions were set such that these parameters were exactly the same between sequences.
2. Checking the gas supply prior to commencing.
3. Using a manual pre-scan option for the dynamic sequence.
4. Attention to detail of the timing of the gas.

After the 1st five participants, the protocol was adjusted to protocol 2 (see Table 4-2). This was done to reduce a banding artefact as indicated by the red arrows in Figure 4-4. Banding is thinner and less evident in the new protocol than in the old protocol (Figure 4-4).

Table 4-2: Shows settings for protocol 1 and 2 for dynamic oxygen enhanced acquisition.

	Protocol number 1	Protocol number 2
Total scan duration [mm:ss]	Approx 15:00	Approx 13:00
TR/TE [ms]	4/0.73	3000
Flip Angle [deg]	9	9
Dynamic scans	180	138
Acq matrix	88x88	64x64
Slices number / slice thickness	18 / 5 mm	18 / 5 mm
Gas delivered to patient	Start: medical air 25 th dyn/2 min: O ₂ 120 th dyn/ 10 min: medical air	Start: medical air 16 th dyn/1 min 30 sec: O ₂ 86 th dyn/ 8 min: medical air

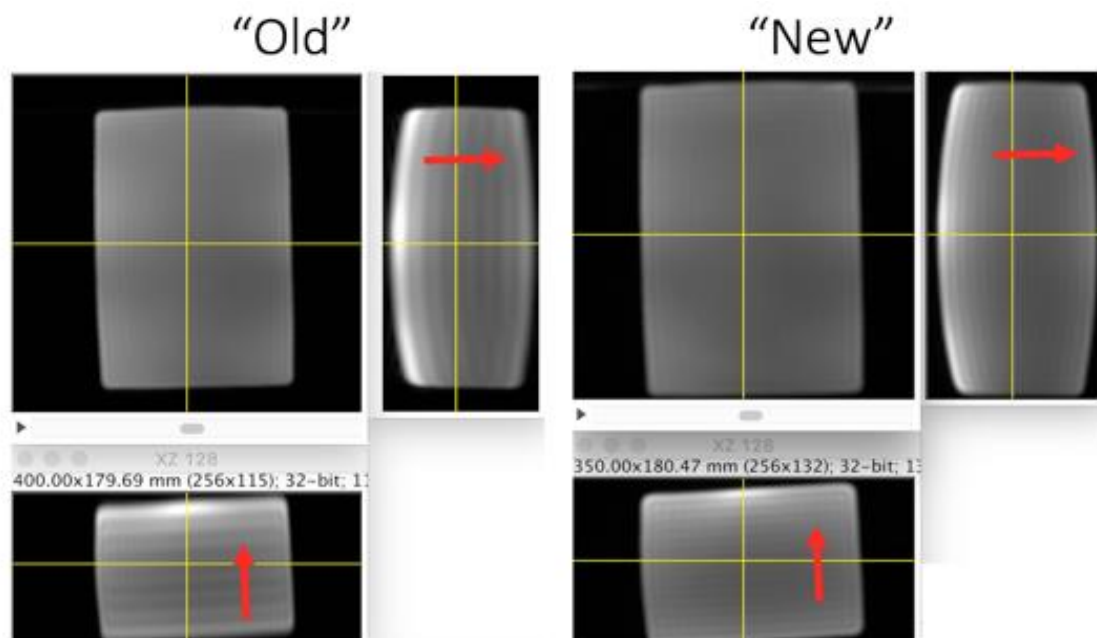


Figure 4-4: Shows the different between two protocols.

4.2.6.4 HASTE Structural Imaging

4.2.6.4.1 Anatomical Images – 2D Coronal Scan

Anatomic images that matched the previous functional images were acquired by applying a multi-slice 2D Coronal Fast Spin Echo (HASTE) with respiratory triggering. Moreover, we used a factor 2 ASSET/SENSE acceleration option (see Table 4-3), which required a calibration scan. This calibration was done in free breathing, without triggering. These HASTE sequences were captured whilst the patient was breathing medical air (21% O₂). A breath hold was not required in this acquisition. The scan required the respiratory belt, which allowed respiratory triggering.

1. The calibration scan was executed in normal breathing without triggering.
2. The same geometry was copied from the preceding dynamic scan.
3. The respiratory trigger was run when gating control is tapped on to activate the respiratory belt.
4. The gating trigger option was set as follows:
 - a. "Respiratory interval" was set to 5.
 - b. "Trigger point" and "Trigger window" were set to 30.
 - c. The respiratory rate was derived from the signal by clicking on "Update rate".

If the system could not catch the appropriate rate, or if the breathing was irregular, the respiratory interval value was reduced.

Table 4-3: Shows a protocol for Multi-slice HASTE with respiratory triggering.

Total scan duration [mm:ss]	Approx 6:00
TR/TE [ms]	550/30.9
Flip angle [deg]	180
Acq matrix	128x128
Slice numbers / slice thickness	18 / 5 mm
SENSE/ASSET factor	2
Gas delivered to patient at start:	medical air

4.2.6.5 Protocol 2

After reviewing the initial images from protocol 1, the following modifications were made to protocol 1 to become protocol 2. The acquisition matrix was reduced from 88 x 88 to 64 x 64, and the number of dynamic scans from 180 to 139. This led to a scanning time of 13 minutes, of which the first 1 minute 30 is in air, then in oxygen until 8 minutes 30 seconds, followed by air until the end of the scan (see Table 4-2). This was done to reduce a banding artefact as it was shown in Figure 4-4.

4.2.7 Statistical Analysis

Our initial planned sample size was 25 participants. This represents approximately 25% of all children in the UK who have AT. This is a sample size of convenience; in that we feel it is unlikely that we will be able to

recruit more than 25% of the eligible pool of participants based on our previous experience in recruiting participants with AT to a brain MRI imaging study. In addition to assessing feasibility of OE-MRI, a goal of this study is to allow the research team to undertake sample size calculations in future studies with OE-MRI as the outcome measure. Because of the Covid pandemic 15 subjects were actually contacted.

We initially aimed to approach 20 volunteers for imaging scanning protocol development in children. Eleven responded to the first and second adverts. Nine consented to take part. One was excluded due to motion artefact preventing image analysis. Further rounds of recruitment were prevented due to the COVID-19 pandemic.

Demographic data of the study group and comparison group were calculated with summary statistics (median and interquartile range). For comparisons, $p < 0.05$ was the pre-specified threshold for statistical significance. For normally distributed data, a t-test was used to compare OE-MRI outcome measures (delta-PO₂ whole lung, delta-PO₂ aorta, wash-in-time whole lung and VVF) between healthy controls and children with AT (see Table 4-4). The Mann-Whitney test was used for non-parametric data. Additional analyses were performed in SPSS using linear regression to compare healthy controls with children with AT after accounting for height, age, and gender as pre-specified co-variates.

Table 4-4: Description of the OE-MRI's parameters.

Parameter	Description
Delta-PO ₂ whole lung	Oxygen enhancement as change in partial pressure of oxygen [mmHg].
VVF	Fraction of the region presenting with oxygen enhancement (max 1, min 0).
Wash-in-time whole lung	Wash in time in the region considered [s].
Delta-PO ₂ aorta	Oxygen enhancement as change in partial pressure of oxygen [mmHg].

4.3 Results

4.3.1 Study Recruitment and Study Population Characteristics

Fifteen children (9 males and 6 females (see Table 4-5)) diagnosed with AT were initially approached to take part in the study (see Figure 4-5). The research, its potential future benefits and how the technique was going to be used were explained clearly to the parents of the participants. Twelve out of the 15 children underwent OE-MRI (see Figure 4-5).

In addition, 9 healthy children (6 males and 3 females (see Table 6)) were approached to take part in the study as part of the control group (see Table 4-7). Eight of the 9 children underwent OE-MRI (see Figure 4-6).

Figure 4-5: Displays the consort diagram of the children with AT who participated in this study.

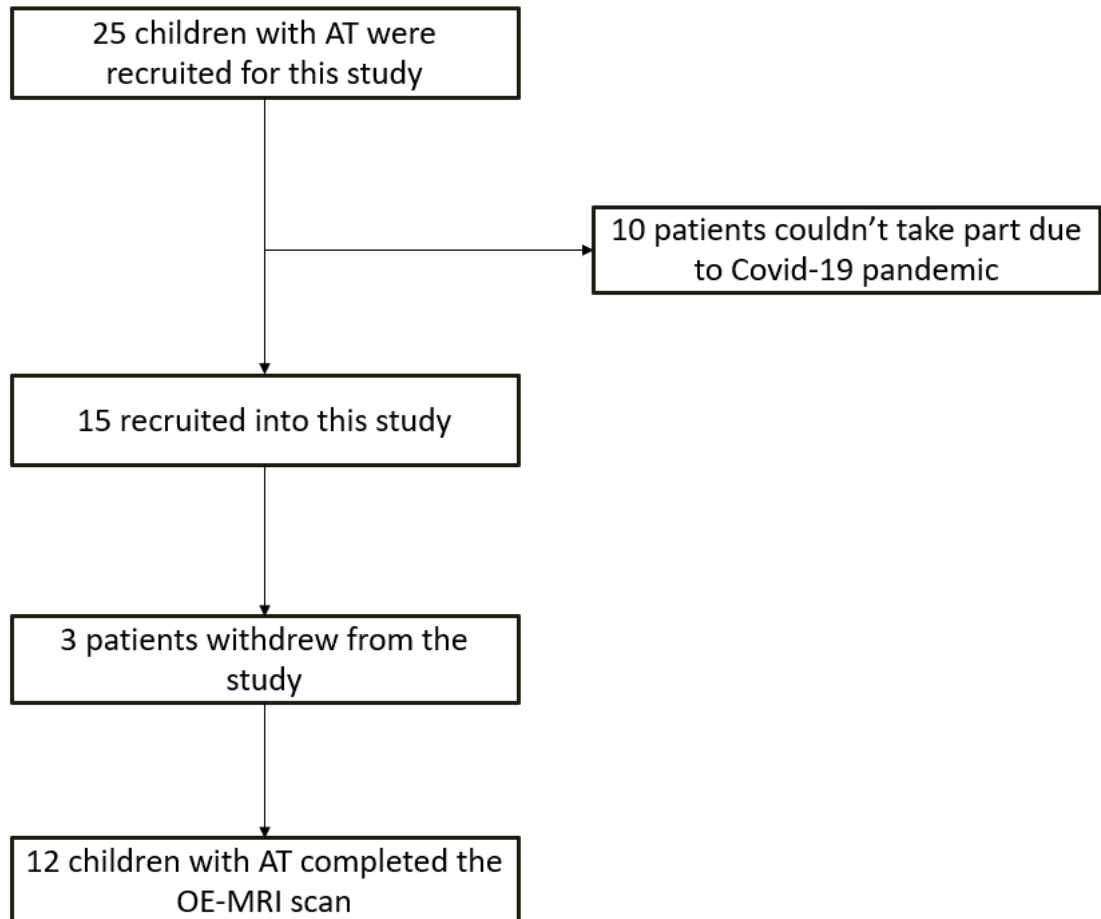


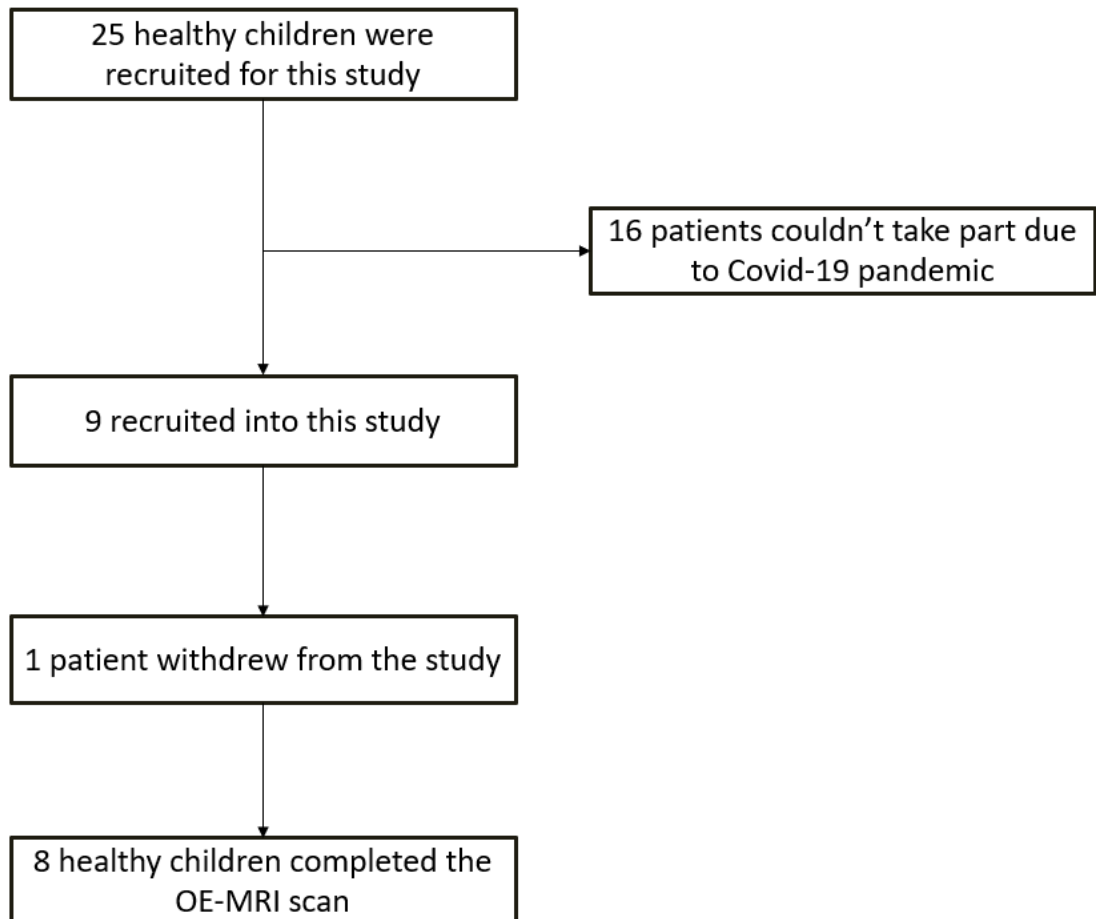
Table 4-5: Descriptive characteristics of individuals in the AT group. The participants who withdrew from the study were marked by a star (*).

NO	Age	Gender	Height	Weight
1	12	Male	125 cm	24 kg
2	14	Female	137 cm	33 kg
3	14	Female	151 cm	42 kg
4	14	Female	151.3 cm	45 kg
5	9	Male	126 cm	40 kg
6	12	Male	141 cm	30 kg
7*	6	Male	119 cm	21 kg
8	8	Male	125 cm	27 kg
9*	8	Female	129 cm	35 kg
10	9	Male	145 cm	35 kg
11	11	Male	141 cm	31 kg
12	7	Female	109 cm	17 kg
13*	7	Female	121 cm	23 kg
14	9	Male	132 cm	29 kg
15	9	Male	131 cm	33 kg

Table 4-6: Characteristics for the AT group.

Descriptive Parameter	Results
Age (median, IQR)	9 years (4 years)
Sex (%)	Male= 60%
	Female= 40%
Height (median, IQR)	131cm (16 cm)
Weight (median, IQR)	31 kg (11 kg)

Figure 4-6: Displays the consort diagram of the healthy volunteers who participated in this study.



We aimed to recruit up to 20 patients for imaging scanning protocol development in children. Eleven responded to the first and second adverts. Nine consented to take part. One was excluded due to motion artefact preventing image analysis. Further rounds of recruitment were prevented due to the COVID-19 pandemic.

Table 4-7: Descriptive characteristics of individuals in the control group. The participants who withdrew from the study were marked by a star (*).

NO	Age	Gender	Height	Weight
1	10	Female	164 cm	65 kg
2	16	Male	172 cm	56.8 kg
3	11	Male	140 cm	32 kg
4*	8	Male	122 cm	22.25 kg
5	12	Male	161 cm	46.4 g
6	11	Male	147 cm	36.6 g
7	8	Male	126 cm	23.85 kg
8	13	Female	165 cm	48.45 kg
9	10	Female	145 cm	37.5 kg

Table 4-8: Characteristics for the AT group and control group (healthy volunteer).

Descriptive Parameter	Statistical Results (HV)	Statistical Results (AT)
Number completed scan and scan analysis possible	8	12
Age (median, IQR)	11 years (3.5 years)	9 years (4 years)
Sex (%)	Male= 66.66%	Male= 60%
	Female= 33.33%	Female= 40%
Height (median, IQR)	147 cm, (31.5 cm)	131cm (16 cm)
Weight (median, IQR)	37.5 kg, (24.7 kg)	31 kg (11 kg)

Table 4-9: Shows the OE-MRI parameters and its region for AT group.

No.	Delta-PO ₂	Wash-in-time	Delta-PO ₂	VVF
	Whole-lung wash-in-ef-mask	Whole-lung wash-in-ef-mask	Aorta wash-in-ef-mask	Whole-lung
1	-503.3592274	88247.32576	699.4225552	0.923855876
2	264.362051	17430.33136	555.061472	0.986768888
3	221.5518556	31069.78098	471.1955261	0.94469795
4	-607.0005163	54487.47581	446.2573977	0.946412987
5	-12.45403388	98794.35517	639.1731977	0.901159679
6	-177.5327632	25482.73986	442.0260719	0.868487691
7	-90.78568791	32027.31093	571.0040665	0.689534707
8	-139.8360102	19291.93639	581.1024679	0.79158348
9	-368.4653647	43946.50224	273.2879796	0.889218319
10	185.8318303	12200.55475	451.0579732	0.95360046
11	-6061.653856	485780.3571	1541.607414	0.613758531
12	-115.4391835	23686.9248	367.3967734	0.678639091

Table 4-10: Shows the OE-MRI parameters and its region for healthy volunteer.

No.	Delta-PO ₂	Wash-in-time	Delta-PO ₂	VVF
	Whole-lung wash-in-ef-mask	Whole-lung wash-in-ef-mask	Aorta wash-in-ef-mask	Whole-lung
1	-522.3830082	124738.9126	535.3173724	0.925091221
2	-1605.330936	130696.9631	-382.3462938	0.836706523
3	173.3280394	13480.11569	703.1467278	0.893670363
4	-256.9409701	31192.19248	436.4764303	0.895667299
5	-5188.380696	393156.9126	451.194753	0.890176645
6	-2190.798876	133420.6856	356.8131707	0.79393903
7	-16.551803	21936.28947	363.5350812	0.957821812
8	-1555.19466	98517.27657	531.2142519	0.520154843

4.3.2 Image Acquisition and Artefact

A single 3D-MRI was taken of the dynamic OE-MRI protocol, which goes into the image analysis pipeline for OE-MRI analysis. There is concern that

there is imaging artefact from the receiver coil and bed projecting within the lung fields. Artefacts were noted in the raw data, appearing as horizontal lines, which were attributed to the straps, scanner bed and receiver projecting into the thorax (see Figure 4-7). These were resolved by increasing the field of view and changing the straps from plastic to cotton. This reduced the number of horizontal lines artefacts and prevented them from appearing within the thorax (see Figure 4-8).

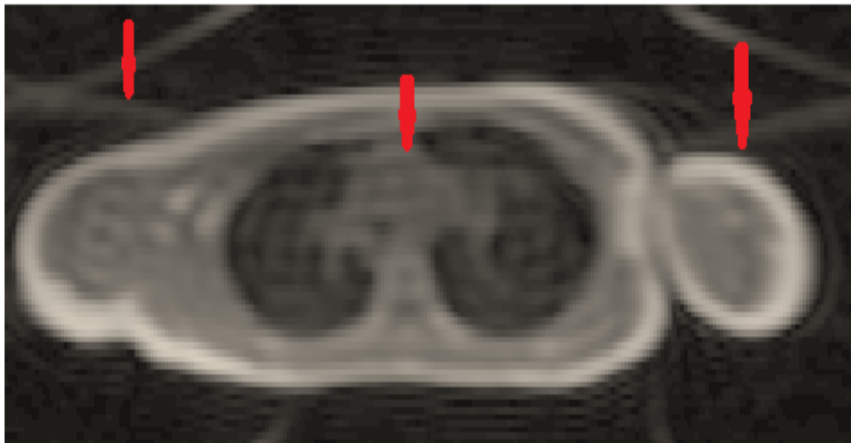


Figure 4-7: Shows an axial lung MR image which captured by protocol 1 with an artefact of horizontal lines, indicated by red arrows.

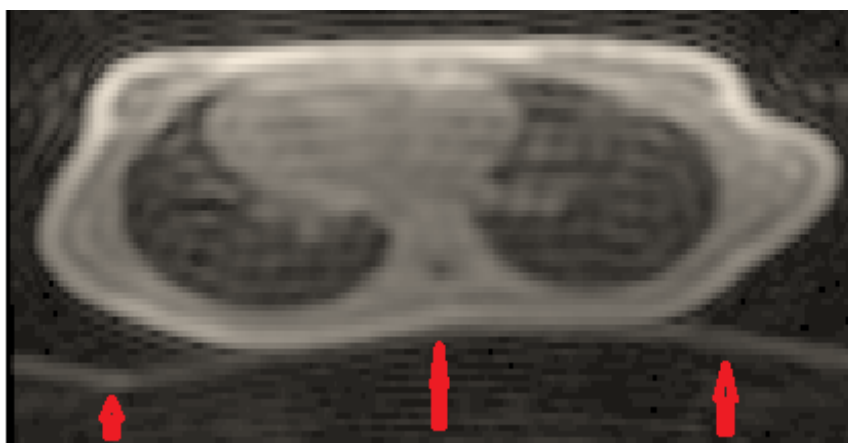


Figure 4-8: Shows an axial lung MR image which captured by protocol 2 with an artefact horizontal line as indicated by red arrows.

4.3.3 Example Processed Data

Example data from the OE-MRI pipeline shows an area of ventilation defect. In any area of the lungs where the dissolved oxygen ratio is increased, the MRI signal (T1) will spontaneously increase, and vice versa (see Figure 4-9). Data for the OE-MRI scans were processed by BioxyDyn with their imaging pipeline and returned to the Nottingham team for further analysis.

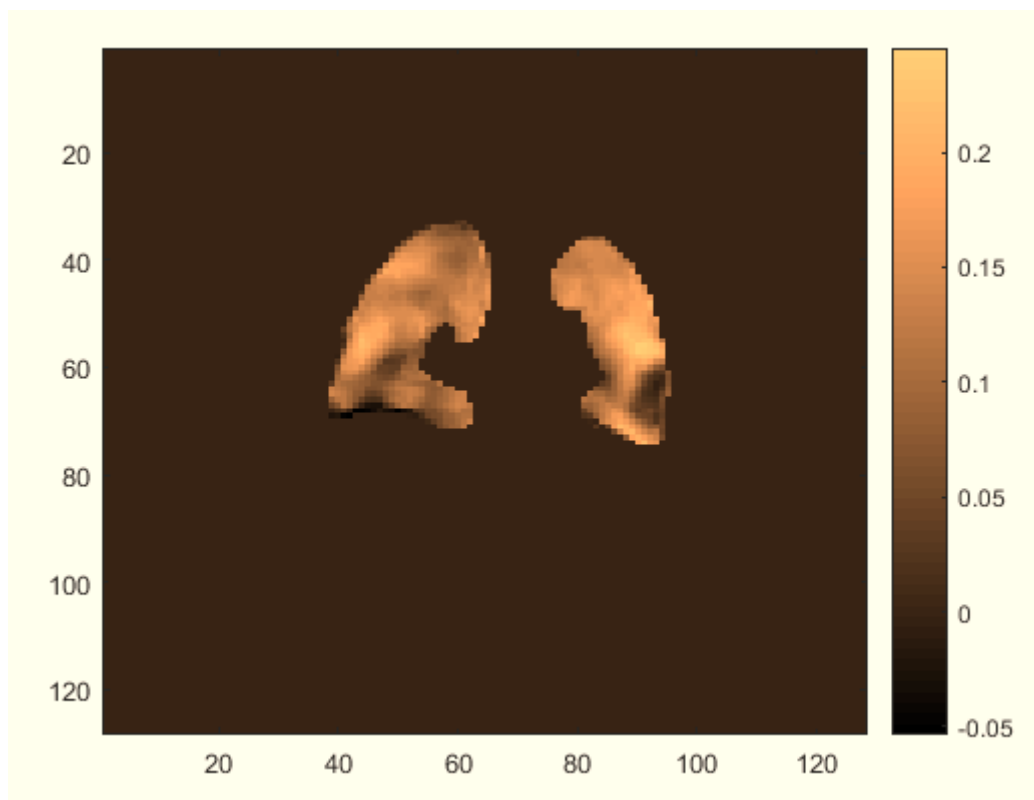


Figure 4-9: Shows an area of ventilation defect in the lungs (coloured by black). Units are arbitrary and are calibrated later in the pipeline.

4.3.4 Histogram and Normality Test

Histogram and test of normality were conducted to determine the proper statistical method of analysing OE-MRI's data for both the AT group and healthy volunteers' group.

4.3.4.1 Histogram and Test of Normality of Delta-PO₂ Whole Lung

A histogram and test of normality were conducted and showed that the distribution of these data for both groups is not normal (see Figure 4-10). Using the Kolmogorov-Smirnov and the Shapiro-Wilk tests, the data of AT group did not have a normal distribution (P-value <0.001, which is less than the pre-specified 0.05; see Table 4-11). Likewise, the same test has been used for healthy volunteer group, it did not have a normal distribution (P-value 0.06, which is less than the pre-specified 0.05; see Table 4-11). Therefore, these data are analysed by non-parametric test.

Table 4-11: Shows the normality test of delta-PO₂ in whole lung for AT group and healthy volunteer group.

Tests of Normality							
	Groups	Kolmogorov-Smirnov ^a			Shapiro-Wilk		
		Statistic	df	Sig.	Statistic	df	Sig.
Delta PO ₂ whole lung	AT	0.419	12	<.001	0.474	12	<.001
	HV	0.202	8	.200*	0.83	8	0.06

a. Lilliefors Significance Correction

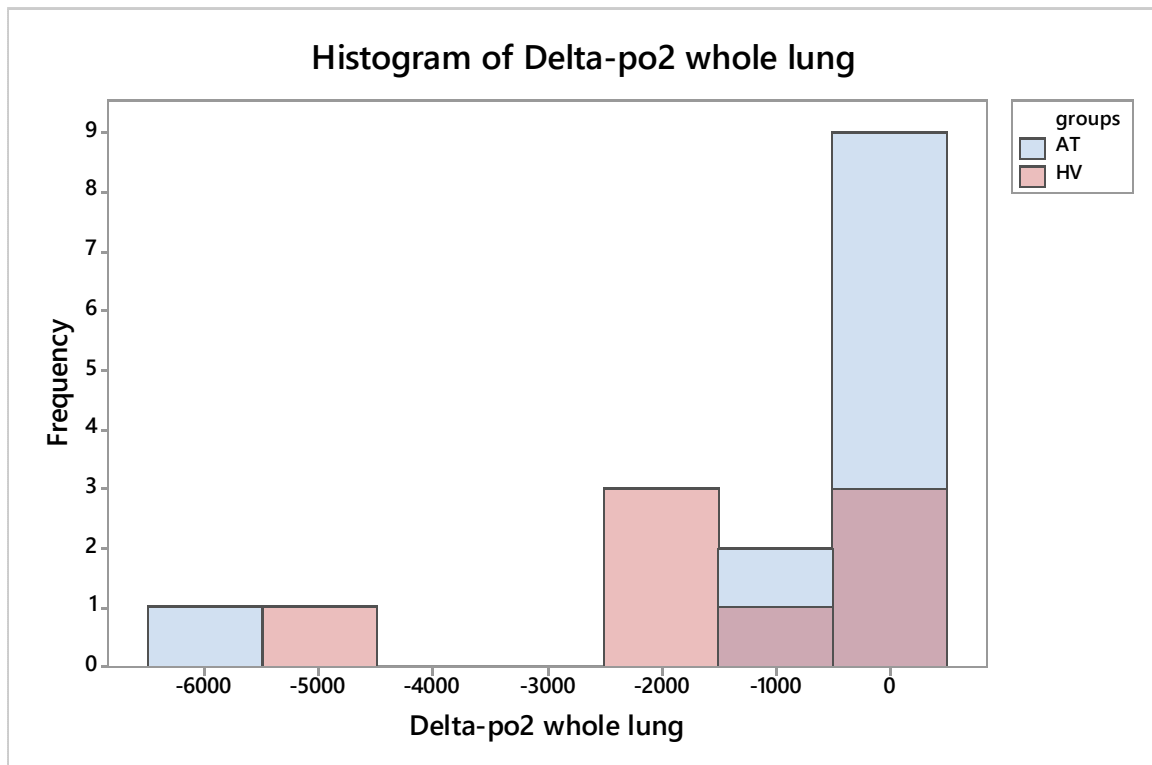


Figure 4-10: Shows the distribution of delta-PO₂ data in whole lung for AT group and healthy volunteer group.

4.3.4.2 Histogram and Test of Normality of Wash-in-time Whole Lung

A histogram and normality tests were conducted. These too showed that the distribution of these data for both groups is not normal (see Figure 4-11). The P-value for AT group was <0.001 and P-value for the healthy volunteers' group was 0.015, which is less than the pre-specified 0.05; see table 4-12.

Table 4-12: Shows the normality test of wash in time in whole lung for AT group and healthy volunteer group.

Tests of Normality							
	Groups	Kolmogorov-Smirnov ^a			Shapiro-Wilk		
		Statistic	df	Sig.	Statistic	df	Sig.
Wash in time whole lung	AT	0.353	12	<.001	0.503	12	<.001
	HV	0.326	8	0.012	0.773	8	0.015

a. Lilliefors Significance Correction

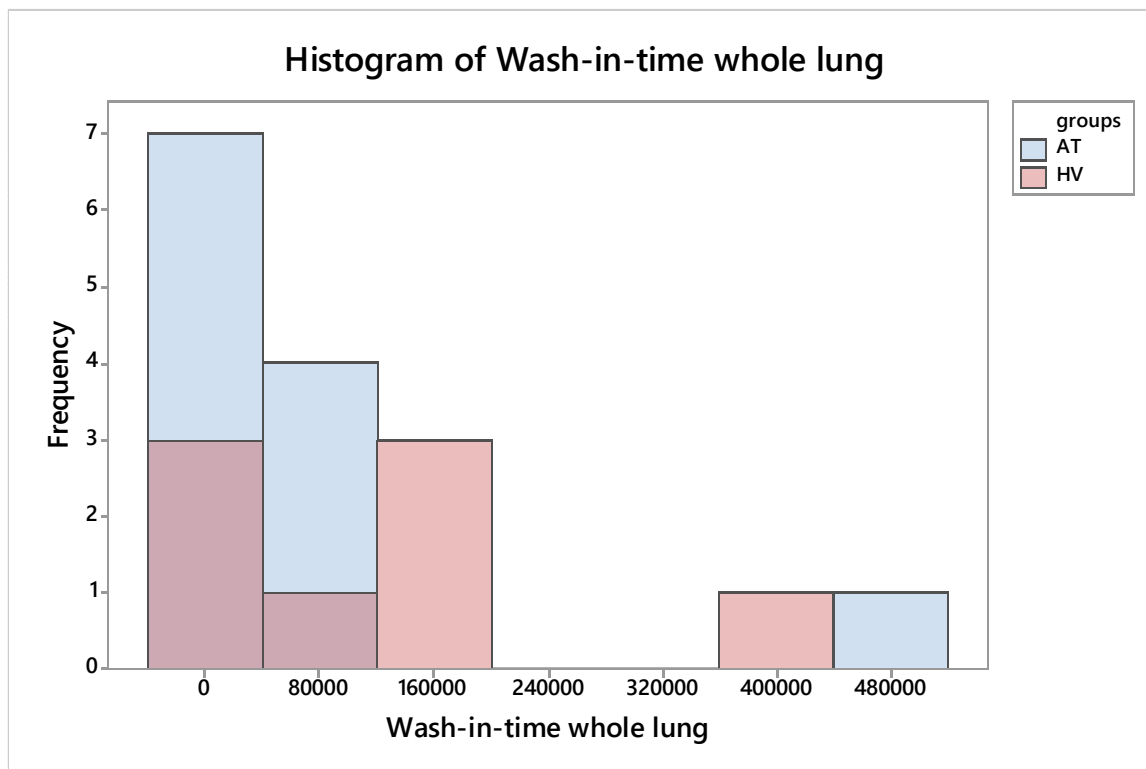


Figure 4-11: Shows the distribution of wash in time data in whole lung for AT group and healthy volunteer group.

4.3.4.3 Histogram and Test of Normality of Delta-PO₂ Aorta

A Histogram and normality tests also were conducted, which showed that the distribution of these data for both groups is not normal (see Figure 4-

12). The P-value for AT group was <0.001 and for P-value for the healthy volunteers' group was 0.007, which is less than the pre-specified 0.05; see table 4-13.

Table 4-13: Shows the normality test of delta-PO₂ in aorta for AT group and healthy volunteer group.

Tests of Normality							
	Groups	Kolmogorov-Smirnov ^a			Shapiro-Wilk		
		Statistic	df	Sig.	Statistic	df	Sig.
Delta PO ₂ aorta	AT	0.28	12	0.01	0.684	12	<.001
	HV	0.353	8	0.004	0.745	8	0.007

a. Lilliefors Significance Correction



Figure 4-12: Shows the distribution of delta-PO₂ data in aorta for AT group and healthy volunteer group.

4.3.2.4 Histogram and Test of Normality of VVF

A Histogram and normality tests also were conducted, which showed that the distribution of these data for both groups is not normal (see Figure 4-13). The P-value for AT group was 0.057 and for P-value for the healthy volunteers' group was 0.008, which is less than the pre-specified 0.05; see table 4-14.

Table 4-14: Shows the normality test of VVF for AT group and healthy volunteer group.

Tests of Normality							
	Groups	Kolmogorov-Smirnov ^a			Shapiro-Wilk		
		Statistic	df	Sig.	Statistic	df	Sig.
VVF	AT	0.229	12	0.083	0.865	12	0.057
	HV	0.269	8	0.092	0.749	8	0.008

a. Lilliefors Significance Correction

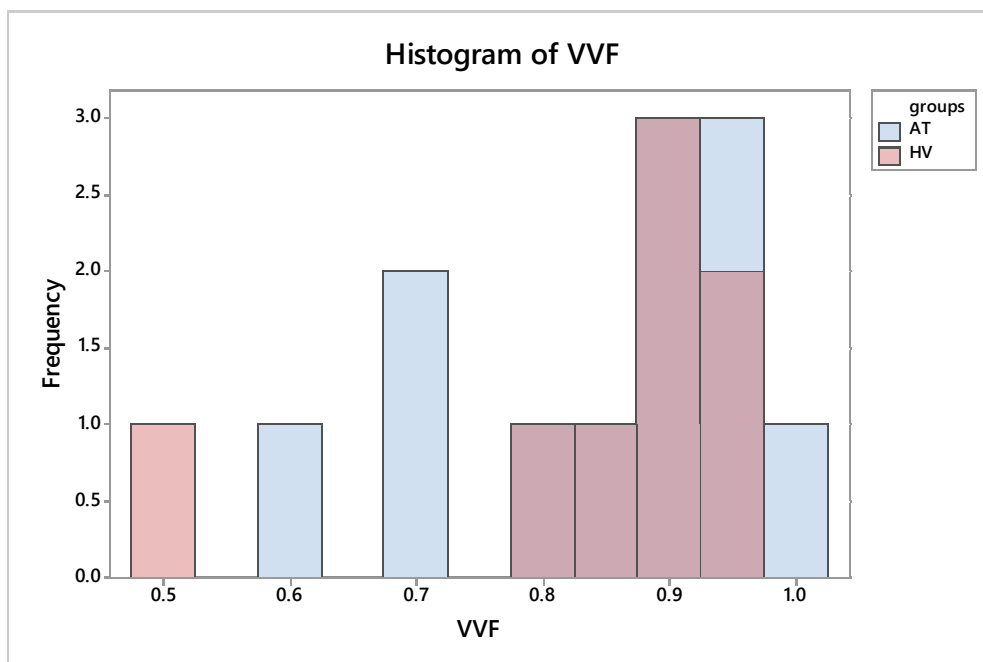


Figure 4-13 Shows the distribution of VVF data in whole lung for AT group and healthy volunteer group. VVF: Fraction of the region presenting with oxygen enhancement (max 1, min 0).

4.3.5 Boxplot

4.3.5.1 Boxplot of Delta-PO₂ in Whole Lung for AT Group and Control Group

The boxplot suggests that there is a difference in the delta-PO₂ in whole lung median between the two groups (AT median= -127.6, healthy volunteer group median= -1038.8). The data for the AT group is more concentrated and exhibits less variability with an extreme value downwards. In contrast, the data in healthy volunteer group is less concentrated and has more variability with an extreme value downwards as well (see Figure 4-14).

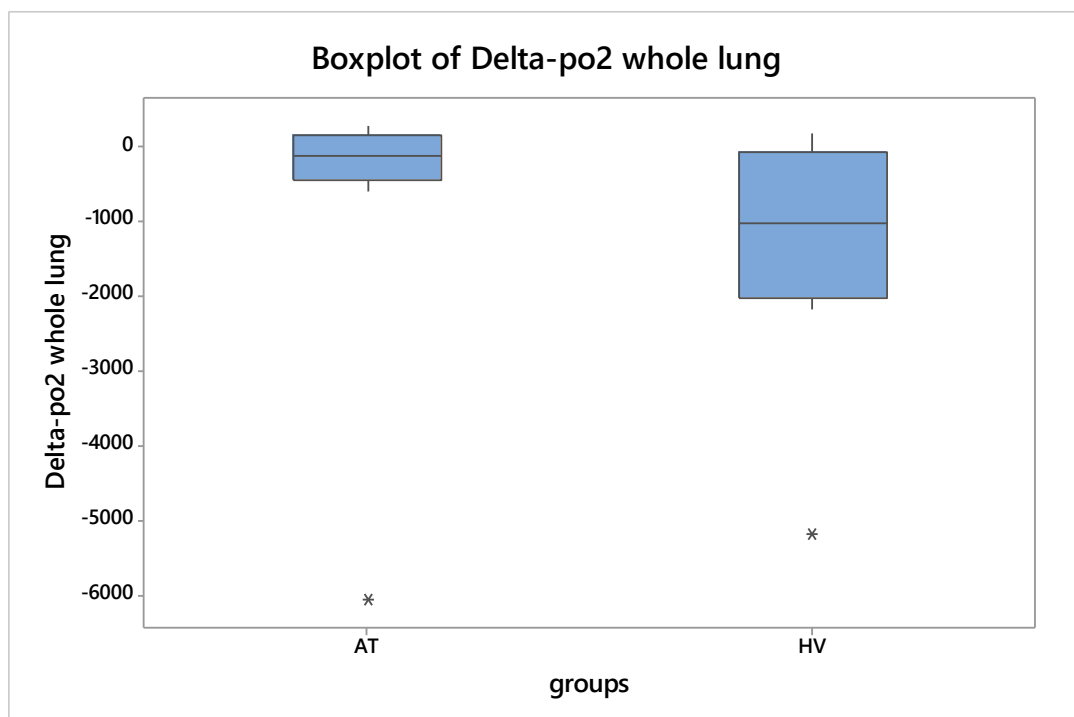


Figure 4-14: Shows the distribution of delta-PO₂ data in the whole lung for AT group with a lower extreme outlier and the healthy volunteer group with a lower extreme outlier as well.

4.3.5.2 Boxplot of Wash-in-Time in the Whole Lung for the AT Group and Control Group

The boxplot suggests that there is difference in the median wash-in-time in the whole lung between two groups. (AT median= 31549, healthy volunteer median= 111628). The data in the AT group is more concentrated and less variable in the first quartile. Moreover, it is less concentrated and more variable in the third quartile with an extreme upwards value. In contrast, the data in healthy volunteer group is less concentrated and more variable in the first quartile. In addition, it is more concentrated in the third quartile, with an extreme upwards value as well (see Figure 4-15).

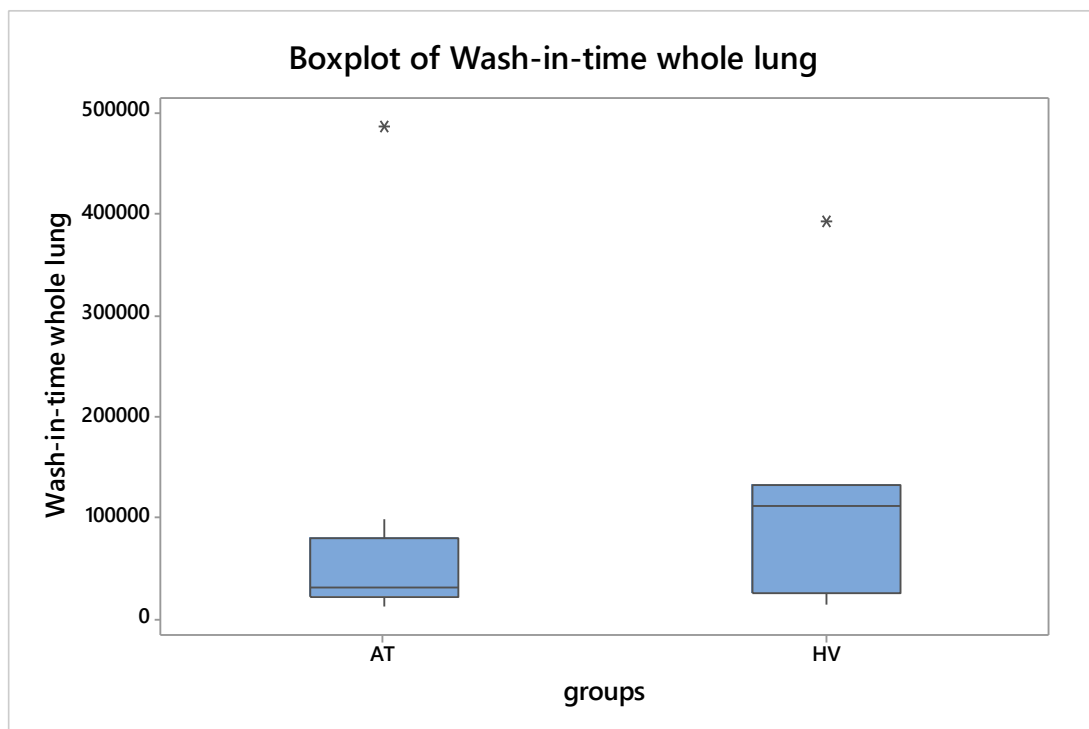


Figure 4-15: Shows the distribution of wash-in-time data in the whole lung for AT group with an upper extreme outlier and the healthy volunteer group with an upper extreme outlier as well.

4.3.5.3 Boxplot of Delta-PO₂ Aorta for AT Group and Control Group

The boxplot suggests that there is no difference in the median of the delta-PO₂ aorta between the two groups (AT median= 513.1, healthy volunteer median= 443.8). The data for the AT group is more concentrated and less variable in the first and third quartiles with an extreme upwards value. In contrast, the data in healthy volunteer group is more concentrated and less variable in the first and third quartiles with an extreme downwards value (see Figure 4-16).

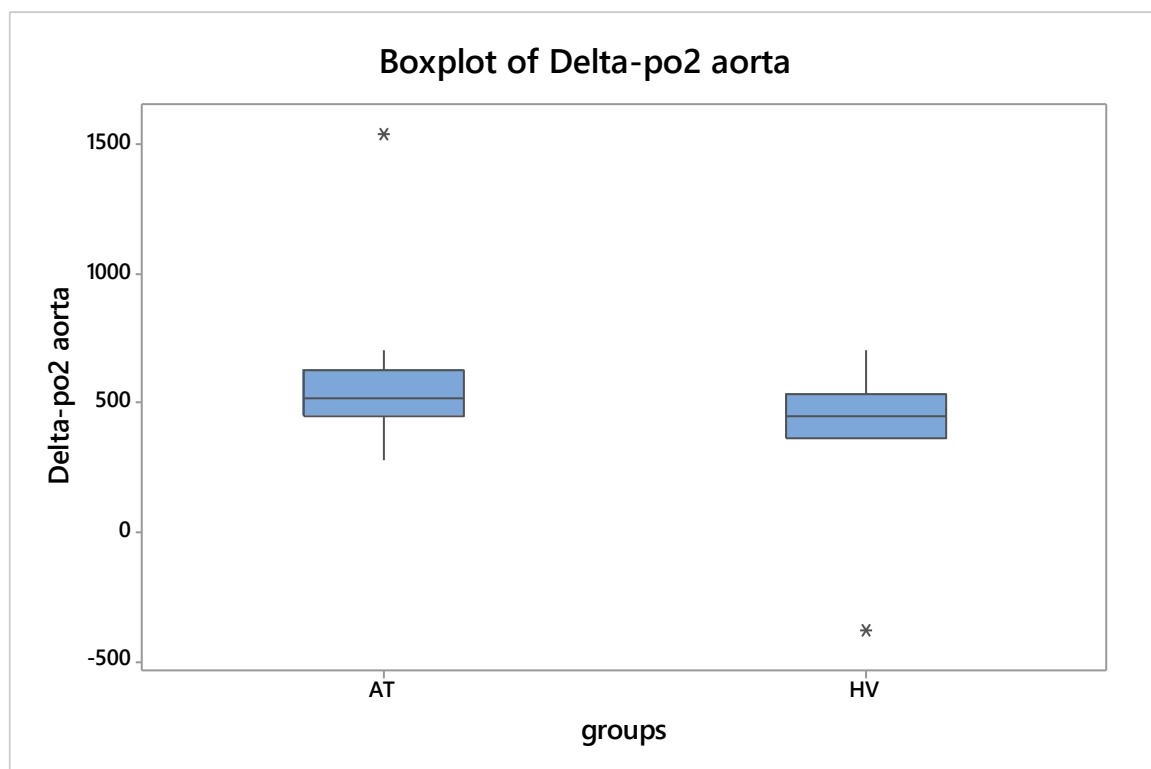


Figure 4-16: Shows the distribution of delta-PO₂ data in aorta for AT group with an upper extreme outlier and the healthy volunteer's group with a lower extreme outlier.

4.3.5.4 Boxplot of VVF for AT Group and Control Group

The boxplot suggests that there is no difference in the VVF in whole lung median between the two groups (AT median= 0.8952, healthy volunteer median= 0.8919). The AT group appears to have a more variable VVF than the HV group. In contrast, the data for the healthy volunteer group is less variable overall (see Figure 4-17).

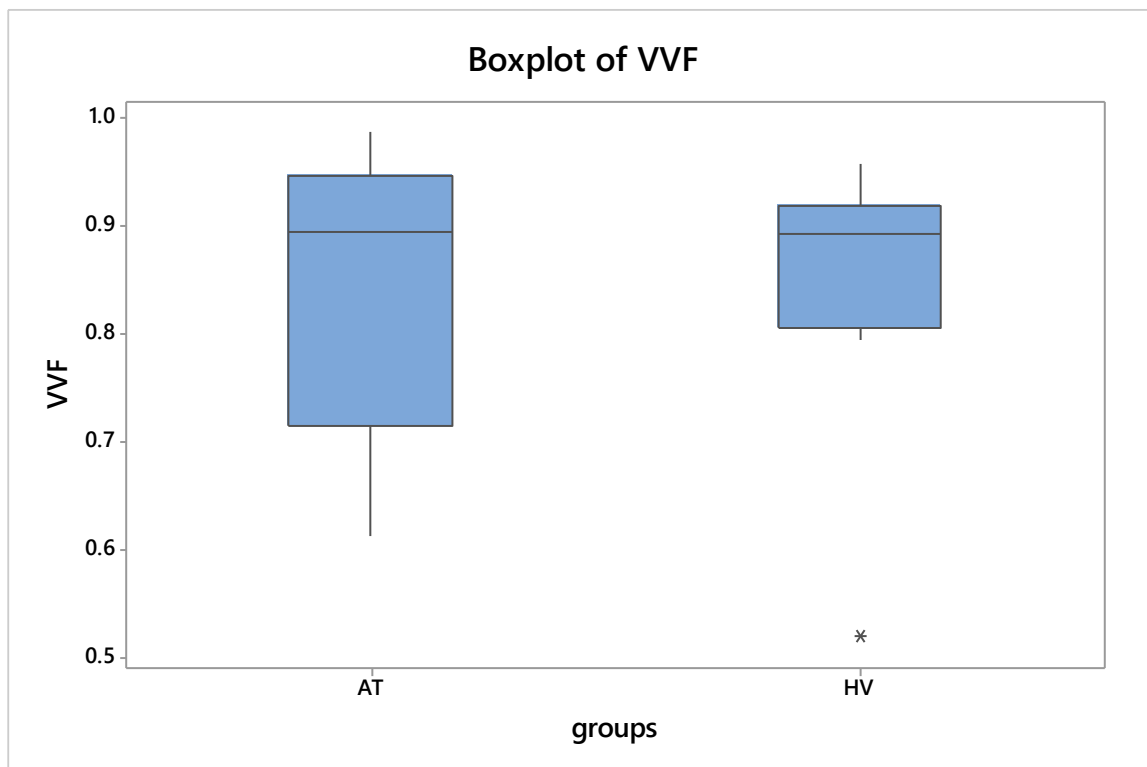


Figure 4-17: Shows the distribution of VVF data in whole lung for AT group and healthy volunteer group with a lower extreme outlier. VVF: Fraction of the region presenting with oxygen enhancement (max 1, min 0).

4.3.6 The Difference in OE-MRI Parameters (Delta-PO₂ Whole Lung, Wash-in-Time, Delta-PO₂ Aorta and VVF) between Both Groups

In this study, the Mann-Witney test was conducted to determine the difference between the two groups. I hypothesised that if there were no lung disease present in the children with AT, there would be no variation between the two groups. Therefore, the null hypothesis is that there is no significant difference between the two groups, unless lung disease is present.

4.3.6.1 The Difference in the Delta-PO₂ in the Whole Lung between the AT Group and Control

The delta-PO₂ parameter in whole lung was compared between the two groups using Mann-Whitney. The result of this test showed that there is not enough evidence to reject the null hypothesis, as the P-value (0.105) is greater than the pre-specified threshold of 0.05. There is no evidence for a difference between the two groups (see Table 4-15).

Table 4-15: Demonstrates the results of the Mann-Whitney test of delta-PO₂ in whole for AT group and healthy volunteers.

Test Statistics ^a	Delta PO ₂ whole lung
Mann-Whitney U	27.000
Wilcoxon W	63.000
Z	-1.620
Asymp. Sig. (2-tailed)	.105
Exact Sig. [2*(1-tailed Sig.)]	.115 ^b

4.3.6.2 The Difference in the Wash-in-Time between the AT Group and Control

Next, the wash-in-time parameter in whole lung of the two groups was compared using Mann-Whitney. The result of this test show that there is not enough evidence to reject the null hypothesis, as the P-value (0.217) is greater than 0.05, There is no evidence for a difference between the two groups (see Table 4-16).

Table 4-16: Demonstrates the Mann-Whitney test of the wash-in-time in whole lung for the AT group and healthy volunteers.

Test Statistics ^a	Wash in time whole lung
Mann-Whitney U	32.000
Wilcoxon W	110.000
Z	-1.234
Asymp. Sig. (2-tailed)	.217
Exact Sig. [2*(1-tailed Sig.)]	.238 ^b

4.3.6.3 The Difference in Delta-PO₂ Aorta between the AT Group and Control

The delta-PO₂ parameter in aorta of the two groups was compared using Mann-Whitney. The result of this test showed that there is not enough evidence to reject the null hypothesis, as the P-value (0.217) is greater than 0.05, There is no evidence for a difference between the two group (see Table 4-17).

Table 4-17: Demonstrates the Mann-Whitney test of delta-PO₂ in aorta for AT group and healthy volunteers.

Test Statistics ^a	Delta-PO ₂ aorta
Mann-Whitney U	32.000
Wilcoxon W	68.000
Z	-1.234
Asymp. Sig. (2-tailed)	.217
Exact Sig. [2*(1-tailed Sig.)]	.238 ^b

4.3.6.4 The Difference in VVF between the AT Group and Control

Mann-Whitney was used to compare a VVF parameter between the two groups. The result of this test showed that there is not enough evidence to reject the null hypothesis, as the P-value (0.817) is greater than 0.05, There is no evidence for a difference between the two groups (see Table 4-18).

Table 4-18: Demonstrates the Mann-Whitney test result of VVF for the AT group and healthy volunteers.

Test Statistics ^a	VVF
Mann-Whitney U	45.000
Wilcoxon W	81.000
Z	-.231
Asymp. Sig. (2-tailed)	.817
Exact Sig. [2*(1-tailed Sig.)]	.851 ^b

4.3.7 The Relationship between OE-MRI Parameters and Height in the AT Group and Control

As mentioned before, height plays a key role in determining the range of these values, which increases with height unless there is significant lung disease present. Therefore, I assessed the relationship between these values (delta-PO₂ whole lung, wash-in-time whole lung, delta-PO₂ aorta,

VVF) and height in the groups using multivariable regression model (Minitab 17.2.1) (see Figure 4-18). The OE-MRI parameters are the key values obtained from OE-MRI scan.

When the ratio of these values is high, it implies there is good ventilation and perfusion and vice versa. Therefore, I hypothesise that there is relationship between height and OE-MRI parameters; also, that there is a relationship between the two groups unless there is significant lung disease present. The null hypothesis is that there is no relationship between two groups and the OE-MRI parameters and the height.

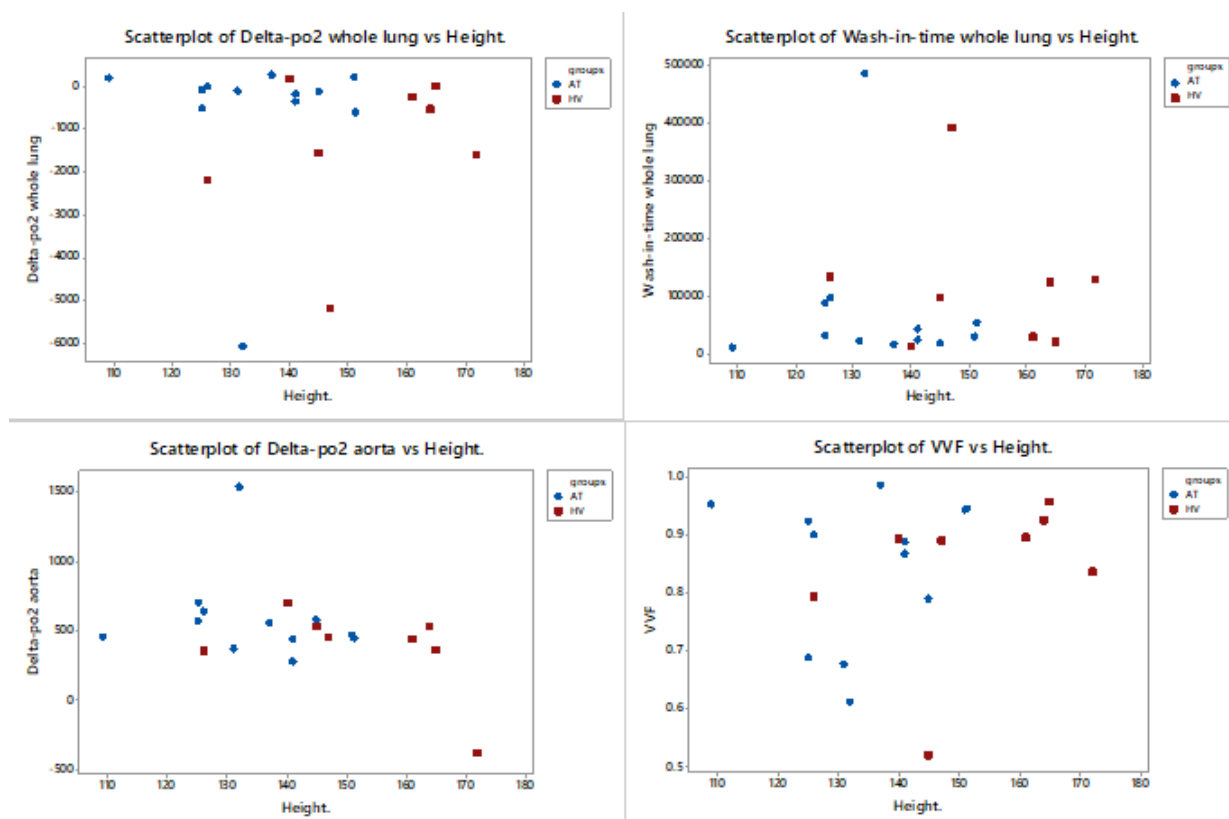


Figure 4-18: Shows the OE-MRI parameters versus height for 12 children with AT (blue dots and line) and 8 healthy volunteers (red dots and line).

4.3.7.1 Regression Analysis: Delta-PO₂ the Whole Lung versus Height

After accounting for height as a co-variable in the multivariable linear regression model, the delta PO₂ in whole lung was 1111 less in the group of healthy volunteers compared to the AT group. The average delta PO₂ the of healthy volunteers' group (-1111) is lower than the AT group (-3107) (see Table 4-19). With each unit increase in the height, the whole lung delta-PO₂ goes up by 18.5 units. However, the P-value was 0.272 for the group, which means there no evidence of a difference in the delta-PO₂ for the whole lung after accounting for height (see Table 4-19). Based on this, the null hypothesis of no association with height was accepted, and the increase in delta-PO₂ for the whole lung with height could be a chance finding.

Table 4-19: Demonstrates the linear regression model of the delta-PO₂ in whole lung versus height as covariable in healthy volunteer group and AT group.

Term	Coef	SE Coef	T-Value	P-Value	VIF
Constant	-3107	4148	-0.75	0.464	
Height.	18.5	30.6	0.60	0.553	1.46
Groups					
HV	-1111	979	-1.13	0.272	1.46

4.3.7.2 Regression Analysis: Wash-in-Time in Whole Lung versus Height

After accounting for height as a co-variable in the linear regression model, the wash-in-time in the whole lung was 59779 higher in the group of healthy volunteers compared to the AT group. The average wash-in-time of the healthy volunteers' group of 59779, is lower than the AT group (220575) (see Table 4-20). With each unit increase in the height, the wash-in-time in the whole lung goes down by -1062 units. Based on this significant value the null hypothesis is accepted. However, the P-value was 0.419 for group, which means that there was no evidence of a difference in the wash-in-time after accounting for height (see Table 4-20). Based on this, the null hypothesis of no association with height was accepted, and the decrease in wash-in-time with height could be a chance finding.

Table 4-20: Demonstrates the linear regression model of the wash-in-time in whole lung versus height as covariable in healthy volunteer group and AT group.

Term	Coef	SE Coef	T-Value	P-Value	VIF
Constant	220575	305545	0.72	0.480	
Height.	-1062	2254	-0.47	0.643	1.46
Groups					
HV	59779	72115	0.83	0.419	1.46

4.3.7.3 Regression Analysis: Delta-PO₂ in the Aorta versus Height

After accounting for height as a co-variable in the linear regression model, the delta PO₂ in the aorta was 80 less in the group of healthy volunteers

compared to the AT group. The average delta PO₂ of healthy volunteers' group of-80, is lower than the AT group (1573) (see Table 4-21). With each unit increase in the height, the delta-PO₂ in the aorta goes down by -7.33 units. However, the P-value was 0.652 for group, which means that there was no evidence of a difference in the delta-PO₂ in the aorta after accounting for height (see Table 4-21). Based on this, the null hypothesis of no association with height was accepted, and the decrease in delta-PO₂ aorta with height could be a chance finding.

Table 4-21: Demonstrates the linear regression model of the delta-PO₂ in the aorta versus height as covariable in healthy volunteer group and AT group.

Term	Coef	SE Coef	T-Value	P-Value	VIF
Constant	1573	741	2.12	0.049	
Height.	-7.33	5.47	-1.34	0.197	1.46
Groups					
HV	-80	175	-0.46	0.652	1.46

4.3.7.4 Regression Analysis: VVF versus Height

After accounting for height as a co-variable in the linear regression model, the VVF was 0.0513 less in the group of healthy volunteers compared to the AT group. The average VVF of the healthy volunteers' group was 0.0513, which is lower than the AT group (0.539) (see Table 4-22). With each unit increase in the height, the VVF goes up by 0.00231 units. However, the P-value was 0.485 for group, which means that there was no

evidence of a difference in VVF after accounting for height (see Table 4-22). Based on this, the null hypothesis of no association with height was accepted, and the increase in VVF with height could be a chance finding.

Table 4-22: Demonstrates the linear regression model of the VVF versus height as covariable in healthy volunteer group and AT group.

Term	Coef	SE Coef	T-Value	P-Value	VIF
Constant	0.539	0.304	1.77	0.095	
Height.	0.00231	0.00224	1.03	0.319	1.46
Groups					
HV	-0.0513	0.0718	-0.71	0.485	1.46

4.3.8 The relationship among OE-MRI Parameters versus Age with the AT group and control group

As mentioned before, age plays a key role in determining the range of these values, which will increase as lung growth continues during childhood unless significant lung disease is present. Therefore, I assessed the relationship between these values ($\Delta\text{-PO}_2$ for the whole lung, wash-in-time for the whole lung, $\Delta\text{-PO}_2$ in the aorta and VVF) versus age in the AT group and the control group using multivariable regression model (Minitab 17.2.1) (see Figure 4-19).

When the ratio of these values is high, it implies there are good ventilation and perfusion, and vice versa. Therefore, I hypothesise that there is relationship between age and the OE-MRI parameters, and there is a relationship between two groups unless significant lung disease is present.

The null hypothesis is that there is no relationship between the two groups and the OE-MRI parameters versus age.

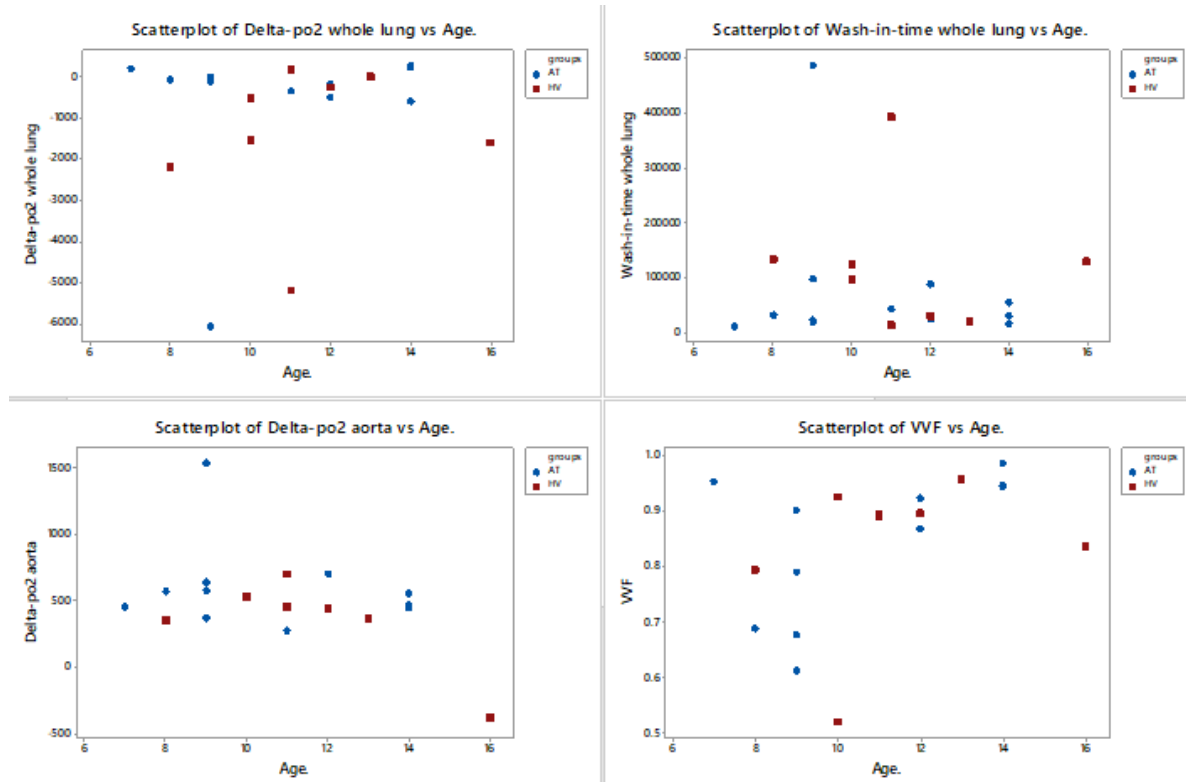


Figure 4-19: Shows the OE-MRI parameters versus age for 12 children with AT (blue dots and line) and 8 healthy volunteers (red dots and line).

4.3.8.1 Regression Analysis: Delta-PO₂ in Whole Lung versus Age

After accounting for age as a co-variable in the linear regression model, the delta PO₂ in whole lung was 864 less in the group of healthy volunteers compared to the AT group. The average delta PO₂ of healthy volunteers' group was -864, which is lower than the AT group (-1914) (see Table 4-23). With each unit increase in age, the delta-PO₂ in whole lung goes up by

122 units. However, the P-value was 0.304 for group, which means that there was no evidence of a difference in the delta-PO₂ for the whole lung after accounting for age (see Table 4-23). Based on this, the null hypothesis of no association with age was accepted, and the increase in delta-PO₂ in the whole lung with age could be a chance finding.

Table 4-23: Demonstrates the linear regression model of the delta-PO₂ in whole lung versus age as covariable in the healthy volunteer group and AT group.

Term	Coef	SE Coef	T-Value	P-Value	VIF
Constant	-1914	1879	-1.02	0.323	
Age	122	170	0.72	0.483	1.02
Groups					
HV	-864	815	-1.06	0.304	1.02

4.3.8.2 Regression Analysis: Wash-in-time for the Whole Lung versus Age

After accounting for age as a co-variable in the linear regression model, the wash-in-time in the whole lung was 46670 higher in the group of healthy volunteers compared to the AT group. The average wash-in-time of the healthy volunteers' group was 46670, which is lower than the AT group (167783) (see Table 4-24). With each unit increase in age, the wash-in-time in the whole lung goes down by -8445 units. Based on this significant value, the null hypothesis is accepted. However, the P-value was 0.447 for group, which means that there was no evidence of a difference in the wash-in-time after accounting for height (see Table 4-24). Based on this, the null

hypothesis of no association with age was accepted, and the decrease in wash-in-time with age could be a chance finding.

Table 4-24: Demonstrates the linear regression model of the wash-in-time in the whole lung versus age as covariable in the healthy volunteer group and AT group.

Term	Coef	SE Coef	T-Value	P-Value	VIF
Constant	167783	138092	1.22	0.241	
Age	-8445	12460	-0.68	0.507	1.02
Groups					
HV	46670	59906	0.78	0.447	1.02

4.3.8.3 Regression Analysis: Delta-PO₂ in Aorta versus Age

After accounting for age as a co-variable in the linear regression model, the delta PO₂ in the aorta was 174 less in the group of healthy volunteers compared to the AT group. The average delta PO₂ of healthy volunteers was -174, which is lower than the AT group (1164) (see Table 4-25). With each unit increase in age, the delta-PO₂ in the whole lung goes down by -54.2 units. The P-value is 0.232, which means that is highly likely there is no difference between two groups (see Table 4-25).

Based on this significance value, the null hypothesis is accepted. However, the P-value was 0.232 for group, which means that there was no evidence of difference in delta-PO₂ in the aorta after accounting for age (see Table 4-25). Based on this, the null hypothesis of no association with age was

accepted, and the decrease in delta-PO₂ in the aorta with age could be a chance finding.

Table 4-25: Demonstrates the linear regression model of the delta-PO₂ in aorta versus age as covariable in the healthy volunteer group and AT group.

Term	Coef	SE Coef	T-Value	P-Value	VIF
Constant	1164	323	3.60	0.002	
Age	-54.2	29.2	-1.86	0.081	1.02
Groups					
HV	-174	140	-1.24	0.232	1.02

4.3.8.4 Regression Analysis: VVF versus Age

After accounting for age as a co-variable in the linear regression model, the VVF was 0.0269 less in the group of healthy volunteers compared to AT group. The average VVF of the healthy volunteers was -0.0269, which is lower than the AT group (0.592) (see Table 4-26). With each unit increase in the age, the VVF goes up by 0.0241 units. However, the P-value was 0.632 for group, which means that there was no evidence of a difference in VVF after accounting for age (see Table 4-26). Based on this, the null hypothesis of no association with age was accepted, and the increase in VVF with age could be a chance finding.

Table 4-26: Demonstrates the linear regression model of the VVF in whole lung versus age as covariable in the healthy volunteer group and AT group.

Term	Coef	SE Coef	T-Value	P-Value	VIF
Constant	0.592	0.127	4.65	0.000	
Age	0.0241	0.0115	2.10	0.051	1.02
Groups					
HV	-0.0269	0.0552	-0.49	0.632	1.02

4.3.9 The relationship among OE-MRI Parameters versus Gender in the AT group and control group

Gender plays a key role in determining the range of these values. Males' lung size is greater than females' lung size when there is similarity in the race, height, and weight, unless significant lung disease is present. Therefore, I assessed the relationship between these values (delta-PO₂ in the whole lung, delta-PO₂ in the aorta, wash-in-time whole and VVF) versus gender for the AT group and the control group using multivariable regression model (Minitab 17.2.1).

When the ratio of these values is high, it implies there are good ventilation and perfusion and vice versa. Therefore, I hypothesise that there is relationship between the age and OE-MRI parameters and there is a relationship between two groups unless significant lung disease is present. The null hypothesis is that there is no relationship between two groups and the OE-MRI parameters versus gender.

4.3.9.1 Regression Analysis: Delta-PO₂ in the whole Lung versus Gender

After accounting for gender as a co-variable in the linear regression model, there was no evidence of a difference between the AT and HV groups (P-value= 0.309) (see Table 4-27).

Table 4-27: Demonstrates the linear regression model of the delta-PO₂ in whole lung versus gender as covariable in the healthy volunteer group and AT group.

Term	Coef	SE Coef	T-Value	P-Value	VIF
Constant	-1975	1181	-1.67	0.113	
Gender	1018	804	1.27	0.223	1.00
Groups					
HV	-821	783	-1.05	0.309	1.00

4.3.9.2 Regression Analysis: Wash-in-Time for the Whole Lung versus Gender

After accounting for gender as a co-variable in the linear regression model, there was no evidence of a difference between the AT and HV groups (P-value= 0.463) (see Table 4-28).

Table 4-28: Demonstrates the linear regression model of the wash-in-time in whole lung versus gender as covariable in the healthy volunteer group and AT group.

Term	Coef	SE Coef	T-Value	P-Value	VIF
Constant	167425	87422	1.92	0.072	
Gender	-67291	59535	-1.13	0.274	1.00
Groups					
HV	43492	57964	0.75	0.463	1.00

4.3.9.3 Regression Analysis: Delta-PO₂ in the Aorta versus Gender

After accounting for gender as a co-variable in the linear regression model, there was no evidence of a difference between the AT and HV groups (P-value= 0.183) (see Table 4-29).

Table 4-29: Demonstrates the linear regression model of the delta-PO₂ in the aorta versus gender as covariable in the healthy volunteer group and AT group.

Term	Coef	SE Coef	T-Value	P-Value	VIF
Constant	621	229	2.70	0.015	
Gender	-26	156	-0.16	0.872	1.00
Groups					
HV	-211	152	-1.39	0.183	1.00

4.3.9.4 Regression Analysis: VVF in the Whole Lung versus Gender

After accounting for gender as a co-variable in the linear regression model, there was no evidence of a difference between the AT and HV groups (P-value= 0.831) (see Table 4-30).

Table 4-30: Demonstrates the linear regression model of the VVF versus gender as covariable in the healthy volunteer group and AT group.

Term	Coef	SE Coef	T-Value	P-Value	VIF
Constant	0.7547	0.0890	8.48	0.000	
Sex	0.0707	0.0606	1.17	0.259	1.00
Groups					
HV	-0.0128	0.0590	-0.22	0.831	1.00

4.4 Discussion

In the work described in this chapter, I set out to assess whether or not OE-MRI is feasible in children with AT. I further contributed to the development and optimisation of the scanning protocol. I went on to undertake exploratory analyses of the initial data. The main finding of the work described in this chapter is that it is possible to undertake an OE-MRI scan in children with AT.

There are limitations in this study. First and foremost, I acknowledge that the number of study sample is small, and this small number of participants has reduced the power of the exploratory statistical analysis. As mentioned beforehand, the main outcome measure was whether children with a significant movement disorder could undertake the OE-MRI protocol. Although the reduced sample size means that the study has less power to undertake exploratory interim analyses in which we compared children with AT and healthy controls, the overall objective to understand feasibility was met.

Fifteen children with AT were recruited into the study to compare OE-MRI parameters against those of healthy volunteers. Twelve of the 15 children successfully completed the MRI scan (see Figure 4-5). The underlying reason for this withdrawal of those participants was claustrophobia and the noisy sound produced by the MRI machine during the scan.

Claustrophobia can occur in anyone, regardless of his/ her health condition. Nevertheless, claustrophobia may be overcome by fully explaining the

procedure, encouraging the subject and rehearsing it before initiating the actual scan. Changing the patient's position from prone to supine may also help to solve this issue. The issue of noisy sounds may be solved by using music provided via headphones, which can minimise the sound and distract participants.

We encountered artefacts in the raw data, which constituted a major obstacle in this technique, and which we resolved by making adjustments in the scanning protocol. Artefacts were noted in the raw data as horizontal lines, which were thought to be due to the straps, scanner bed and receiver projecting into the thorax field of view (see Figure 4-7). However, this issue was minimised by using a large field of view and changing the plastic straps to cotton ones. This reduced the number of horizontal lines artefacts and prevented them from appearing within the images (see Figure 4-8).

When analysing the data, we initially looked at graphical plots (the box plots), which showed possible differences between the HV and AT groups. We went on to undertake a Mann-Whitney test, which did not find a difference. However, we knew that the AT and HV groups were not matched for height and age; therefore, we undertook multivariate regression, accounting for height and age. For completeness, and easy viewing of the results, each parameter of OE-MRI was separately presented in different statistical ways (Mann-Whitney, multivariable regression model, boxplot).

I undertook an exploratory analysis of multiple outcomes to obtain an initial understanding of what we can expect in future studies of OE-MRI. The

main outcomes defined to have potential value were as follows. Delta- PO_2 in the whole lung represents oxygen enhancement as the change in partial pressure of oxygen in whole lung [mmHg]. Delta- PO_2 in the aorta represents oxygen enhancement as the change in the partial pressure of oxygen in the aorta [mmHg] and is a measure of whole lung transfer of oxygen – more effective oxygen transfer leads to higher PO_2 in the aorta. Wash-in-time in the whole lung is the time taken to reach maximum PO_2 after administering pure oxygen. A higher wash in time implies greater heterogeneity of alveolar ventilation. VVF of the whole lung was the last OE-MRI parameter evaluated. VVF is the fraction of the region presenting with oxygen enhancement (max 1, min 0) – and a higher number implies better ventilation of the lung as a whole. In the exploratory analysis, there was no difference between the whole lung delta- PO_2 , aortal delta- PO_2 , or wash in time.

However, there was a difference in the ventilation fraction of the lung, with more of the healthy volunteers having higher ventilation fraction. This makes intuitive sense – we expect that all of the healthy volunteers will have well-ventilated lungs. However, whilst some of the children with AT will have normal ventilation, some will have reduced ventilation, as can be seen in the boxplot of ventilation.

We used a multivariable model to account for the fact that there were more tall children in healthy group than in the AT group. We could not match children with AT to healthy controls of both the same age and height,

because children with AT are short. If we match for height, we would get younger children in the controls compared to the AT groups. If we matched for age, we would get taller children in the control compared to the children with AT. That is why a multivariable model was used, because it allows for the simultaneous account for both, without having to match the cases in the controls. As there is some evidence that VVF in the whole lung may be lower in a proportion of children in the AT group, this encourages us to continue this work and collect more data.

According to Zeng et al. (2019), using lung MRI in conjunction with a MultiVane technique, can produce high-resolution, motion-suppressed images that allow for the characterisation of different pulmonary diseases, especially TB, due to the consistent results of the CT scan (see Figure 1-8). A MultiVane works as a beam of several parallel lines, which are collected in a multi-echo acquisition, instead of a single radial line.

AT patients are prone to sinopulmonary infection, which constitutes the primary cause of death. Therefore, we anticipate that the OE-MRI results of the AT group would be less than the results for the healthy volunteers. This technique depends on the ratio of pure oxygen dissolved in the blood, which increases the MRI signal (T1). Failure to increase the signal may imply that there is a defect in this part of the lung. Therefore, the lung size of AT patients would be smaller than the lung size of healthy volunteers.

Finally, the strength point of this study is that the technique was practically applied to AT patients, rather than based on theoretical considerations,

making it is the first study in this field. Although the study sample is small, it constitutes 12% of the total UK paediatric AT population. In addition, OE-MRI is a safe (non-ionising), non-invasive method of providing temporal and spatial lung information. Also, MRI machines are available in most hospitals and the cost of OE-MRI technique is lower than other techniques, like hyperpolarised noble gases. Children with AT also find difficulty to hold their breath; therefore, free breathing is regarded as a suitable way for them due to their neuromuscular degeneration.

The main limitation in this study is that it had to be paused due to the COVID-19 pandemic. This was because all non-essential research was initially stopped due to the pandemic. It was not safe for children with an immunodeficiency to come into hospital during lockdown, or later, when restrictions were limited, as they are considered to be clinically extremely vulnerable. Moreover, the scanning artefacts discussed above constitute another potential obstacle, which are caused by free breathing. Nevertheless, using respiratory gate and optimising the protocol helps to minimise this issue. Furthermore, increasing the field of view also helps to overcome wrap artefacts. In addition, recruiting controls for this study proved to be very difficult. We advertised in the whole of Nottingham, but only eleven people came forward to participate.

4.5 Conclusion

In conclusion, this study of OE-MRI demonstrates it is feasible to undertake scans in children with AT, providing evidence to support further evaluation in AT patients. Since the OE-MRI is a free-breathing technique, there is no need for coordinated forced effort, unlike spirometry. All of the children with AT who could tolerate getting into the scanner did not find it difficult to undertake this technique. Our exploratory analysis showed possible differences between the HV and AT group particularly in VVF, with a trend towards greater VVF in the AT group compared to the control group. In spite of the fact that the artefact has a negative effect on the quality of OE-MR images, artefacts should affect both groups similarly. Therefore, this encourages us to continue this work and collect more data by optimising the protocol.

Finally, further investigations are required to assess the feasibility of OE-MRI in children and young adults with AT and assess their suitability as clinical trial endpoints.

In the next chapter of my thesis, I present the final discussion and conclusion of this thesis. Comparing all three methods used in this thesis (spirometry, LCI and OE-MRI) to determine which technique might be most effective for use in this group of patients.

Chapter 5

General Discussion and Conclusion

5.1 Background

As discussed in chapter 1, AT is a genetic disorder, which is characterised by neurodegeneration, genomic instability, immunodeficiency and radio-sensitivity; the latter increases the patient's susceptibility to cancer. Progressive cerebellar ataxia is the severest form of the disorder (Schoenaker et al., 2016). As of now, there are no therapies available to cure this disorder or to prevent it from developing. It is only possible to suppress some of the symptoms and complications associated with immunodeficiency and deteriorating lung functioning. However, the neurodegeneration and predisposition to cancer are incurable. The immunodeficiency results in many of these patients developing lung disease. In other patient groups, CT scan is the standard method for anatomical lung imaging; but it is a less safe solution in AT due to the sensitivity of patients to ionising radiation. Spirometry, LCI and OE-MRI are potentially safer solutions to look for underlying lung disease in AT patients. Therefore, the aim of the studies described in this thesis was to assess the utility of these techniques in patients with AT.

5.2 Hypothesis and Aims of the Study

The hypothesis underlying this project was that OE-MRI could be a more suitable technique for lung imaging in children with AT. Furthermore, it was considered it could provide more useful physiological information about lung disease than LCI and spirometry. Moreover, OE-MRI and LCI had not been studied in those patients.

The overall aim of this thesis was to assess the feasibility of OE-MRI, LCI and spirometry in children and young adults with AT. In addition, I hoped to monitor trends in parameters derived from OE-MRI, LCI and spirometry and assess their suitability as clinical trial endpoints.

5.3 Key Findings of the Study

In this section I have summarised the key findings from the work described in this thesis.

5.3.1 Assessing Reliability of Spirometry Measurements Patients with Ataxia Telangiectasia

In Chapter 2, I set out to determine whether children with AT are capable of performing spirometry and to explore potential correlations between age and the ability to perform spirometry. The results of this study showed that the children with AT are less able to perform spirometry compared to a control group of children who were attending respiratory clinics for other reasons. The main finding of this work was that only 11 of 34 children with AT were able to complete spirometry to a standard completely fulfilling established guidelines. The main reasons for this were cough, lack of reproducibility and an inability to maintain prolonged expiration, potentially resulting in underestimates of FVC. Nonetheless, estimates of FEV₁ and FVC could be obtained from a reasonable number of children, allowing some additional analyses to be performed. In general, younger children are less able to comply with spirometry instructions than older children or adults.

However, I found that younger children with AT were more able to do spirometry than the older ones. The most likely explanation is that the older children's ability to co-ordinate respiratory effort decreases with age as their ataxia worsens.

In contrast, the capacity of older children in the control group to do spirometry to adequate standards was greater than the capacity of younger children. This shows that in children being referred to a respiratory clinic for problems other than AT, the ability to comply with spirometry to achieve satisfactory recordings increased with age. In children in the AT group there was a weak correlation between FEV₁ and FVC versus age ($r= 0.22$ and $r= 0.15$) respectively. This analysis should obviously be treated with caution, as only one of the 34 children in the AT group was able to achieve fully satisfactory FEV₁ and FVC measurements. The potential explanations for this weak correlation are either that spirometry underestimates lung function in older children with AT, or that the lung disease caused by infection in AT impairs normal lung function.

In contrast, there was a moderate/high positive correlation between the FEV₁ and FVC, and age in the children in the control group ($r=0.68$ and $r=0.70$) respectively. In addition, 44 out of 68 in the control group were able to achieve predicted FEV₁ and FVC. Furthermore, the numbers of children who were unable to reach the lower limited of normal was higher in the AT group than in the control group (see result section in Chapter 2).

These results need to be considered in the light of experience in performing spirometry in other cohorts involving children. A number of studies have been performed which have included spirometry in children: one good example is The Avon Longitudinal Study of Parents and Children (the ALSPAC) study, which was designed to explore risk factors for allergic disease (in particular asthma) and other diseases in young children. In this study, of the 13,963 originally recruited, 5276 at age 8 were able to complete spirometry to a satisfactory standard (Cai et al., 2020). As well as poor technique, many of those not completing spirometry will have been lost to follow up or withdrew from the study. The percentage of those who underwent spirometry who produced adequate results is not recorded but will therefore be substantially higher than at first it might appear.

In adult populations, spirometry has been widely performed, usually with high success rates, although minor errors in technique are common. As an example, large genetic association studies of lung function have been performed in UK Biobank, as part of which spirometry quality control was formally assessed. In the initial study, of the 426,797 who performed 2 satisfactory spirometry blows, 275,939 (65%) met strict ATS/ERS criteria for reproducibility (Wain et al., 2015). However, many of the error calls were minor and the true number with usable spirometry has risen to over 333,515 (Shrine et al., 2023) following further evaluation. These and other studies show that even when using strict ATS/ERS criteria in adult populations and other general children's cohorts' successful spirometry can be performed much more frequently than the rate seen in children with AT.

5.3.2 Assessing Reliability of LCI Measurements Patients with Ataxia Telangiectasia

In Chapter 3, I set out to assess whether or not children with AT are able to undertake the LCI technique. This technique is safe, as it does not use ionising radiation, and as it depends on tidal breathing, it does not require any effort from the participants and hence it seemed possible it might be more reliable as a way of assessing lung function than spirometry. However, although normal tidal breathing does not require any coordinated effort, in the first four breaths before the wash-out and the first three breaths after the wash-out, none of the participants with AT was able to fulfil the accepted criteria for LCI in terms of similarity of tidal breathing range (10% less or greater).

However, the reason for this difference in these breaths may be due to the click sound produced when starting the examination. This issue can potentially be solved providing music via headphones to minimise this sound to distract participants. Better encouragement and explanation before starting the test might also help. The results of the study on compliance of AT children with LCI criteria revealed that all the participants were able to achieve two criteria (LCI5 and maintain no leakage), whereas 11 out of 13 have also been able to fulfil two additional criteria (the LCI2.5 and the trajectory's consistency) (see Table 3-7). Therefore, the LCI5 may be more appropriate because of the shorter time it takes, which is about half the time of the LCI2.5. Two out of 15 subjects withdrew, not because

LCI induces anxiety or is difficult to apply but because LCI was conducted after doing OE-MRI which made them anxious due to claustrophobia. Eleven out of 13 participants were able to provide acceptable results.

The study result revealed that overall, 85% of the participants were able to undertake the LCI technique. In general, children with AT are able to comply with LCI instructions, because these instructions do not require the same controlled effort required to undertake spirometry. I also explored the relationship between age and the ability to comply with LCI technique. The group of children with AT was divided into two groups based on age (aged 11 or under and over 11). No difference was seen between the two age groups in their ability to complete LCI.

I used the initial analyses of the lung function values obtained (regardless of quality) for LCI2.5, LCI5 and FRC to determine the relationship between these values versus demographic factors (age, height, and weight). These were explored using scatterplot and regression in SPSS. The result of these analyses revealed that for children in the AT group, there was no relationship between LCI2.5 and age ($R^2= 0.004$) and a very weak relationship between LCI5 and FRC, and age ($R^2= 0.118$ and $R^2= 0.178$) respectively. Additionally, relationships between LCI2.5, LCI5, and FRC versus height were determined. The study's findings indicated that there was no relationship between LCI2.5 and LCI5 and height in children in the AT group ($R^2= 0.034$ and $R^2= 0.01$) respectively, but that there was a positive correlation between FRC and height ($R^2=0.452$). Likewise, the

relationships between LCI2.5, LCI5, and FRC versus height were determined. I also found that there was no relationship between LCI2.5, LCI5 and FRC and weight in children in the AT group ($R^2 < 0.01$, $R^2 = 0.010$, and $R^2 = 0.083$) respectively.

To the best of my knowledge, these data are the first to describe the use of LCI in children with AT. The study's findings have been compared to previous published data on children with CF, asthma, PCD and neuromuscular diseases, such as SMA. The result of LCI2.5 for the eleven participants with AT was (median, interquartile (IQR)) (9.76, (1.445)), which is higher than the values obtained in healthy volunteers in studies of asthma (median= 6.48) and CF (mean= 6.7 ± 0.5); this is anticipated. Also, it is higher than children with severe and mild/ moderate asthmatic patients (median= 7.49 and median= 6.69) respectively. Furthermore, it is lower than the result of LCI in children with CF (mean= 12 ± 3) (for references see Table 5-1).

In contrast, the LCI result for children with AT was (median= 9.76), which is fairly similar to the LCI results for children with PCD and SMA (median= 9.70 and median= 9.30) respectively. I noticed some interesting similarity in the results of LCI between children with AT and SMA, another condition characterised by muscle weakness (see Table 5-1). According to Sommerburg et al. (2021), the normal range in adults is between 5.9 and 7.5, and in children up to 16 years, this ranges from 5.3 to 7.3. The LCI result value is increased due to the different rates of nitrogen coming from

multiple compartments (Bates & Peters, 2018). In summary, the data presented in this thesis shows that children with AT can undertake LCI, but that their technique is not to the standard required to meet accepted guidelines, meaning results obtained must be interpreted with caution.

Table 5-1: This table summarises selected results of LCI studies, as well as the LCI result of this study.

Clinical conditions		Sample size	Age Median (IQR range)	LCI result Median (IQR range)	Reference
Asthma	Mild/ moderate	7	12.5 (8.6 to 14.0)	6.69 (6.11 to 6.90)	Nuttall et al., 2021
	Severe	23	11.8 (9.2 to 15.3)	7.49 (6.63 to 7.84)	
	Healthy	7	13.9 (10.5 to 14.4)	6.48 (6.13 to 6.78)	
Cystic fibrosis/ healthy [Mean \pm SD range]]		10	13 \pm 2.5 (10–17)	12 \pm 3 (6.7–16)	Kanhere et al., 2017
		5	12.4 \pm 2.4 (10–17)	6.7 \pm 0.5 (5.9–7.2)	
Primary ciliary dyskinesia Median (IQR range)		90	12.8 (9.1 to 17.8)	9.70 (8.24 to 11.74)	Singer et al., 2021
Spinal muscular atrophy (Median, IQR)		15	8.06 (2.44)	9.30 (4.67)	Kapur et al., 2019
Ataxia Telangiectasia (Median, IQR)		11	10 (4)	9.76 (1.445)	This thesis

5.3.3 Assessing Reliability of OE-MRI Measurements Patients with Ataxia Telangiectasia

In the work described in this chapter, I set out to assess whether oxygen-enhanced magnetic resonance imaging (OE-MRI) is feasible in children with AT. I further contributed to the development and optimisation of the

scanning protocol and proceeded to perform an exploratory analysis of the initial data.

The study group determined in advance that the results of this feasibility study (if it proved feasible) would allow us to undertake future power calculations using OE-MRI. This technique is safe because it uses non-ionising radiation and requires no effort on the part of the participant, who simply breathes normally. Surprisingly, this technique has not yet been applied to such patients. This chapter's key finding is that it is possible to perform OE-MRI scans on children with AT.

This study has several limitations. First and foremost, the study sample is small, which diminishes the power of the statistical analysis. However, as mentioned above, the main outcome measure was whether children with a significant movement disorder could undertake the OE-MRI protocol. Although the small sample size diminishes the study's suitability for exploratory interim analyses comparing children with AT and healthy controls, the overall objective to understand feasibility was met.

The healthy controls were recruited as part of our OE-MRI development programme, and the comparison between the two groups is exploratory in nature.

Fifteen children with AT were recruited into the study to compare OE-MRI parameters against those of healthy volunteers. Twelve of the 15 children successfully completed the MRI scan (see Figure 4-5). The underlying

reason for the withdrawal of three participants was claustrophobia and aversion to the noise produced by the MRI machine during the scan.

Anyone may experience claustrophobia, regardless of their health condition. Nevertheless, subjects may be supported in overcoming their claustrophobia if technicians fully explain the procedure, provide encouragement and rehearse the process before initiating the actual scan. Changing the patient's position from prone to supine may also help to resolve the issue. The problem of noise aversion may be resolved by providing the subject with headphones through which music is played, which can minimise the sound and provide a source of distraction for the participants.

We encountered artefacts in the raw data, which constituted a major obstacle to performing this technique and which we solved in protocol 2. Artefacts were noted in the raw data as horizontal lines and were thought to be due to the straps, scanner bed and receiver projecting into the thorax (see Figure 4-7). However, this issue was minimised with the use of large field of view and by replacing the plastic straps with cotton ones. This reduced the occurrence of horizontal lines and prevented the artefacts from appearing within the thorax (see Figure 4-8).

When analysing the data, we initially examined graphical plots (the box plots), which revealed potential differences between the HV and AT groups. We proceeded to perform a Mann-Whitney test, which did not find a difference. However, we knew that the AT and HV groups were not matched

for height and age; therefore, we performed multivariate regression, accounting for height and age. For completeness and, easy viewing of the results, each parameter of OE-MRI was presented separately in different statistical modes (i.e., Mann–Whitney, multivariable regression model, boxplot).

I undertook an exploratory analysis of multiple outcomes to obtain an initial understanding of what might be expected in future studies of OE-MRI. Delta- PO_2 in the whole lung represents oxygen enhancement as the change in partial pressure of oxygen in whole lung [mmHg]. Delta- PO_2 in the aorta represents oxygen enhancement as the change in partial pressure of oxygen in the aorta [mmHg] and is a measure of whole lung transfer of oxygen—more effective oxygen transfer leads to higher PO_2 in the aorta. Wash-in time in the whole lung indicates the time taken to reach maximum PO_2 after administering pure oxygen. A higher wash-in time implies greater heterogeneity of alveolar ventilation. VVF of the whole lung was the last OE-MRI parameter evaluated. VVF is the fraction of the region presenting with oxygen enhancement (max 1, min 0), and a higher number implies better ventilation of the lung overall. The exploratory analysis revealed no difference between the whole-lung delta- PO_2 , aortal delta- PO_2 and the wash-in time.

However, a difference was observed in the ventilation fraction of the lung, with more of the healthy volunteers having higher ventilation fraction. This makes intuitive sense – we expect that all of the healthy volunteers will

have well-ventilated lungs. However, whilst some of the children with AT will have normal ventilation, some will have reduced ventilation, as can be seen in the boxplot of ventilation.

We used a multivariable model to account for the fact that the healthy control group included more tall children than the AT group. We could not match children with AT to healthy controls of both the same age and height, because children with AT are short. Had we matched for height, we would have had younger children in the controls than in the AT groups. Had we matched for age, the control group would have had taller children than those with AT. For this reason, a multivariable model was used, because it simultaneously accounts for both without the need to match the cases in the controls. The emergence of evidence that VVF in the whole lung may be lower in a proportion of children in the AT group encourages us to continue this work and collect more data.

AT patients are prone to sinopulmonary infection, which constitutes the primary cause of death among this population. Therefore, we anticipated that the OE-MRI results of the AT group would be lower than the results for the healthy volunteers. This technique depends on the ratio of pure oxygen dissolved in the blood, which increases the MRI signal (T1). Failure to increase the signal may imply a defect in this part of the lung. Therefore, AT patients' lung size would be smaller than that of healthy volunteers.

Since AT patients are more prone to sinopulmonary infection, one might anticipate that the OE-MRI parameters of the AT group would be different

to those of healthy volunteers. The technique depends on the ratio of pure oxygen dissolved in the blood, which increases the MRI signal (T1). Failure to increase the signal may imply that there is a defect in gas transfer in the relevant part of the lung. In addition, the lung size of AT patients might be anticipated to be small compared to healthy volunteers.

According to Zeng et al. (2019), using lung MRI in conjunction with the MultiVane technique can produce high-resolution, motion-suppressed images that allow for the characterisation of different pulmonary diseases. This has been assessed in tuberculosis patients, where the results obtained were consistent with those from CT scans (see Figure 1-6). MultiVane works as a beam of several parallel lines, which are collected in a multi-echo acquisition instead of a single radial line.

There are a range of other MR based approaches to study lung ventilation/perfusion which have not yet been evaluated in patients with AT and could potentially be of value. These include hyperpolarised inert gas imaging using ^{129}Xe , and structural imaging with UTE and similar sequences. Both these approaches have been evaluated in children with cystic fibrosis with some success.

There is a recent study which has been conducted by Willmering. The aim of the study was to improve pulmonary imaging ^{129}Xe ventilation by three-dimension spiral UTE technique. The findings of the study showed that a developed spiral 3D UTE sequence called FLORET (Fermat looped, orthogonally encoded trajectories) sampling pattern results in higher-

resolution images and/or shorter breath-holds, without the need for high-performance gradients. The FLORET images obtained demonstrate an approximate 3-fold higher resolution and a 40% higher relative SNRn in a 15% shorter breath-hold duration compared with 2D GRE. This should result in higher sensitivity, and more accurate quantification of ventilation, and make ^{129}Xe ventilation imaging more feasible for subjects with more advanced lung disease or less compliant subjects who are unable to complete longer-duration breath-holds. Due to children with AT facing difficulties in holding their breath and the problems caused by artefacts when using OE-MRI these findings suggest it may be possible to adopt alternative approaches for MR imaging in AT patients. However, ^{129}Xe lung imaging also requires a breath hold (ideally of around 10 seconds) and hence this technique may also be sub-optimal for children with AT (Willmering et al., 2020).

Finally, there has been recent work to try and develop free breathing proton-based imaging approaches to explore ventilation and perfusion, for example using PREFUL (Klimeš et al., 2021). Klimeš and his team states that repeatability of all ventilation parameters derived from 3D PREFUL MRI during free breathing in healthy subjects and COPD patients was good. 3D PREFUL ventilation parameters are sensitive for changes of regional lung ventilation and may add value to established pulmonary lung function testing. The big advantage of free breathing techniques is that they do not require breath holds. Image acquisition times for PREFUL and related approaches are generally around 10 minutes.

This area of research is still at a relatively early stage and the advantages and disadvantages of using these different techniques in children with suspected lung disease needs further study to discover which is the most useful in terms of sensitivity and specificity for identifying underlying lung disease, and which has the greatest patient acceptability.

5.4 Strength and Limitation

5.4.1 Potential Strength

The strength of the studies described in this thesis is the pragmatic approach taken, where the different techniques explored in patients with AT were practically applied in those patients rather than just considering theoretical considerations. This is the first such study to be performed exploring all of these modalities in this field. Although the study sample is relatively small, it constitutes 13% of the entire UK childhood population with AT. These approaches are all potentially possible in any regional hospital as the equipment required is fairly standard. Further modifications may also improve reliability of these approaches, for example using a facemask for children with AT as an alternative to a mouthpiece.

OE-MRI is a safe, non-invasive technique, which unlike CT, does not involve the use of ionising radiation, which is a specific problem in this patient group. Whilst we have shown that the majority of subjects with AT can undergo MR scanning, further evaluation is required in a larger group of subjects with more severe lung disease to assess the sensitivity and

specificity of this technique fully. OE-MRI does have the advantage of being easier to perform and cheaper than some other MR based lung imaging modalities. such as those using hyperpolarised noble gases.

5.4.2 Potential Limitation

The research described in this thesis was unfortunately affected significantly by the global COVID-19 pandemic. At an early stage of my studies, all clinical research was effectively halted due to concerns over the transmission of COVID-19, and this meant that planned repeat imaging sessions using OE-MRI were not feasible. In view of this, and in addition to the spirometry work I had been able to undertake, I used previously collected LCI data to explore the value of using LCI in patients with AT. In addition to the direct effects of the pandemic on the ability to complete all the planned imaging studies, my research was also affected indirectly by travel restrictions and family illness caused by COVID-19. Later LCI and spirometry were considered aerosol generating procedures so research using them was not straightforward to undertake. Another limitation of this study is the sample size in this study is very small to make any meaningful analysis. Therefore, we recommend increasing the number of participants in the future.

5.5 Future Work

As discussed above, further refinements are required to assess fully the value of using OE-MRI and LCI in children and young adults with AT and to

assess their suitability as clinical trial endpoints. Furthermore, a longitudinal study is recommended that uses a larger number of participants, and the lung status of those patients be monitored. Finally, AT groups and healthy volunteers should be matched according to the factors of age and gender. There are also interesting developments using other proton-based MRI techniques, such as phase-resolved functional lung (PREFUL) (Pöhler et al., 2021) and ultra-short echo time and zero echo time (UTE/ZTE) based approaches, which could also provide complimentary information (Bae et al., 2019).

5.6 Conclusion

In conclusion, children with AT find it difficult to comply with spirometry for a range of reasons, the main one being ataxia. Two-thirds of children with AT are unable to perform spirometry to an adequate level. Spirometry is a technique that needs co-ordinated effort to be used successfully. In contrast, children with AT find it less difficult to comply with LCI or to undertake an OE-MRI scan. Because LCI and OE-MRI are free breathing techniques, there is no need for a coordinated forced effort, unlike spirometry. The work presented in this thesis provides evidence to support the further development of the LCI technique and OE-MRI for evaluating AT patients. Larger numbers of subjects are required to define fully the reproducibility and the sensitivity of these techniques to detect early disease.

References

- Agustí, Alvar, and James C. Hogg. "Update on the pathogenesis of chronic obstructive pulmonary disease." *New England Journal of Medicine* 381.13 (2019): 1248-1256.
- Aksamit, T. R., O'Donnell, A. E., Barker, A., Olivier, K. N., Winthrop, K. L., Daniels, M. L. A., ... & Bronchiectasis Research Registry Consortium. (2017). Adult patients with bronchiectasis: a first look at the US bronchiectasis research registry. *Chest*, 151(5), 982-992.
- ALAM, D., OLSSON, L. & ALAMIDI, D. Lung imaging using oxygen-enhanced MRI in small animals. 2010.
- ALSOP, D., HATABU, H., BONNET, M., LISTERUD, J. AND GEFTER, W. 1995. Multi-Slice, Breath hold Imaging of the Lung with Sub millisecond Echo Times. *Magnetic Resonance in Medicine*, 33 (5), 678-682.
- Ambrose M, Gatti RA (2013). Pathogenesis of ataxiatelangiectasia: the next generation of ATM functions. *Blood* 121: 4036–4045. Amromin GD, Boder E, Teplitz R (1979).
- Amirifar, P., Ranjouri, M. R., Yazdani, R., Abolhassani, H., & Aghamohammadi, A. (2019). Ataxia-telangiectasia: A review of clinical features and molecular pathology. *Pediatric Allergy and Immunology*, 30(3), 277-288.

- Aurora, P., Stocks, J., Oliver, C., Saunders, C., Castle, R., Chaziparasidis, G., & Bush, A. (2004). Quality control for spirometry in preschool children with and without lung disease. *American journal of respiratory and critical care medicine*, 169(10), 1152-1159.
- Backman, H., Lindberg, A., Oden, A., Ekerljung, L., Hedman, L., Kainu, A., ... & Rönmark, E. (2015). Reference values for spirometry—report from the Obstructive Lung Disease in Northern Sweden studies. *European clinical respiratory journal*, 2(1), 26375.
- Bae, K., Jeon, K. N., Hwang, M. J., Lee, J. S., Ha, J. Y., Ryu, K. H., & Kim, H. C. (2019). Comparison of lung imaging using three-dimensional ultrashort echo time and zero echo time sequences: preliminary study. *European radiology*, 29(5), 2253-2262.
- Bannas, P., Bell, L. C., Johnson, K. M., Schiebler, M. L., François, C. J., Motosugi, U., ... & Nagle, S. K. (2016). Pulmonary embolism detection with three-dimensional ultrashort echo time MR imaging: experimental study in canines. *Radiology*, 278(2), 413-421.
- Bates, J. H., & Peters, U. (2018). A model-based approach to interpreting multibreath nitrogen washout data. *Journal of Applied Physiology*, 124(5), 1155-1163.
- BAUMAN, G. & EICHINGER, M. 2012. Ventilation and perfusion magnetic resonance imaging of the lung. *Polish journal of radiology*, 77, 37.

- BEAMISH, H. & LAVIN, M. F. 1994. Ionizing radiation and cell cycle progression in ataxia telangiectasia. *Radiation research*, 138, S130-S133.
- Beeckman-Wagner, L. A. F., & Freeland, D. (2012). Spirometry quality assurance; common errors and their impact on test results.
- Benseler, A., Stanojevic, S., Jensen, R., Gustafsson, P., & Ratjen, F. (2015). Effect of equipment dead space on multiple breath washout measures. *Respirology*, 20(3), 459-466.
- BERGIN, C., GLOVER, G. AND PAULY, J. 1991. Lung Parenchyma: Magnetic Susceptibility in MR Imaging. *Radiology*, 180 (3), 845-848.
- BERGIN, C., PAULY, J. & MACOVSKI, A. 1991. Lung parenchyma: projection reconstruction MR imaging. *Radiology*, 179, 777-781.
- Bhandary, A., Prabhu, G. A., Rajinikanth, V., Thanaraj, K. P., Satapathy, S. C., Robbins, D. E., ... & Raja, N. S. M. (2020). Deep-learning framework to detect lung abnormality—A study with chest X-Ray and lung CT scan images. *Pattern Recognition Letters*, 129, 271-278.
- Bhatt, J. M. (2013). Treatment of pulmonary exacerbations in cystic fibrosis. *European Respiratory Review*, 22(129), 205-216.
- Bhatt, J. M., Bush, A., van Gerven, M., Nissenkorn, A., Renke, M., Yarlett, L., ... & Merkus, P. J. (2015). ERS statement on the multidisciplinary respiratory management of ataxia telangiectasia. *European Respiratory Review*, 24(138), 565-581.

Blog, B., 2021. *Molecular Mechanisms of Inflammatory Signaling in COPD*. [online] The Biophysical Society. Available at: <<https://www.biophysics.org/blog/molecular-mechanisms-of-inflammatory-signaling-in-copd>> [Accessed 18 October 2021].

Boulet, L. P., Reddel, H. K., Bateman, E., Pedersen, S., FitzGerald, J. M., & O'Byrne, P. M. (2019). The global initiative for asthma (GINA): 25 years later. *European Respiratory Journal*, 54(2).

Bryan, M. R., Uhouse, M. A., Nordham, K. D., Joshi, P., Rose, D. I., O'Brien, M. T., ... & Bowman, A. B. (2018). Phosphatidylinositol 3 kinase (PI3K) modulates manganese homeostasis and manganese-induced cell signaling in a murine striatal cell line. *Neurotoxicology*, 64, 185-194.

Burkhardt, R., & Pankow, W. (2014). The diagnosis of chronic obstructive pulmonary disease. *Deutsches Ärzteblatt International*, 111(49), 834.

BUXTON, R. B. 2013. The physics of functional magnetic resonance imaging (fMRI). *Reports on Progress in Physics*, 76, 096601.

Cai, Y., Hansell, A. L., Granell, R., Blangiardo, M., Zottoli, M., Fecht, D., ... & Elliott, P. (2020). Prenatal, early-life, and childhood exposure to air pollution and lung function: the ALSPAC cohort. *American journal of respiratory and critical care medicine*, 202(1), 112-123.

- Candemir, S., & Antani, S. (2019). A review on lung boundary detection in chest X-rays. *International journal of computer assisted radiology and surgery*, 14(4), 563-576.
- Carpaij, O. A., Burgess, J. K., Kerstjens, H. A., Nawijn, M. C., & van den Berge, M. (2019). A review on the pathophysiology of asthma remission. *Pharmacology & therapeutics*, 201, 8-24.
- Carpenter, D. M., Jurdi, R., Roberts, C. A., Hernandez, M., Horne, R., & Chan, A. (2018). A review of portable electronic spirometers: implications for asthma self-management. *Current allergy and asthma reports*, 18(10), 1-10.
- Celli, B. R., & Wedzicha, J. A. (2019). Update on clinical aspects of chronic obstructive pulmonary disease. *New England Journal of Medicine*, 381(13), 1257-1266.
- Chalmers, J. D., Chang, A. B., Chotirmall, S. H., Dhar, R., & McShane, P. J. (2018). Bronchiectasis (Primer). *Nature Reviews: Disease Primers*.
- Chandra, S., Skali, H., & Blankstein, R. (2011). Novel techniques for assessment of left ventricular systolic function. *Heart failure reviews*, 16(4), 327-337.
- Chiang, J., Mehta, K., & Amin, R. (2018). Respiratory diagnostic tools in neuromuscular disease. *Children*, 5(6), 78.
- Choate, R., Aksamit, T. R., Mannino, D., Addrizzo-Harris, D., Barker, A., Basavaraj, A., ... & Stone, G. (2021). *Pseudomonas aeruginosa*

associated with severity of non-cystic fibrosis bronchiectasis measured by the modified bronchiectasis severity score (BSI) and the FACED: The US bronchiectasis and NTM Research Registry (BRR) study. *Respiratory Medicine*, 177, 106285.

Choi, J. Y., & Rhee, C. K. (2020). Diagnosis and treatment of early chronic obstructive lung disease (COPD). *Journal of Clinical Medicine*, 9(11), 3426.

Chorepsima, S., Kechagias, K. S., Kalimeris, G., Triarides, N. A., & Falagas, M. E. (2018). Spotlight on inhaled ciprofloxacin and its potential in the treatment of non-cystic fibrosis bronchiectasis. *Drug Design, Development and Therapy*, 4059-4066.

Choy, K. R., & Watters, D. J. (2018). Neurodegeneration in ataxia-telangiectasia: Multiple roles of ATM kinase in cellular homeostasis. *Developmental Dynamics*, 247(1), 33-46.

COLLIEZ, F., SAFRONOVA, M. M., MAGAT, J., JOUDIQU, N., PEETERS, A. P., JORDAN, B. F., GALLETZ, B. & DUPREZ, T. 2015. Oxygen mapping within healthy and acutely infarcted brain tissue in humans using the NMR relaxation of lipids: a proof-of-concept translational study. *PLoS One*, 10, e0135248.

Condino-Neto, A., Costa-Carvalho, B. T., Grumach, A. S., King, A., Bezrodnik, L., Oleastro, M., ... & Sorensen, R. U. (2014). Guidelines for the use of human immunoglobulin therapy in patients with

primary immunodeficiencies in Latin America. *Allergologia et immunopathologia*, 42(3), 245-260.

Cremona, C. A., & Behrens, A. (2014). ATM signalling and cancer. *Oncogene*, 33(26), 3351-3360.

CRUICKSHANK, S. & HIRSCHAUER, N. 2004. The alveolar gas equation. Continuing Education in Anaesthesia, Critical Care & Pain, 4, 24-27.

Currie, S., Hoggard, N., Craven, I. J., Hadjivassiliou, M., & Wilkinson, I. D. (2013). Understanding MRI: basic MR physics for physicians. *Postgraduate medical journal*, 89(1050), 209-223.

Daugherty, J., Lin, X., Baxter, R., Suruki, R., & Bradford, E. (2018). The impact of long-term systemic glucocorticoid use in severe asthma: a UK retrospective cohort analysis. *Journal of Asthma*, 55(6), 651-658.

Deligianni, X. (2013). *Exploring T^* 2 decay: new methods for short echo time imaging and fat-water quantification* (Doctoral dissertation, University_of_Basel).

DONG, Z., ANDREWS, T., XIE, C. & YOKOO, T. 2015. Advances in MRI techniques and applications. Hindawi.

DREGELY, I., RUSET, I. C., MATA, J. F., KETEL, J., KETEL, S., DISTELBRINK, J., ALTES, T. A., MUGLER III, J. P., WILSON MILLER, G. & WILLIAM HERSMAN, F. 2012. Multiple-exchange-time xenon polarization transfer contrast (MXTC) MRI: initial results in animals and healthy volunteers. *Magnetic resonance in medicine*, 67, 943-953.

DRIEHUYS B, MÖLLER HE, CLEVELAND ZI, POLLARO J, HEDLUND LW.

Pulmonary perfusion and xenon gas exchange in rats: MR imaging with intravenous injection of hyperpolarized ^{129}Xe . *Radiology*, 2009; 252: 386–393.

DRIEHUYS, B., MARTINEZ-JIMENEZ, S., CLEVELAND, Z.I., METZ, G.M., BEAVER, D.M., NOULS, J.C., KAUSHIK, S.S., FIRSZT, R., WILLIS, C., KELLY, K.T. AND WOLBER, J. 2012. Chronic obstructive pulmonary disease: safety and tolerability of hyperpolarized ^{129}Xe MR imaging in healthy volunteers and patients. *Radiology*, 262(1), pp.279-289.

Dunn, J. O., Mythen, M. G., & Grocott, M. P. (2016). Physiology of oxygen transport. *Bja Education*, 16(10), 341-348.

Ebner, L., Kammerman, J., Driehuys, B., Schiebler, M. L., Cadman, R. V., & Fain, S. B. (2017). The role of hyperpolarized ^{129}Xe in MR imaging of pulmonary function. *European journal of radiology*, 86, 343-352.

EBNER, L., KAMMERMAN, J., DRIEHUYS, B., SCHIEBLER, M. L., CADMAN, R. V. & FAIN, S. B. 2017. The role of hyperpolarized ^{129}Xe in MR imaging of pulmonary function. *European journal of radiology*, 86, 343-352.

EDELMAN, R. 1996. Hatabu H, Tadamura E, Li W, and Prasad PV. Noninvasive assessment of regional ventilation in the human lung

using oxygen-enhanced magnetic resonance imaging. *Nat Med*, 2, 1236-1239.

Edelman, R. R., Hatabu, H., Tadamura, E., Li, W., & Prasad, P. V. (1996). Noninvasive assessment of regional ventilation in the human lung using oxygen-enhanced magnetic resonance imaging. *Nature medicine*, 2(11), 1236-1239.

Ernst, M. M., Johnson, M. C., & Stark, L. J. (2010). Developmental and psychosocial issues in cystic fibrosis. *Child and Adolescent Psychiatric Clinics*, 19(2), 263-283.

FABICH, H., BENNING, M., SEDERMAN, A. AND HOLLAND, D. 2014. Ultrashort Echo Time (UTE) Imaging Using Gradient Pre-Equalization and Compressed Sensing. *Journal of Magnetic Resonance*, 245, 116-124.

Federighi, P., Ramat, S., Rosini, F., Pretegianni, E., Federico, A., & Rufa, A. (2017). Characteristic eye movements in ataxia-telangiectasia-like disorder: an explanatory hypothesis. *Frontiers in neurology*, 8, 596.

Feher, J. J. (2017). *Quantitative human physiology: an introduction*. Academic press.

Fehrenbach, H., Wagner, C., & Wegmann, M. (2017). Airway remodeling in asthma: what really matters. *Cell and tissue research*, 367(3), 551-569.

Fowler, W. S., Cornish, E. R., & Kety, S. S. (1952). *Lung function studies. VIII. Analysis of alveolar ventilation by pulmonary N₂ clearance curves. The Journal of clinical investigation, 31(1), 40-50.*

Fretzayas, A., Douros, K., Moustaki, M., & Loukou, I. (2019). Applications of lung clearance index in monitoring children with cystic fibrosis. *World journal of clinical pediatrics, 8(2), 15.*

FUSEYA, Y., MURO, S., SATO, S., TANABE, N., SATO, A., TANIMURA, K., HASEGAWA, K., UEMASU, K., KUBO, T. & KIDO, A. 2018. Complementary regional heterogeneity information from COPD patients obtained using oxygen-enhanced MRI and chest CT. *PloS one, 13, e0203273.*

Ge, X. Q., & Blow, J. J. (2010). Chk1 inhibits replication factory activation but allows dormant origin firing in existing factories. *Journal of Cell biology, 191(7), 1285-1297.*

Gold, W. M., & Koth, L. L. (2016). Pulmonary function testing. *Murray and Nadel's Textbook of Respiratory Medicine, 407.*

Gonem, S., Scadding, A., Soares, M., Singapuri, A., Gustafsson, P., Ohri, C., ... & Siddiqui, S. (2014). Lung clearance index in adults with non-cystic fibrosis bronchiectasis. *Respiratory research, 15(1), 1-9.*

Graham, B. L., Steenbruggen, I., Miller, M. R., Barjaktarevic, I. Z., Cooper, B. G., Hall, G. L., ... & Thompson, B. R. (2019). Standardization of spirometry 2019 update. An official American thoracic society and

European respiratory society technical statement. *American journal of respiratory and critical care medicine*, 200(8), e70-e88.

Gustafsson, P. M., Aurora, P., & Lindblad, A. (2003). Evaluation of ventilation maldistribution as an early indicator of lung disease in children with cystic fibrosis. *European Respiratory Journal*, 22(6), 972-979.

HALAWEISH, A. F. & CHARLES, H. C. 2014. Physiorack: an integrated MRI safe/conditional, gas delivery, respiratory gating, and subject monitoring solution for structural and functional assessments of pulmonary function. *Journal of Magnetic Resonance Imaging*, 39, 735-741.

Hannon, D., Bradley, J. M., Bradbury, I., Bell, N., Elborn, J. S., & O'Neill, K. (2014). Shortened Lung Clearance Index is a repeatable and sensitive test in children and adults with cystic fibrosis. *BMJ open respiratory research*, 1(1), e000031.

Hatziagorou, E., Avramidou, V., Kirvassilis, F., & Tsanakas, J. (2015). Use of lung clearance index to assess the response to intravenous treatment in cystic fibrosis. *Hippokratia*, 19(1), 47.

Haynes, J. M. (2018). Basic spirometry testing and interpretation for the primary care provider. *Canadian journal of respiratory therapy: CJRT= Revue canadienne de la therapie respiratoire: RCTR*, 54(4).

HERSMAN, F.W., RUSET, I.C., KETEL, S., MURADIAN, I., COVRIG, S.D., DISTELBRINK, J., PORTER, W., WATT, D., KETEL, J., BRACKETT, J. AND HOPE, A. 2008. Large production system for hyperpolarized ¹²⁹Xe for human lung imaging studies. *Academic radiology*, 15(6), pp.683-692.

Horsley, A. (2009). Lung clearance index in the assessment of airways disease. *Respiratory medicine*, 103(6), 793-799.

Horsley, A. R., Alrumuh, A., Bianco, B., Bayfield, K., Tomlinson, J., Jones, A., ... & Gilchrist, F. J. (2020). Lung clearance index in healthy volunteers, measured using a novel portable system with a closed circuit wash-in. *PloS one*, 15(2), e0229300.

Hough, K. P., Curtiss, M. L., Blain, T. J., Liu, R. M., Trevor, J., Deshane, J. S., & Thannickal, V. J. (2020). Airway remodeling in asthma. *Frontiers in Medicine*, 7, 191.

HSIA, C. C., HYDE, D. M. & WEIBEL, E. R. 2011. Lung structure and the intrinsic challenges of gas exchange. *Comprehensive physiology*, 6, 827-895.

HSIA, C. C., SCHMITZ, A., LAMBERTZ, M., PERRY, S. F. & MAINA, J. N. 2013. Evolution of air breathing: oxygen homeostasis and the transitions from water to land and sky. *Comprehensive Physiology*, 3, 849-915.

Iheanacho, I., Zhang, S., King, D., Rizzo, M., & Ismaila, A. S. (2020). Economic burden of chronic obstructive pulmonary disease (COPD): a systematic literature review. *International journal of chronic obstructive pulmonary disease*, 439-460.

JAKOB, P.M., WANG, T., SCHULTZ, G., HEBESTREIT, H., HEBESTREIT, A. AND HAHN, D. 2004. Assessment of human pulmonary function using oxygen-enhanced T1 imaging in patients with cystic fibrosis. *Magnetic Resonance in Medicine: An Official Journal of the International Society for Magnetic Resonance in Medicine*, 51(5), pp.1009-1016.

Jat, K. R. (2013). Spirometry in children. *Primary Care Respiratory Journal*, 22(2), 221-229.

Johns, D. P., Walters, J. A., & Walters, E. H. (2014). Diagnosis and early detection of COPD using spirometry. *Journal of thoracic disease*, 6(11), 1557.

JOHNSON KM,, FAIN SB, , SCHIEBLER ML, , NAGLE S. 2013. Optimized 3D ultrashort echo time pulmonary MRI. *Magn Reson Med*, 70(5):1241–1250.

Kamsler A, Daily D, Hochman A et al. (2001). Increased oxidative stress in ataxia telangiectasia evidenced by alterations in redox state of brains from Atm-deficient mice. *Cancer Res* 61: 1849–1854..

Kanhere, N., Couch, M. J., Kowalik, K., Zanette, B., Rayment, J. H., Manson, D., ... & Santyr, G. (2017). Correlation of lung clearance

index with hyperpolarized ^{129}Xe magnetic resonance imaging in pediatric subjects with cystic fibrosis. *American journal of respiratory and critical care medicine*, 196(8), 1073-1075.

Kapur, N., Deegan, S., Parakh, A., & Gauld, L. (2019). Relationship between respiratory function and need for NIV in childhood SMA. *Pediatric pulmonology*, 54(11), 1774-1780.

Kelkar, K. V. (2015). Post-operative pulmonary complications after non-cardiothoracic surgery. *Indian journal of anaesthesia*, 59(9), 599.

Kern, A. L., & Vogel-Claussen, J. (2018). Hyperpolarized gas MRI in pulmonology. *The British journal of radiology*, 91(1084), 20170647.

Kiley, J., Smith, R., & Noel, P. (2007). Asthma phenotypes. *Current opinion in pulmonary medicine*, 13(1), 19-23.

KINDVALL, S. S. I., DIAZ, S., SVENSSON, J., WOLLMER, P. & OLSSON, L. E. 2017. The change of longitudinal relaxation rate in oxygen enhanced pulmonary MRI depends on age and BMI but not diffusing capacity of carbon monoxide in healthy never-smokers. *Plos one*, 12, e0177670.

King, L., White, H., Clifton, I., Spoletini, G., Ispoglou, T., & Peckham, D. G. (2021). Nutritional status and intake in patients with non-cystic fibrosis bronchiectasis (NCFB)-a cross sectional study. *Clinical Nutrition*, 40(9), 5162-5168.

KIRBY M, COXSON HO, PARRAGA G. 2013. Pulmonary functional magnetic resonance imaging for paediatric lung disease. *Paediatric Respir Rev.*, 14:180–189.

Klimeš, F., Voskrebenezv, A., Gutberlet, M., Obert, A. J., Pöhler, G. H., Grimm, R., ... & Vogel-Claussen, J. (2021). Repeatability of dynamic 3D phase-resolved functional lung (PREFUL) ventilation MR Imaging in patients with chronic obstructive pulmonary disease and healthy volunteers. *Journal of Magnetic Resonance Imaging*, 54(2), 618-629.

Komoda, T., & Matsunaga, T. (2015). *Biochemistry for Medical Professionals*. Academic Press.

KRISHNAMURTHY, R., PEDNEKAR, A., ATWEH, L. A., VOGELIUS, E., CHU, Z. D., ZHANG, W., MASKATIA, S., MASAND, P., MORRIS, S. A. & KRISHNAMURTHY, R. 2015. Clinical validation of free breathing respiratory triggered retrospectively cardiac gated cine balanced steady-state free precession cardiovascular magnetic resonance in sedated children. *Journal of Cardiovascular Magnetic Resonance*, 17, 1-7.

Kroft, L. J., van der Velden, L., Girón, I. H., Roelofs, J. J., de Roos, A., & Geleijns, J. (2019). Added value of ultra-low-dose computed tomography, dose equivalent to chest x-ray radiography, for diagnosing chest pathology. *Journal of thoracic imaging*, 34(3), 179.

- Kuo, W., Kemner-van de Corput, M. P., Perez-Rovira, A., De Bruijne, M., Fajac, I., Tiddens, H. A., & Van Straten, M. (2016). Multicentre chest computed tomography standardisation in children and adolescents with cystic fibrosis: the way forward. *European Respiratory Journal*, *47*(6), 1706-1717.
- LARSON, P. E., HAN, M., KRUG, R., JAKARY, A., NELSON, S. J., VIGNERON, D. B., HENRY, R. G., MCKINNON, G. & KELLEY, D. A. 2016. Ultrashort echo time and zero echo time MRI at 7T. *Magnetic Resonance Materials in Physics, Biology and Medicine*, *29*, 359-370.
- Li, J., Han, Y. R., Plummer, M. R., & Herrup, K. (2009). Cytoplasmic ATM in neurons modulates synaptic function. *Current Biology*, *19*(24), 2091-2096.
- Lilburn, D. M., Pavlovskaya, G. E., & Meersmann, T. (2013). Perspectives of hyperpolarized noble gas MRI beyond ^3He . *Journal of magnetic resonance*, *229*, 173-186.
- Lo, D., Maniyar, A., Gupta, S., & Gaillard, E. (2019). High prevalence of bronchiectasis on chest CT in a selected cohort of children with severe Asthma. *BMC pulmonary medicine*, *19*(1), 1-9.
- Lopes-Pacheco, M. (2020). CFTR modulators: the changing face of cystic fibrosis in the era of precision medicine. *Frontiers in pharmacology*, *10*, 1662.

LOUED-KHENISSI, L., DÖLL, O. & PREUSCHOFF, K. 2019. An overview of functional magnetic resonance imaging techniques for organizational research. *Organizational Research Methods*, 22, 17-45.

Lum, S., Stocks, J., Stanojevic, S., Wade, A., Robinson, P., Gustafsson, P., ... & Sonnappa, S. (2013). Age and height dependence of lung clearance index and functional residual capacity. *European Respiratory Journal*, 41(6), 1371-1377.

MA, W., SHEIKH, K., SVENNINGSEN, S., PIKE, D., GUO, F., ETEMAD-REZAI, R., LEIPSIC, J., COXSON, H. O., MCCORMACK, D. G. & PARRAGA, G. 2015. Ultra-short echo-time pulmonary MRI: Evaluation and reproducibility in COPD subjects with and without bronchiectasis. *Journal of Magnetic Resonance Imaging*, 41, 1465-1474.

MAI, V. M., LIU, B., POLZIN, J. A., LI, W., KURUCAY, S., BANKIER, A. A., KNIGHT-SCOTT, J., MADHAV, P., EDELMAN, R. R. & CHEN, Q. 2002. Ventilation-perfusion ratio of signal intensity in human lung using oxygen-enhanced and arterial spin labeling techniques. *Magnetic Resonance in Medicine: An Official Journal of the International Society for Magnetic Resonance in Medicine*, 48, 341-350.

Makaju, S., Prasad, P. W. C., Alsadoon, A., Singh, A. K., & Elchouemi, A. (2018). Lung cancer detection using CT scan images. *Procedia Computer Science*, 125, 107-114.

- Marek, W., Marek, E., Mückenhoff, K., Smith, H. J., Degens, P., Kotschy-Lang, N., & Kohlhäufel, M. (2009). Time for new reference values for ventilatory lung function. *European Journal of Medical Research*, 14(4), 1-7.
- Martinez-Pitre, P. J., Sabbula, B. R., & Cascella, M. (2020). Restrictive Lung Disease. *StatPearls [Internet]*.
- Matteo, V., Marina, A., Giuseppina, B., Ernesto, C., & Alfredo, C. (2018). Flow and volume response to bronchodilator in patients with COPD. *Acta Bio Medica: Atenei Parmensis*, 89(3), 332.
- MAXIEN, D., DIETRICH, O., THIEME, S. F., FÖRSTER, S., BEHR, J., REISER, M. F. & NIKOLAOU, K. 2012. Value of oxygen-enhanced MRI of the lungs in patients with pulmonary hypertension: A qualitative and quantitative approach. *Journal of Magnetic Resonance Imaging*, 35, 86-94.
- McCarthy, B., Casey, D., Devane, D., Murphy, K., Murphy, E., & Lacasse, Y. (2015). Pulmonary rehabilitation for chronic obstructive pulmonary disease. *Cochrane database of systematic reviews*, (2).
- McFarlin DE, Strober W, Waldmann TA (1972). Ataxiatelangiectasia. *Medicine (Baltimore)* 51: 281-314.
- McGrath-Morrow, S. A., Gower, W. A., Rothblum-Oviatt, C., Brody, A. S., Langston, C., Fan, L. L., ... & Lederman, H. M. (2010). Evaluation and

management of pulmonary disease in ataxia-telangiectasia. *Pediatric pulmonology*, 45(9), 847-859.

McGrath-Morrow, S., Lefton-Greif, M., Rosquist, K., Crawford, T., Kelly, A., Zeitlin, P., ... & Lederman, H. M. (2008). Pulmonary function in adolescents with ataxia telangiectasia. *Pediatric pulmonology*, 43(1), 59-66.

MCKEOWN, S. 2014. Defining normoxia, physoxia and hypoxia in tumours—implications for treatment response. *The British journal of radiology*, 87, 20130676.

McNulty, W., & Usmani, O. S. (2014). Techniques of assessing small airways dysfunction. *European clinical respiratory journal*, 1(1), 25898.

Milanzi, E. B., Koppelman, G. H., Oldenwening, M., Augustijn, S., Aalders-de Ruijter, B., Farenhorst, M., ... & Gehring, U. (2019). Considerations in the use of different spirometers in epidemiological studies. *Environmental Health*, 18(1), 1-8.

Miller, A. (2016). Practical approach to lung ultrasound. *Bja Education*, 16(2), 39-45.

Miller, M. R., Hankinson, J. A. T. S., Brusasco, V., Burgos, F., Casaburi, R., Coates, A., ... & Wanger, J. A. T. S. (2005). Standardisation of spirometry. *European respiratory journal*, 26(2), 319-338.

MOLINARI, F., EICHINGER, M., RISSE, F., PLATHOW, C., PUDERBACH, M., LEY, S., HERTH, F., BONOMO, L., KAUCZOR, H.U. AND FINK, C. 2007. Navigator-triggered oxygen-enhanced MRI with simultaneous cardiac and respiratory synchronization for the assessment of interstitial lung disease. *Journal of Magnetic Resonance Imaging: An Official Journal of the International Society for Magnetic Resonance in Medicine*, 26(6), pp.1523-1529.

MOLNAR, C. & GAIR, J. 2013. 20.4 Transport of Gases in Human Bodily Fluids. *Concepts of Biology-1st Canadian Edition*.

Moore, V. C. (2012). Spirometry: step by step. *Breathe*, 8(3), 232-240.

MORATAL, D., VALLÉS-LUCH, A., MARTÍ-BONMATÍ, L. & BRUMMER, M. E. 2008. k-Space tutorial: an MRI educational tool for a better understanding of k-space. *Biomedical imaging and intervention journal*, 4.

MUGLER, J. P., & ALTES, T. A. 2013. Hyperpolarized ¹²⁹Xe MRI of the Human Lung. *Journal of Magnetic Resonance Imaging: JMRI*, 37(2), 313–331. <http://doi.org/10.1002/jmri.23844>.

MUGLER, J.P., ALTES, T.A., RUSSET, I.C., DREGELY, I.M., MATA, J.F., MILLER, G.W., KETEL, S., KETEL, J., HERSMAN, F.W. AND RUPPERT, K. 2010. Simultaneous magnetic resonance imaging of ventilation distribution and gas uptake in the human lung using hyperpolarized

xenon-129. Proceedings of the National Academy of Sciences, p.201011912.

Nissenkorn, A., Levi, Y. B., Vilozni, D., Berkun, Y., Efrati, O., Frydman, M., ... & Ben-Zeev, B. (2011). Neurologic presentation in children with ataxia-telangiectasia: is small head circumference a hallmark of the disease?. *The Journal of pediatrics*, 159(3), 466-471.

Nonas, S. (2015). Pulmonary manifestations of primary immunodeficiency disorders. *Immunol Allergy Clin North Am*, 35(4), 753-766.

Nuttall, A. G., Beardsmore, C. S., & Gaillard, E. A. (2021). Ventilation heterogeneity in children with severe asthma. *European Journal of Pediatrics*, 1-6.

Nuttall, A. G., Velásquez, W., Beardsmore, C. S., & Gaillard, E. A. (2019). Lung clearance index: assessment and utility in children with asthma. *European Respiratory Review*, 28(154).

Obi, O. N., & Baughman, R. P. (2020). Mixed Obstructive and Restrictive Ventilatory Defect in Sarcoidosis: A New Phenotype?. *Chest*, 158(5), 1816-1817.

O'BRIEN, K., MYERSON, S., COWAN, B., YOUNG, A. AND ROBSON, M. 2009. Phase Contrast Ultrashort TE: A More Reliable Technique for Measurement of High-Velocity Turbulent Stenotic Jets'. *Magnetic Resonance in Medicine*, 62 (3), 626-636

O'CONNOR, J. P., BOULT, J. K., JAMIN, Y., BABUR, M., FINEGAN, K. G., WILLIAMS, K. J., LITTLE, R. A., JACKSON, A., PARKER, G. J. & REYNOLDS, A. R. 2016. Oxygen-enhanced MRI accurately identifies, quantifies, and maps tumor hypoxia in preclinical cancer models. *Cancer research*, 76, 787-795.

O'Connor, J. P., Robinson, S. P., & Waterton, J. C. (2019). Imaging tumour hypoxia with oxygen-enhanced MRI and BOLD MRI. *The British journal of radiology*, 92(1096), 20180642.

O'CONNOR, J.P., NAISH, J.H., PARKER, G.J., WATERTON, J.C., WATSON, Y., JAYSON, G.C., BUONACCORSI, G.A., CHEUNG, S., BUCKLEY, D.L., MCGRATH, D.M. AND WEST, C.M., 2009. Preliminary study of oxygen-enhanced longitudinal relaxation in MRI: a potential novel biomarker of oxygenation changes in solid tumours. *International Journal of Radiation Oncology* Biology* Physics*, 75(4), pp.1209-1215.

OHNO, Y. & HATABU, H. 2007. Basics concepts and clinical applications of oxygen-enhanced MR imaging. *European journal of radiology*, 64, 320-328.

OHNO, Y., CHEN, Q. AND HATABU, H. 2001. Oxygen-Enhanced Magnetic Resonance Ventilation Imaging of Lung. *European Journal of Radiology*, 37 (3), 164-171.

OHNO, Y., HATABU, H., HIGASHINO, T., KAWAMITSU, H., WATANABE, H., TAKENAKA, D., VAN CAUTEREN, M. & SUGIMURA, K. 2004. Centrally reordered inversion recovery half-Fourier single-shot turbo spin-echo sequence: improvement of the image quality of oxygen-enhanced MRI. *European journal of radiology*, 52, 200-205.

OHNO, Y., HATABU, H., TAKENAKA, D., VAN CAUTEREN, M., FUJII, M. AND SUGIMURA, K., 2002. Dynamic oxygen-enhanced MRI reflects diffusing capacity of the lung. *Magnetic Resonance in Medicine: An Official Journal of the International Society for Magnetic Resonance in Medicine*, 47(6), pp.1139-1144.

OHNO, Y., KOYAMA, H., MATSUMOTO, K., ONISHI, Y., NOGAMI, M., TAKENAKA, D., MATSUMOTO, S. AND SUGIMURA, K. 2011. Oxygen-enhanced MRI vs. quantitatively assessed thin-section CT: pulmonary functional loss assessment and clinical stage classification of asthmatics. *European journal of radiology*, 77(1), pp.85-91.

OHNO, Y., KOYAMA, H., YOSHIKAWA, T., MATSUMOTO, K., TAKAHASHI, M., VAN CAUTEREN, M. AND SUGIMURA, K. 2011. T2* measurements of 3-T MRI with ultrashort TEs: capabilities of pulmonary function assessment and clinical stage classification in smokers. *American Journal of Roentgenology*, 197(2), pp.W279-W285.

OHNO, Y., SUGIMURA, K. & HATABU, H. 2003. Clinical oxygen-enhanced magnetic resonance imaging of the lung. *Topics in Magnetic Resonance Imaging*, 14, 237-243.

- Panchbhai, A. S. (2015). Wilhelm Conrad Röntgen and the discovery of X-rays: Revisited after centennial. *Journal of Indian academy of oral medicine and radiology*, 27(1), 90.
- Panitch, H. B. (2009). The pathophysiology of respiratory impairment in pediatric neuromuscular diseases. *Pediatrics*, 123(Supplement 4), S215-S218.
- Pellegrino, R., Viegi, G., Brusasco, V., Crapo, R. O., Burgos, F., Casaburi, R. E. A., ... & Wanger, J. (2005). Interpretative strategies for lung function tests. *European respiratory journal*, 26(5), 948-968.
- Phillips, S. M., Summerbell, C., Hobbs, M., Hesketh, K. R., Saxena, S., Muir, C., & Hillier-Brown, F. C. (2021). A systematic review of the validity, reliability, and feasibility of measurement tools used to assess the physical activity and sedentary behaviour of pre-school aged children. *International Journal of Behavioral Nutrition and Physical Activity*, 18(1), 1-28.
- Pittman, R. N. (2011, April). Regulation of tissue oxygenation. In *Colloquium series on integrated systems physiology: from molecule to function* (Vol. 3, No. 3, pp. 1-100). Morgan & Claypool Life Sciences.
- Pöhler, G. H., Klimeš, F., Behrendt, L., Voskrebenezv, A., Gonzalez, C. C., Wacker, F., ... & Vogel-Claussen, J. (2021). Repeatability of phase-resolved functional lung (PREFUL)-MRI ventilation and perfusion

parameters in healthy subjects and COPD patients. *Journal of Magnetic Resonance Imaging*, 53(3), 915-927.

POWERS, K. A. & DHAMOON, A. S. 2020. Physiology, Pulmonary Ventilation and Perfusion. StatPearls [Internet].

Pranata, R., Soeroto, A. Y., Huang, I., Lim, M. A., Santoso, P., Permana, H., & Lukito, A. A. (2020). Effect of chronic obstructive pulmonary disease and smoking on the outcome of COVID-19. *The International Journal of Tuberculosis and Lung Disease*, 24(8), 838-843.

PRAYLE, A., TIBILETTI, M., YOULE, C., SAFAVI, S., ALENAZI, S., PAUL, J. A., COOPER, A., HAYWOOD, B., BARLOW, M. & DINEEN, R. 2018. Early experience of oxygen enhanced magnetic resonance imaging (OE-MRI) in ataxia telangiectasia (AT). *Eur Respiratory Soc*.

Prayle, D. J. B. a. D. A., 2017. IMAGIN-AT – advanced lung imaging and function testing in Ataxia Telangiectasia. Nottingham University Hospitals NHS Trust.

Quanjer, P. H., Stanojevic, S., Cole, T. J., Baur, X., Hall, G. L., Culver, B. H., ... & ERS Global Lung Function Initiative. (2012). Multi-ethnic reference values for spirometry for the 3–95-yr age range: the global lung function 2012 equations.

Quanjer, P. H., Stanojevic, S., Stocks, J., Hall, G. L., Prasad, K. V. V., Cole, T. J., ... & Ip, M. S. M. (2010). *Changes in the FEV1/FVC ratio during*

childhood and adolescence: an intercontinental study. European Respiratory Journal, 36(6), 1391-1399.

Ranu, H., Wilde, M., & Madden, B. (2011). Pulmonary function tests. *The Ulster medical journal, 80(2), 84.*

Raslan, I. R., de Assis Pereira Matos, P. C. A., Boaratti Ciarlariello, V., Daghasanli, K. H., Rosa, A. B. R., Arita, J. H., ... & Pedroso, J. L. (2021). Beyond typical ataxia telangiectasia: how to identify the ataxia telangiectasia-like disorders. *Movement Disorders Clinical Practice, 8(1), 118-125.*

REICHERT, I. L., ROBSON, M. D., GATEHOUSE, P. D., HE, T., CHAPPELL, K. E., HOLMES, J., GIRGIS, S. & BYDDER, G. M. 2005. Magnetic resonance imaging of cortical bone with ultrashort TE pulse sequences. *Magnetic resonance imaging, 23, 611-618.*

ROACH, D., CRÉMILLIEUX, Y., FLECK, R., BRODY, A., SERAI, S., SZCZESNIAK, R., KERLAKIAN, S., CLANCY, J. AND WOODS, J. 2016. Ultrashort Echo-Time Magnetic Resonance Imaging Is A Sensitive Method for The Evaluation Of Early Cystic Fibrosis Lung Disease. *Annals of the American Thoracic Society, 13 (11), 1923-1931.*

Roberts, C., Ward, S., Walsted, E., & Hull, J. H. (2018). Safety of pulmonary function testing: data from 20 years. *Thorax, 73(4), 385-387.*

Robinson, P. D., Goldman, M. D., & Gustafsson, P. M. (2009). Inert gas washout: theoretical background and clinical utility in respiratory disease. *Respiration*, 78(3), 339-355.

Robinson, P. D., Latzin, P., Verbanck, S., Hall, G. L., Horsley, A., Gappa, M., ... & Gustafsson, P. M. (2013). Consensus statement for inert gas washout measurement using multiple-and single-breath tests.

Robinson, P. D., Lindblad, A., & Gustafsson, P. M. (2010). Comparison of the utility of multiple breath inert gas washout parameters in cystic fibrosis. *Thorax*, 65(7), 659-659.

Robinson, P. D., Lum, S., Moore, C., Hardaker, K. M., Benseler, N., Aurora, P., ... & Stanojevic, S. (2018). Comparison of facemask and mouthpiece interfaces for multiple breath washout measurements. *Journal of Cystic Fibrosis*, 17(4), 511-517.

Rossi, G. A., Morelli, P., Galietta, L. J., & Colin, A. A. (2019). Airway microenvironment alterations and pathogen growth in cystic fibrosis. *Pediatric pulmonology*, 54(4), 497-506.

Rothblum-Oviatt, C., Wright, J., Lefton-Greif, M. A., McGrath-Morrow, S. A., Crawford, T. O., & Lederman, H. M. (2016). Ataxia telangiectasia: a review. *Orphanet journal of rare diseases*, 11(1), 1-21.

ROTHBLUM-OVIATT, C., WRIGHT, J., LEFTON-GREIF, M. A., MCGRATH-MORROW, S. A., CRAWFORD, T. O. & LEDERMAN, H. M. 2016. Ataxia telangiectasia: a review. *Orphanet journal of rare diseases*, 11, 1-21.

- RUPPERT, K., BROOKEMAN, J. R., HAGSPIEL, K. D., DRIEHUYS, B. & MUGLER III, J. P. 2000. NMR of hyperpolarized ^{129}Xe in the canine chest: spectral dynamics during a breath-hold. *NMR in Biomedicine: An International Journal Devoted to the Development and Application of Magnetic Resonance In Vivo*, 13, 220-228.
- SAHAMA, I., SINCLAIR, K., PANNEK, K., LAVIN, M. & ROSE, S. 2014. Radiological imaging in ataxia telangiectasia: a review. *The Cerebellum*, 13, 521-530.
- SAKAI, K., BILEK, A. M., OTEIZA, E., WALSWORTH, R. L., BALAMORE, D., JOLESZ, F. A. & ALBERT, M. S. 1996. *Temporal Dynamics of Hyperpolarized ^{129}Xe Resonances in Living Rats*. Academic Press.
- SALERNO M, ALTES TA, MUGLER JP 3RD, NAKATSU M, HATABU H, DE LANGE EE. 2001. Hyperpolarized noble gas MR imaging of the lung: potential clinical applications. *Eur J Radiol*, 40(1), 33-44.
- SALERNO, M., ALTES, T.A., BROOKEMAN, J.R., DE LANGE, E.E. AND MUGLER III, J.P. 2003. Rapid hyperpolarized ^3He diffusion MRI of healthy and emphysematous human lungs using an optimized interleaved-spiral pulse sequence. *Journal of Magnetic Resonance Imaging: An Official Journal of the International Society for Magnetic Resonance in Medicine*, 17(5), pp.581-588.
- SANDERS RD, FRANKS NP, MAZE M. 2003. Xenon: no stranger to anaesthesia. *Br J Anaesth*, 91:709-717.

- Sanders, D. B., Rosenfeld, M., Mayer-Hamblett, N., Stamey, D., & Redding, G. J. (2008). Reproducibility of spirometry during cystic fibrosis pulmonary exacerbations. *Pediatric pulmonology*, *43*(11), 1142-1146.
- Sandlund, J. T., Hudson, M. M., Kennedy, W., Onciu, M., & Kastan, M. B. (2014). Pilot study of modified LMB-based therapy for children with ataxia–telangiectasia and advanced stage high grade mature B-cell malignancies. *Pediatric blood & cancer*, *61*(2), 360-362.
- Savitsky K, Bar-Shira A, Gilad S et al. (1995). A single ataxia telangiectasia gene with a product similar to PI-3 kinase. *Science* 268: 1749–1753.
- Schlüter, D. K., Southern, K. W., Dryden, C., Diggle, P., & Taylor-Robinson, D. (2020). Impact of newborn screening on outcomes and social inequalities in cystic fibrosis: a UK CF registry-based study. *Thorax*, *75*(2), 123-131.
- Schoenaker, M. H. D., Suarez, F., Szczepanski, T., Mahlaoui, N., & Loeffen, J. L. (2016). Treatment of acute leukemia in children with ataxia telangiectasia (AT). *European journal of medical genetics*, *59*(12), 641-646.
- Schubert, R., Reichenbach, J., & Zielen, S. (2005). Growth factor deficiency in patients with ataxia telangiectasia. *Clinical & Experimental Immunology*, *140*(3), 517-519.

Seitz, A. E., Olivier, K. N., Adjemian, J., Holland, S. M., & Prevots, D. R. (2012). Trends in bronchiectasis among medicare beneficiaries in the United States, 2000 to 2007. *Chest*, 142(2), 432-439.

Severiche-Bueno, D., Gamboa, E., Reyes, L. F., & Chotirmall, S. H. (2019). Hot topics and current controversies in non-cystic fibrosis bronchiectasis. *Breathe*, 15(4), 286-295.

Sharon A. McGrath-Morrow, H. M. L. A. D. A. M. A. L.-G. T. O. C. T. R. J. W. a. J. M. C., 2014. Pulmonary Function in Children and Young. *Pediatric Pulmonology*, Volume 49, p. 84-90.

Shrine, N., Izquierdo, A. G., Chen, J., Packer, R., Hall, R. J., Guyatt, A. L., ... & Consortium Lead Principal Investigators Al-Khodor Souhaila 124 Alshafai Mashael 125 Badii Ramin 126 Chouchane Lotfi 127 Estivill Xavier 128 Fakhro Khalid 129 130 131 132 Mokrab Younes 129 130 131 133 Puthen Jithesh V. 131 Tatari Zohreh 134. (2023). Multi-ancestry genome-wide association analyses improve resolution of genes and pathways influencing lung function and chronic obstructive pulmonary disease risk. *Nature genetics*, 55(3), 410-422.

Singer, F., Schlegkendal, A., Nyilas, S., Vermeulen, F., Boon, M., & Koerner-Rettberg, C. (2021). Lung clearance index predicts pulmonary exacerbations in individuals with primary ciliary dyskinesia: a multicentre cohort study. *Thorax*, 76(7), 681-688.

- Sommerburg, O., Hämmerling, S., Schneider, S. P., Okun, J., Langhans, C. D., Leutz-Schmidt, P., ... & Stahl, M. (2021). CFTR modulator therapy with lumacaftor/ivacaftor alters plasma concentrations of lipid-soluble vitamins A and E in patients with cystic fibrosis. *Antioxidants*, *10*(3), 483.
- Stahl, M., Graeber, S. Y., Joachim, C., Barth, S., Ricklefs, I., Diekmann, G., ... & Mall, M. A. (2018). Three-center feasibility of lung clearance index in infants and preschool children with cystic fibrosis and other lung diseases. *Journal of Cystic Fibrosis*, *17*(2), 249-255.
- Staples, E. R., McDermott, E. M., Reiman, A., Byrd, P. J., Ritchie, S., Taylor, A. M. R., & Davies, E. G. (2008). Immunodeficiency in ataxia telangiectasia is correlated strongly with the presence of two null mutations in the ataxia telangiectasia mutated gene. *Clinical & Experimental Immunology*, *153*(2), 214-220.
- Suarez, F., Mahlaoui, N., Canioni, D., Andriamanga, C., Dubois d'Enghien, C., Brousse, N., ... & Stoppa-Lyonnet, D. (2015). Incidence, presentation, and prognosis of malignancies in ataxia-telangiectasia: a report from the French national registry of primary immune deficiencies. *Journal of clinical oncology*, *33*(2), 202-208.
- Subbarao, P., Milla, C., Aurora, P., Davies, J. C., Davis, S. D., Hall, G. L., ... & Morgan, W. (2015). Multiple-breath washout as a lung function test in cystic fibrosis. A Cystic Fibrosis Foundation Workshop Report. *Annals of the American Thoracic Society*, *12*(6), 932-939.

Subbarao, P., Milla, C., Aurora, P., Davies, J. C., Davis, S. D., Hall, G. L., ... & Morgan, W. (2015). Multiple-breath washout as a lung function test in cystic fibrosis. A Cystic Fibrosis Foundation Workshop Report. *Annals of the American Thoracic Society*, 12(6), 932-939.

SUN, Y., O'SULLIVAN, B.P., ROCHE, J.P., WALVICK, R., RENO, A., BAKER, D., MANSOUR, J.K. AND ALBERT, M.S. 2011. Using hyperpolarized ³He MRI to evaluate treatment efficacy in cystic fibrosis patients. *Journal of Magnetic Resonance Imaging*, 34(5), pp.1206-1211.

Taveira-DaSilva, A. M., Julien-Williams, P., Jones, A. M., & Moss, J. (2016). Incidence of pneumothorax in patients with lymphangiomyomatosis undergoing pulmonary function and exercise testing. *Chest*, 150(1), e5-e8.

TAYLOR, A. J., SALERNO, M., DHARMAKUMAR, R. & JEROSCH-HEROLD, M. 2016. T1 mapping: basic techniques and clinical applications. *JACC: Cardiovascular Imaging*, 9, 67-81.

Taylor, A. M. R., Rothblum-Oviatt, C., Ellis, N. A., Hickson, I. D., Meyer, S., Crawford, T. O., ... & Stewart, G. S. (2019). Chromosome instability syndromes. *Nature Reviews Disease Primers*, 5(1), 1-20.

Teive, H. A., Moro, A., Moscovich, M., Arruda, W. O., Munhoz, R. P., Raskin, S., & Ashizawa, T. (2015). Ataxia-telangiectasia—A historical review and a proposal for a new designation: ATM syndrome. *Journal of the neurological sciences*, 355(1-2), 3-6.

- Tibiletti, M., Paul, J., Bianchi, A., Wundrak, S., Rottbauer, W., Stiller, D., & Rasche, V. (2016). Multistage three-dimensional UTE lung imaging by image-based self-gating. *Magnetic resonance in medicine*, 75(3), 1324-1332.
- Torres, L., Kammerman, J., Hahn, A. D., Zha, W., Nagle, S. K., Johnson, K., ... & Fain, S. B. (2019). Structure-function imaging of lung disease using ultrashort echo time MRI. *Academic radiology*, 26(3), 431-441.
- Touw, H. R., Tuinman, P. R., Gelissen, H. P., Lust, E., & Elbers, P. W. (2015). Lung ultrasound: routine practice for the next generation of internists. *Neth J Med*, 73(3), 100-107.
- Townsend, M. C. (2020). Spirometry in Occupational Health—2020. *Journal of occupational and environmental medicine*, 62(5), e208-e230.
- Turcios, N. L. (2020). Cystic fibrosis lung disease: An overview. *Respiratory care*, 65(2), 233-251.
- VAN DEN TOORN, L. M., OVERBEEK, S. E., DE JONGSTE, J. C., Leman, K., HOOGSTEDEN, H. C., & Prins, J. B. (2001). Airway inflammation is present during clinical remission of atopic asthma. *American journal of respiratory and critical care medicine*, 164(11), 2107-2113.
- Vilozni, D., Berkun, Y., Levi, Y., Weiss, B., Jacobson, J. M., & Efrati, O. (2010). The feasibility and validity of forced spirometry in ataxia telangiectasia. *Pediatric pulmonology*, 45(10), 1030-1036.

Vilozni, D., Lavie, M., Sarouk, I., Bar-Aluma, B. E., Dagan, A., Ashkenazi, M., ... & Efrati, O. (2015). FVC deterioration, airway obstruction determination, and life span in Ataxia telangiectasia. *Respiratory medicine*, 109(7), 890-896.

Wain, L. V., Shrine, N., Miller, S., Jackson, V. E., Ntalla, I., Artigas, M. S., ... & Hall, I. P. (2015). Novel insights into the genetics of smoking behaviour, lung function, and chronic obstructive pulmonary disease (UK BiLEVE): a genetic association study in UK Biobank. *The Lancet Respiratory Medicine*, 3(10), 769-781.

Wang, R., Ding, S., Lei, C., Yang, D., & Luo, H. (2021). The contribution of *Pseudomonas aeruginosa* infection to clinical outcomes in bronchiectasis: a prospective cohort study. *Annals of Medicine*, 53(1), 459-469.

WESTBROOK, C. & ROTH, C. K. 2011. MRI in Practice, John Wiley & Sons.

Wheatley, J. R. (2017). Spirometry: key to the diagnosis of respiratory disorders. *Med J Australia*, 422-3.

Willmering, M. M., Niedbalski, P. J., Wang, H., Walkup, L. L., Robison, R. K., Pipe, J. G., ... & Woods, J. C. (2020). Improved pulmonary ¹²⁹Xe ventilation imaging via 3D-spiral UTE MRI. *Magnetic resonance in medicine*, 84(1), 312-320.

Woo, T. E., Lim, R., Heirali, A. A., Acosta, N., Rabin, H. R., Mody, C. H., ... & Parkins, M. D. (2019). A longitudinal characterization of the Non-

Cystic Fibrosis Bronchiectasis airway microbiome. *Scientific reports*, 9(1), 6871.

Yackov Berkun, D. V. Y. L. S. B. D. W. R. S. A. N. a. O. E., 2010. Reversible Airway Obstruction in Children With. *Pediatric Pulmonology*, Volume 45, p. 230–235.

Yeo, A. J., Henningham, A., Fantino, E., Galbraith, S., Krause, L., Wainwright, C. E., ... & Lavin, M. F. (2019). Increased susceptibility of airway epithelial cells from ataxia-telangiectasia to *S. pneumoniae* infection due to oxidative damage and impaired innate immunity. *Scientific reports*, 9(1), 1-10.

YOUNG, I., CLARKE, G., BAFFLES, D., PENNOCK, J., DOYLE, F. & BYDDER, G. 1981. Enhancement of relaxation rate with paramagnetic contrast agents in NMR imaging. *Journal of Computed Tomography*, 5, 543-547.

Zamanian, A., & Hardiman, C. J. H. F. E. (2005). Electromagnetic radiation and human health: A review of sources and effects. *High Frequency Electronics*, 4(3), 16-26.

Zeng, J., Liu, Z., Shen, G., Zhang, Y., Li, L., Wu, Z., ... & Wang, L. (2019). MRI evaluation of pulmonary lesions and lung tissue changes induced by tuberculosis. *International Journal of Infectious Diseases*, 82, 138-146.

Zhang, W. J., Niven, R. M., Young, S. S., Liu, Y. Z., Parker, G. J., & Naish, J. H. (2015). Dynamic oxygen-enhanced magnetic resonance imaging of the lung in asthma—Initial experience. *European journal of radiology*, *84*(2), 318-326.

Zhou-Suckow, Z., Duerr, J., Hagner, M., Agrawal, R., & Mall, M. A. (2017). Airway mucus, inflammation and remodeling: emerging links in the pathogenesis of chronic lung diseases. *Cell and tissue research*, *367*(3), 537-550.

Zwitsersloot, A., Fuchs, S. I., Müller, C., Bisdorf, K., & Gappa, M. (2014). Clinical application of inert gas Multiple Breath Washout in children and adolescents with asthma. *Respiratory medicine*, *108*(9), 1254-12.

PC-QOL-8

Newcombe, P.A., Sheffield, J.K., & Chang, A.B. (2013). Parent cough-specific quality of life: Development and validation of a short form. *Journal of Allergy and Clinical Immunology*, 131(4), 1069-1074. DOI: 10.1016/j.jaci.2012.10.004

SCORING

- Code "All of the time" = 1; "Most of the time" = 2; "Quite often" = 3; "Some of the time" = 4; "Once in a while" = 5; "Hardly any of the time" = 6; "None of the time" = 7.
- Code "Very very worried/concerned" = 1; "Very worried/concerned" = 2; "Fairly worried/concerned" = 3; "Somewhat worried/concerned" = 4; "A little worried/concerned" = 5; "Hardly worried/concerned" = 6; "Not worried/concerned" = 7.

For total score:

- Compute the average of the 8 items. Higher scores reflect better quality of life.

For Domain scores:

- Physical well-being: Compute the average of items #2, 8
- Social well-being: Compute the average of items #5, 7
- Psychological well-being: Compute the average of items #1, 3, 4, 6
- Across each Domain, higher scores reflect better quality of life.

Paediatric Quality of Life inventory - A standardized children quality of life score

ID#	_____
Date:	_____

PedsQL TM
Pediatric Quality of Life
Inventory

Version 4.0

PARENT REPORT for YOUNG CHILDREN (ages 5-7)

DIRECTIONS

On the following page is a list of things that might be a problem for your child. Please tell us how much of a problem each one has been for your child during the past **ONE** month by circling:

- 0 if it is never a problem
- 1 if it is almost never a problem
- 2 if it is sometimes a problem
- 3 if it is often a problem
- 4 if it is almost always a problem

There are no right or wrong answers.
If you do not understand a question, please ask for help.

In the past **ONE month**, how much of a **problem** has your child had with ...

PHYSICAL FUNCTIONING (problems with...)	Never	Almost Never	Sometimes	Often	Almost Always
1. Walking more than one block	0	1	2	3	4
2. Running	0	1	2	3	4
3. Participating in sports activity or exercise	0	1	2	3	4
4. Lifting something heavy	0	1	2	3	4
5. Taking a bath or shower by him or herself	0	1	2	3	4
6. Doing chores, like picking up his or her toys	0	1	2	3	4
7. Having hurts or aches	0	1	2	3	4
8. Low energy level	0	1	2	3	4

EMOTIONAL FUNCTIONING (problems with...)	Never	Almost Never	Sometimes	Often	Almost Always
1. Feeling afraid or scared	0	1	2	3	4
2. Feeling sad or blue	0	1	2	3	4
3. Feeling angry	0	1	2	3	4
4. Trouble sleeping	0	1	2	3	4
5. Worrying about what will happen to him or her	0	1	2	3	4

SOCIAL FUNCTIONING (problems with...)	Never	Almost Never	Sometimes	Often	Almost Always
1. Getting along with other children	0	1	2	3	4
2. Other kids not wanting to be his or her friend	0	1	2	3	4
3. Getting teased by other children	0	1	2	3	4
4. Not able to do things that other children his or her age can do	0	1	2	3	4
5. Keeping up when playing with other children	0	1	2	3	4

SCHOOL FUNCTIONING (problems with...)	Never	Almost Never	Sometimes	Often	Almost Always
1. Paying attention in class	0	1	2	3	4
2. Forgetting things	0	1	2	3	4
3. Keeping up with school activities	0	1	2	3	4
4. Missing school because of not feeling well	0	1	2	3	4
5. Missing school to go to the doctor or hospital	0	1	2	3	4

IN# _____

Date: _____

PedsQL™

Pediatric Quality of Life Inventory

Version 4.0

YOUNG CHILD REPORT (ages 5-7)

Instructions for interviewer:

I am going to ask you some questions about things that might be a problem for some children. I want to know how much of a problem any of these things might be for you.




Show the child the template and point to the responses as you read.

If it is not at all a problem for you, point to the smiling face

If it is sometimes a problem for you, point to the middle face

If it is a problem for you a lot, point to the frowning face

I will read each question. Point to the pictures to show me how much of a problem it is for you. Let's try a practice one first.

	Not at all	Sometimes	A lot
Is it hard for you to snap your fingers			

Ask the child to demonstrate snapping his or her fingers to determine whether or not the question was answered correctly. Repeat the question if the child demonstrates a response that is different from his or her action.

Think about how you have been doing for the last few weeks. Please listen carefully to each sentence and tell me how much of a problem this is for you.

After reading the item, gesture to the template. If the child hesitates or does not seem to understand how to answer, read the response options while pointing at the faces.

PHYSICAL FUNCTIONING (problems with...)	Not at all	Sometimes	A lot
1. Is it hard for you to walk	0	2	4
2. Is it hard for you to run	0	2	4
3. Is it hard for you to play sports or exercise	0	2	4
4. Is it hard for you to pick up big things	0	2	4
5. Is it hard for you to take a bath or shower	0	2	4
6. Is it hard for you to do chores (like pick up your toys)	0	2	4
7. Do you have hurts or aches (<i>Where?</i> _____)	0	2	4
8. Do you ever feel too tired to play	0	2	4

Remember, tell me how much of a problem this has been for you for the last few weeks.

EMOTIONAL FUNCTIONING (problems with...)	Not at all	Sometimes	A lot
1. Do you feel scared	0	2	4
2. Do you feel sad	0	2	4
3. Do you feel mad	0	2	4
4. Do you have trouble sleeping	0	2	4
5. Do you worry about what will happen to you	0	2	4

SOCIAL FUNCTIONING (problems with...)	Not at all	Sometimes	A lot
1. Is it hard for you to get along with other kids	0	2	4
2. Do other kids say they do not want to play with you	0	2	4
3. Do other kids tease you	0	2	4
4. Can other kids do things that you cannot do	0	2	4
5. Is it hard for you to keep up when you play with other kids	0	2	4

SCHOOL FUNCTIONING (problems with...)	Not at all	Sometimes	A lot
1. Is it hard for you to pay attention in school	0	2	4
2. Do you forget things	0	2	4
3. Is it hard to keep up with schoolwork	0	2	4
4. Do you miss school because of not feeling good	0	2	4
5. Do you miss school because you have to go to the doctor's or hospital	0	2	4

How much of a problem is this for you?

Not at all



Sometimes



A lot



SP

ID#	_____
Date:	_____

PedsQLTM

Pediatric Quality of Life Inventory

Version 4.0

PARENT REPORT for CHILDREN (ages 8-12)

DIRECTIONS

On the following page is a list of things that might be a problem for **your child**. Please tell us **how much of a problem** each one has been for **your child** during the past **ONE month** by circling:

- 0 if it is **never** a problem
- 1 if it is **almost never** a problem
- 2 if it is **sometimes** a problem
- 3 if it is **often** a problem
- 4 if it is **almost always** a problem

There are no right or wrong answers.
If you do not understand a question, please ask for help.

*In the past **ONE month**, how much of a **problem** has your child had with ...*

PHYSICAL FUNCTIONING (problems with...)	Never	Almost Never	Sometimes	Often	Almost Always
1. Walking more than one block	0	1	2	3	4
2. Running	0	1	2	3	4
3. Participating in sports activity or exercise	0	1	2	3	4
4. Lifting something heavy	0	1	2	3	4
5. Taking a bath or shower by him or herself	0	1	2	3	4
6. Doing chores around the house	0	1	2	3	4
7. Having hurts or aches	0	1	2	3	4
8. Low energy level	0	1	2	3	4

EMOTIONAL FUNCTIONING (problems with...)	Never	Almost Never	Sometimes	Often	Almost Always
1. Feeling afraid or scared	0	1	2	3	4
2. Feeling sad or blue	0	1	2	3	4
3. Feeling angry	0	1	2	3	4
4. Trouble sleeping	0	1	2	3	4
5. Worrying about what will happen to him or her	0	1	2	3	4

SOCIAL FUNCTIONING (problems with...)	Never	Almost Never	Sometimes	Often	Almost Always
1. Getting along with other children	0	1	2	3	4
2. Other kids not wanting to be his or her friend	0	1	2	3	4
3. Getting teased by other children	0	1	2	3	4
4. Not able to do things that other children his or her age can do	0	1	2	3	4
5. Keeping up when playing with other children	0	1	2	3	4

SCHOOL FUNCTIONING (problems with...)	Never	Almost Never	Sometimes	Often	Almost Always
1. Paying attention in class	0	1	2	3	4
2. Forgetting things	0	1	2	3	4
3. Keeping up with schoolwork	0	1	2	3	4
4. Missing school because of not feeling well	0	1	2	3	4
5. Missing school to go to the doctor or hospital	0	1	2	3	4

ID# _____

Date: _____

PedsQL™

Pediatric Quality of Life Inventory

Version 4.0

CHILD REPORT (ages 8-12)

DIRECTIONS

On the following page is a list of things that might be a problem for you. Please tell us how much of a problem each one has been for you during the past **ONE** month by circling:

- 0 if it is **never** a problem
- 1 if it is **almost never** a problem
- 2 if it is **sometimes** a problem
- 3 if it is **often** a problem
- 4 if it is **almost always** a problem

There are no right or wrong answers.
If you do not understand a question, please ask for help.

In the past **ONE month**, how much of a **problem** has this been for you ...

ABOUT MY HEALTH AND ACTIVITIES (problems with...)	Never	Almost Never	Sometimes	Often	Almost Always
1. It is hard for me to walk more than one block	0	1	2	3	4
2. It is hard for me to run	0	1	2	3	4
3. It is hard for me to do sports activity or exercise	0	1	2	3	4
4. It is hard for me to lift something heavy	0	1	2	3	4
5. It is hard for me to take a bath or shower by myself	0	1	2	3	4
6. It is hard for me to do chores around the house	0	1	2	3	4
7. I hurt or ache	0	1	2	3	4
8. I have low energy	0	1	2	3	4

ABOUT MY FEELINGS (problems with...)	Never	Almost Never	Sometimes	Often	Almost Always
1. I feel afraid or scared	0	1	2	3	4
2. I feel sad or blue	0	1	2	3	4
3. I feel angry	0	1	2	3	4
4. I have trouble sleeping	0	1	2	3	4
5. I worry about what will happen to me	0	1	2	3	4

HOW I GET ALONG WITH OTHERS (problems with...)	Never	Almost Never	Sometimes	Often	Almost Always
1. I have trouble getting along with other kids	0	1	2	3	4
2. Other kids do not want to be my friend	0	1	2	3	4
3. Other kids tease me	0	1	2	3	4
4. I cannot do things that other kids my age can do	0	1	2	3	4
5. It is hard to keep up when I play with other kids	0	1	2	3	4

ABOUT SCHOOL (problems with...)	Never	Almost Never	Sometimes	Often	Almost Always
1. It is hard to pay attention in class	0	1	2	3	4
2. I forget things	0	1	2	3	4
3. I have trouble keeping up with my schoolwork	0	1	2	3	4
4. I miss school because of not feeling well	0	1	2	3	4
5. I miss school to go to the doctor or hospital	0	1	2	3	4

ID# _____

Date: _____

PedsQLTM

Pediatric Quality of Life Inventory

Version 4.0

PARENT REPORT for TEENS (ages 13-18)

DIRECTIONS

On the following page is a list of things that might be a problem for **your teen**. Please tell us **how much of a problem** each one has been for your teen during the **past ONE month** by circling:

- 0 if it is **never** a problem
- 1 if it is **almost never** a problem
- 2 if it is **sometimes** a problem
- 3 if it is **often** a problem
- 4 if it is **almost always** a problem

There are no right or wrong answers.
If you do not understand a question, please ask for help.

In the past **ONE** month, how much of a **problem** has your teen had with ...

PHYSICAL FUNCTIONING (problems with...)	Never	Almost Never	Sometimes	Often	Almost Always
1. Walking more than one block	0	1	2	3	4
2. Running	0	1	2	3	4
3. Participating in sports activity or exercise	0	1	2	3	4
4. Lifting something heavy	0	1	2	3	4
5. Taking a bath or shower by him or herself	0	1	2	3	4
6. Doing chores around the house	0	1	2	3	4
7. Having hurts or aches	0	1	2	3	4
8. Low energy level	0	1	2	3	4

EMOTIONAL FUNCTIONING (problems with...)	Never	Almost Never	Sometimes	Often	Almost Always
1. Feeling afraid or scared	0	1	2	3	4
2. Feeling sad or blue	0	1	2	3	4
3. Feeling angry	0	1	2	3	4
4. Trouble sleeping	0	1	2	3	4
5. Worrying about what will happen to him or her	0	1	2	3	4

SOCIAL FUNCTIONING (problems with...)	Never	Almost Never	Sometimes	Often	Almost Always
1. Getting along with other teens	0	1	2	3	4
2. Other teens not wanting to be his or her friend	0	1	2	3	4
3. Getting teased by other teens	0	1	2	3	4
4. Not able to do things that other teens his or her age can do	0	1	2	3	4
5. Keeping up with other teens	0	1	2	3	4

SCHOOL FUNCTIONING (problems with...)	Never	Almost Never	Sometimes	Often	Almost Always
1. Paying attention in class	0	1	2	3	4
2. Forgetting things	0	1	2	3	4
3. Keeping up with schoolwork	0	1	2	3	4
4. Missing school because of not feeling well	0	1	2	3	4
5. Missing school to go to the doctor or hospital	0	1	2	3	4

ID# _____

Date: _____

PedsQLTM

Pediatric Quality of Life Inventory

Version 4.0

TEEN REPORT (ages 13-18)

DIRECTIONS

On the following page is a list of things that might be a problem for you. Please tell us **how much of a problem** each one has been for you during the **past ONE month** by circling:

- 0 if it is **never** a problem
- 1 if it is **almost never** a problem
- 2 if it is **sometimes** a problem
- 3 if it is **often** a problem
- 4 if it is **almost always** a problem

There are no right or wrong answers.
If you do not understand a question, please ask for help.

In the past **ONE** month, how much of a **problem** has this been for you ...

ABOUT MY HEALTH AND ACTIVITIES (problems with...)	Never	Almost Never	Some-times	Often	Almost Always
1. It is hard for me to walk more than one block	0	1	2	3	4
2. It is hard for me to run	0	1	2	3	4
3. It is hard for me to do sports activity or exercise	0	1	2	3	4
4. It is hard for me to lift something heavy	0	1	2	3	4
5. It is hard for me to take a bath or shower by myself	0	1	2	3	4
6. It is hard for me to do chores around the house	0	1	2	3	4
7. I hurt or ache	0	1	2	3	4
8. I have low energy	0	1	2	3	4

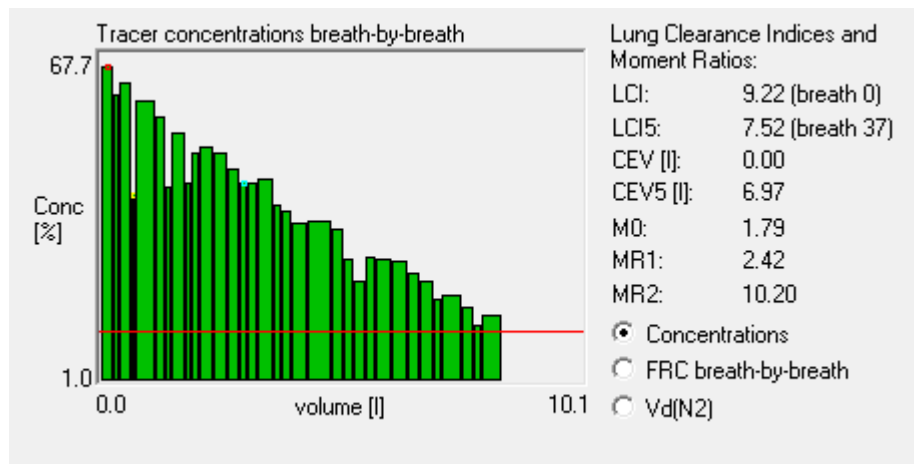
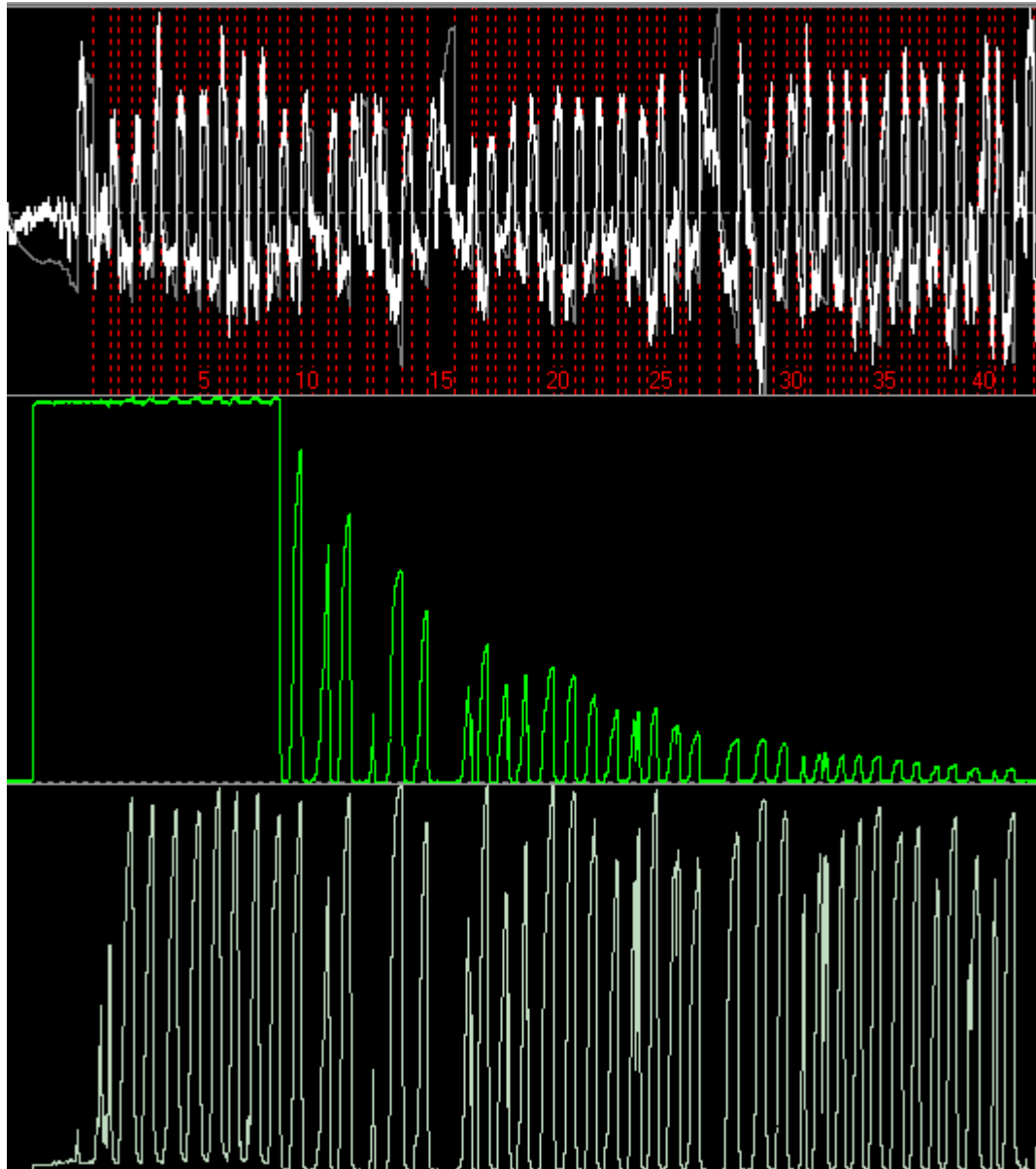
ABOUT MY FEELINGS (problems with...)	Never	Almost Never	Some-times	Often	Almost Always
1. I feel afraid or scared	0	1	2	3	4
2. I feel sad or blue	0	1	2	3	4
3. I feel angry	0	1	2	3	4
4. I have trouble sleeping	0	1	2	3	4
5. I worry about what will happen to me	0	1	2	3	4

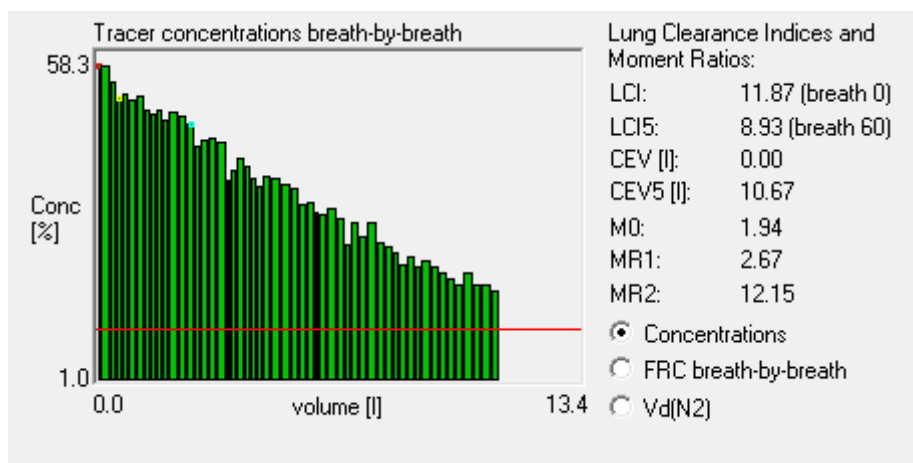
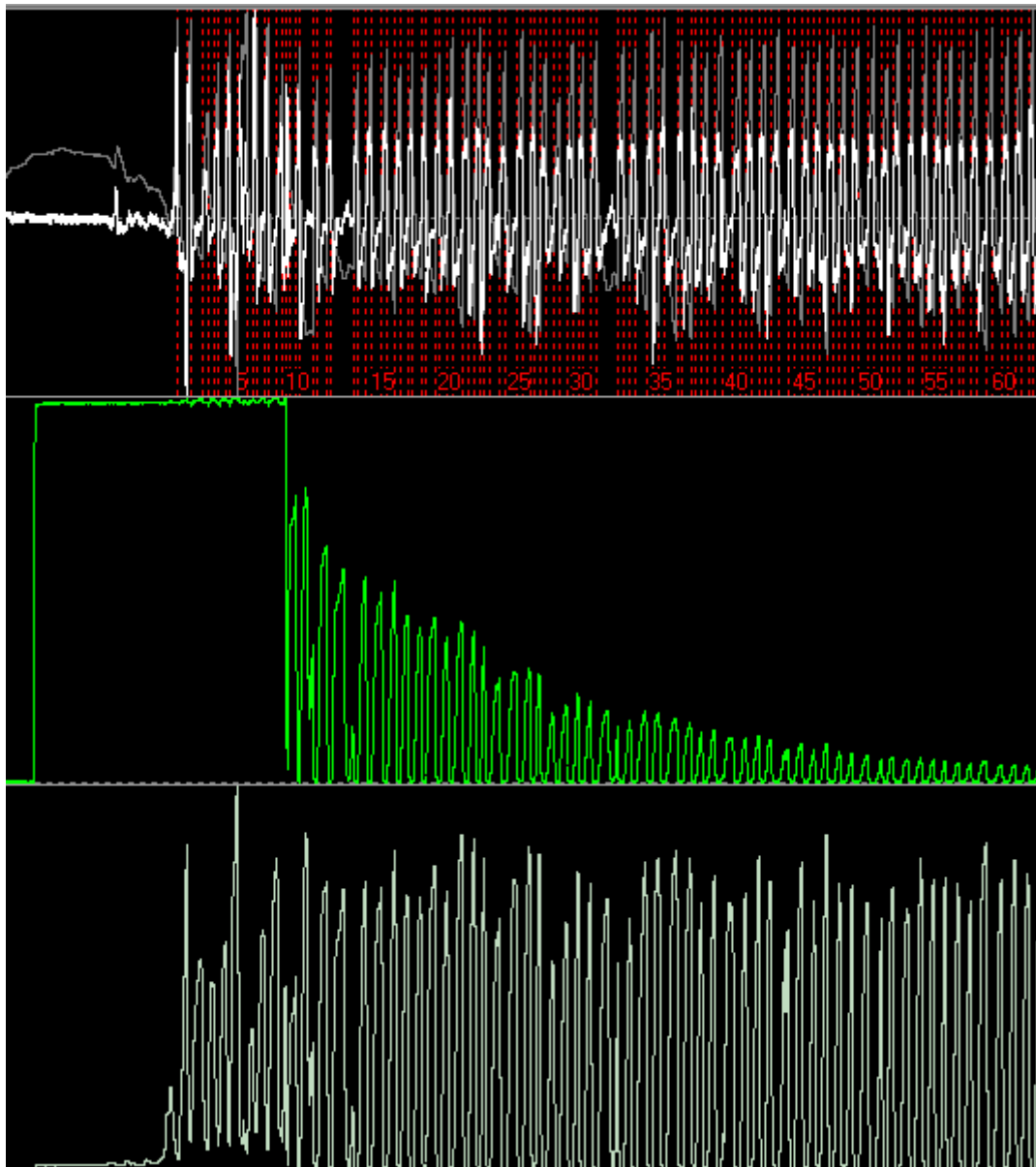
HOW I GET ALONG WITH OTHERS (problems with...)	Never	Almost Never	Some-times	Often	Almost Always
1. I have trouble getting along with other teens	0	1	2	3	4
2. Other teens do not want to be my friend	0	1	2	3	4
3. Other teens tease me	0	1	2	3	4
4. I cannot do things that other teens my age can do	0	1	2	3	4
5. It is hard to keep up with my peers	0	1	2	3	4

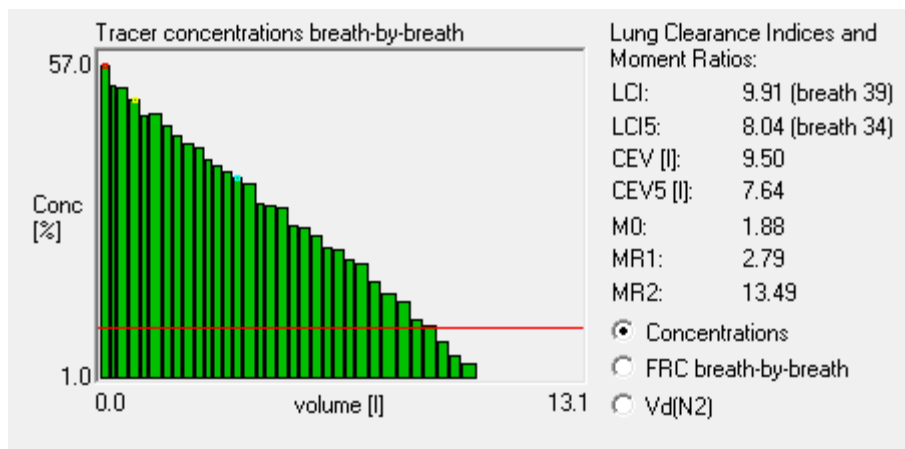
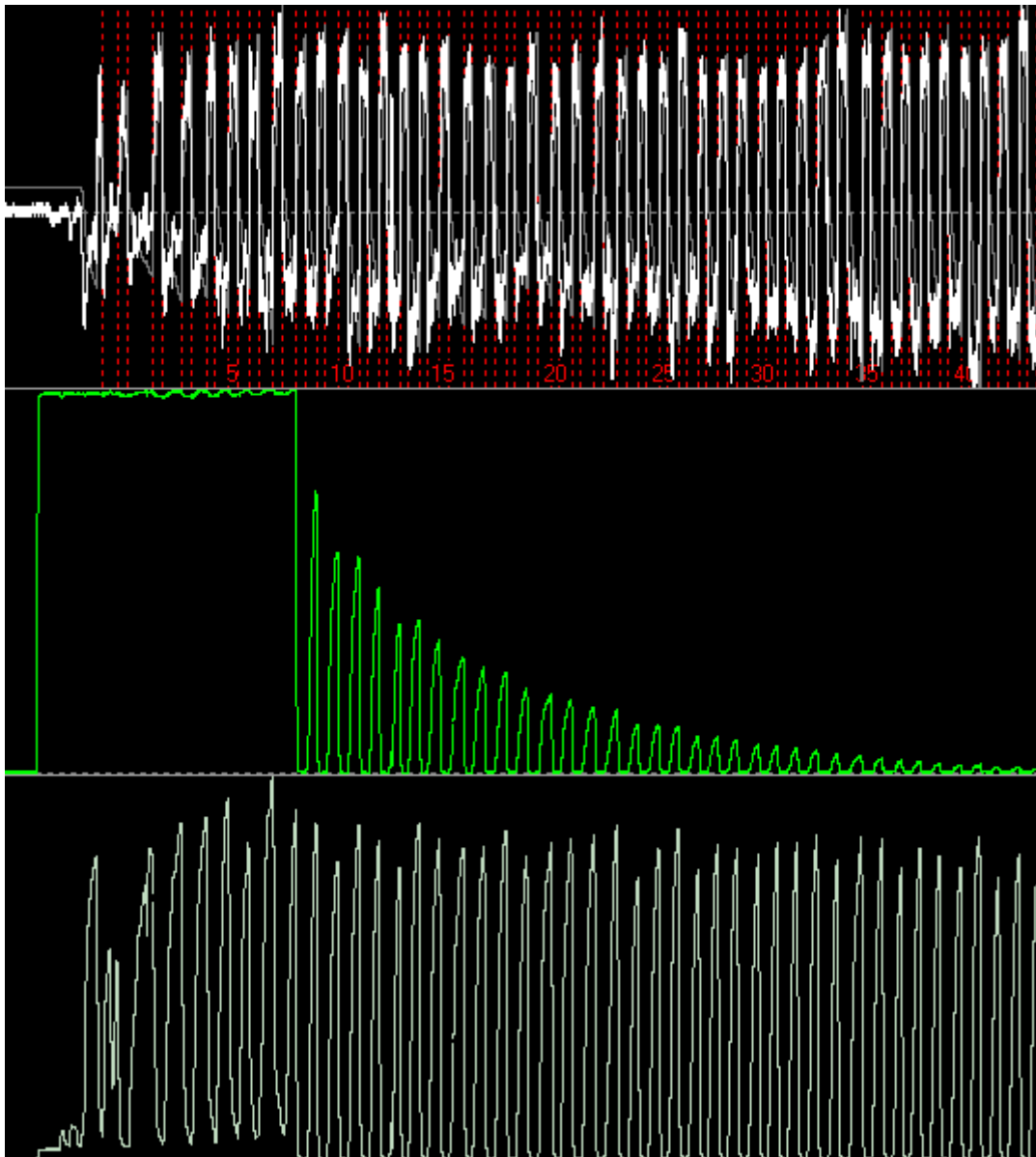
ABOUT SCHOOL (problems with...)	Never	Almost Never	Some-times	Often	Almost Always
1. It is hard to pay attention in class	0	1	2	3	4
2. I forget things	0	1	2	3	4
3. I have trouble keeping up with my schoolwork	0	1	2	3	4
4. I miss school because of not feeling well	0	1	2	3	4
5. I miss school to go to the doctor or hospital	0	1	2	3	4

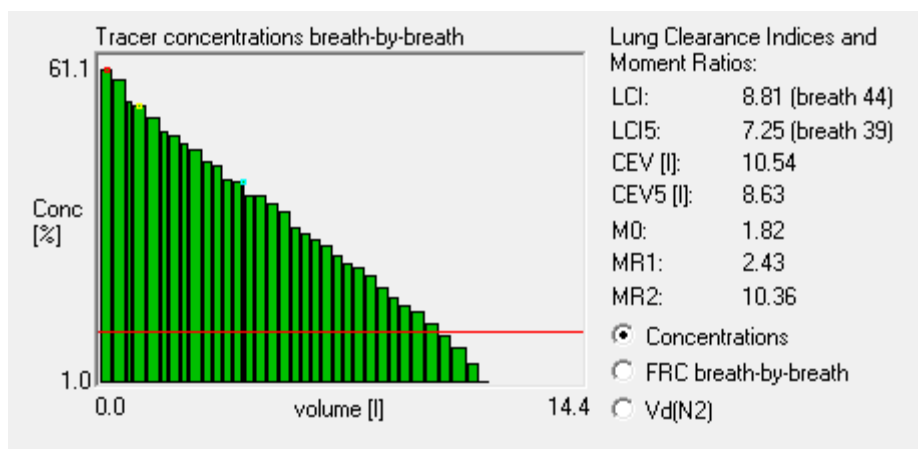
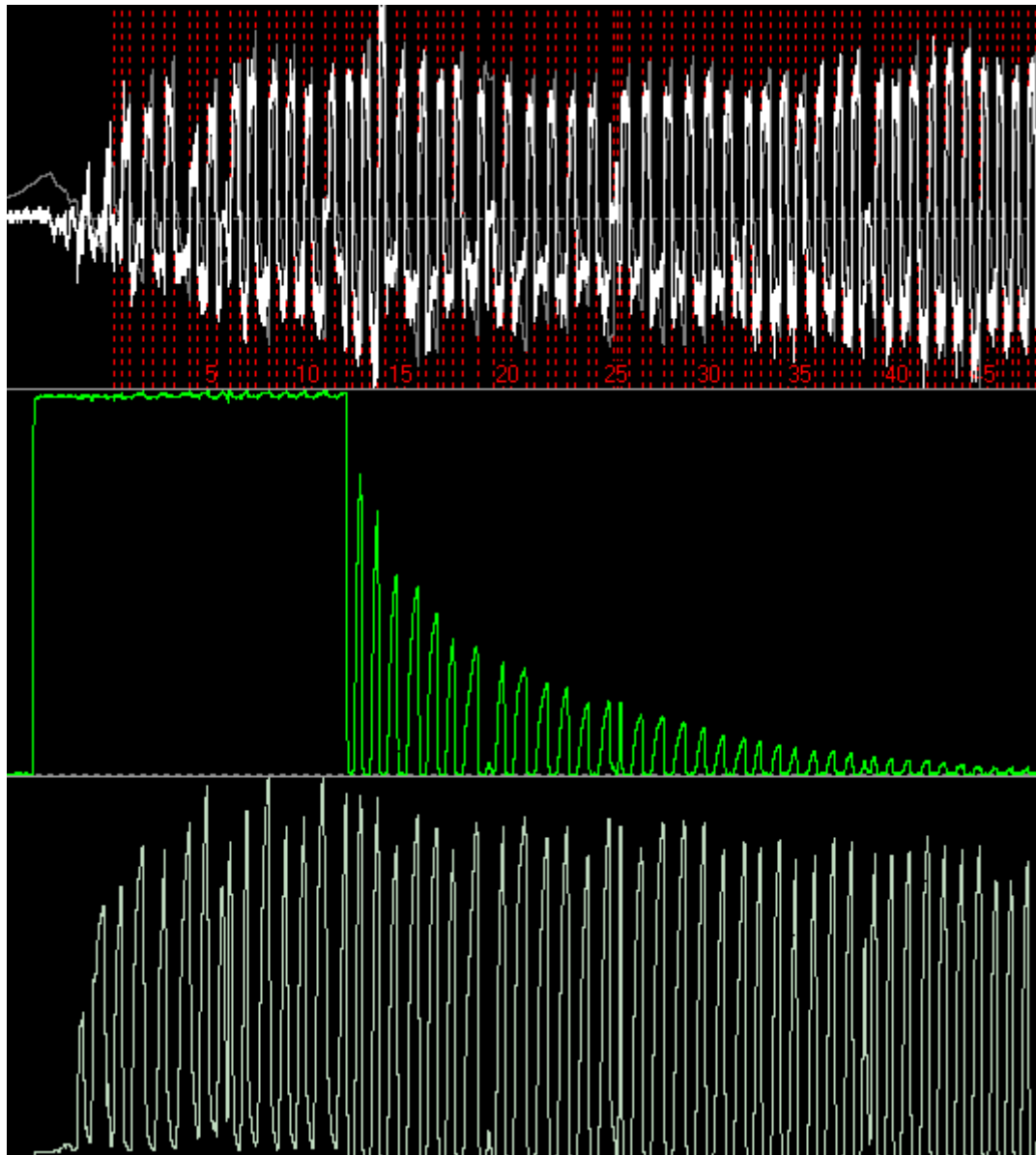
LCI Results of AT Group

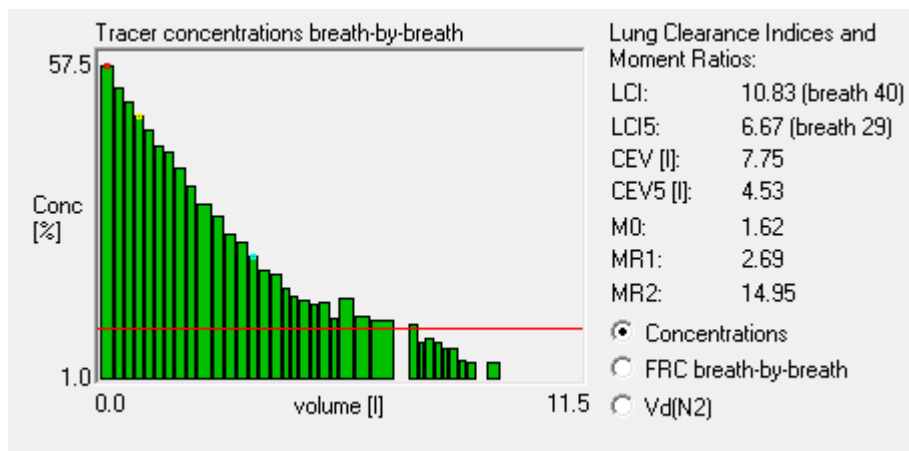
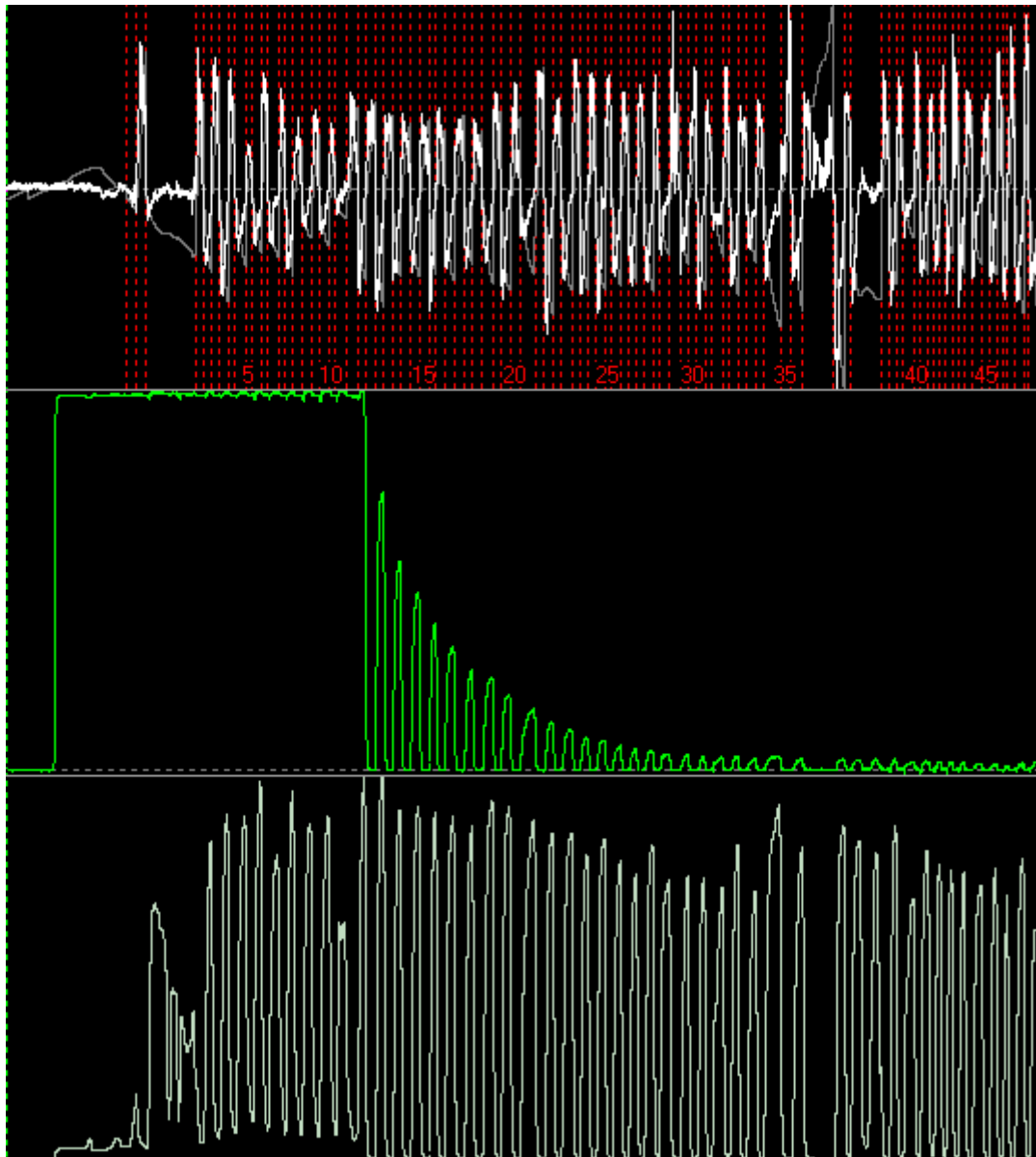
101 (2) 15:12:21

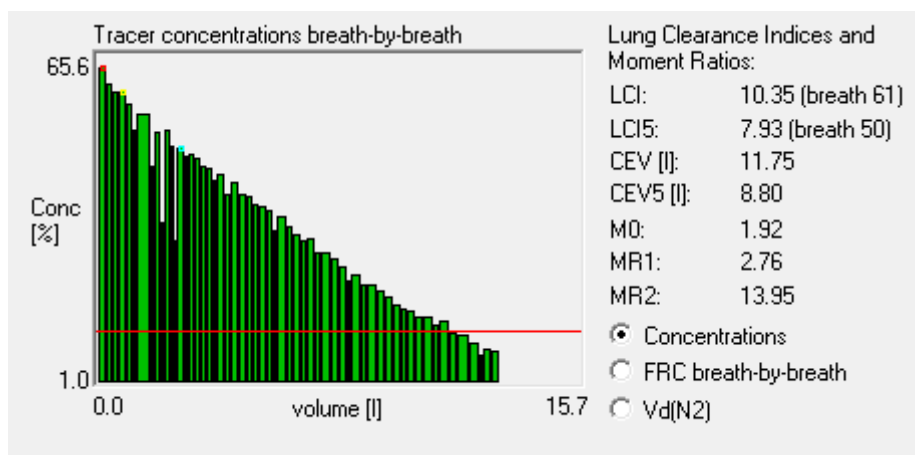
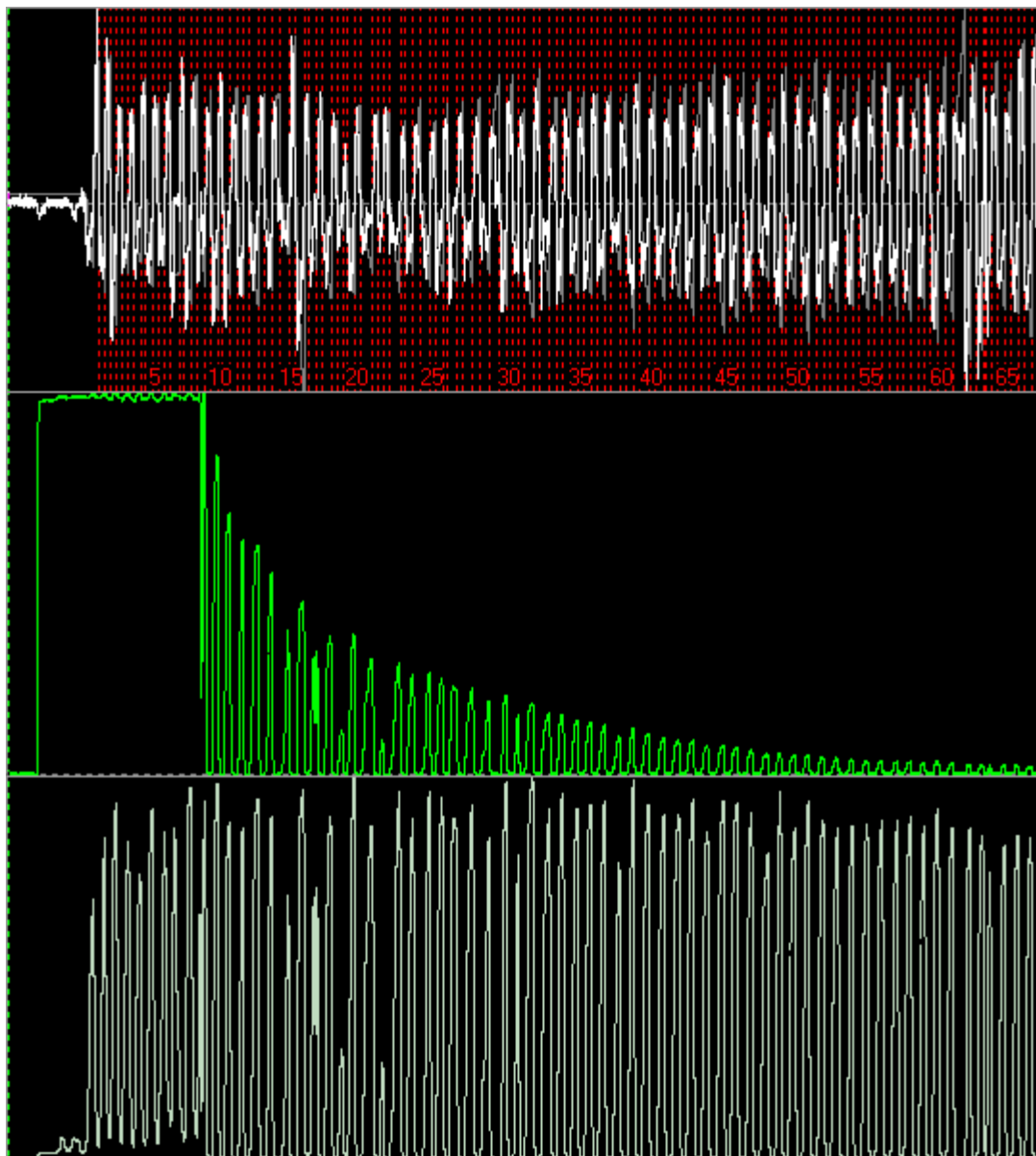


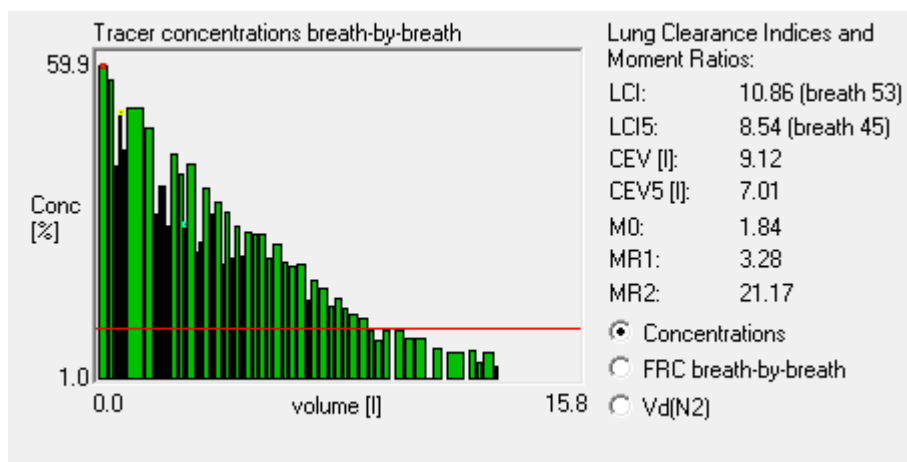
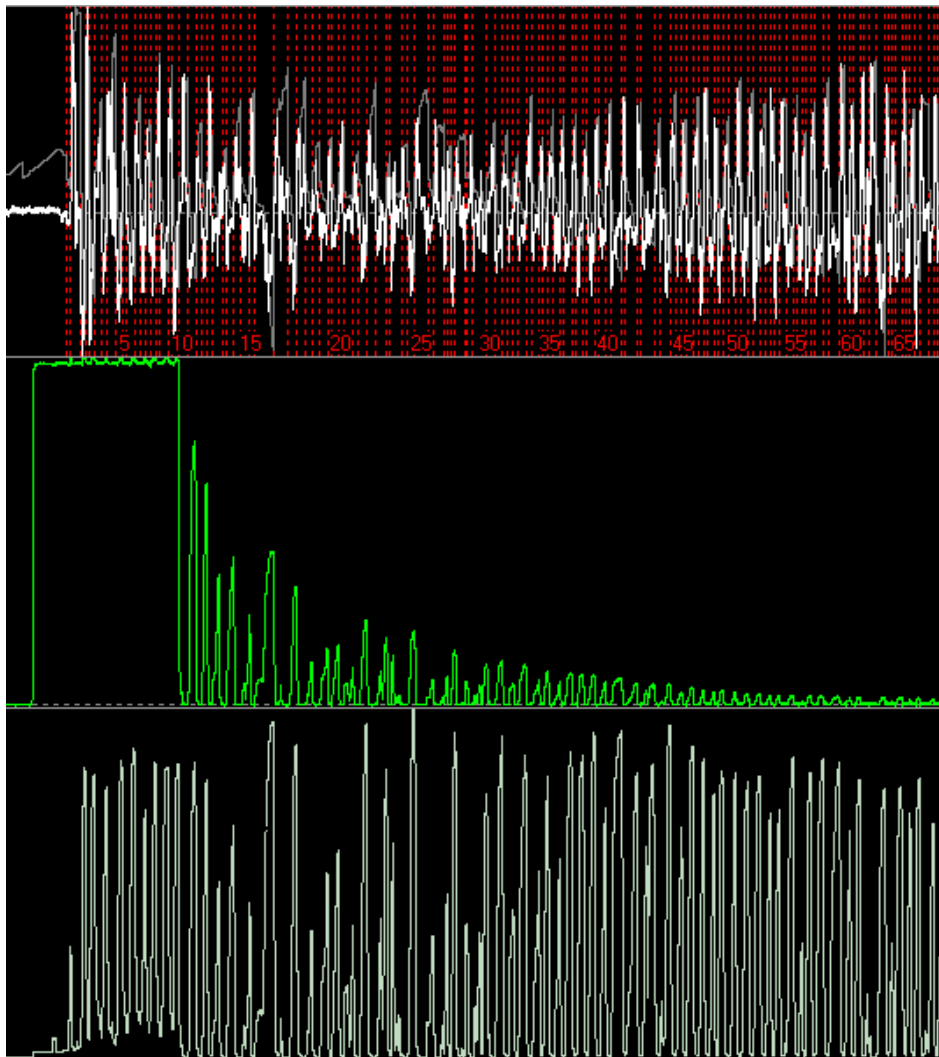


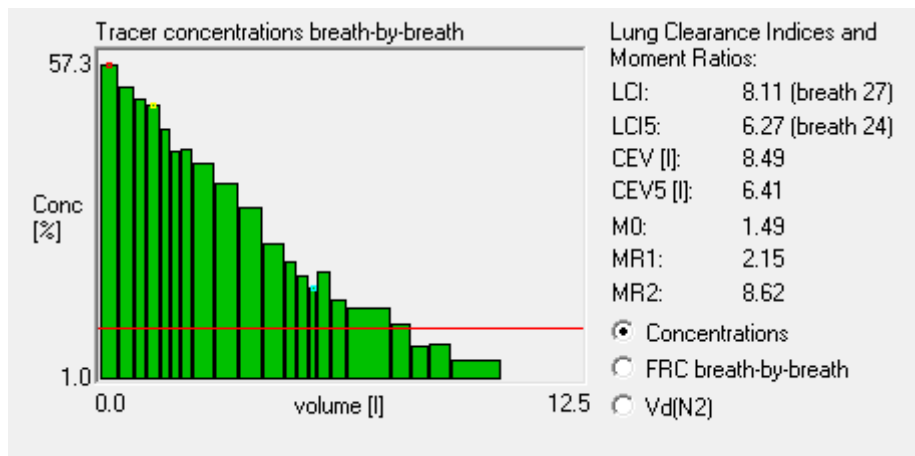
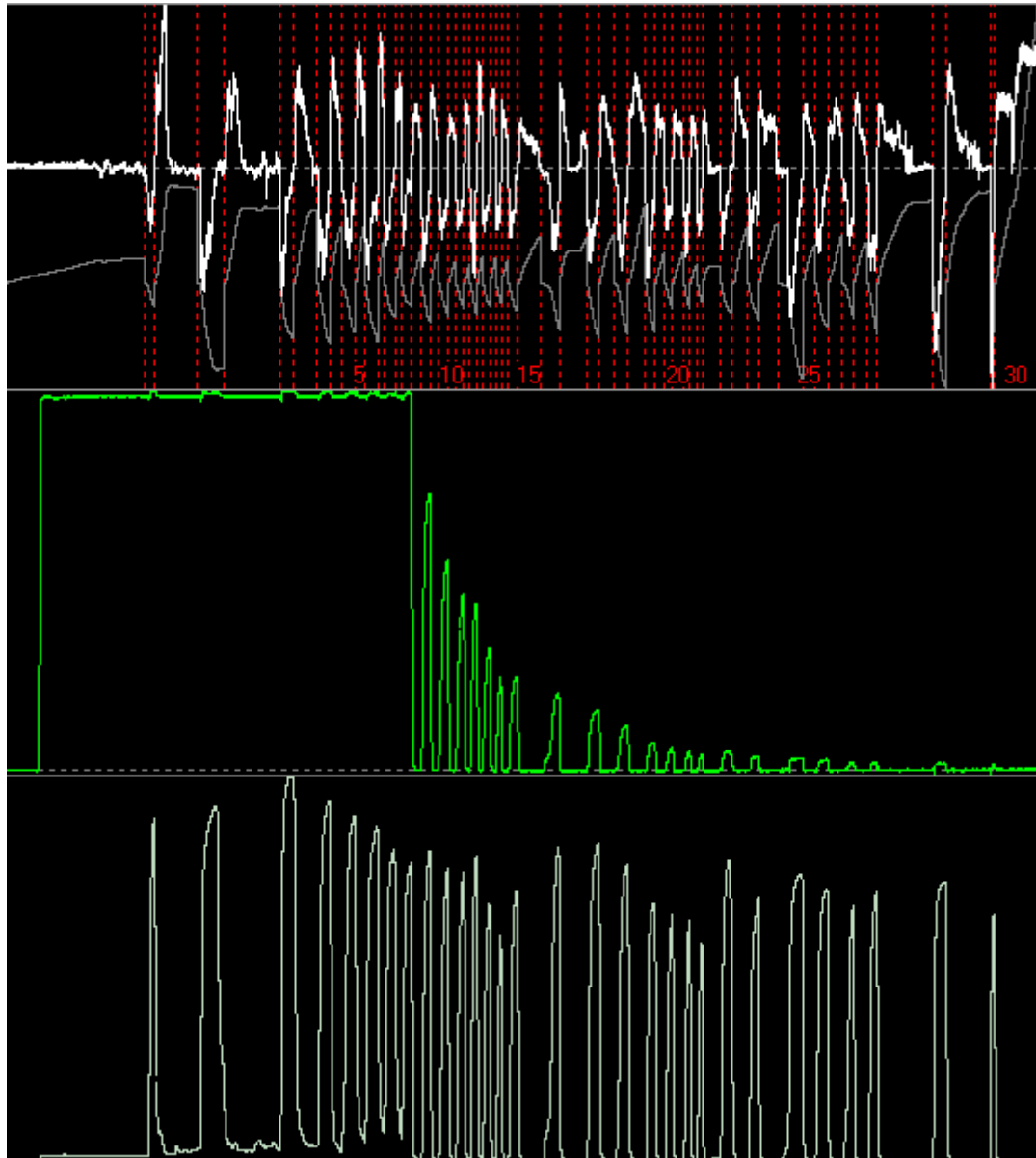


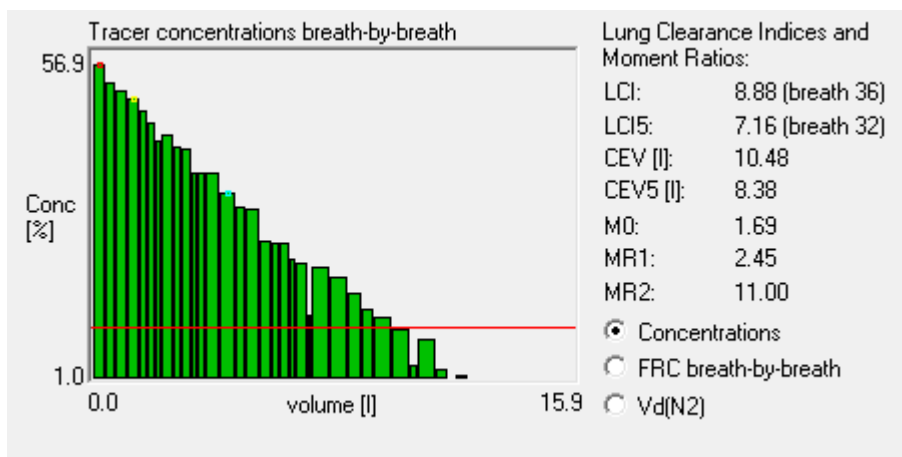
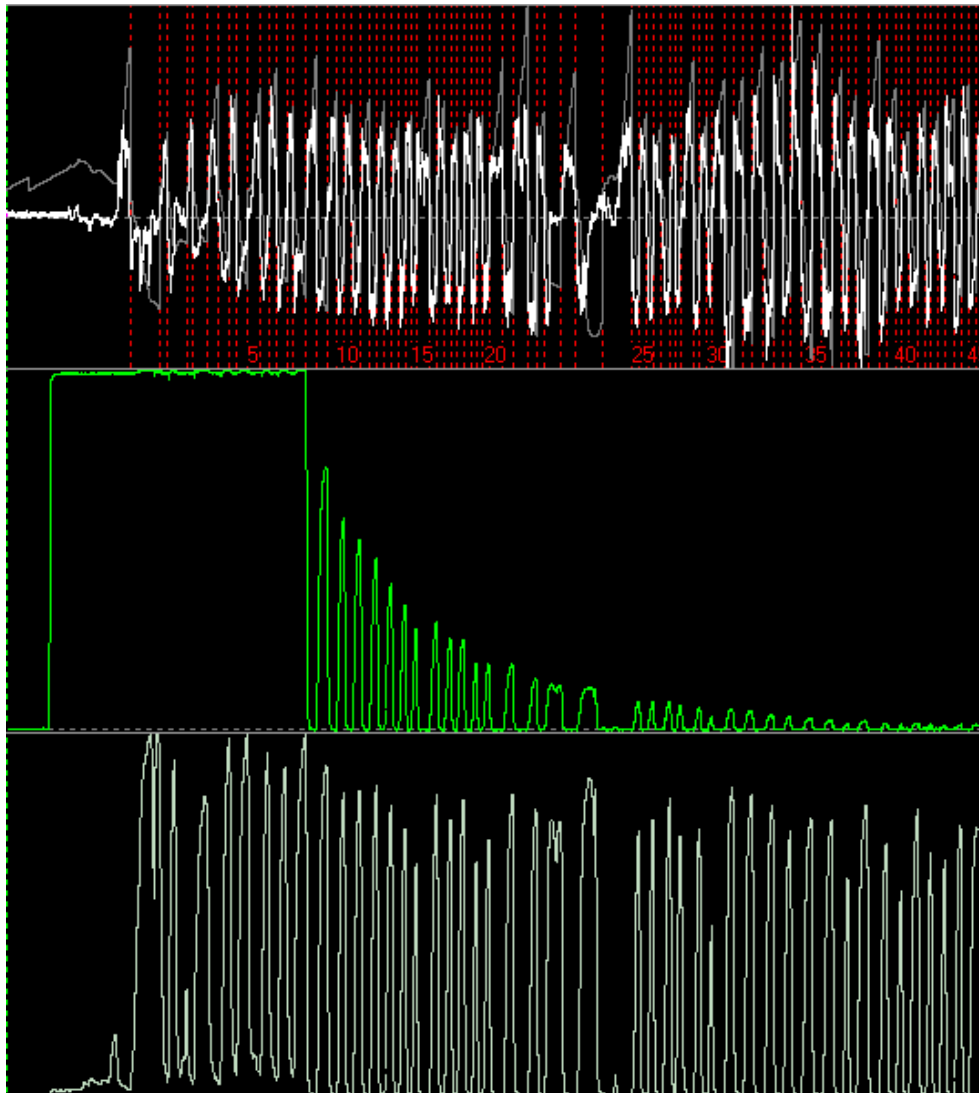


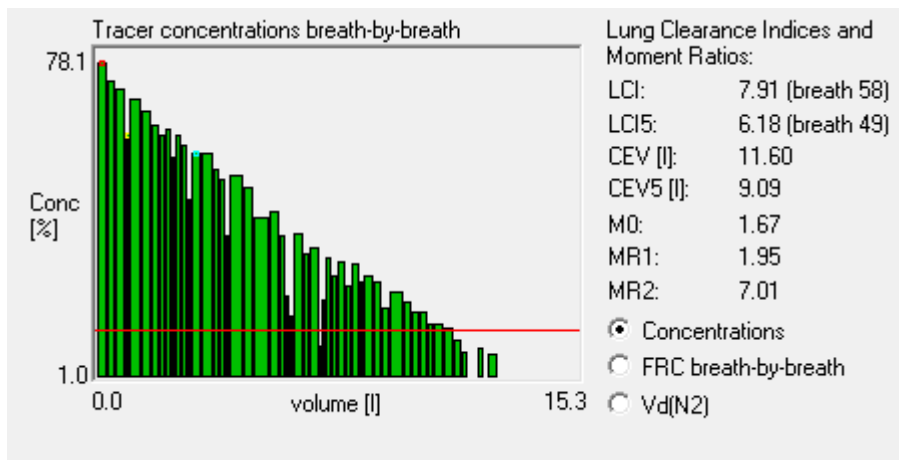
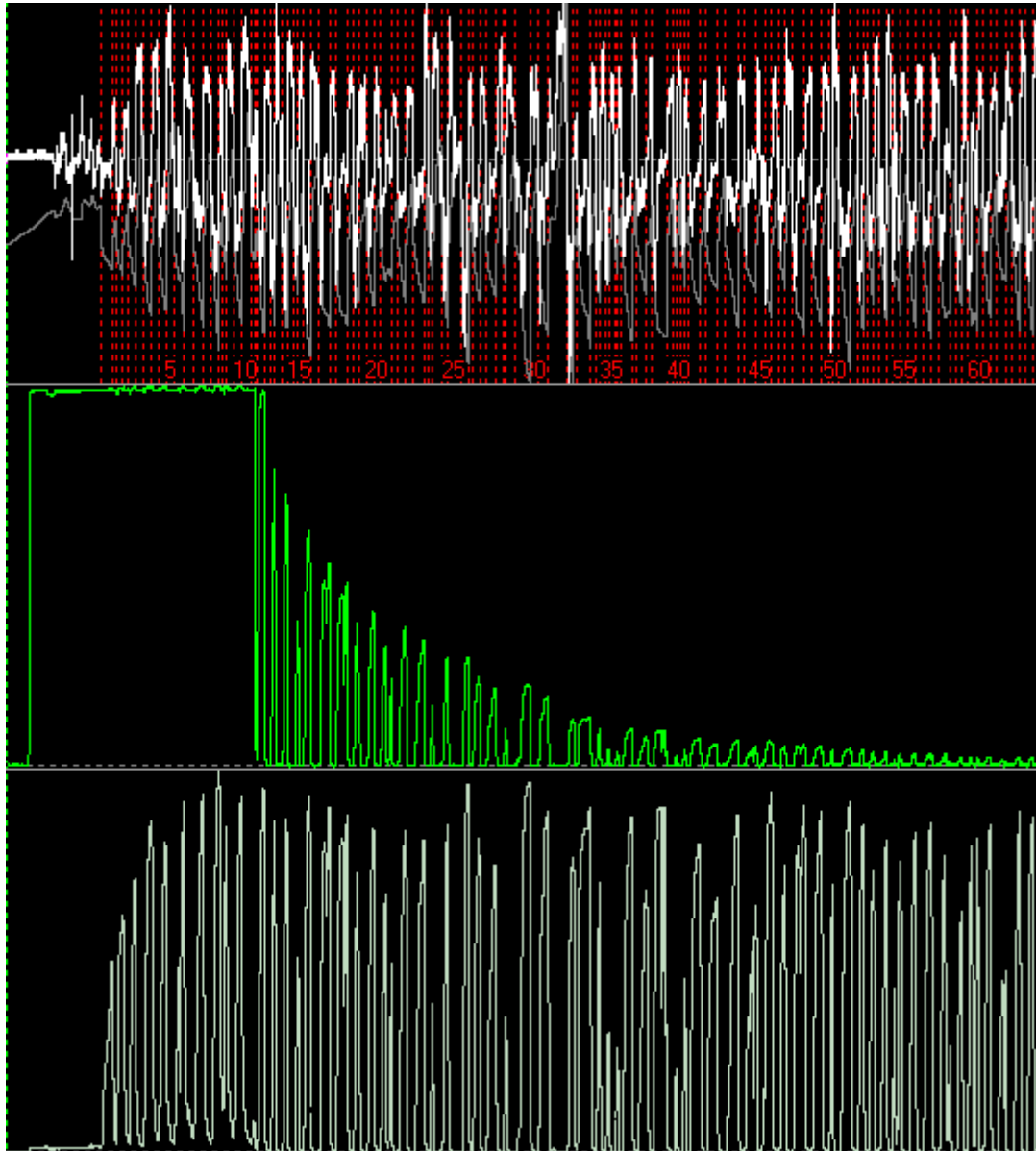


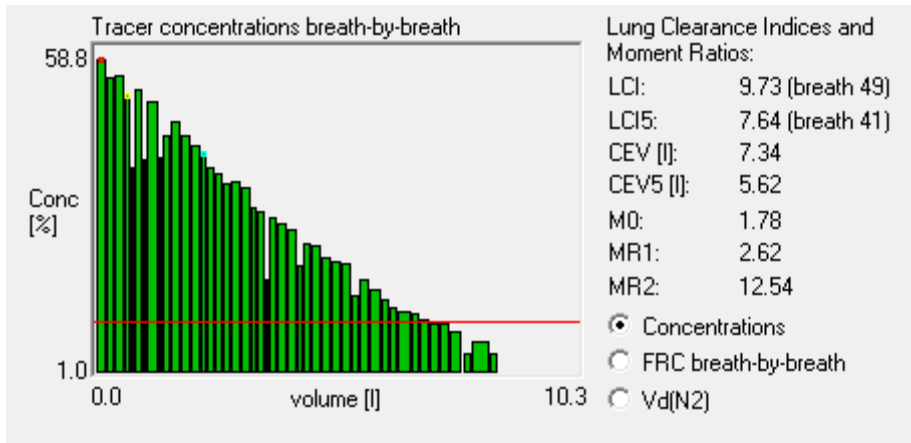
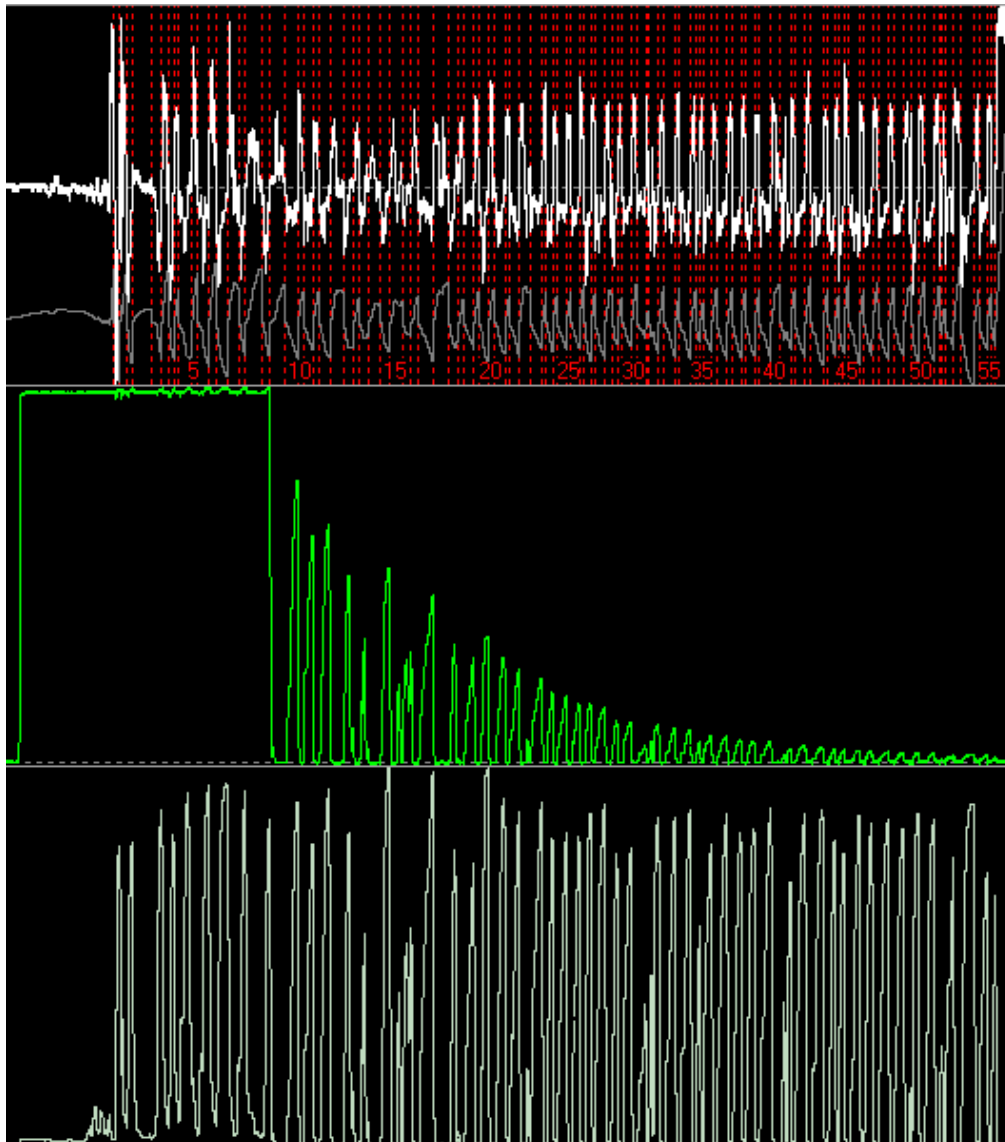


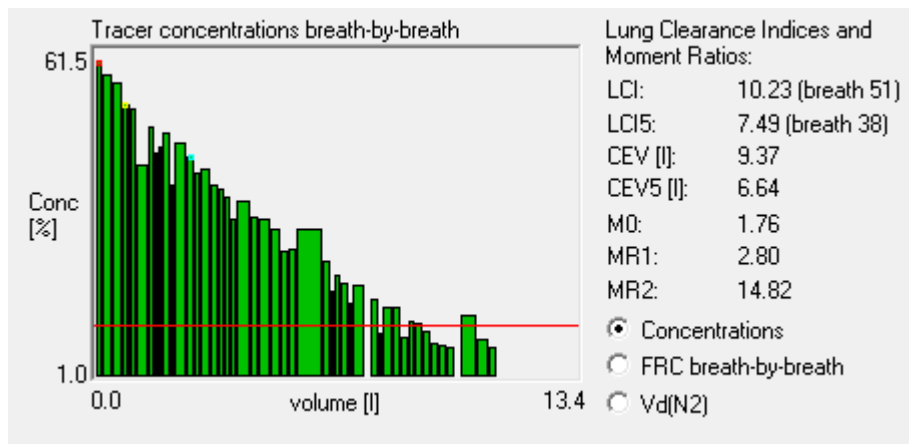
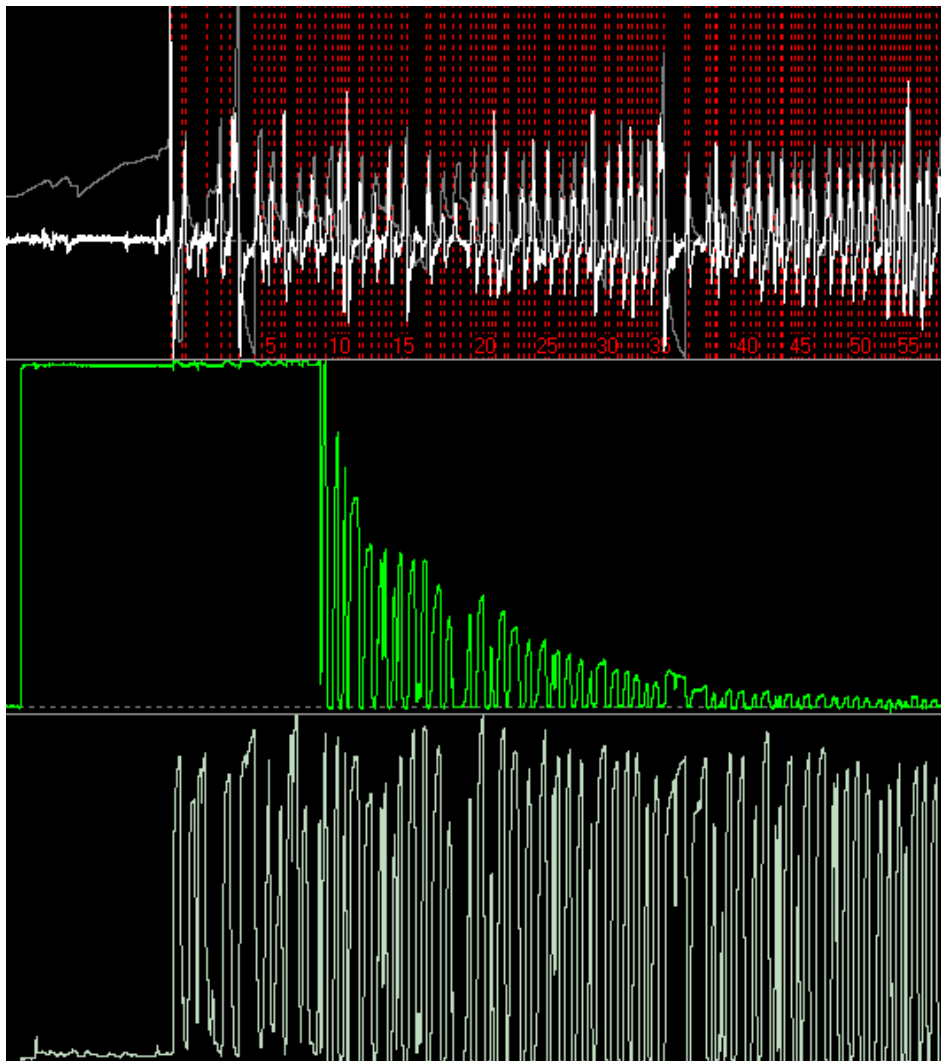


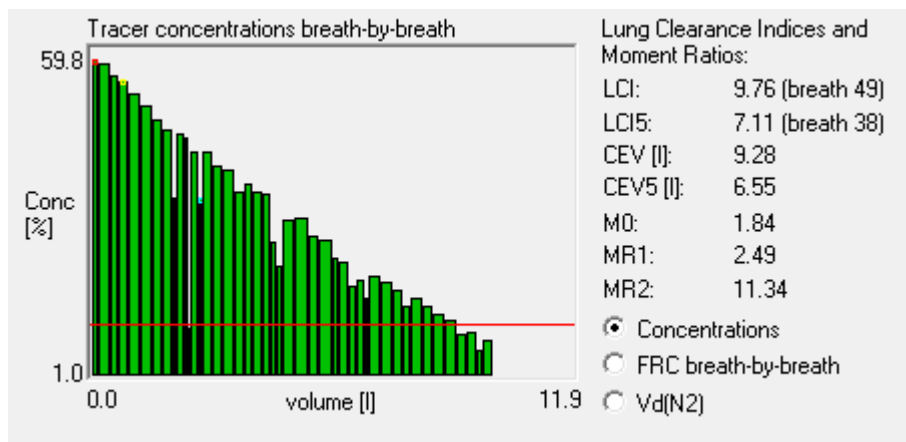
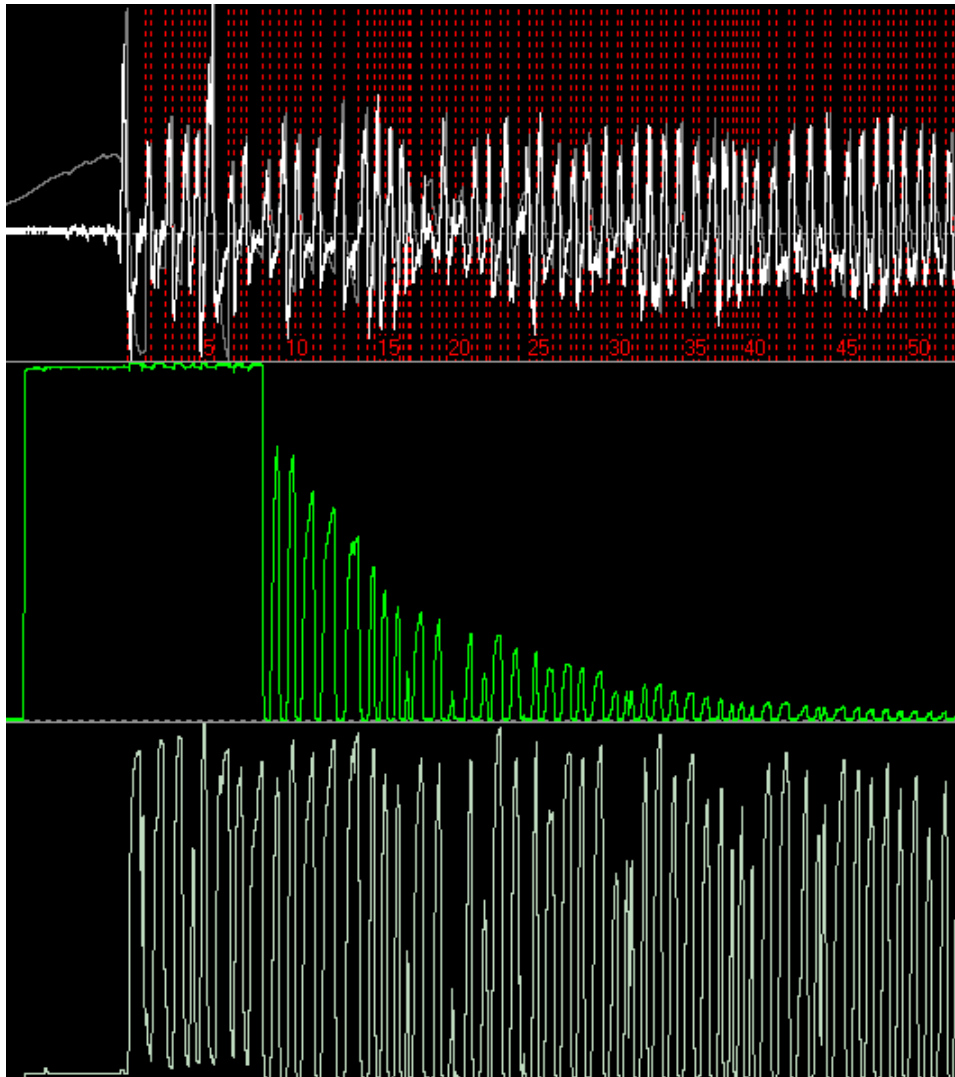






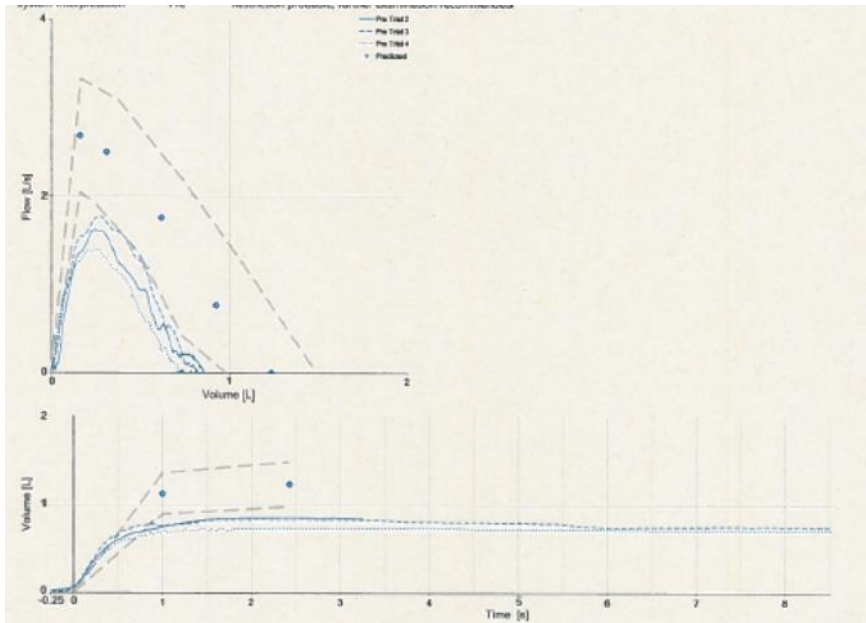




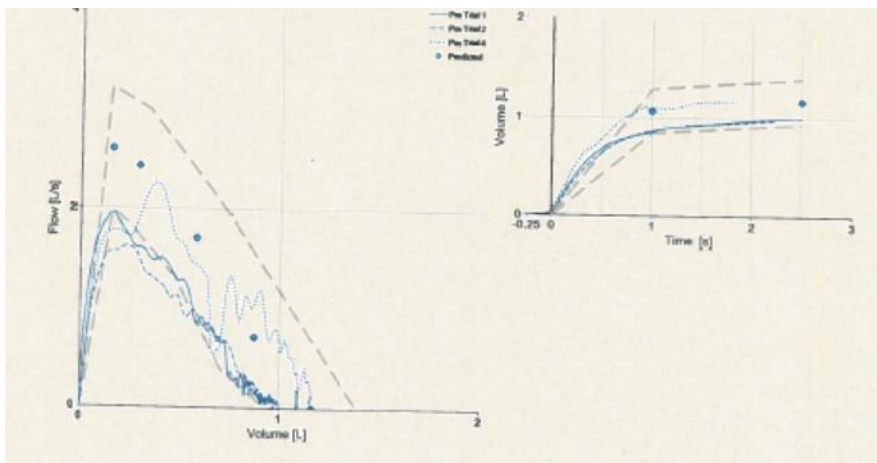


Spirometry Results of AT Group

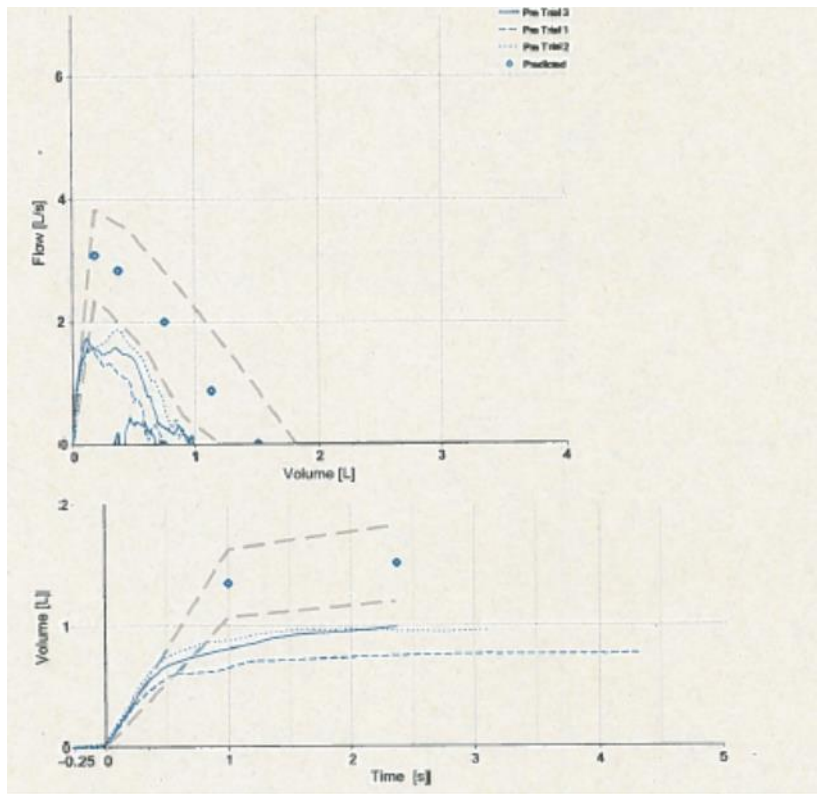
AT-1



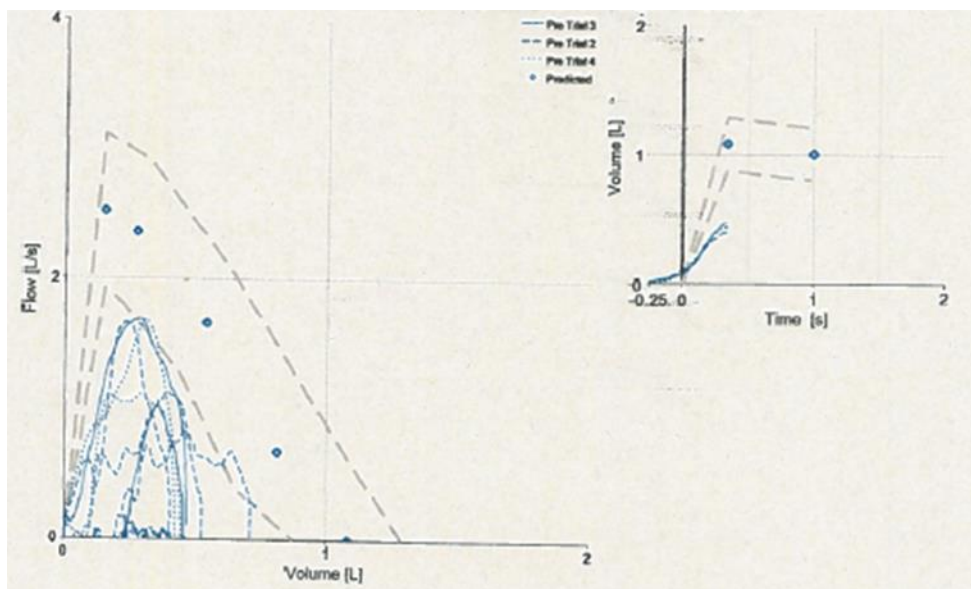
AT-2



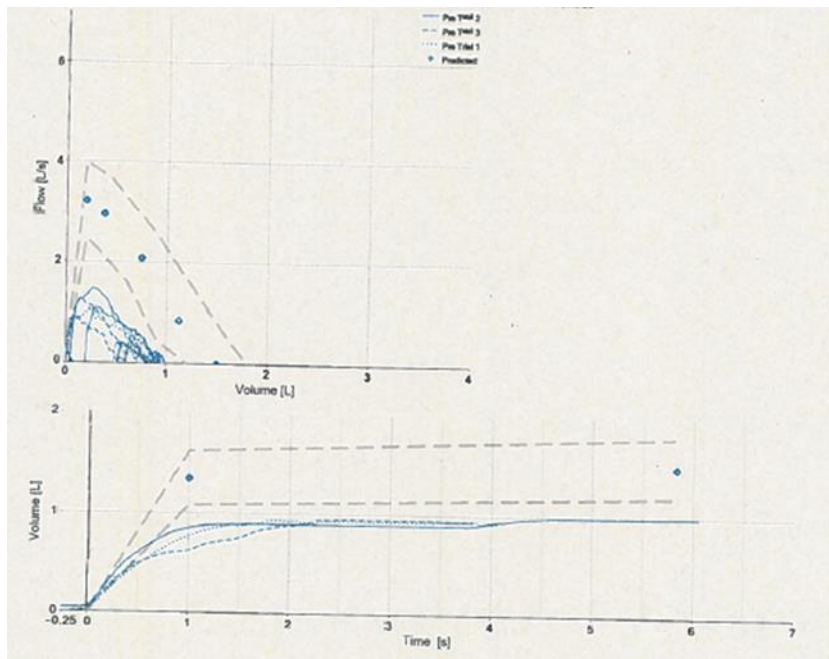
AT-3



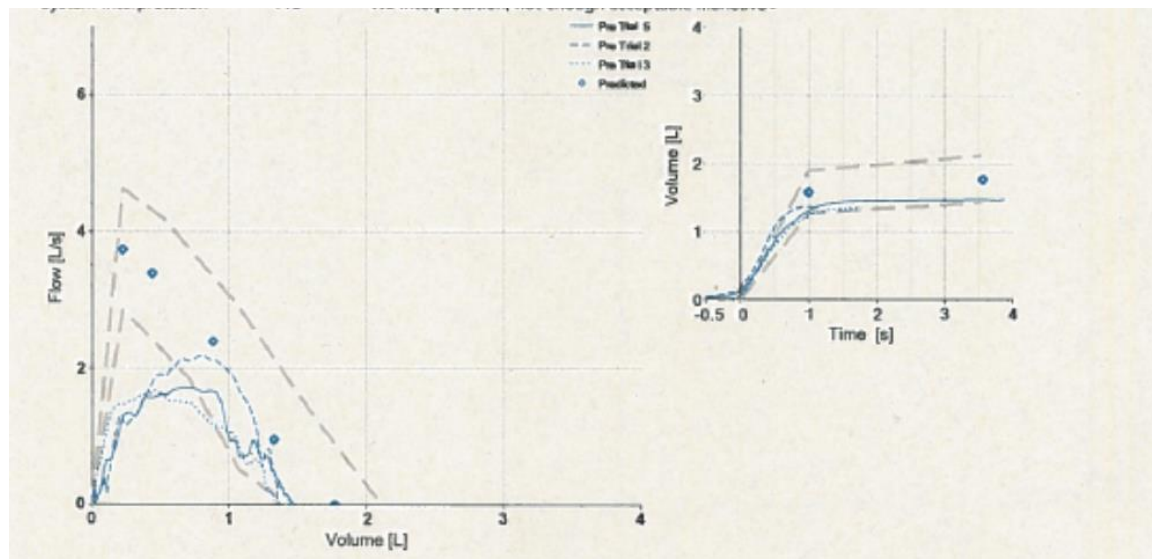
AT-4



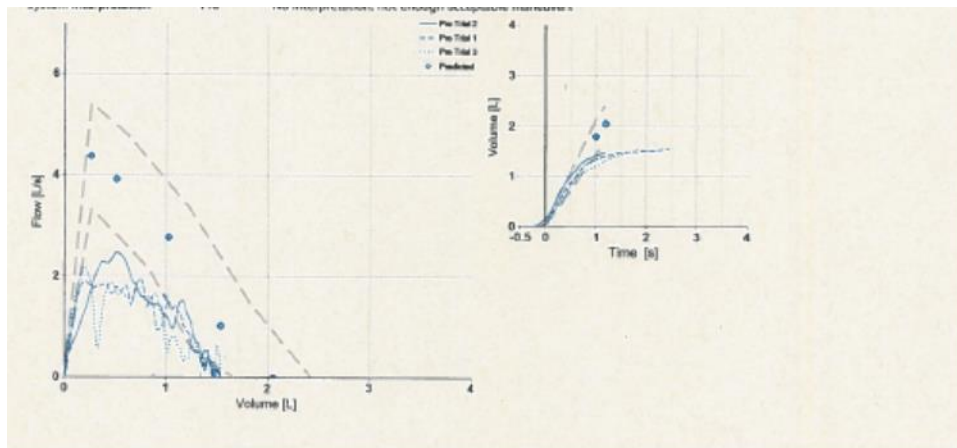
AT-5



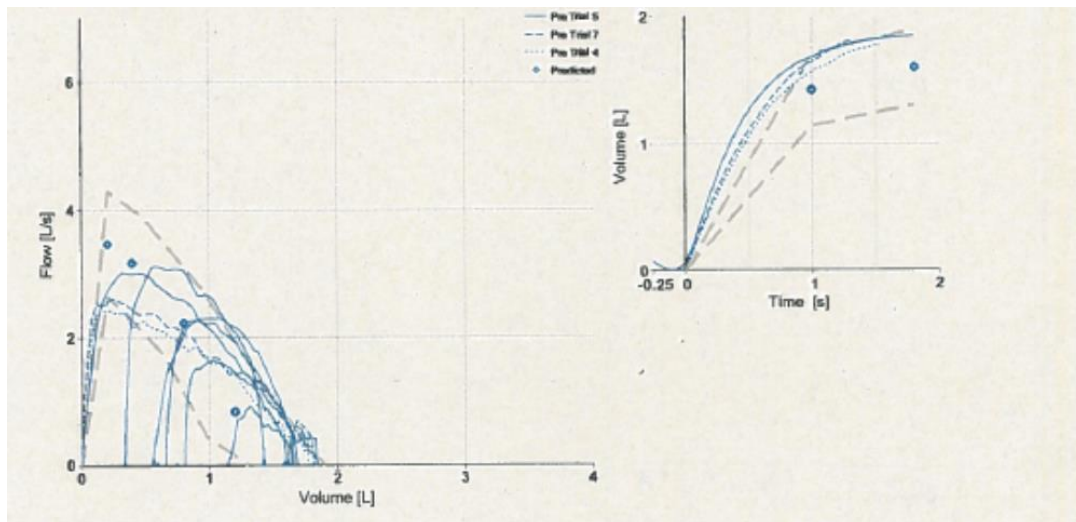
AT-6



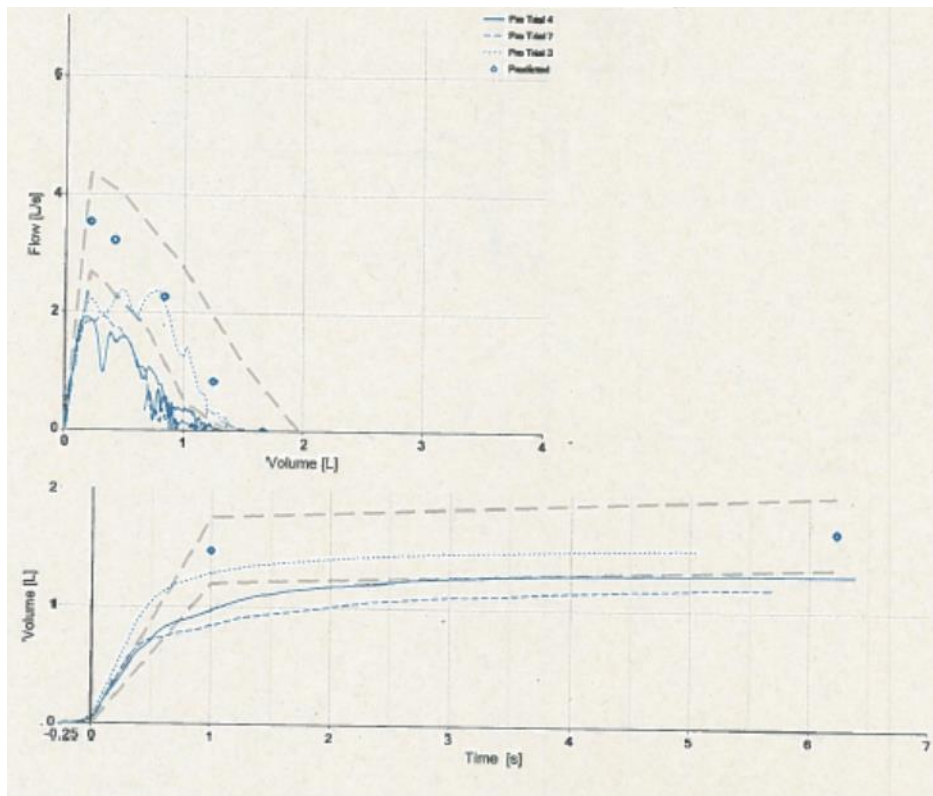
AT-7



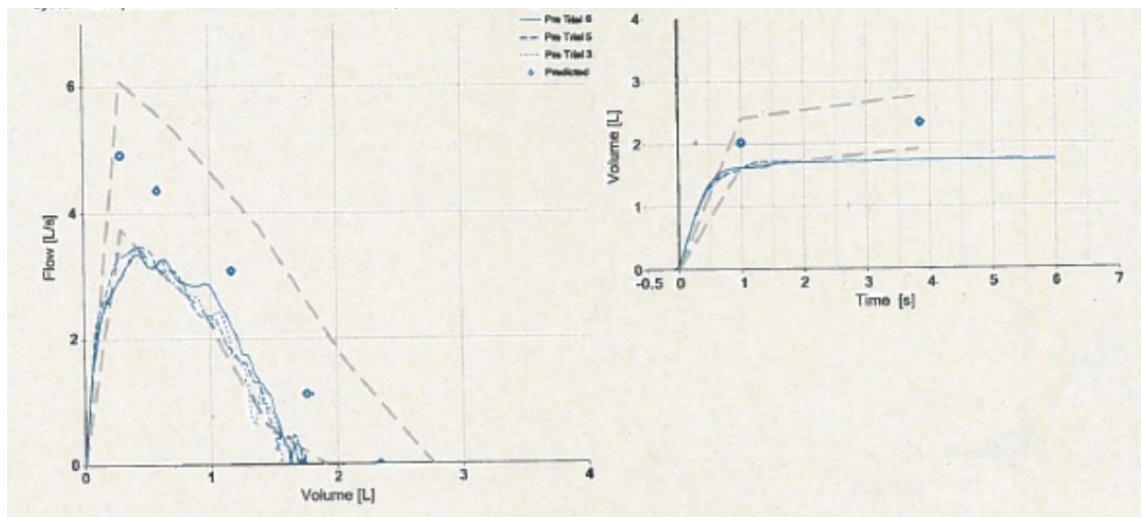
AT-8



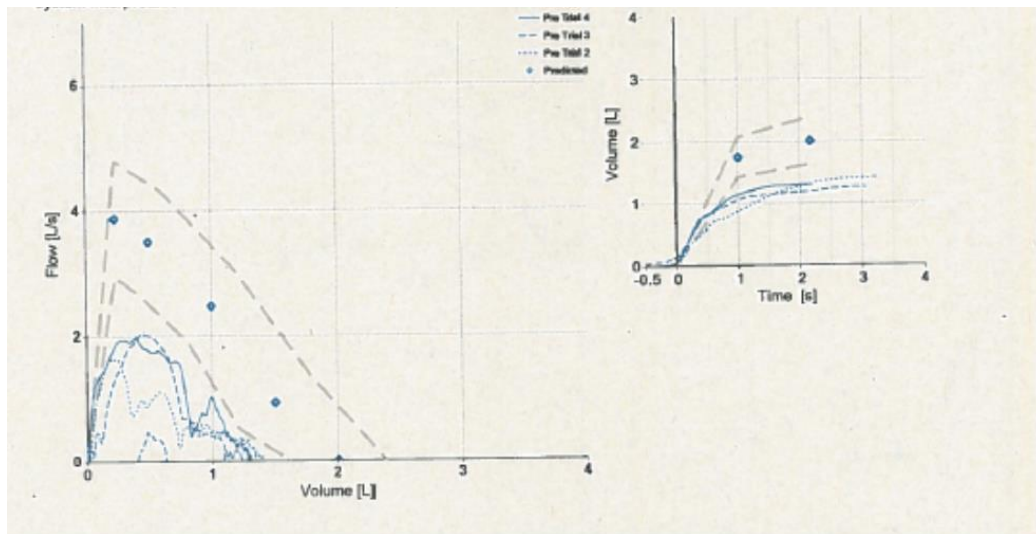
AT-9



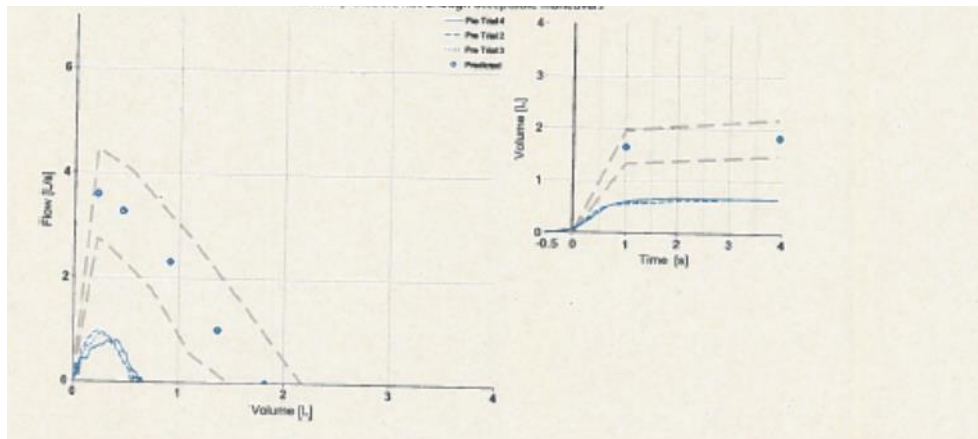
AT-10



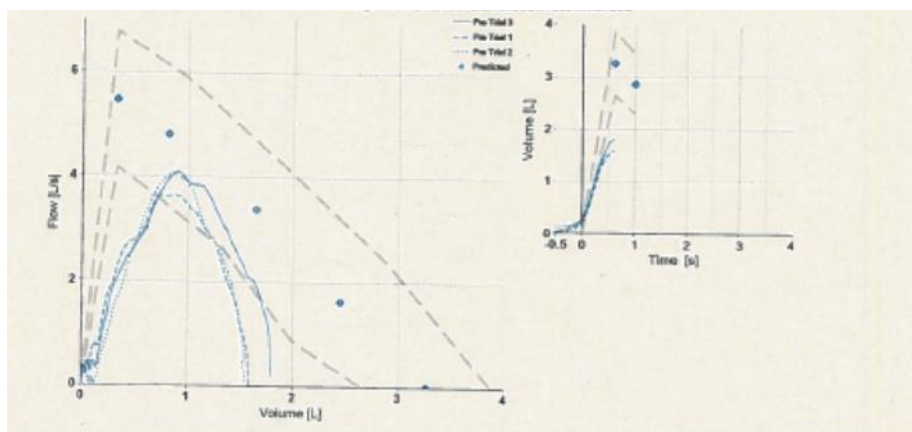
AT-11



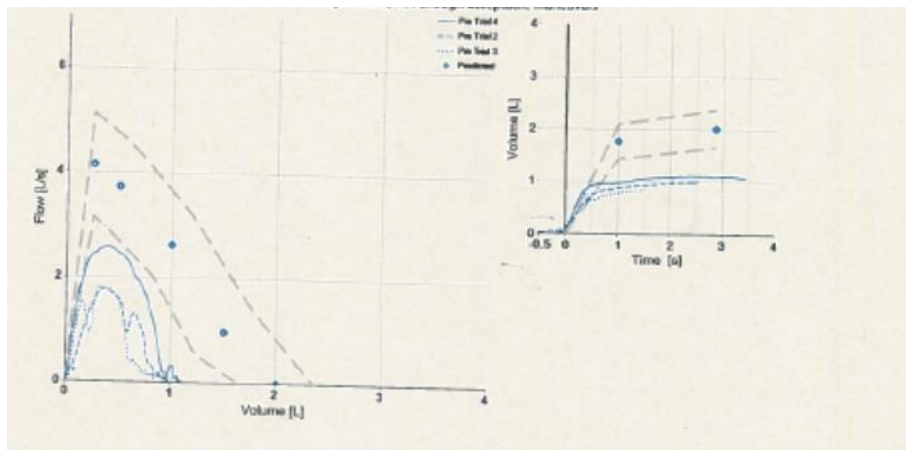
AT-12



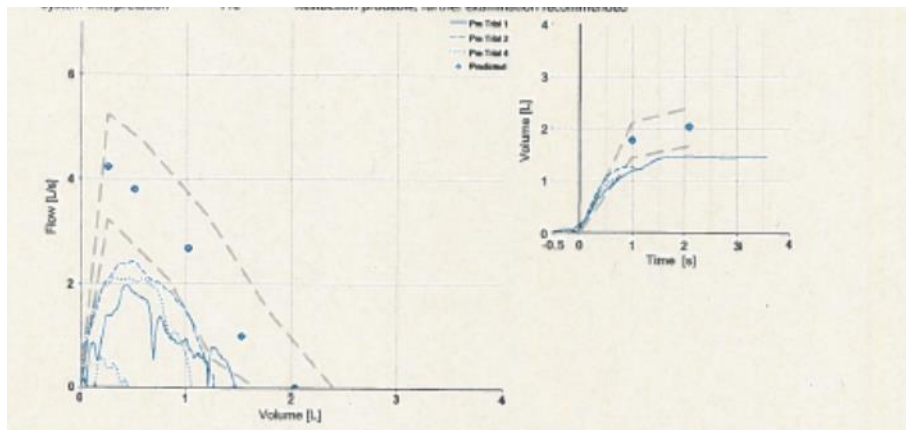
AT-13



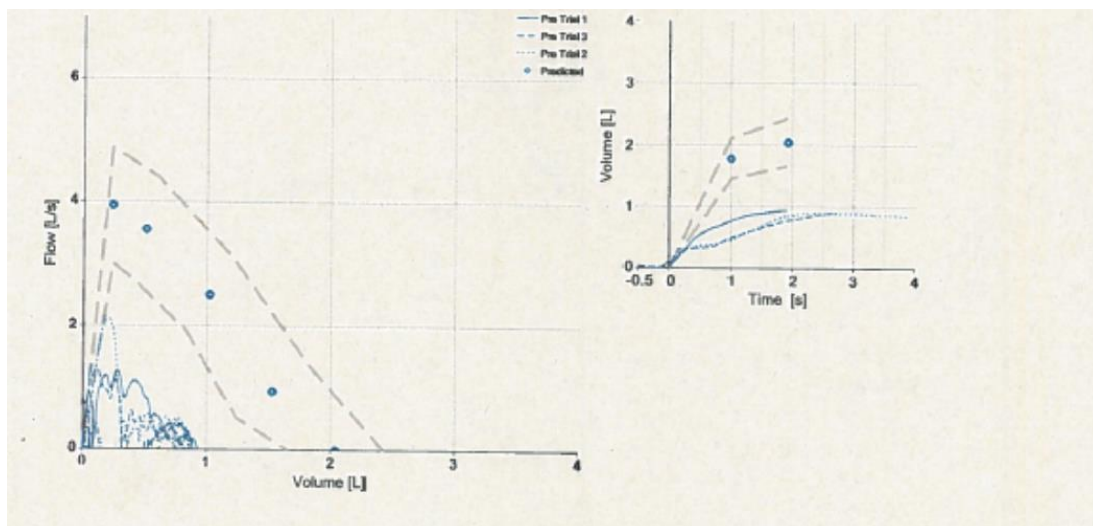
AT-14



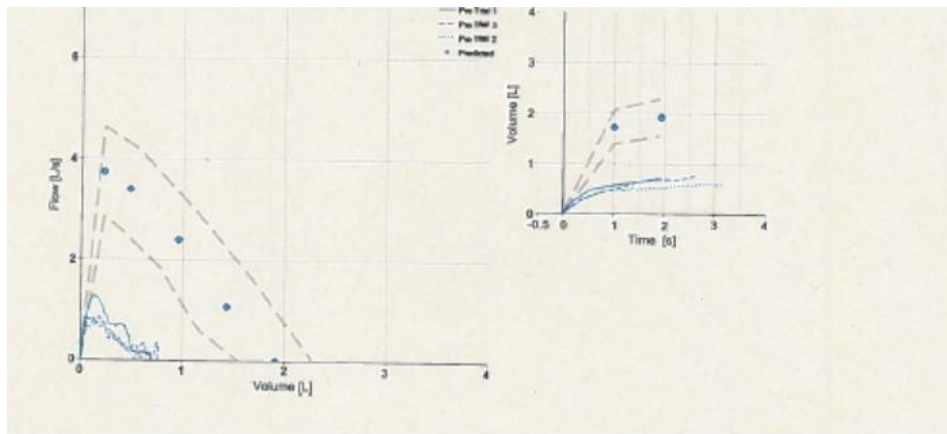
AT-15



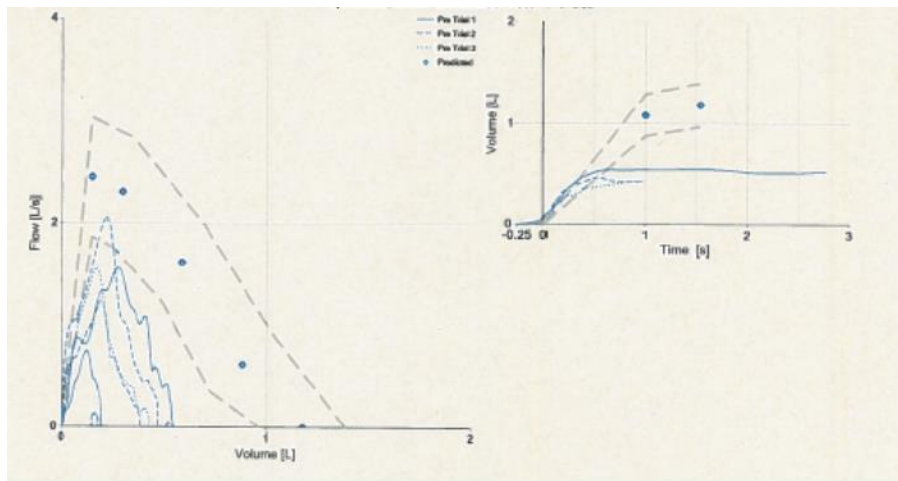
AT-16



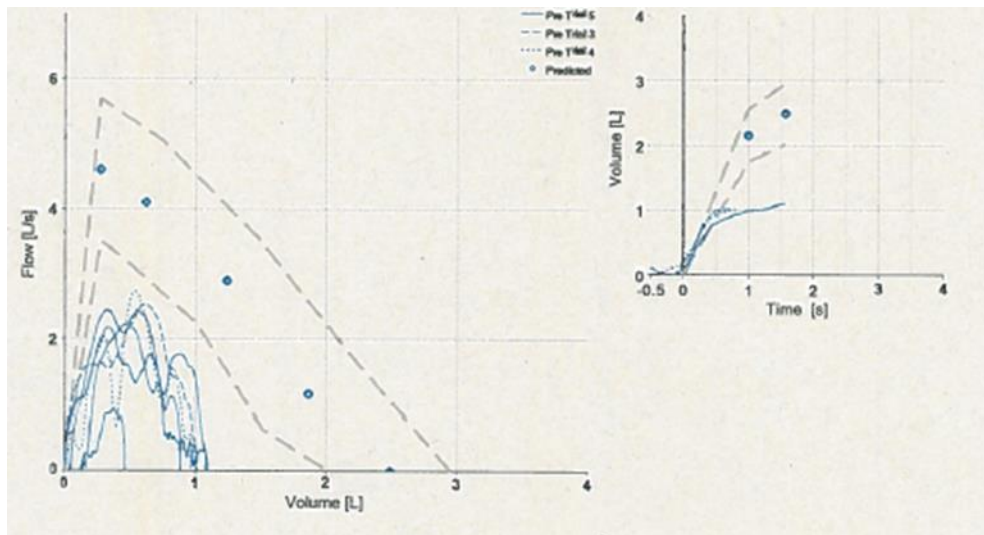
AT-17



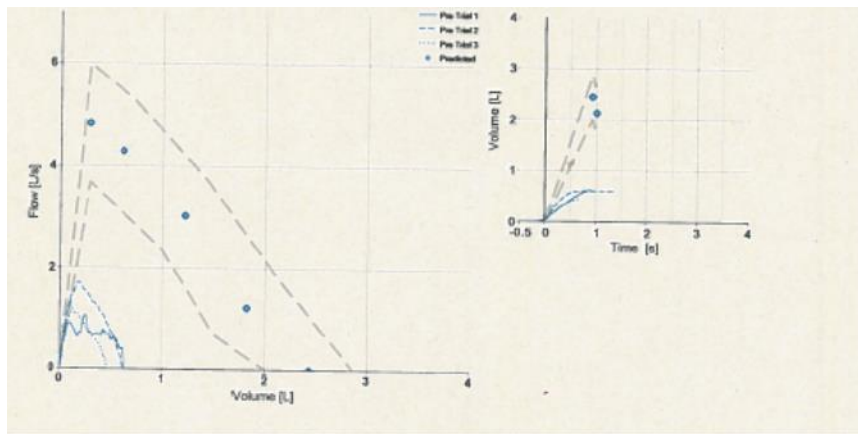
AT-18



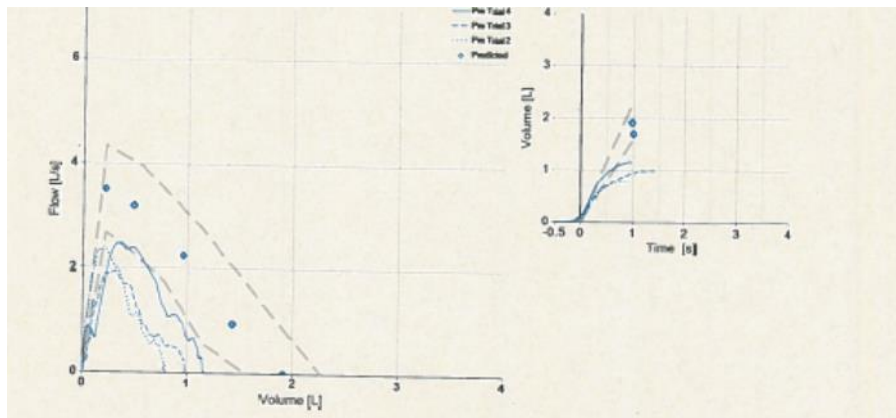
AT-19



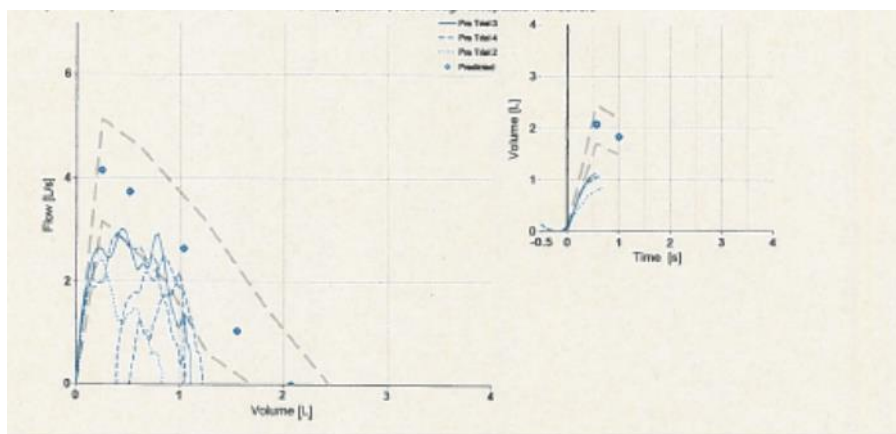
AT-20



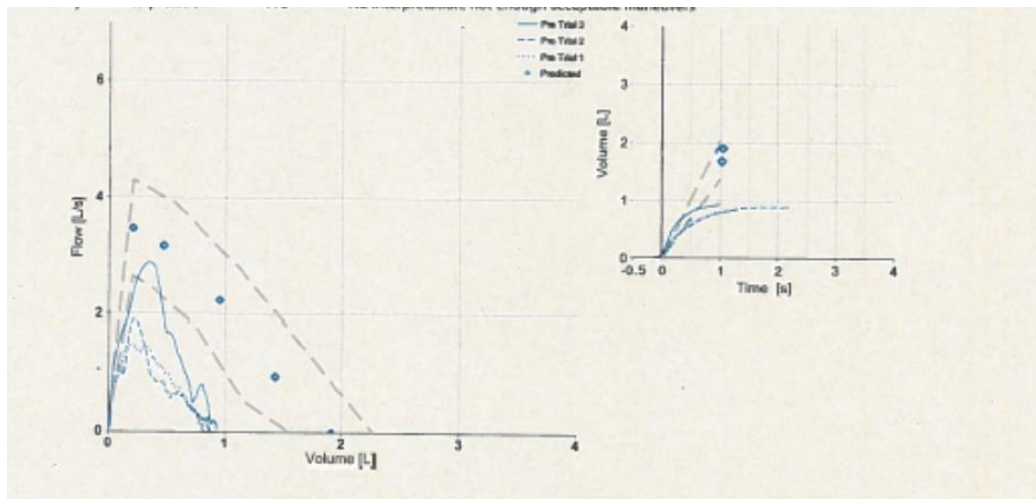
AT-21



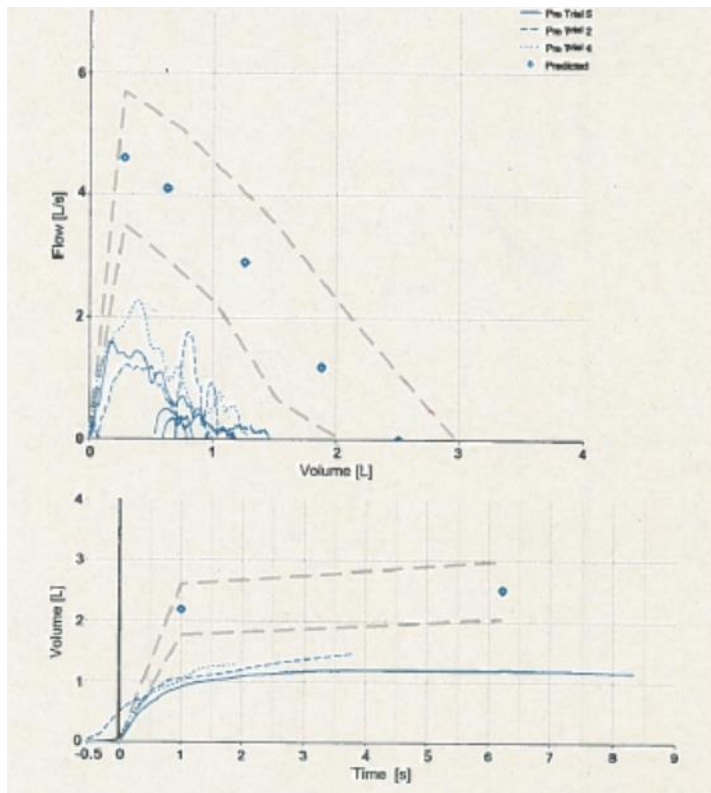
AT-22



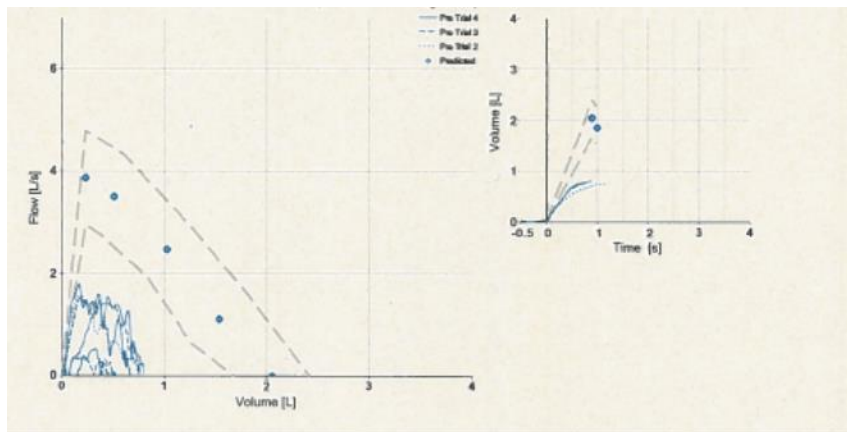
AT-23



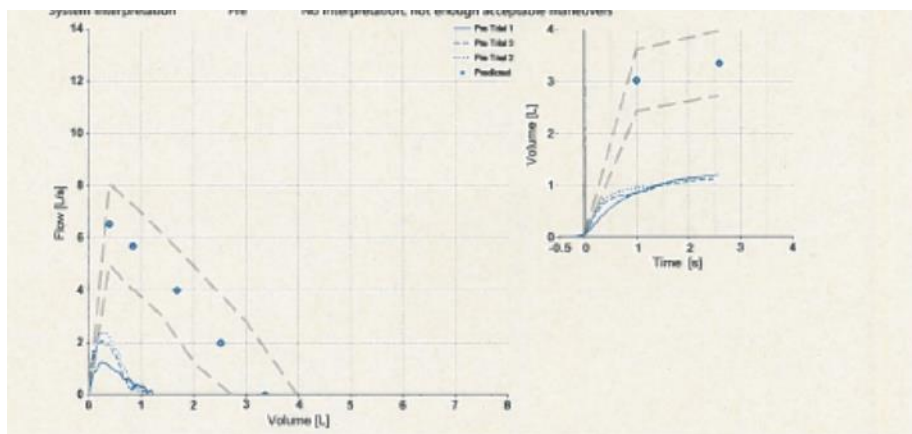
AT-24



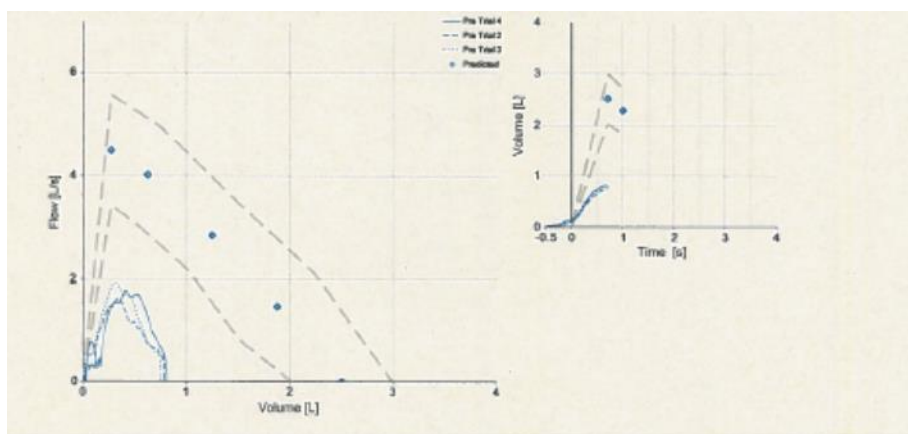
AT-25



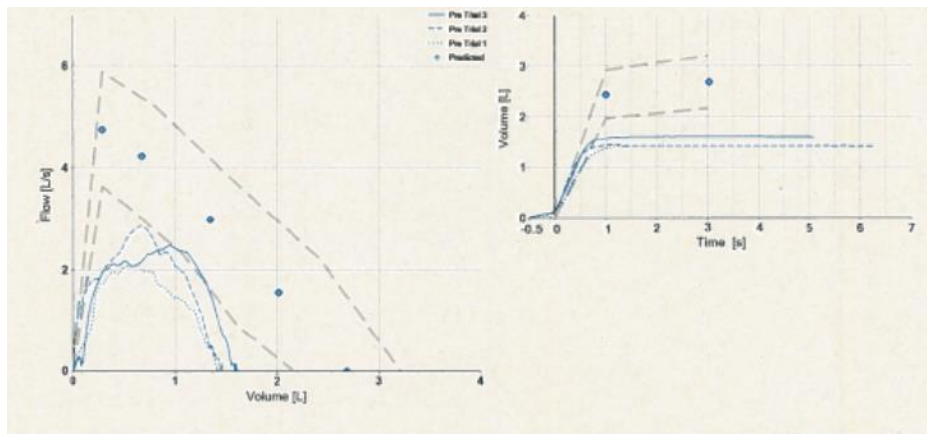
AT-26



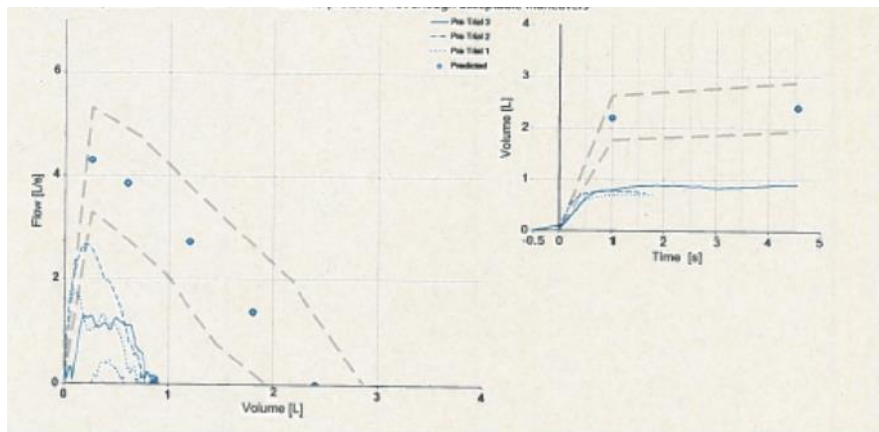
AT-27



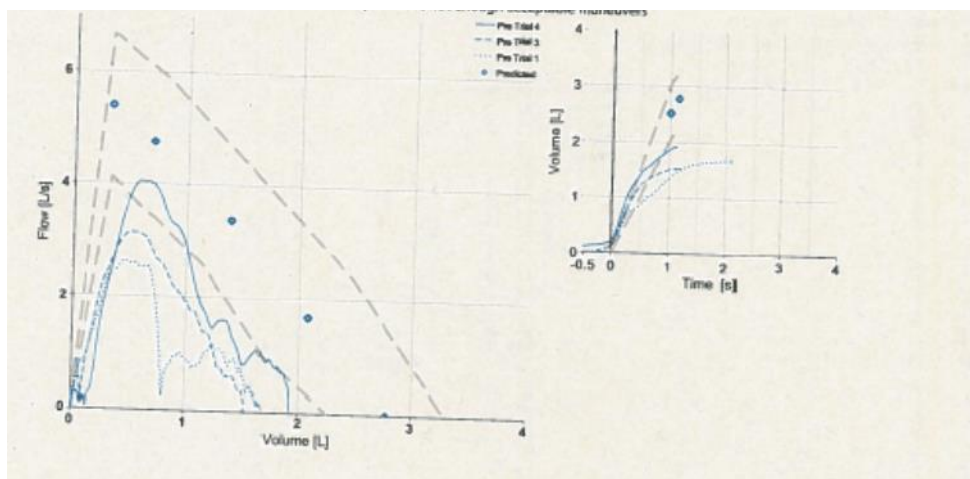
AT-28



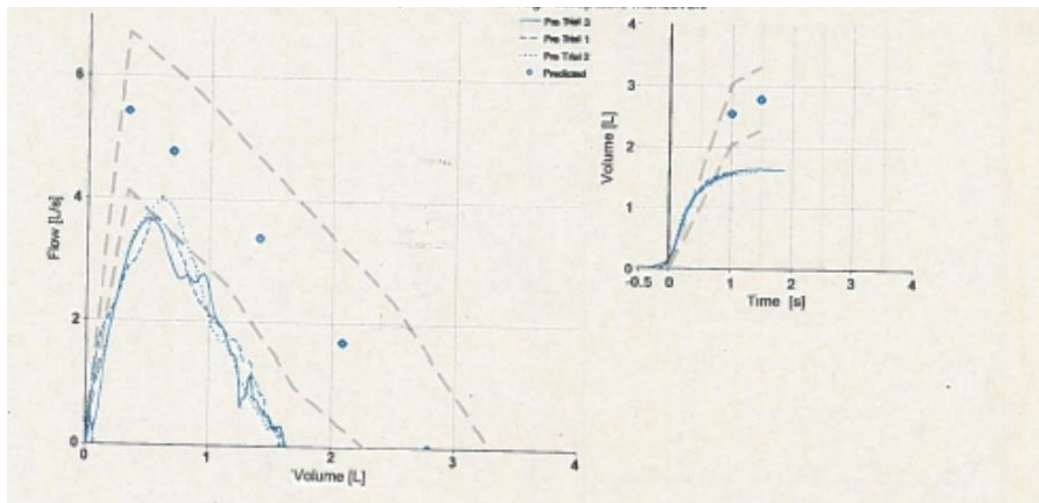
AT-29



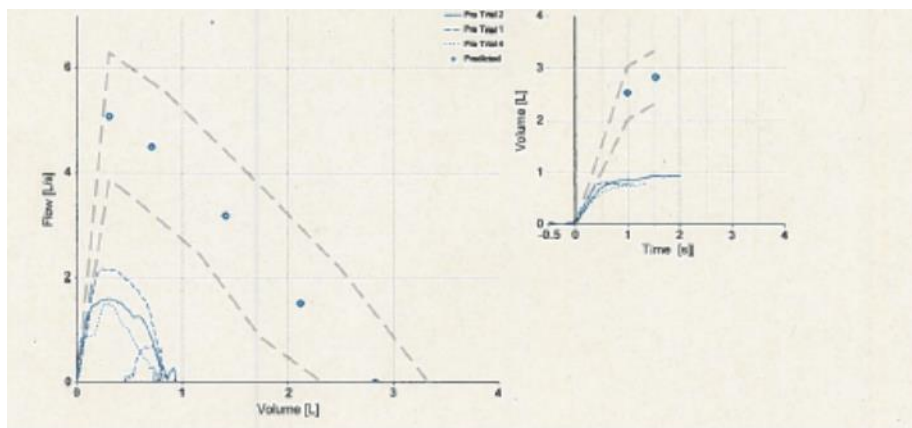
AT-30



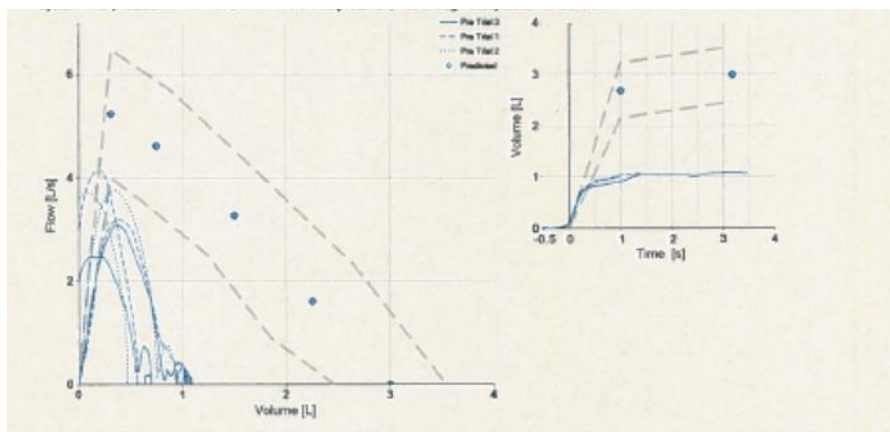
AT-31



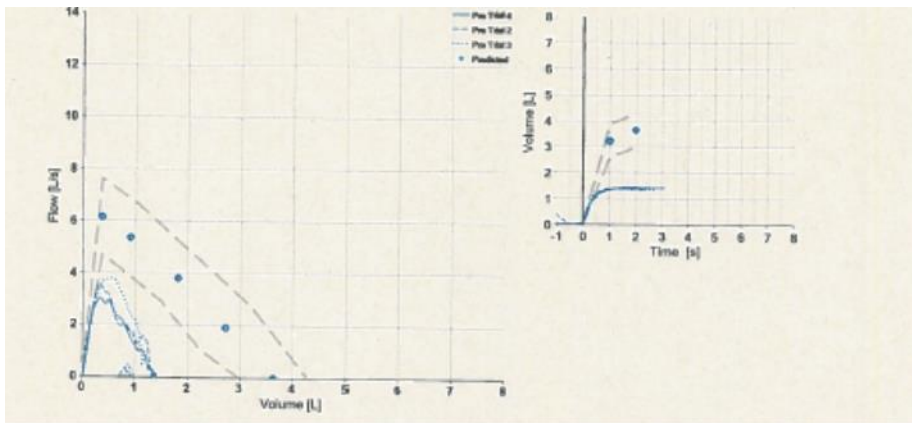
AT-32



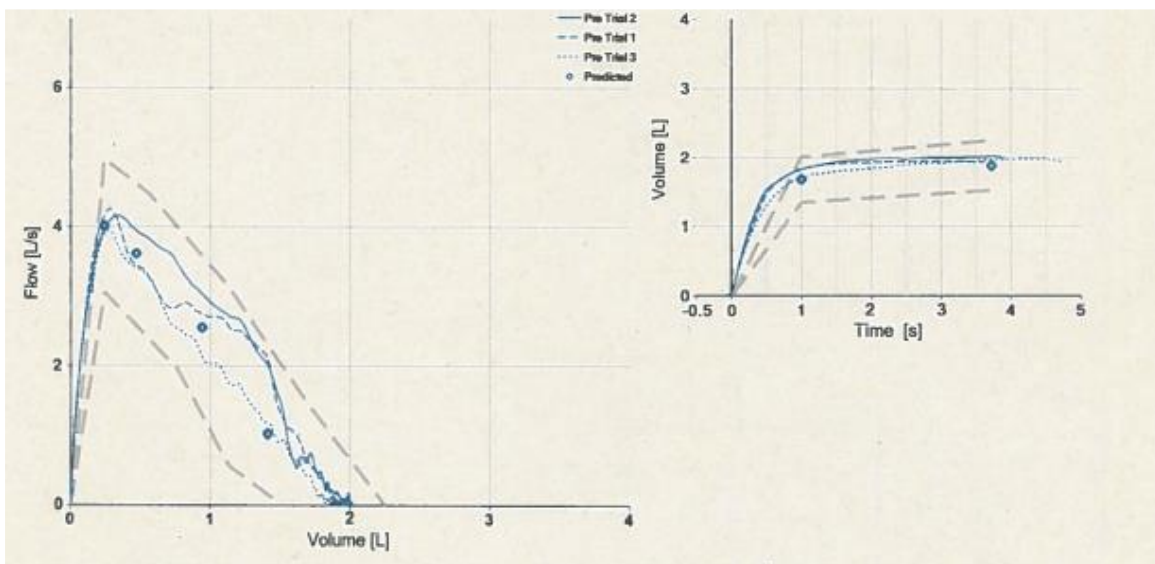
AT-33



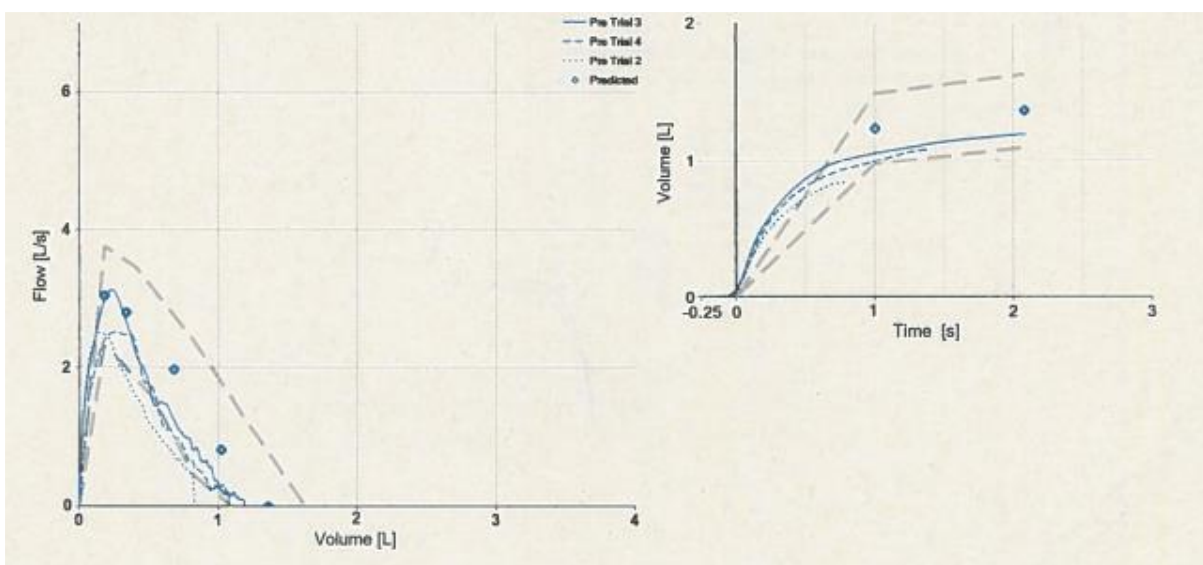
AT-34



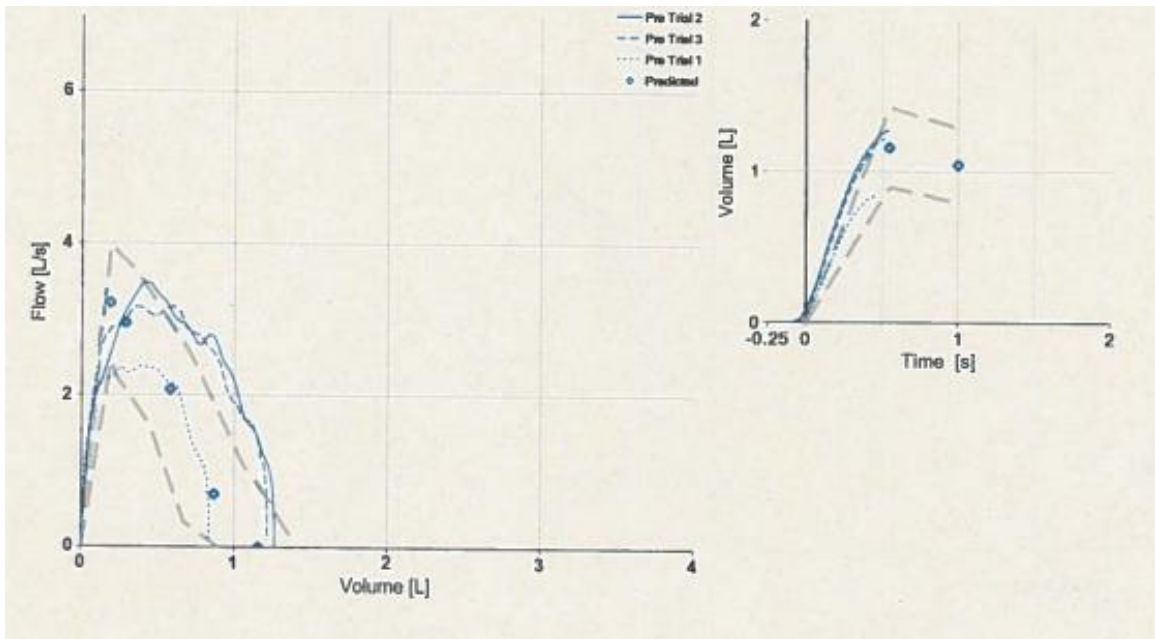
Spirometry Results of Control group 1 CO1- 1



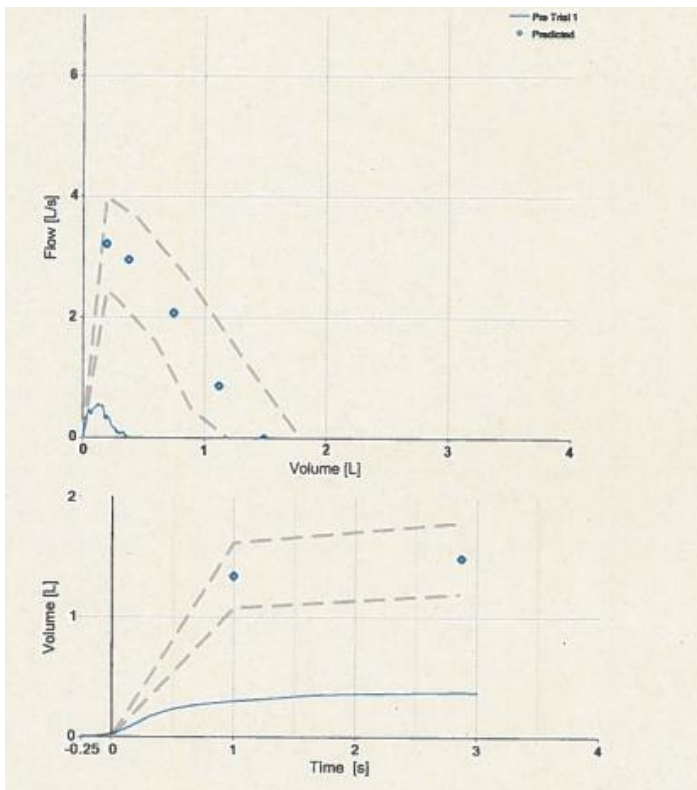
CO1- 2



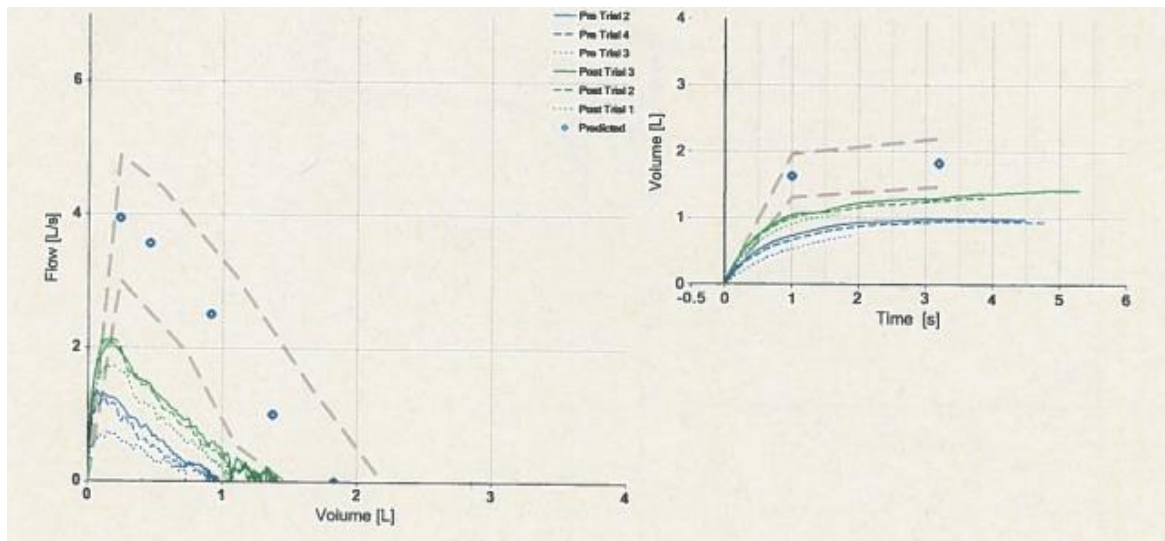
CO1- 3



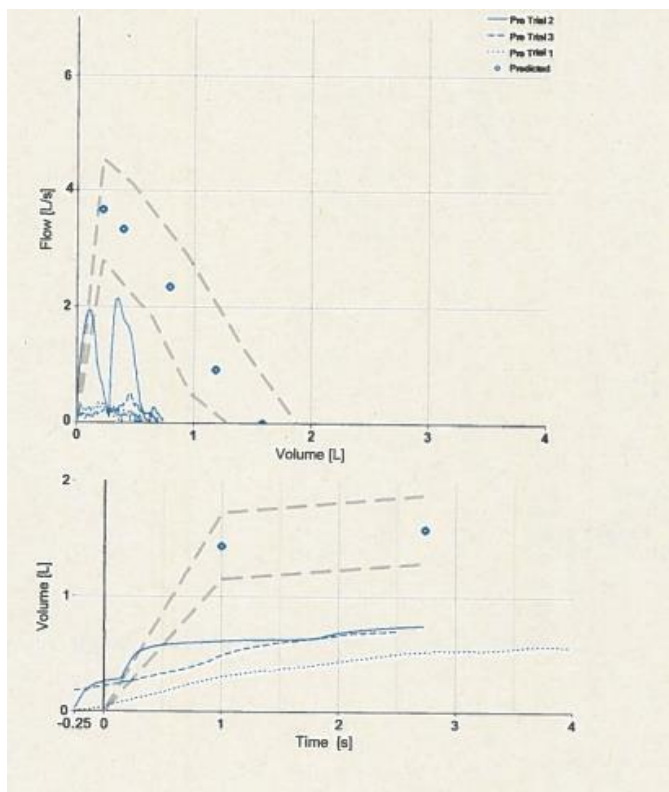
CO2- 4



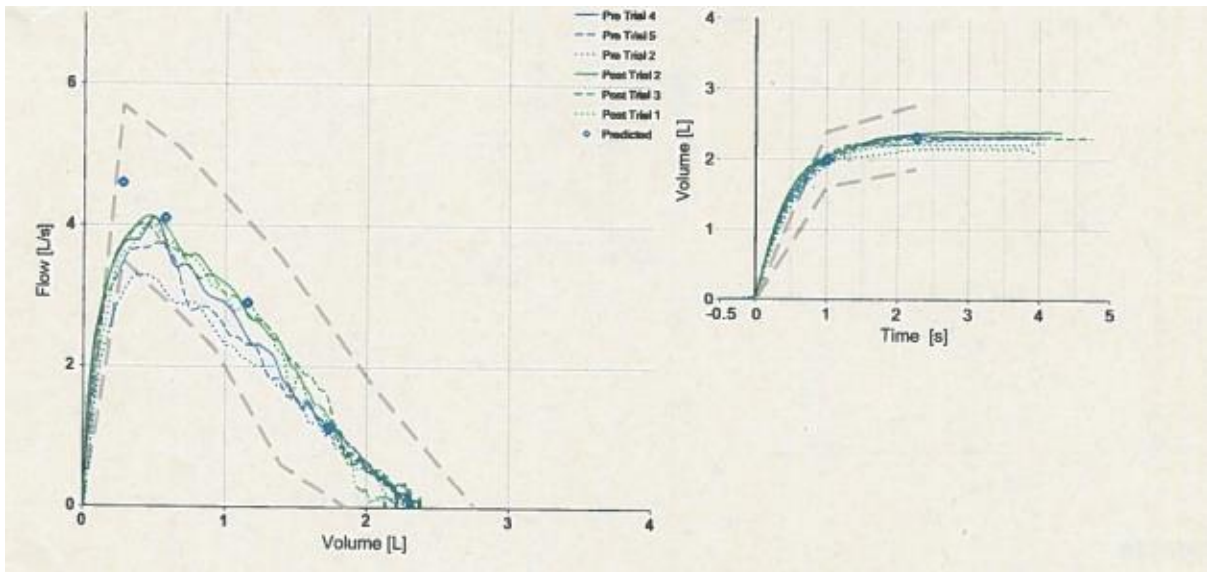
CO1- 5



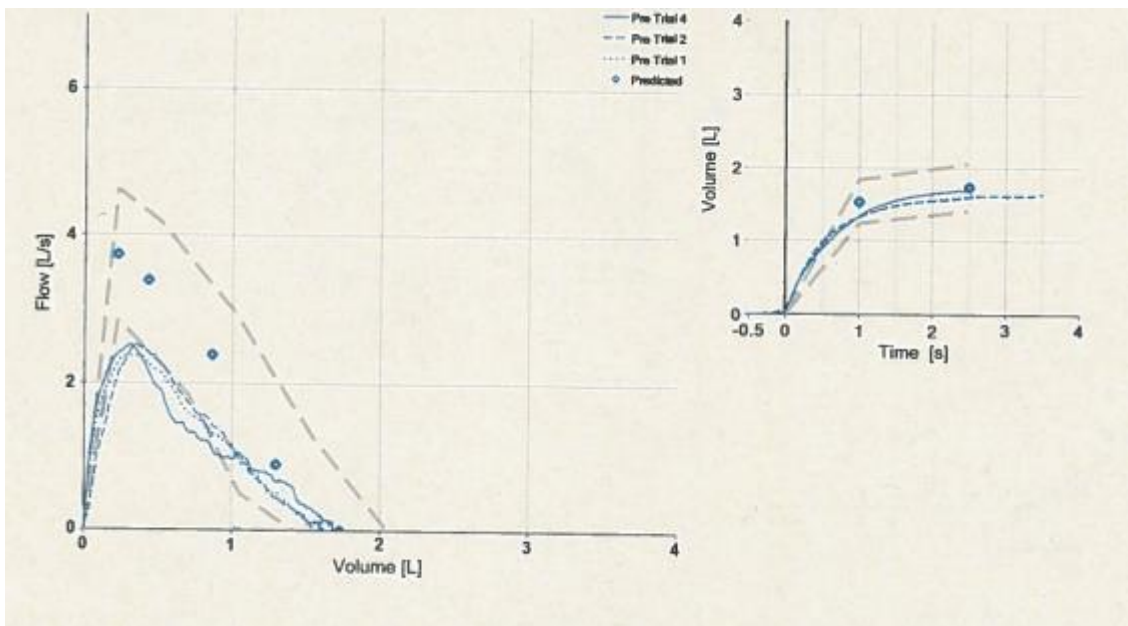
CO1- 6



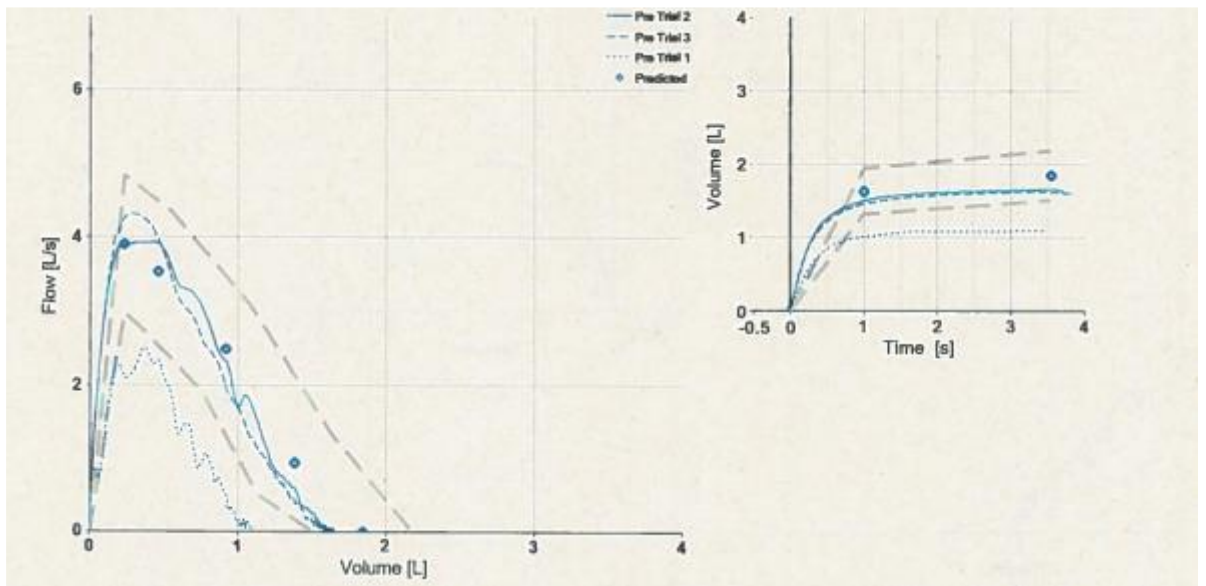
CO1-7



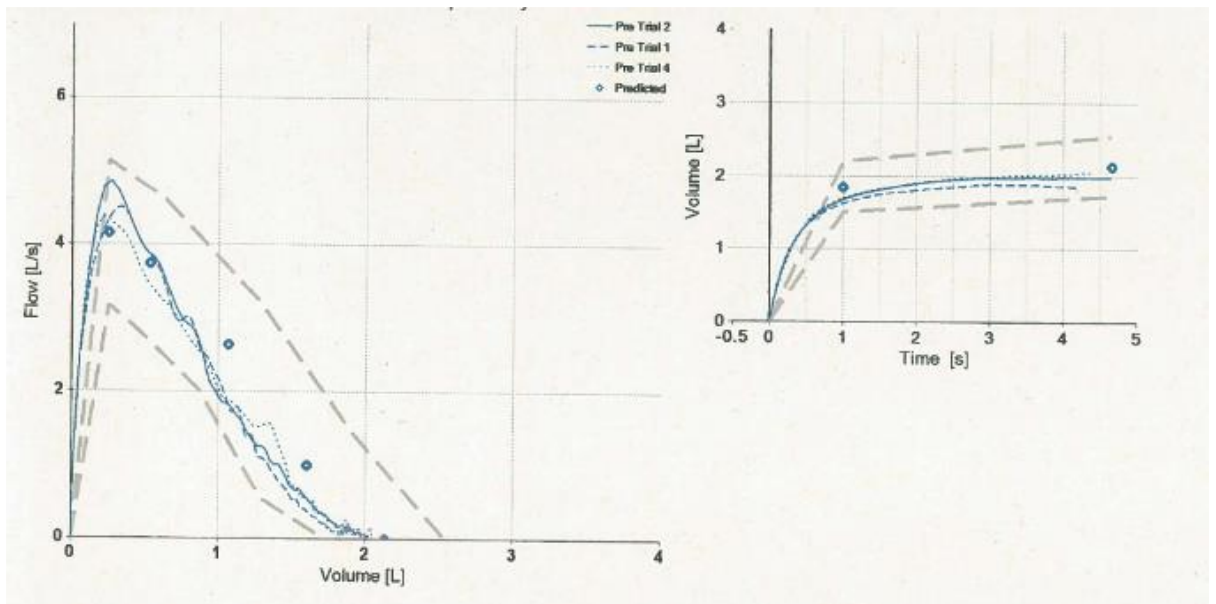
CO1- 8



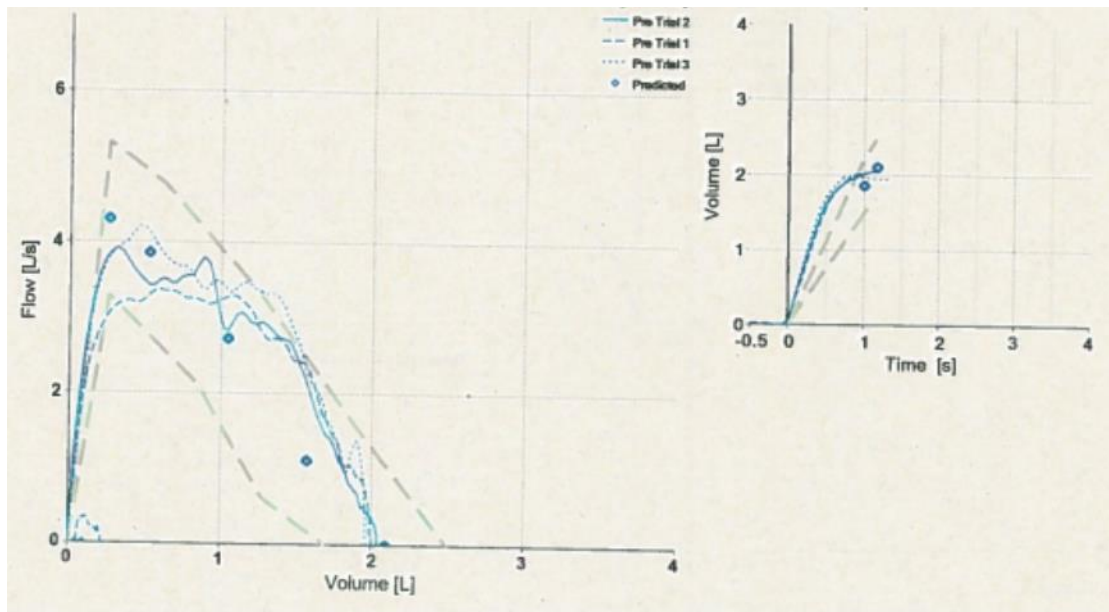
CO1- 9



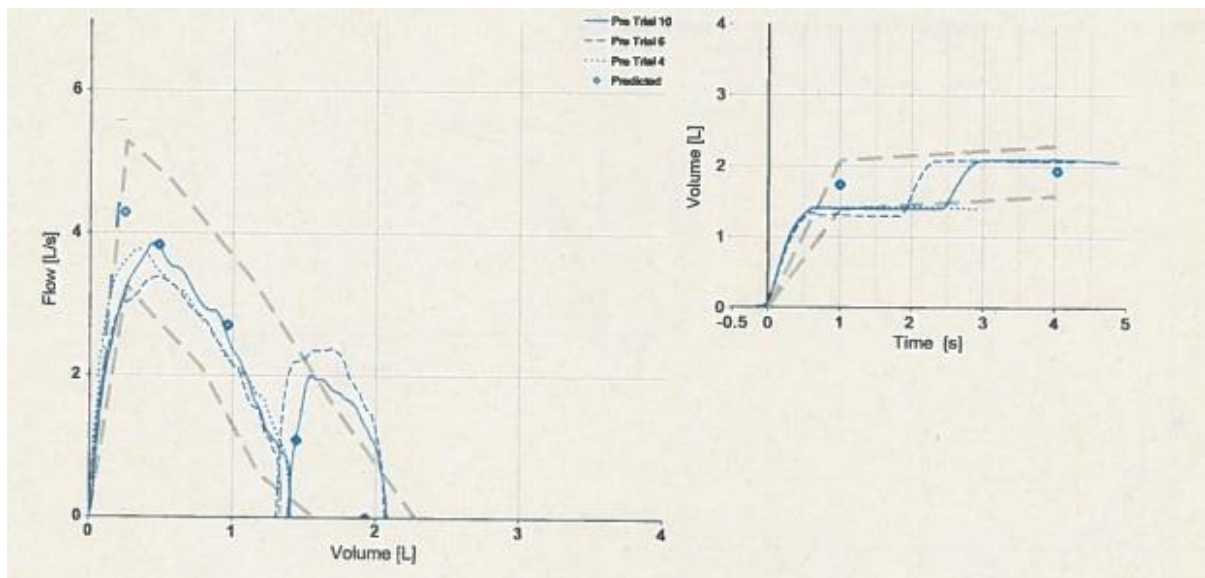
CO1- 10



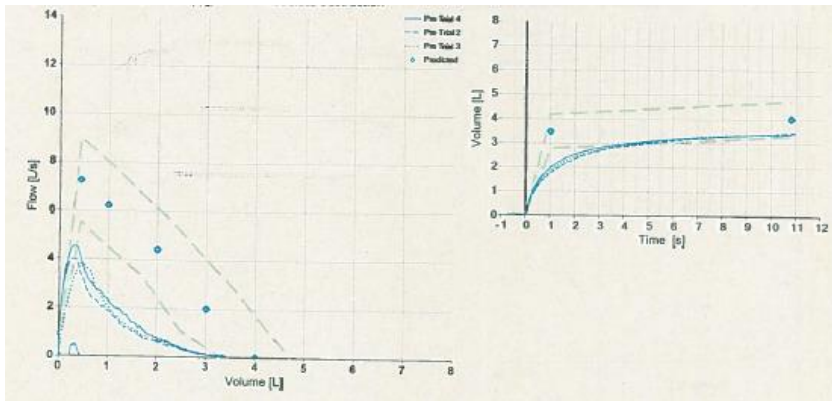
CO1- 11



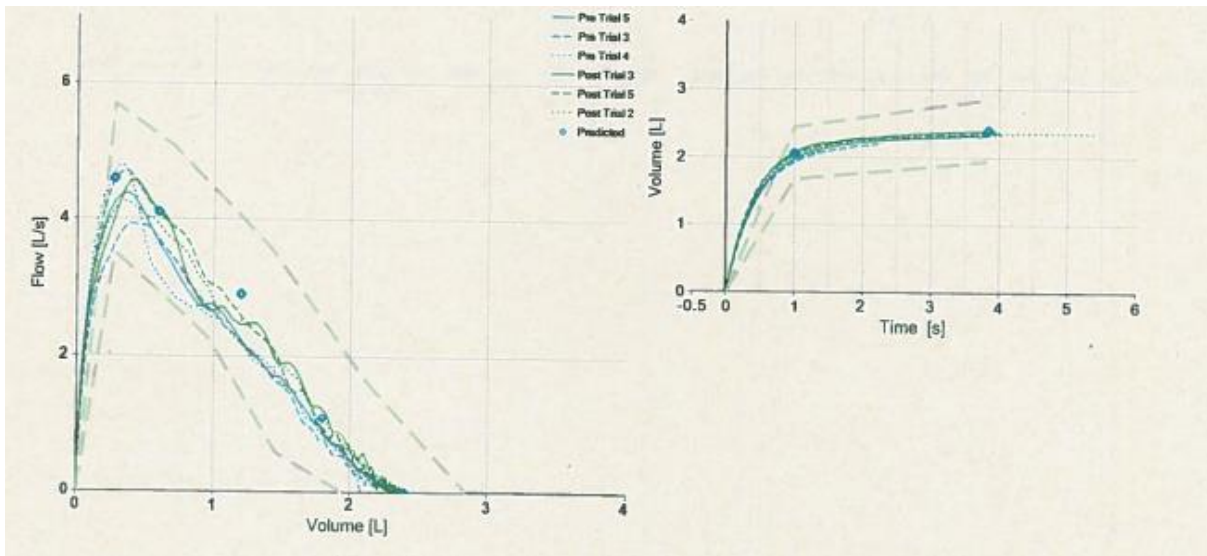
CO1- 12



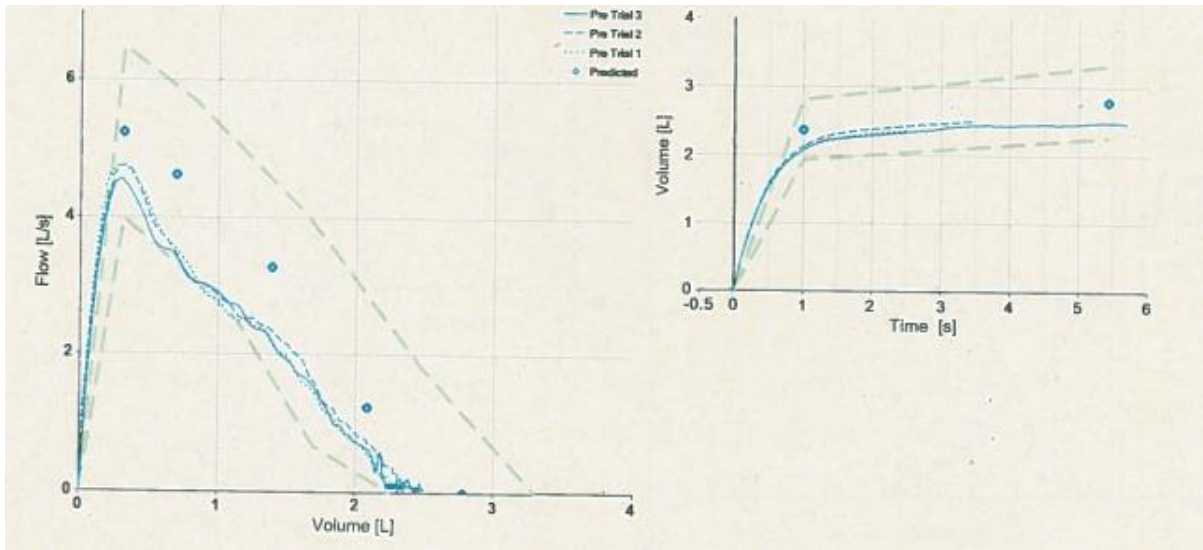
CO1- 13



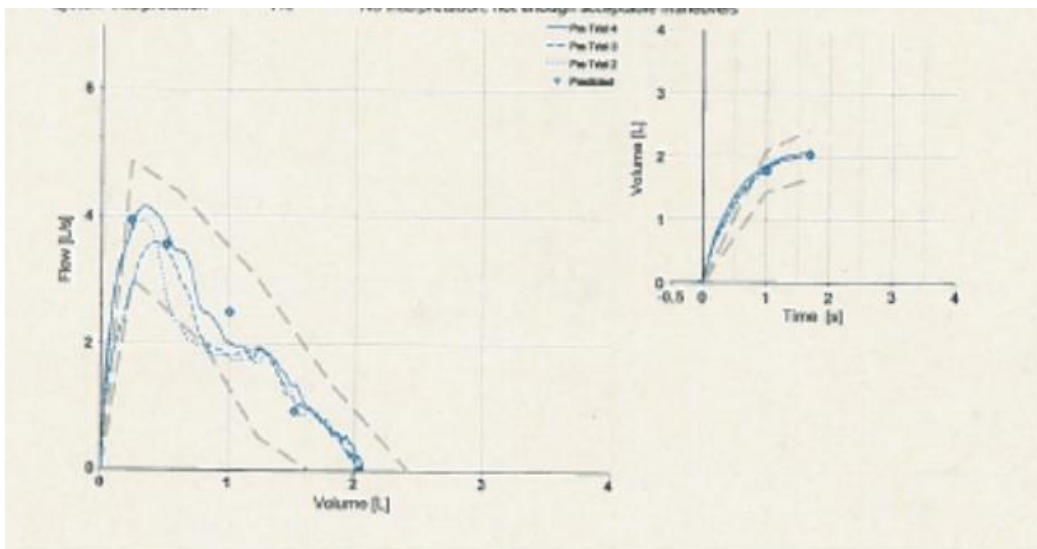
CO1- 14



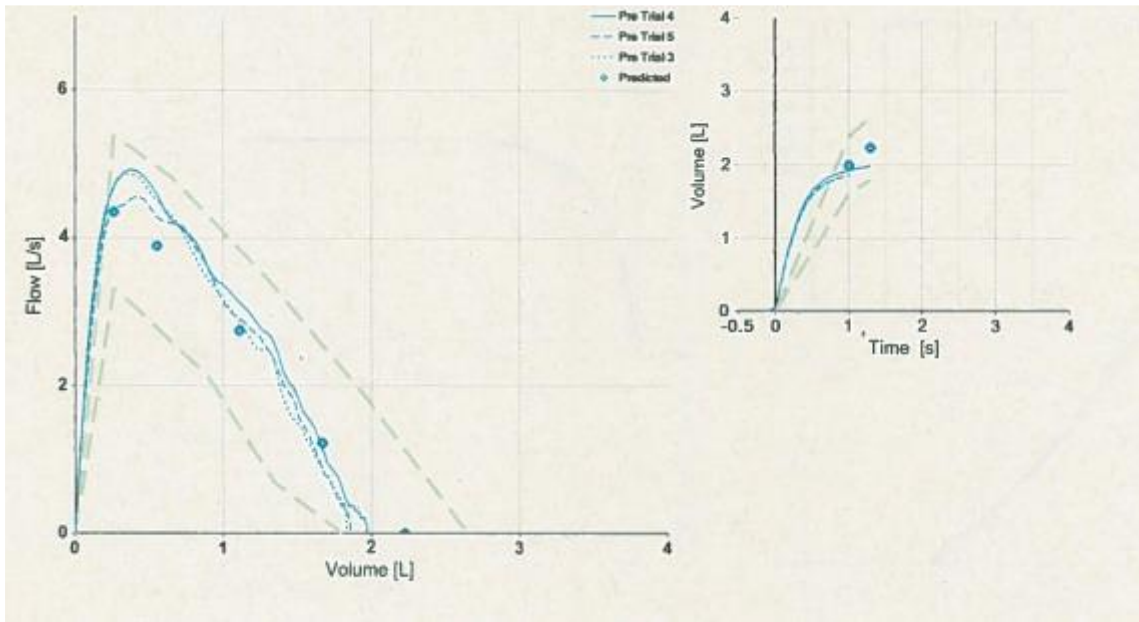
CO1- 15



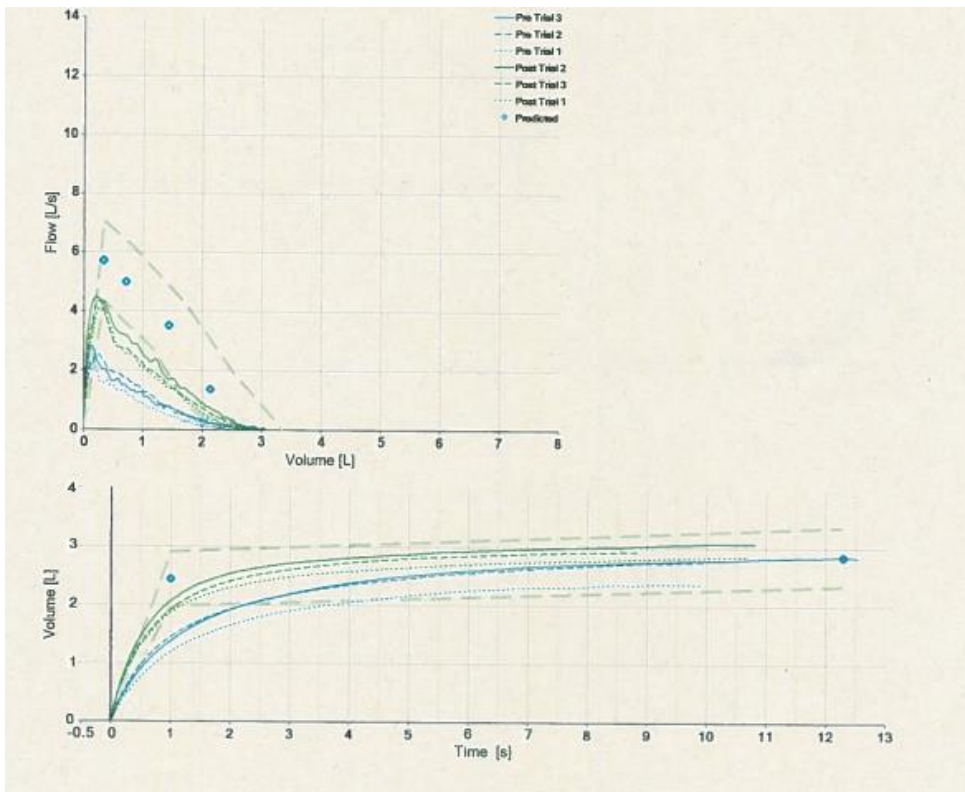
CO1- 16



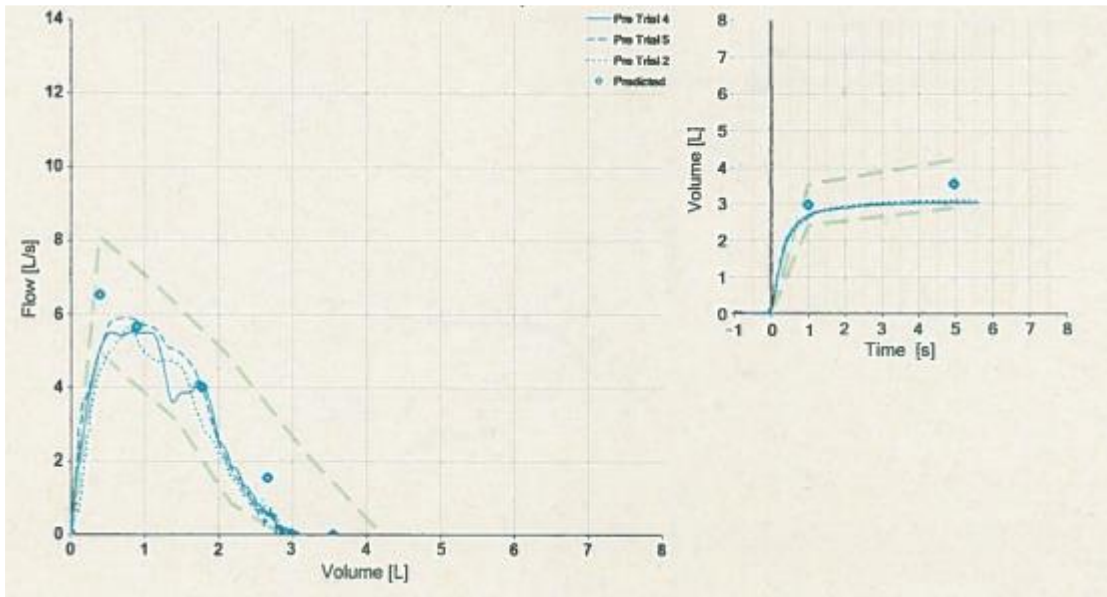
CO1- 17



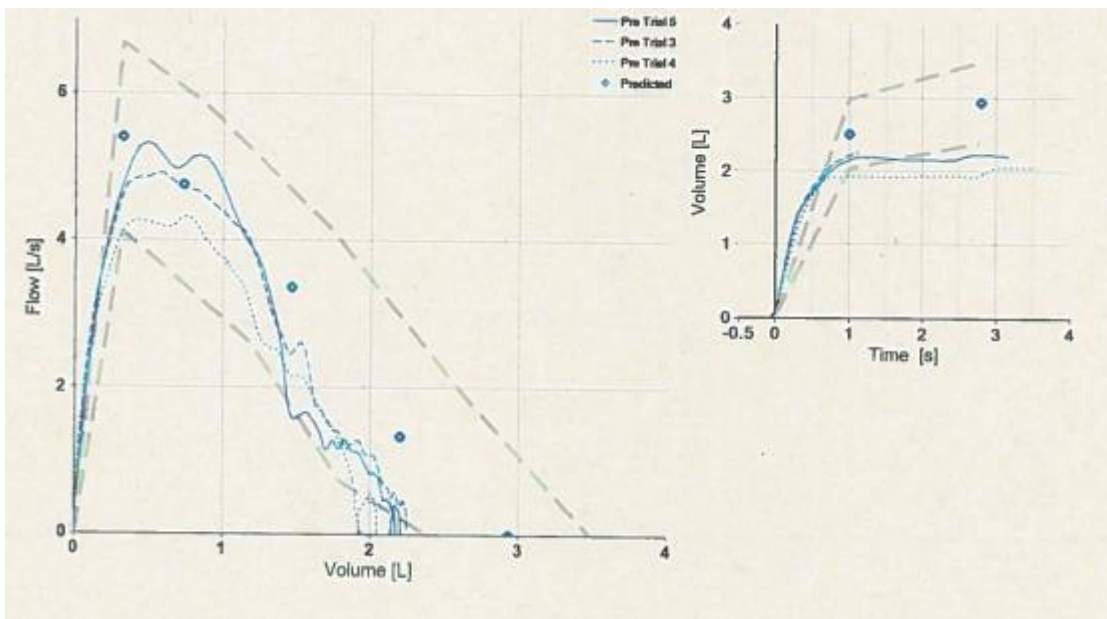
CO1- 18



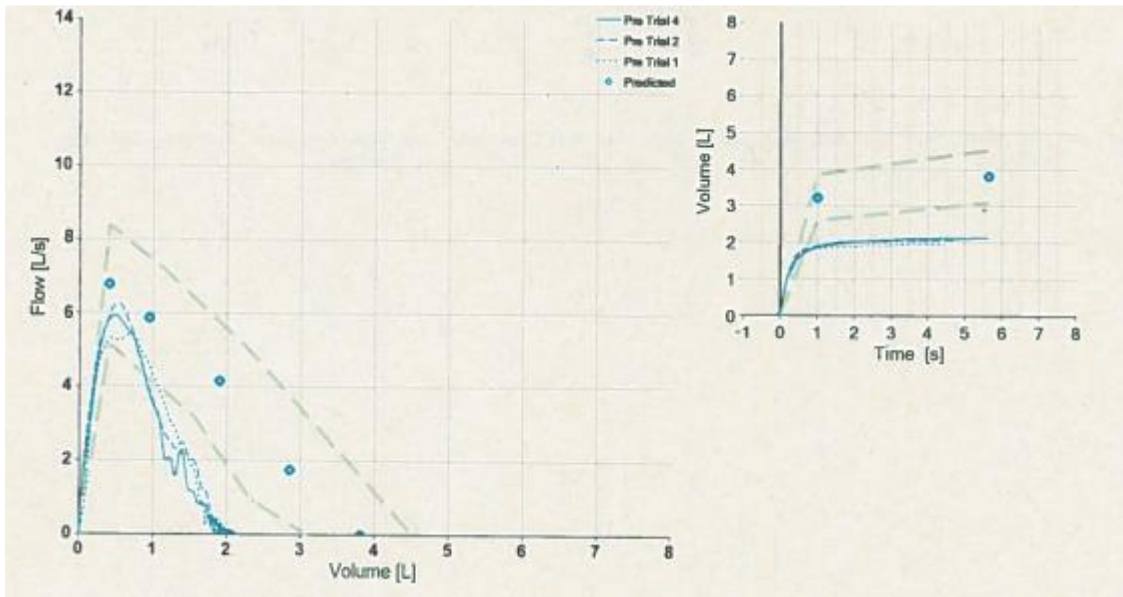
CO1- 19



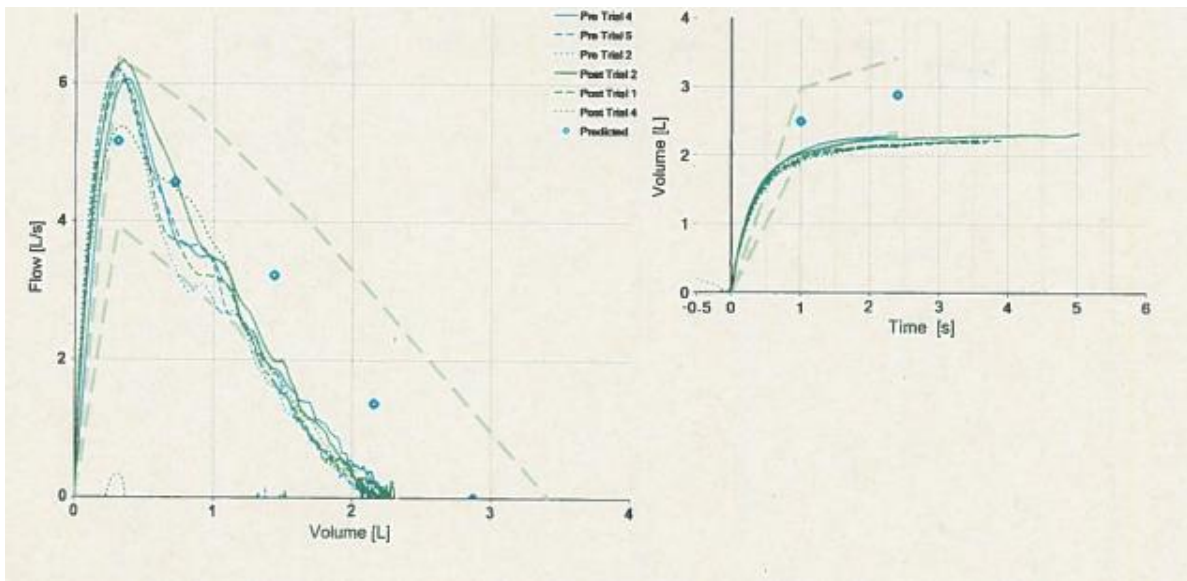
CO- 20



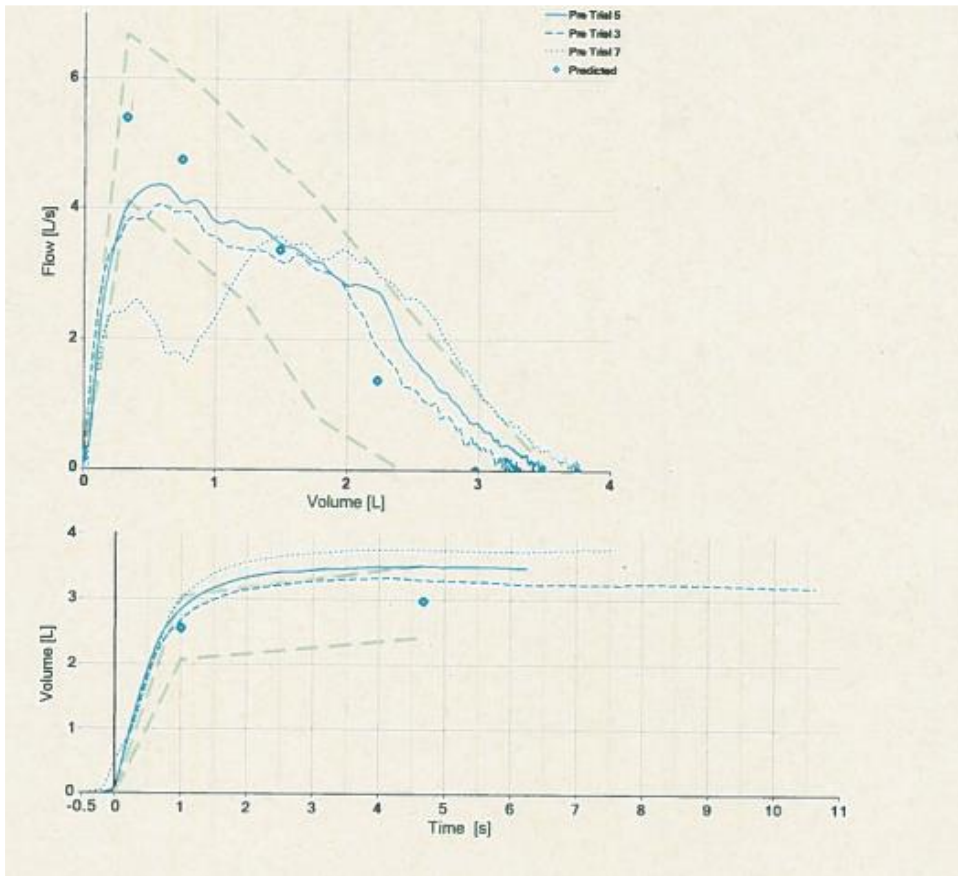
CO1- 21



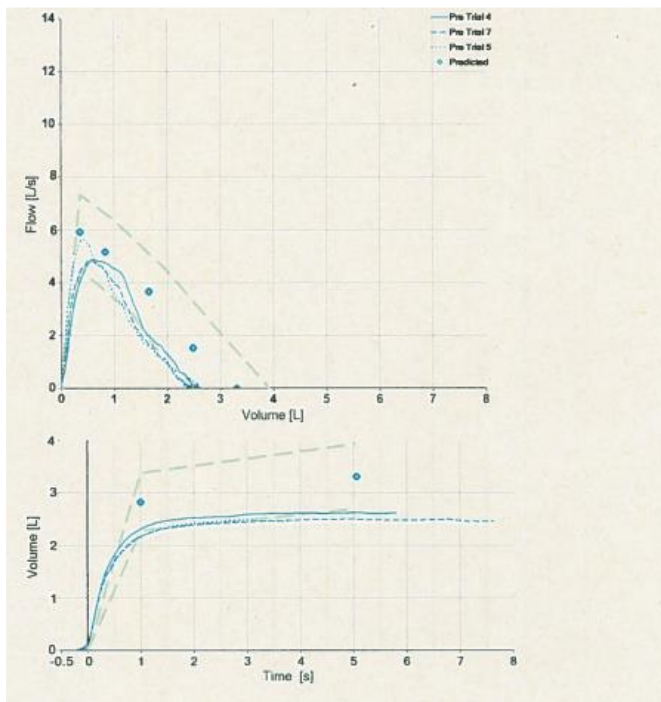
CO1- 22



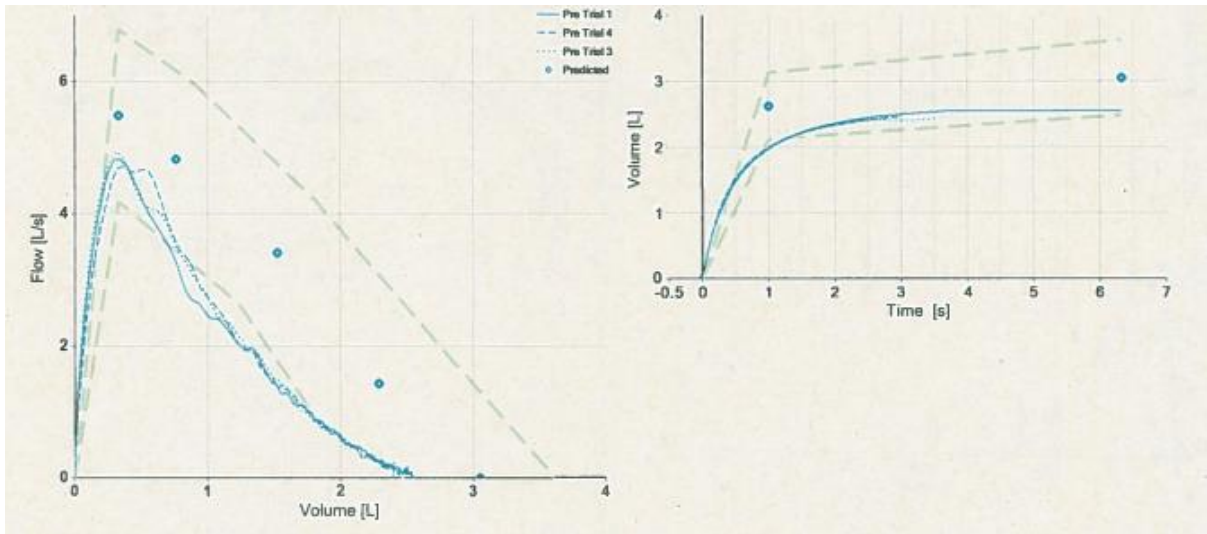
CO1- 23



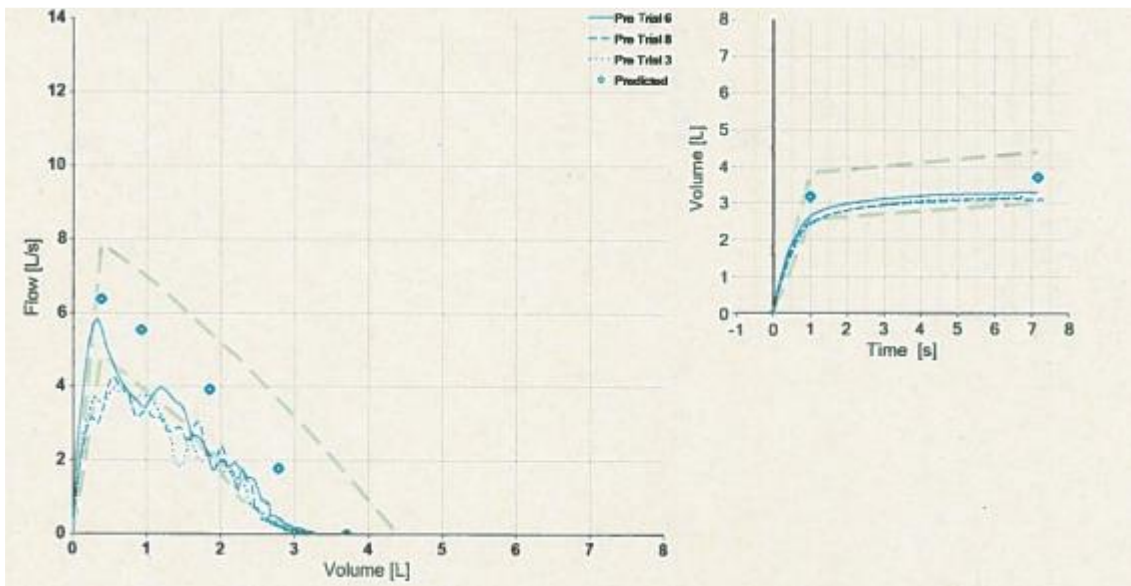
CO1- 24



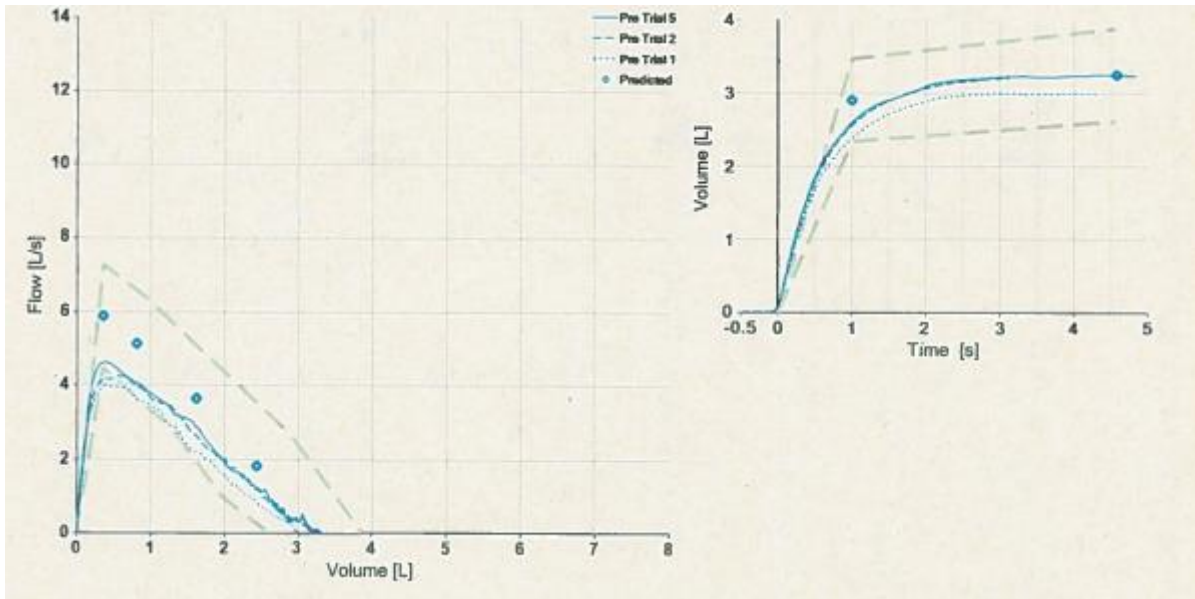
CO1- 25



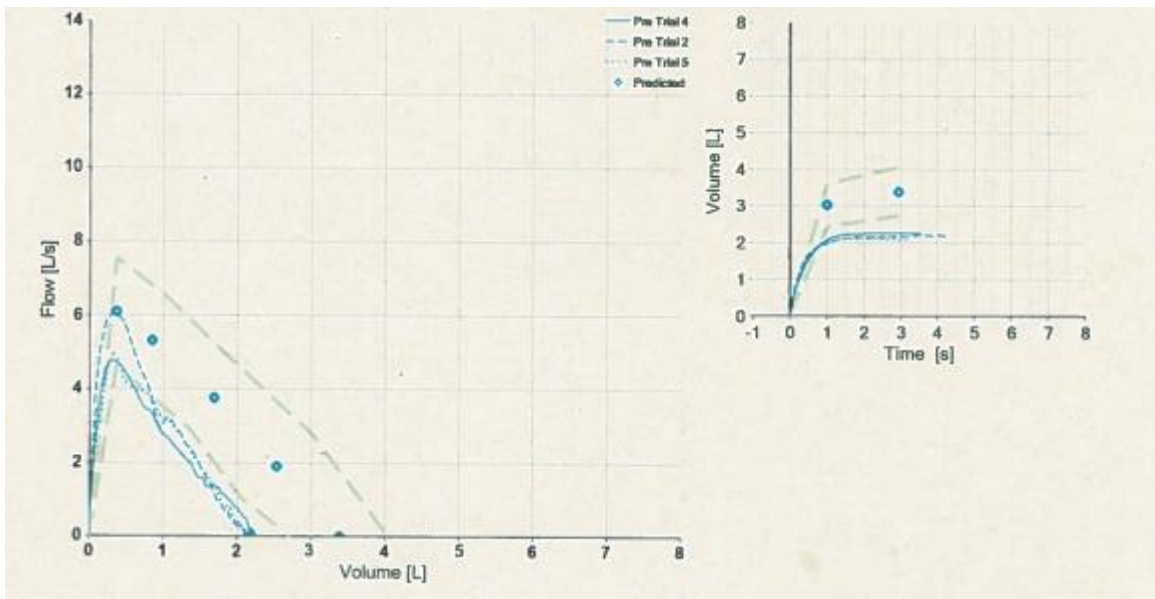
CO1- 26



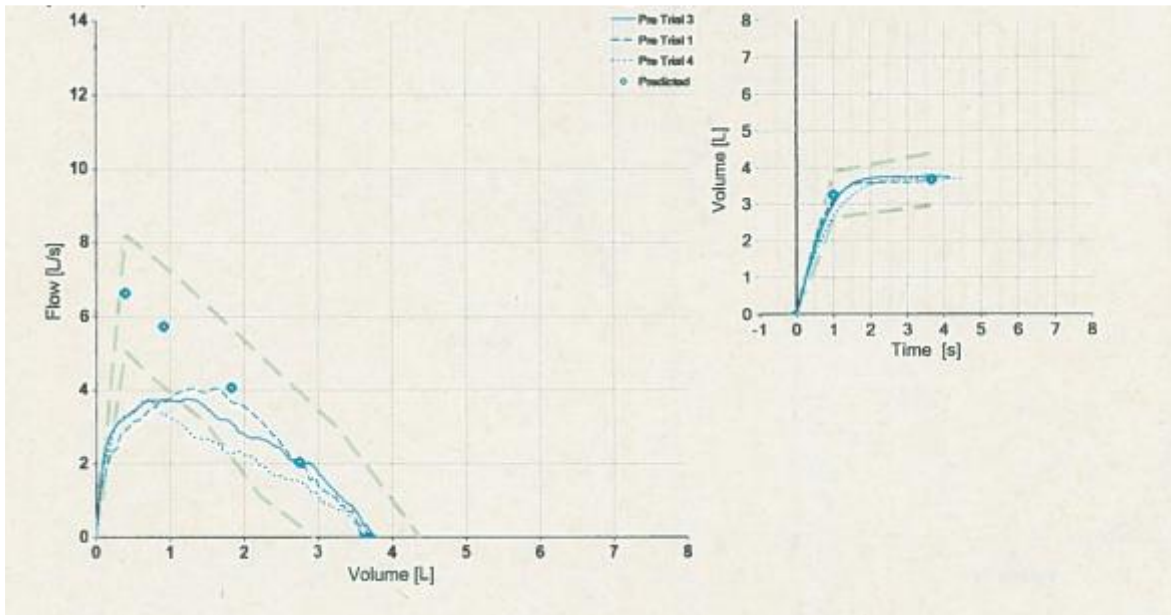
CO1- 27



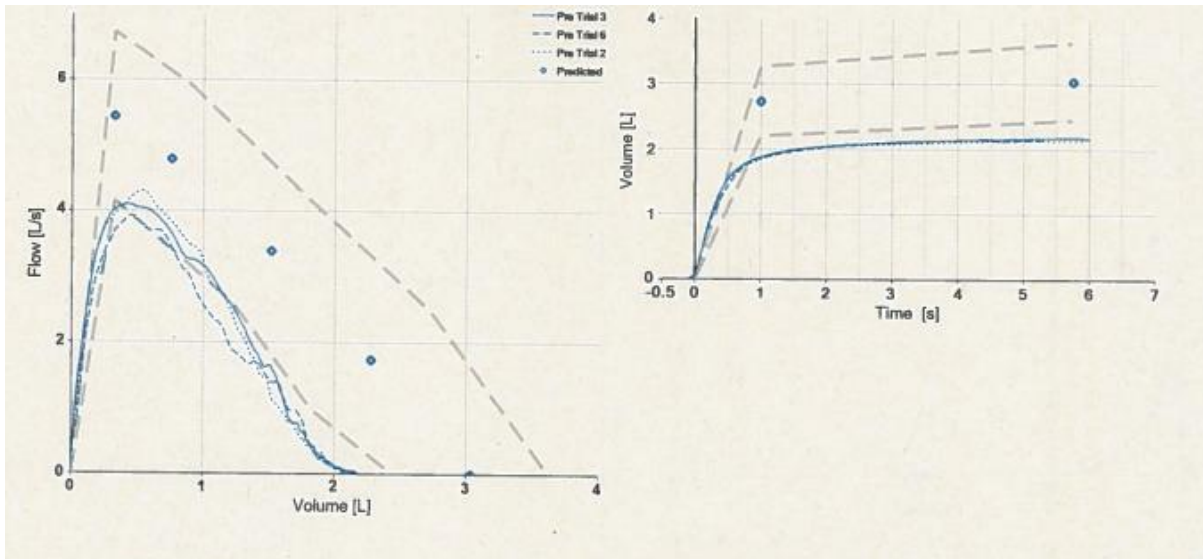
CO1- 28



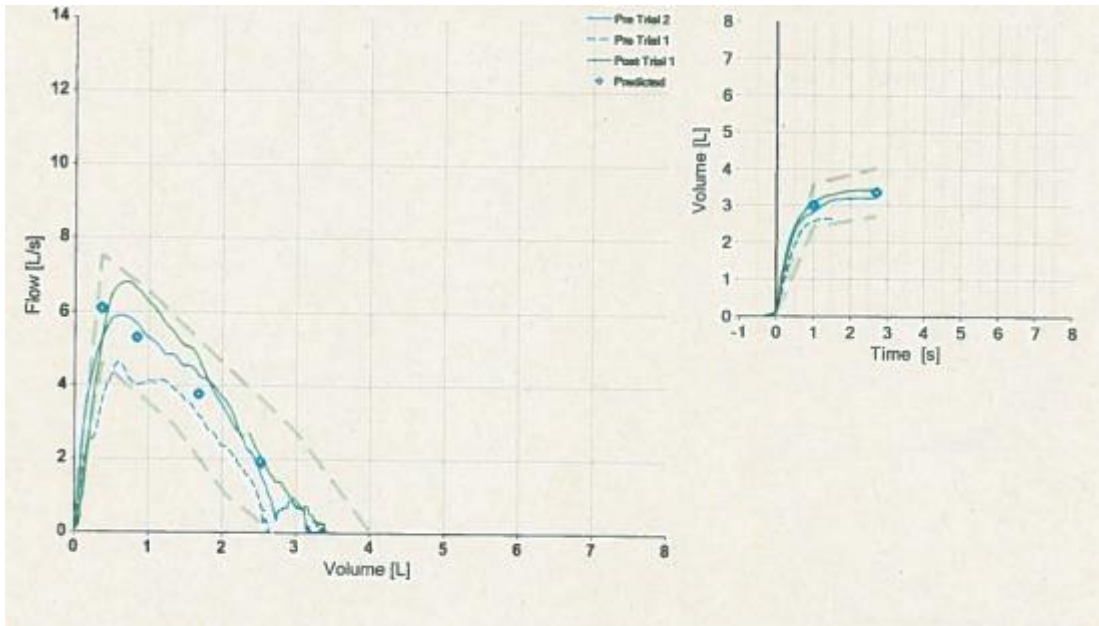
CO1- 29



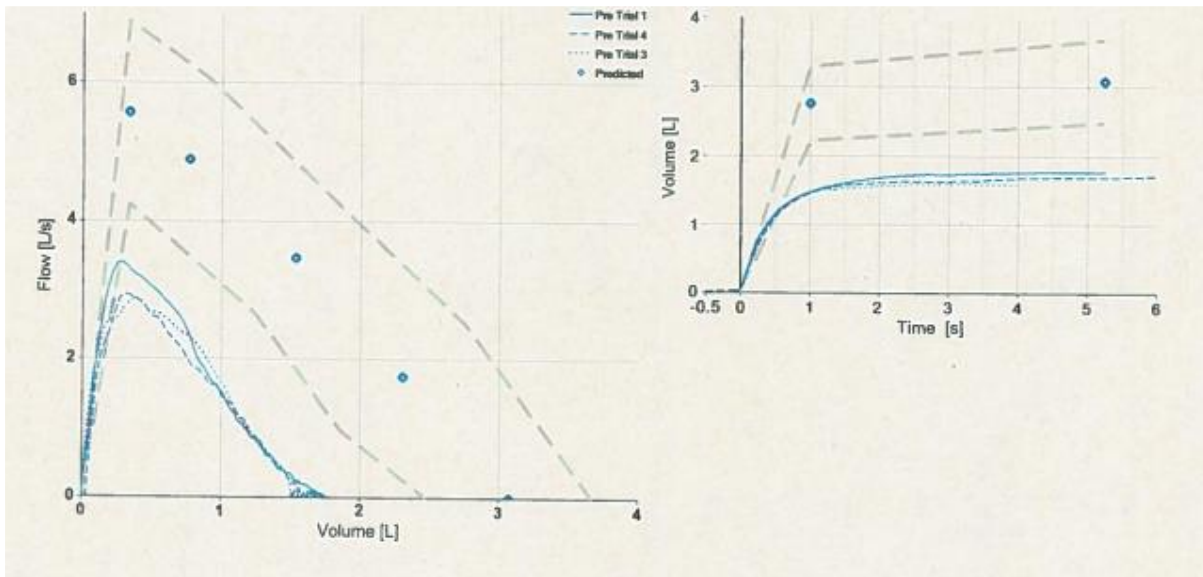
CO1- 30



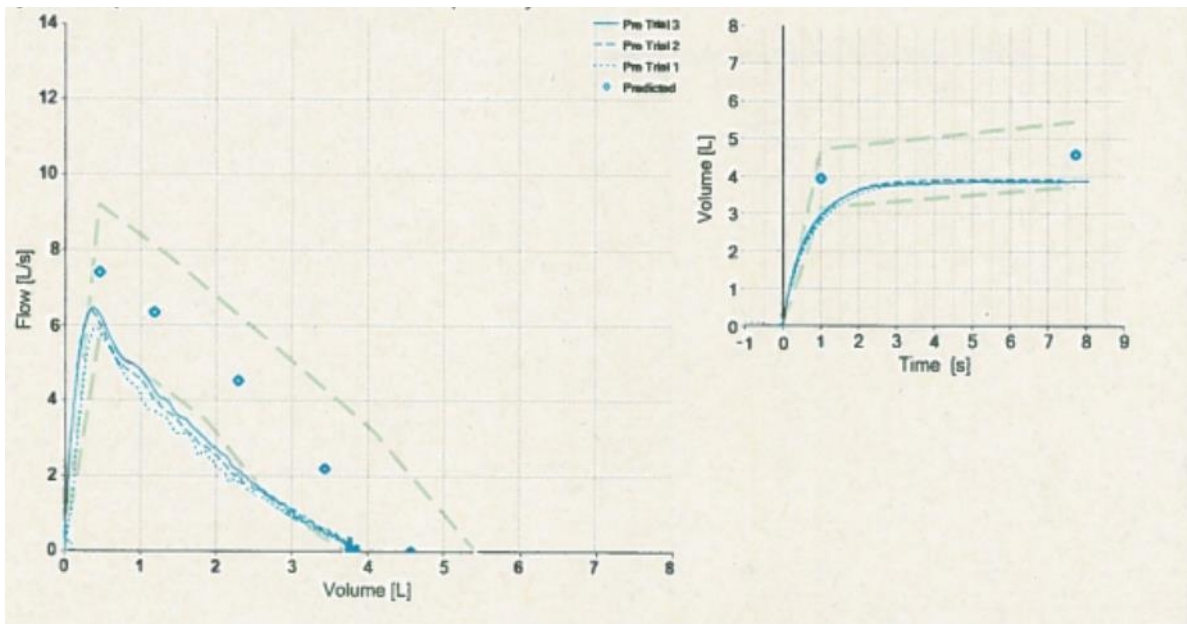
CO1- 31



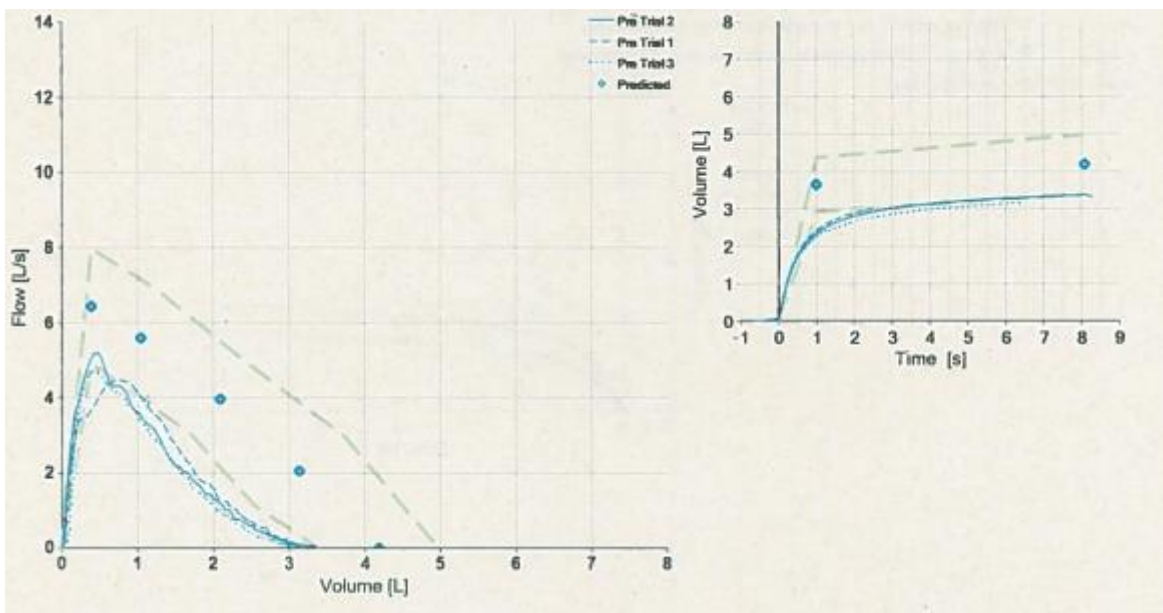
CO1- 32



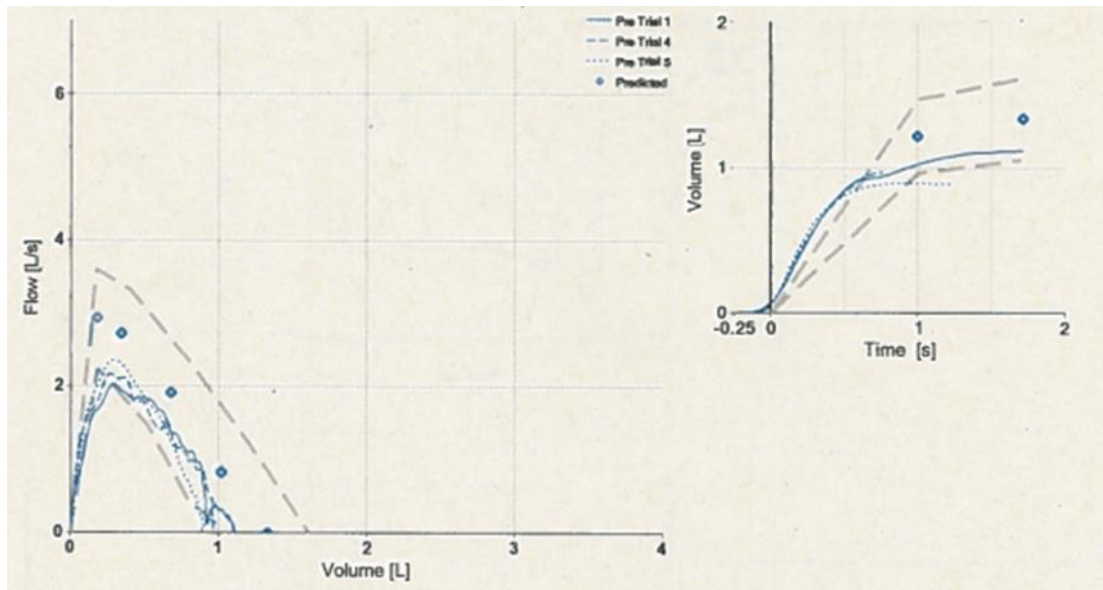
CO1- 33



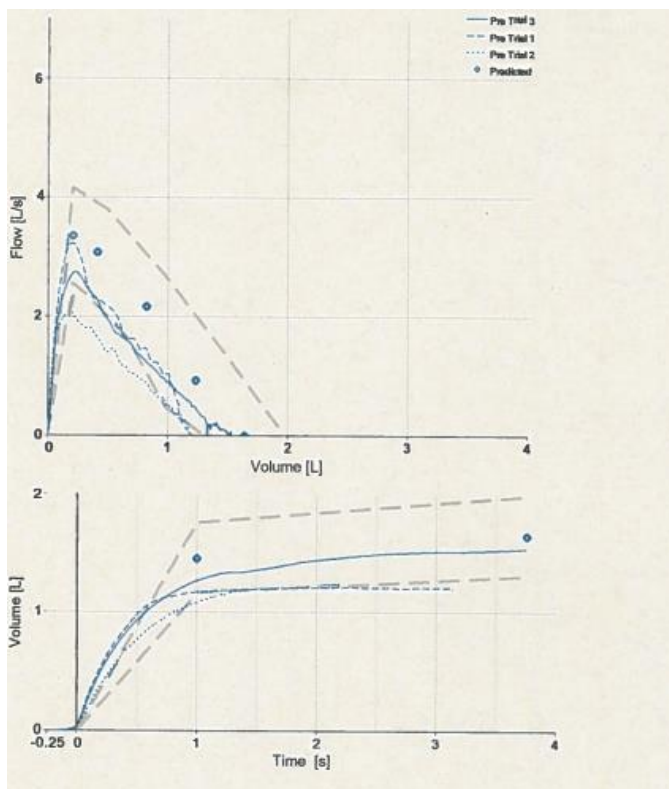
CO1- 34



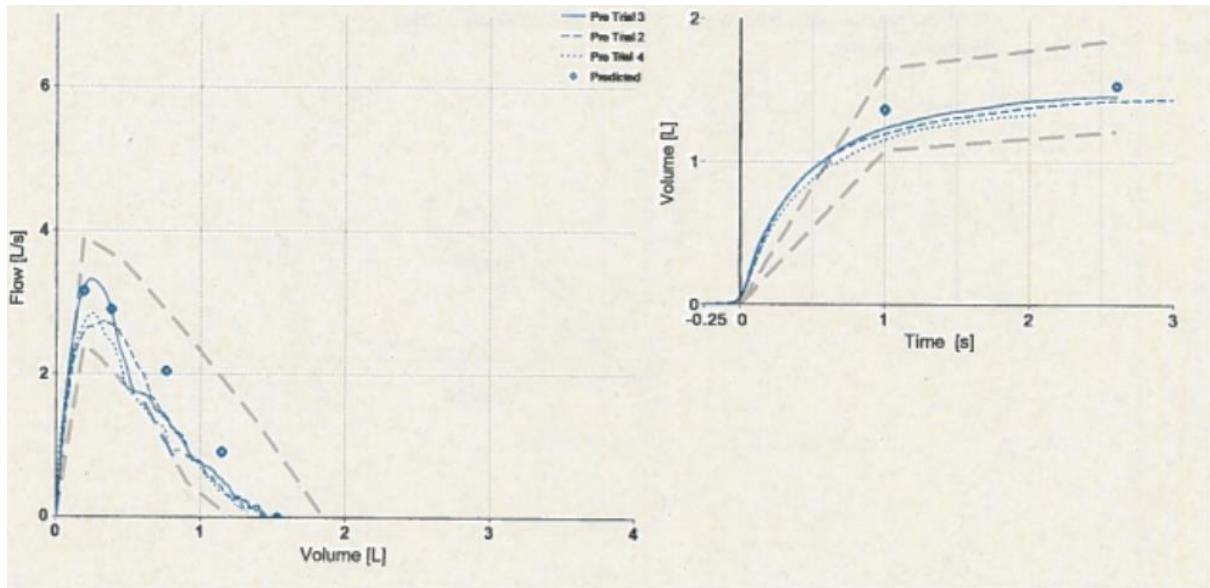
Spirometry Results of Control group 2 CO2- 1



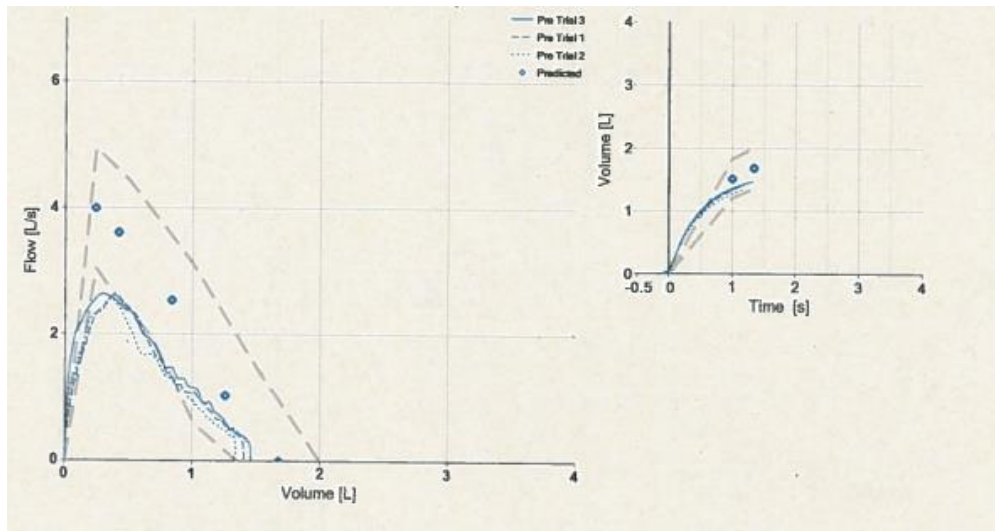
CO2- 2



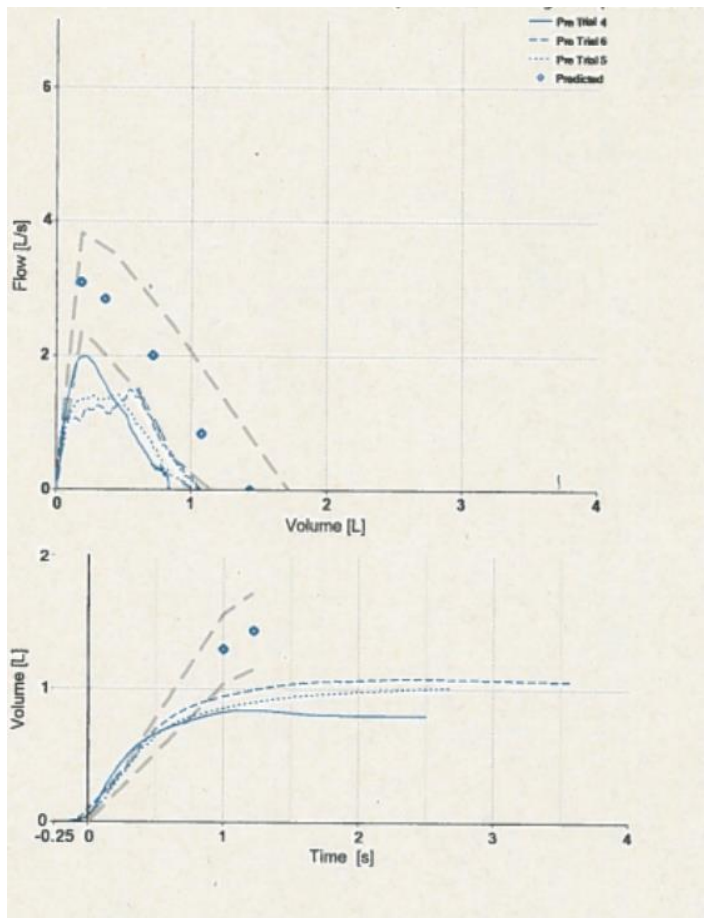
CO2- 3



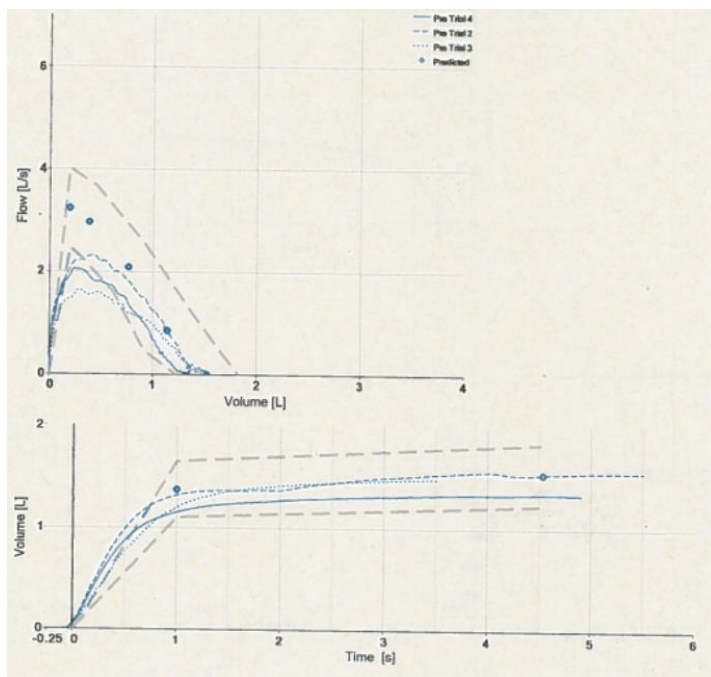
CO2- 4



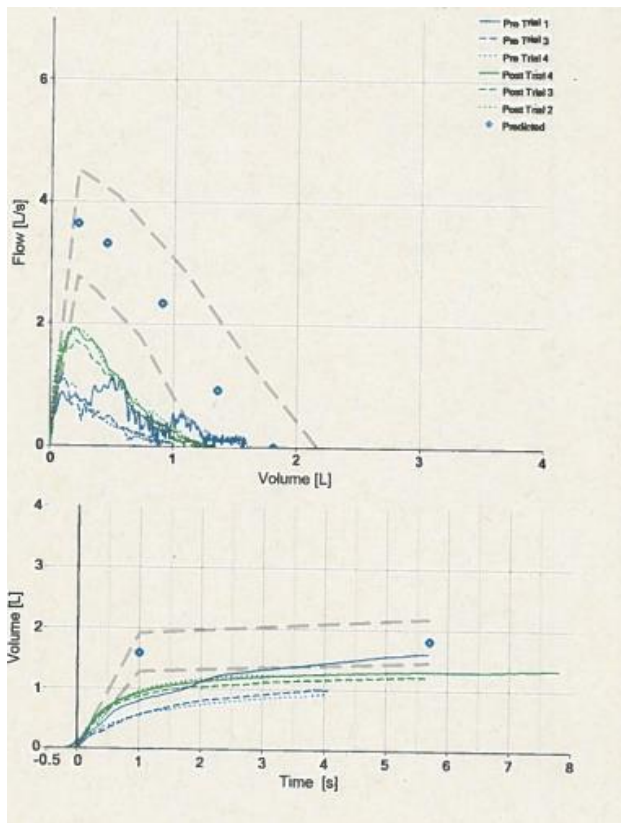
CO2- 5



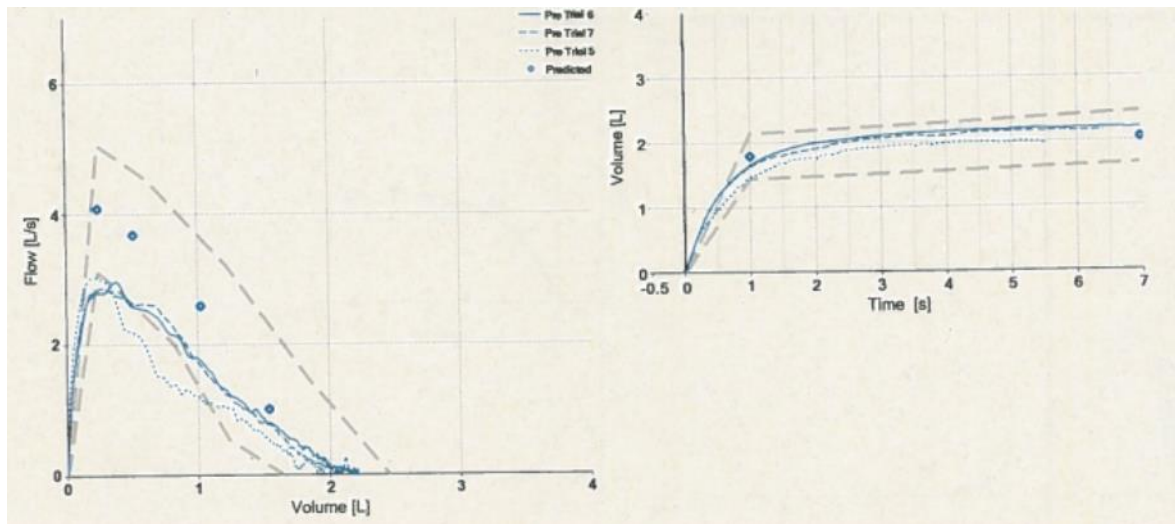
CO2- 6



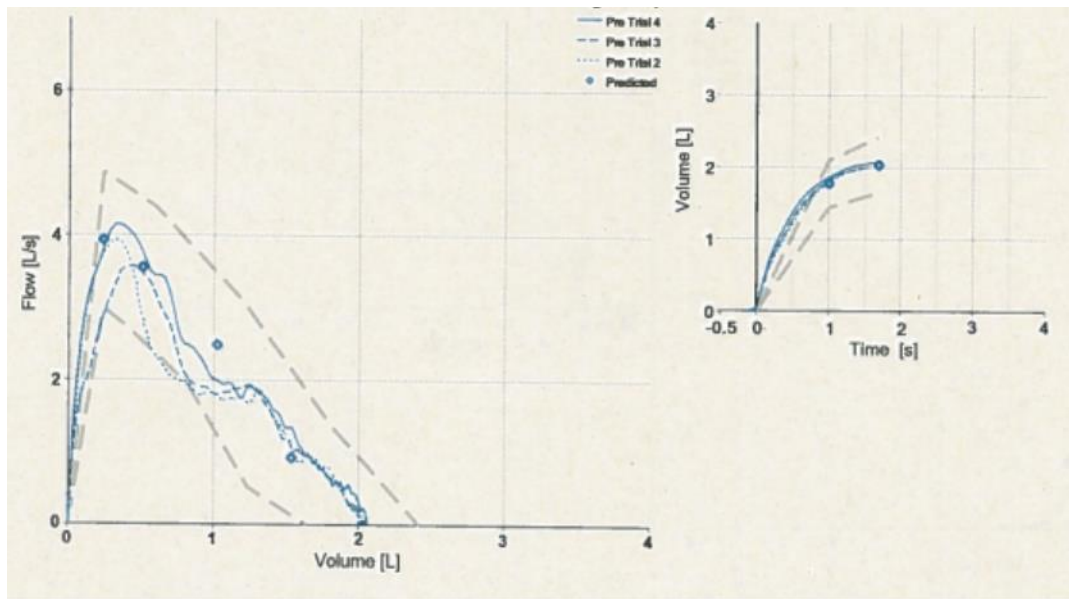
CO2- 7



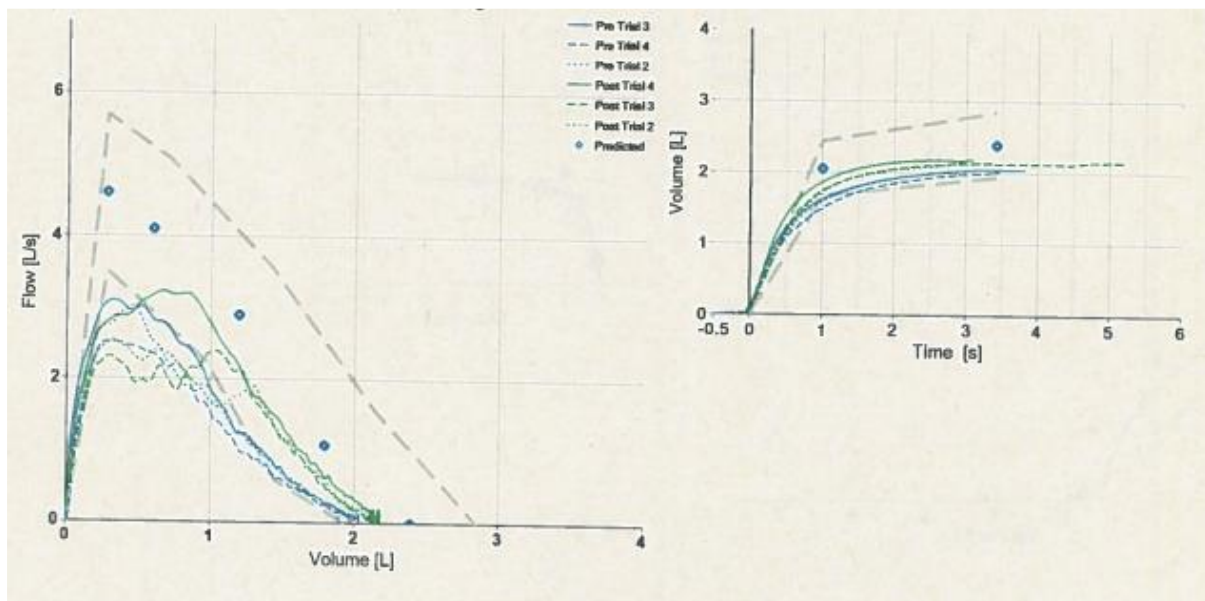
CO2- 8



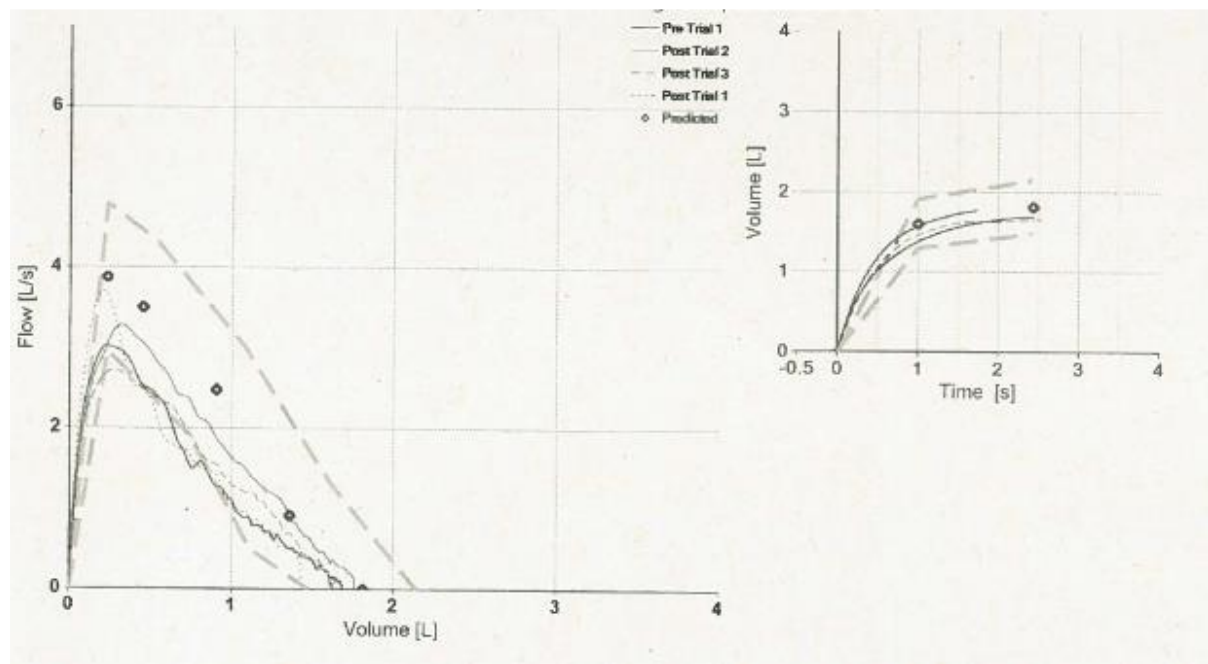
CO2- 9



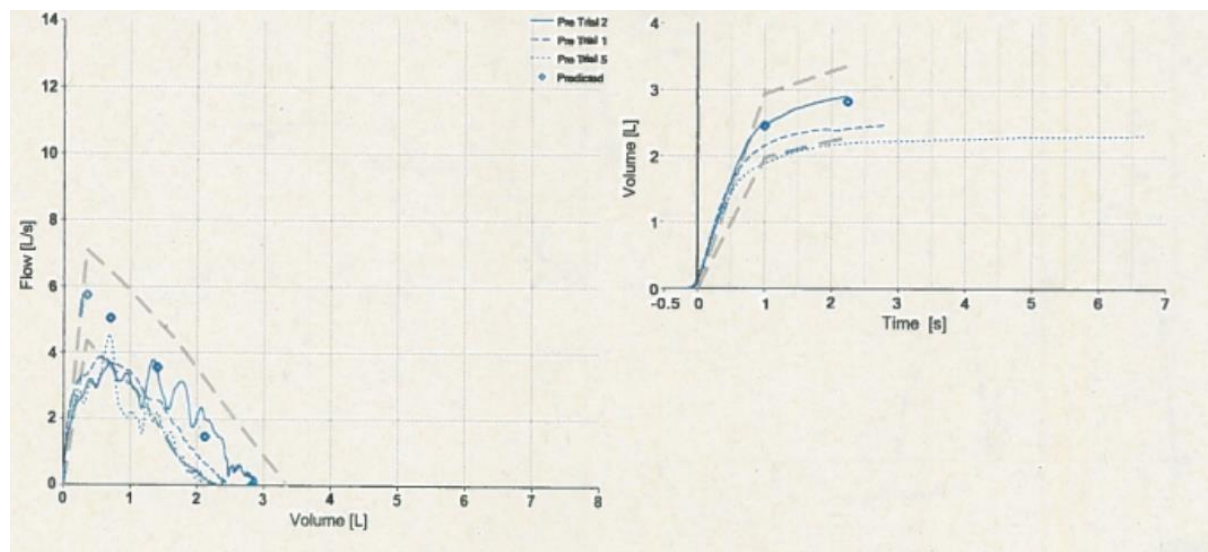
CO2- 10



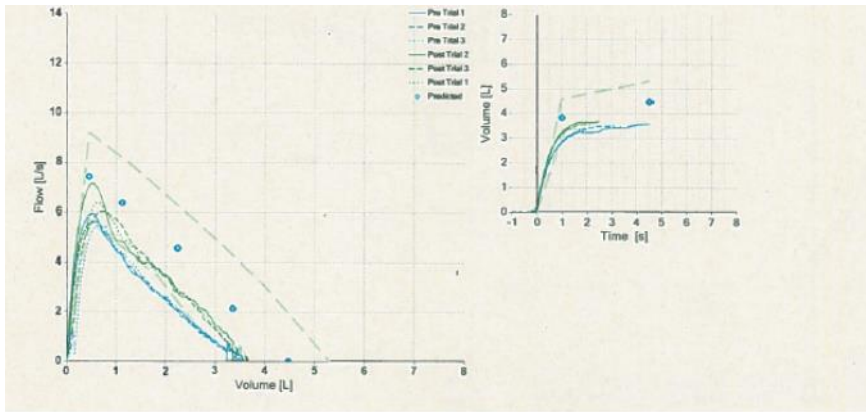
CO2- 11



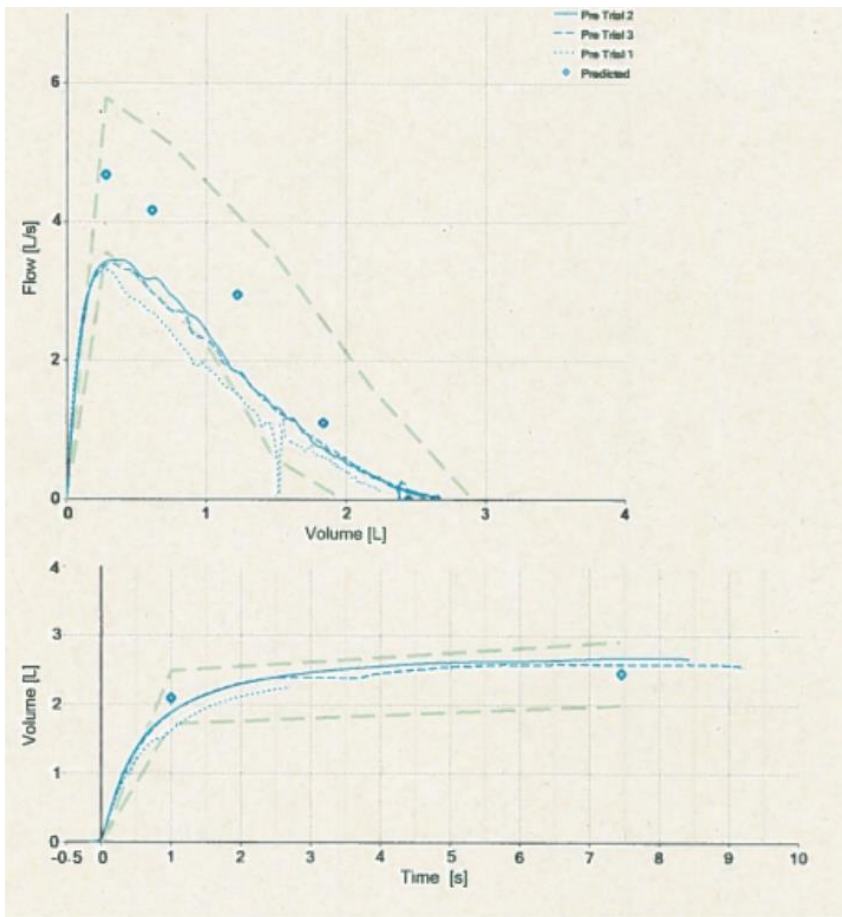
CO2- 12



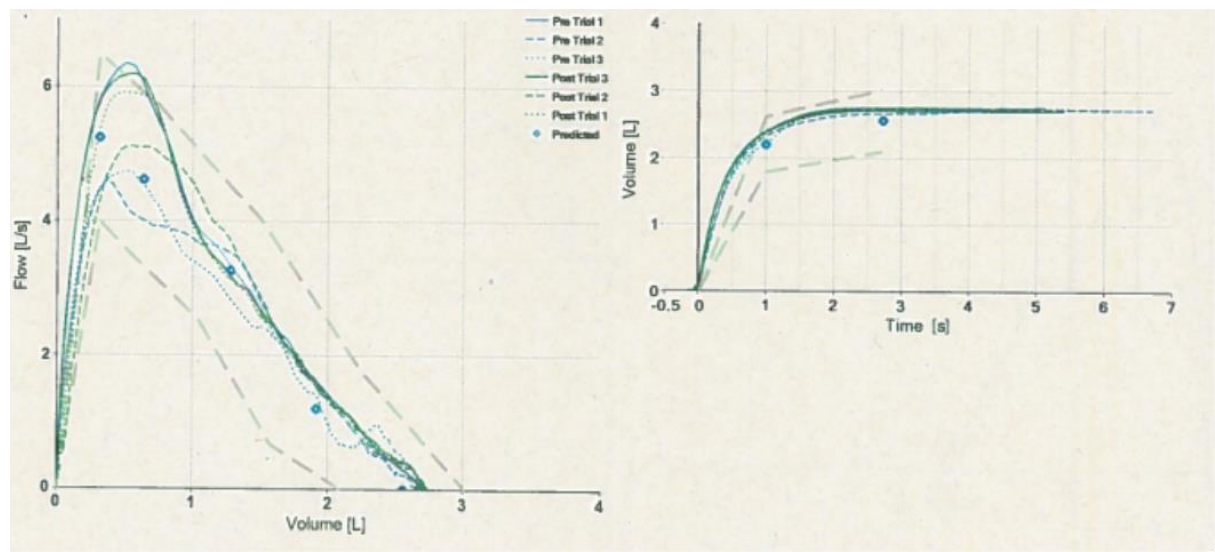
CO2- 13



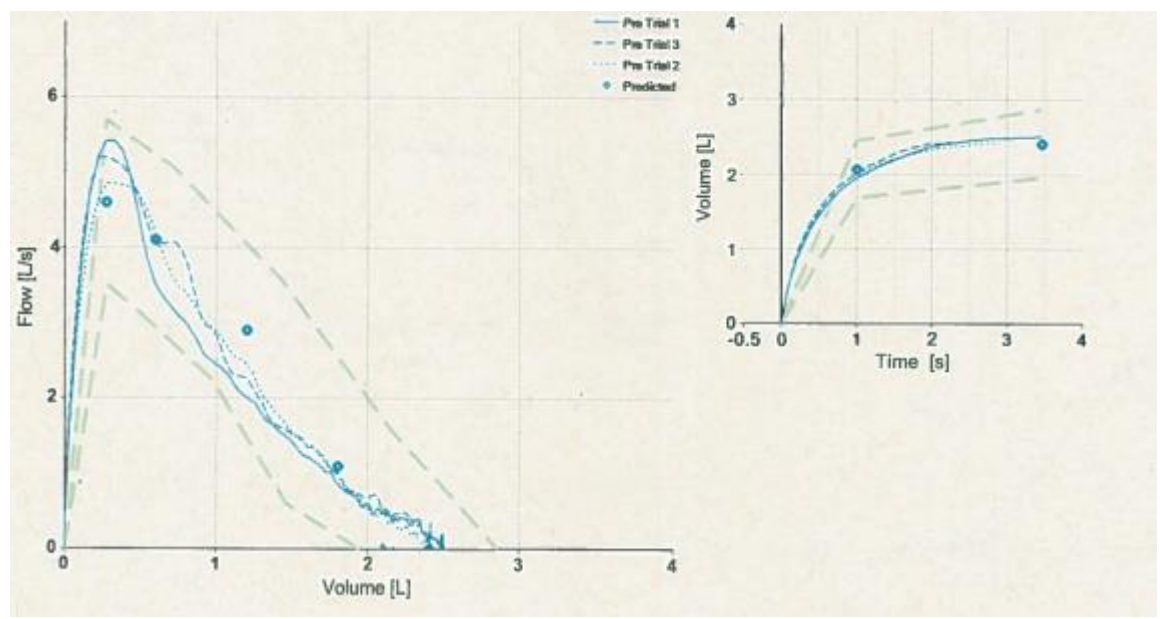
CO2- 14



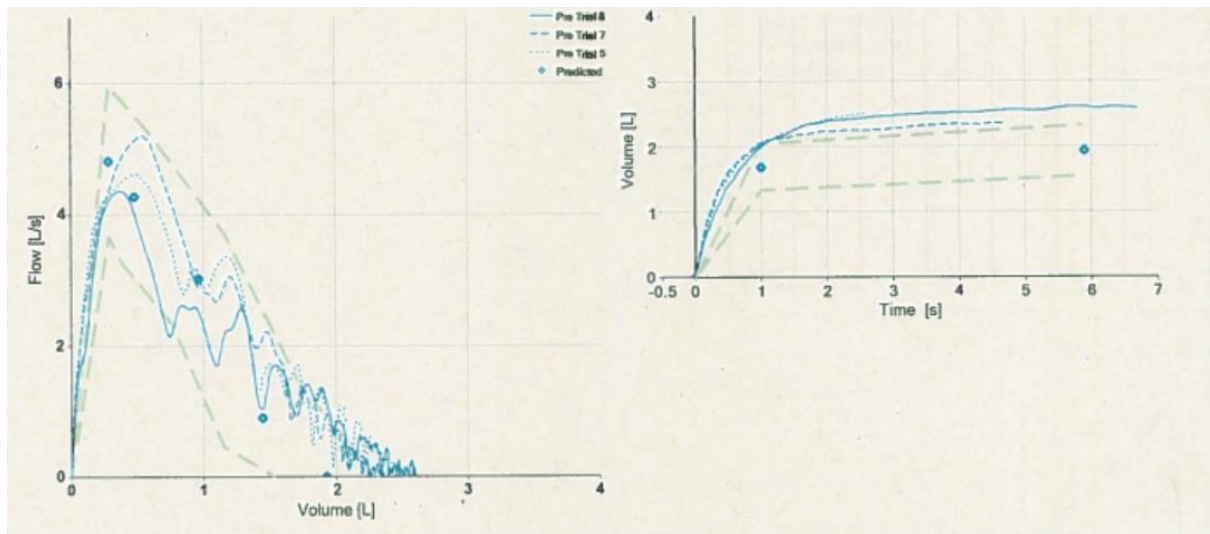
CO2- 15



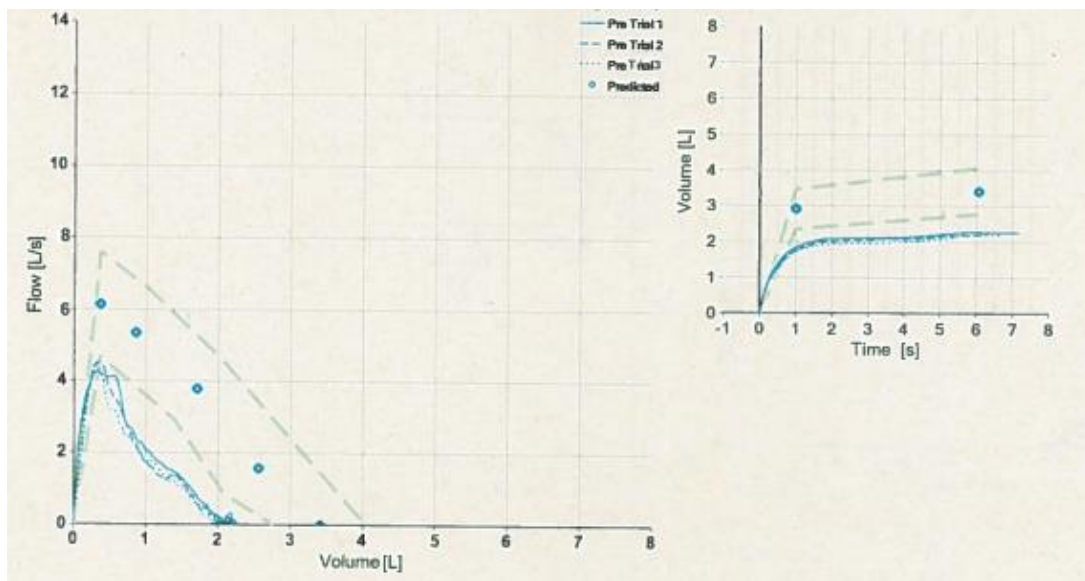
CO2- 16



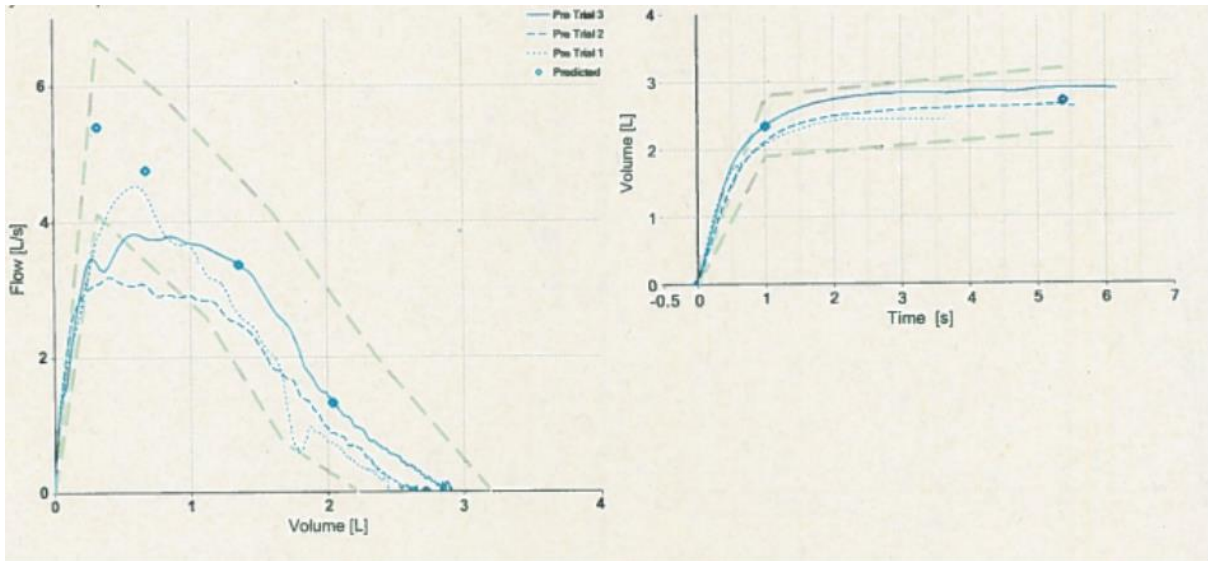
CO2- 17



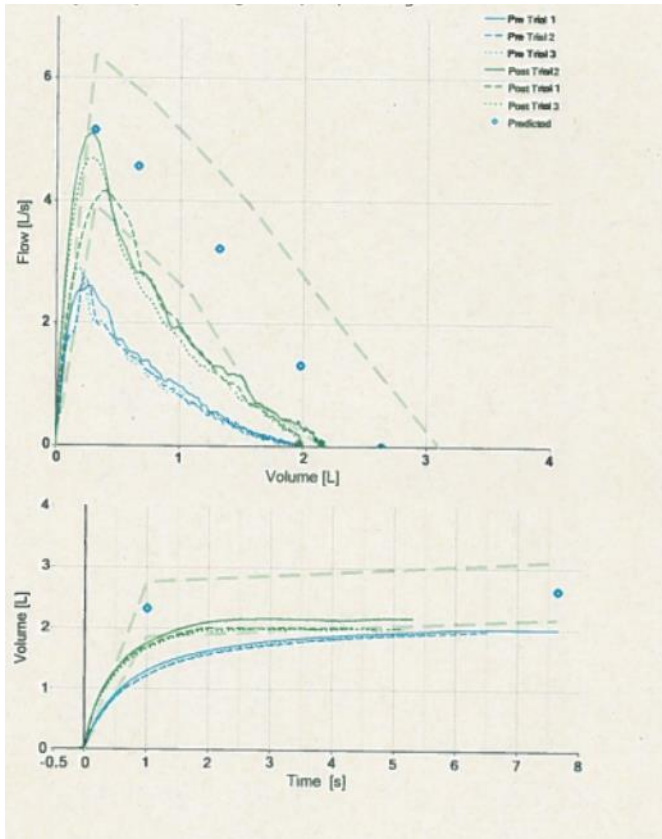
CO2- 18



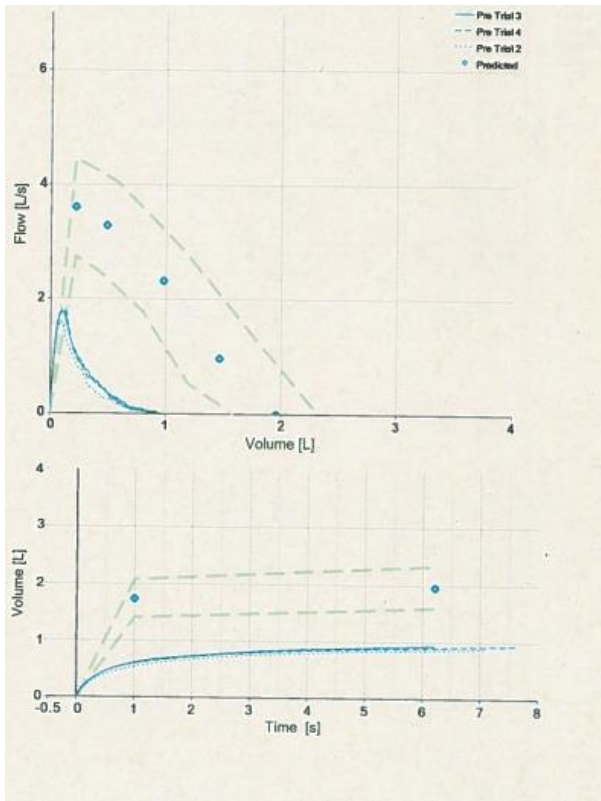
CO2- 19



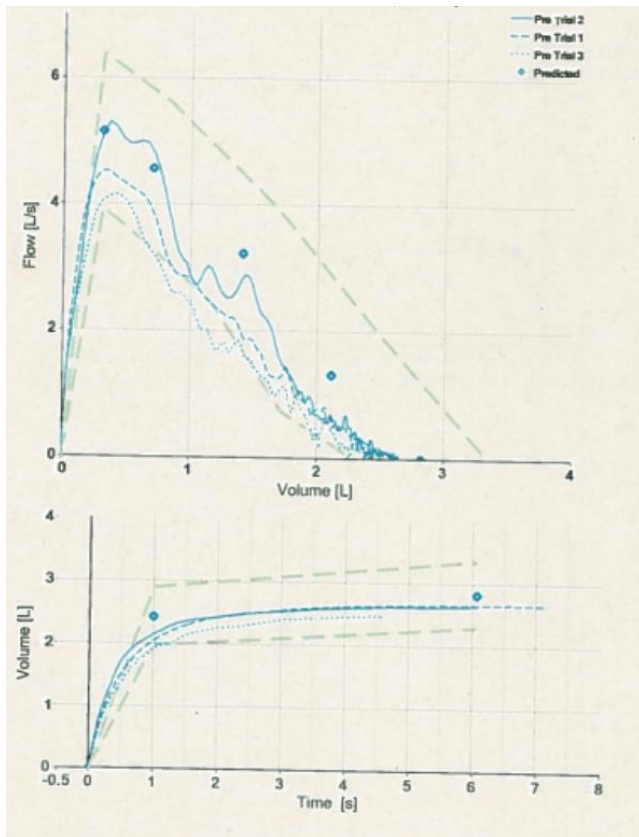
CO2- 20



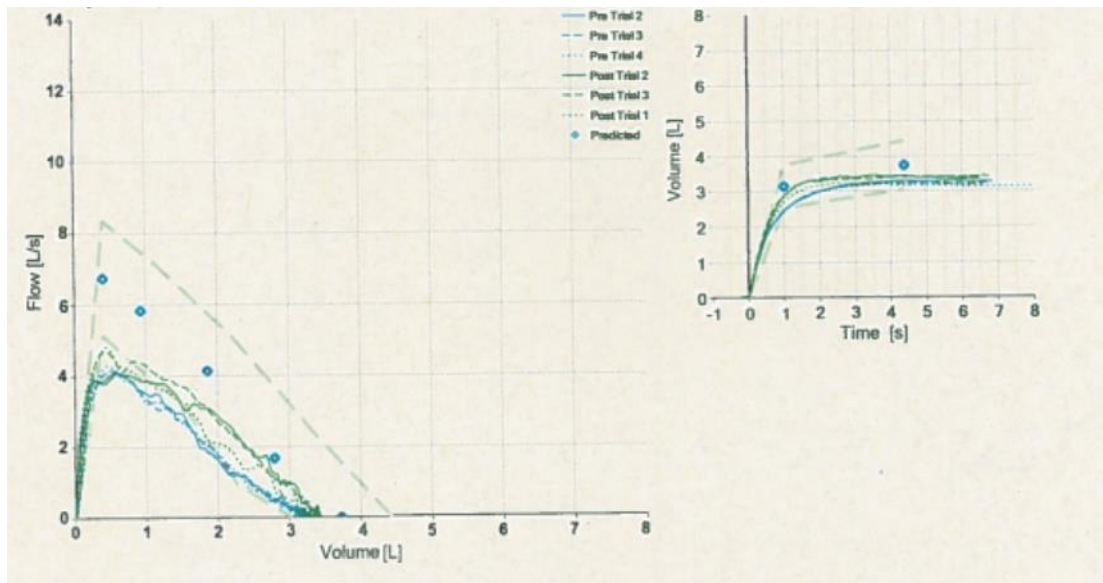
CO2- 21



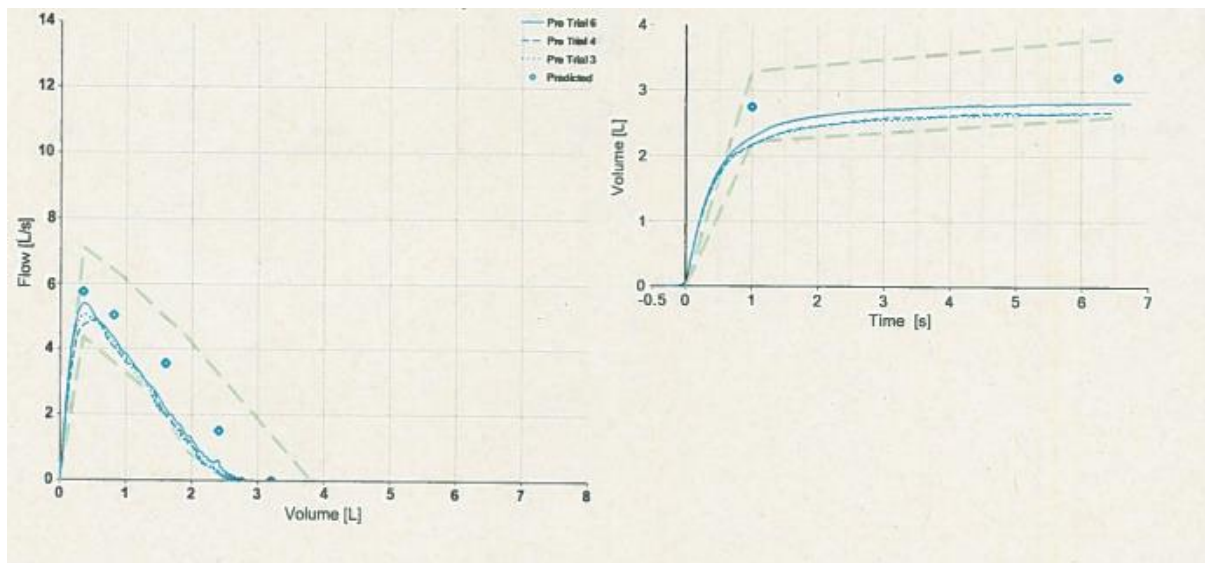
CO2- 22



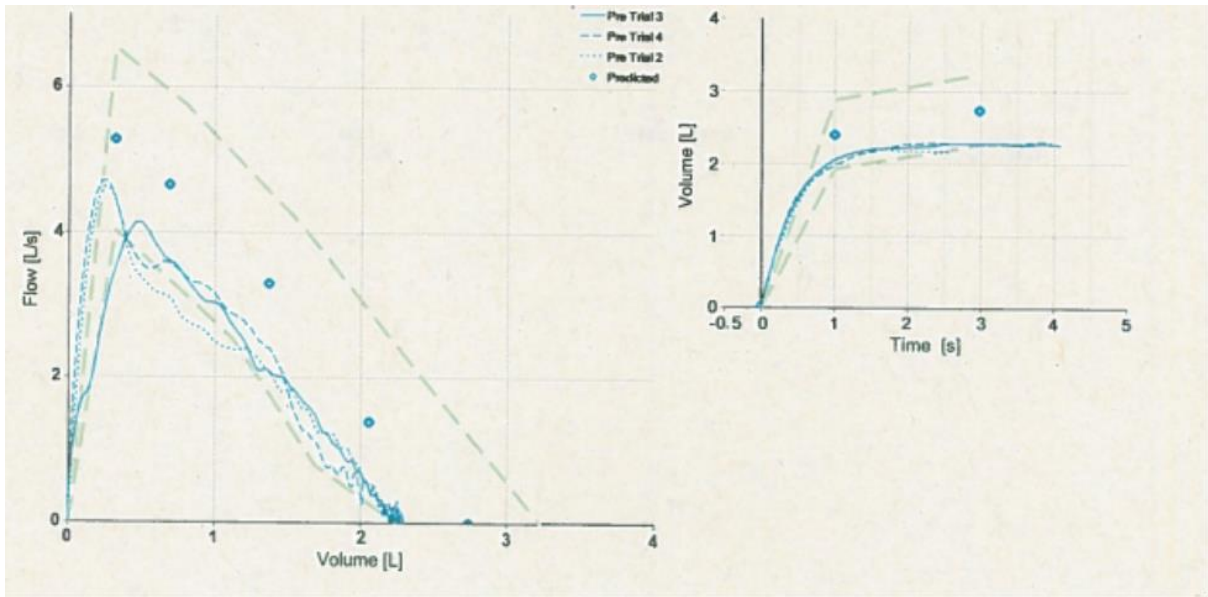
CO2- 23



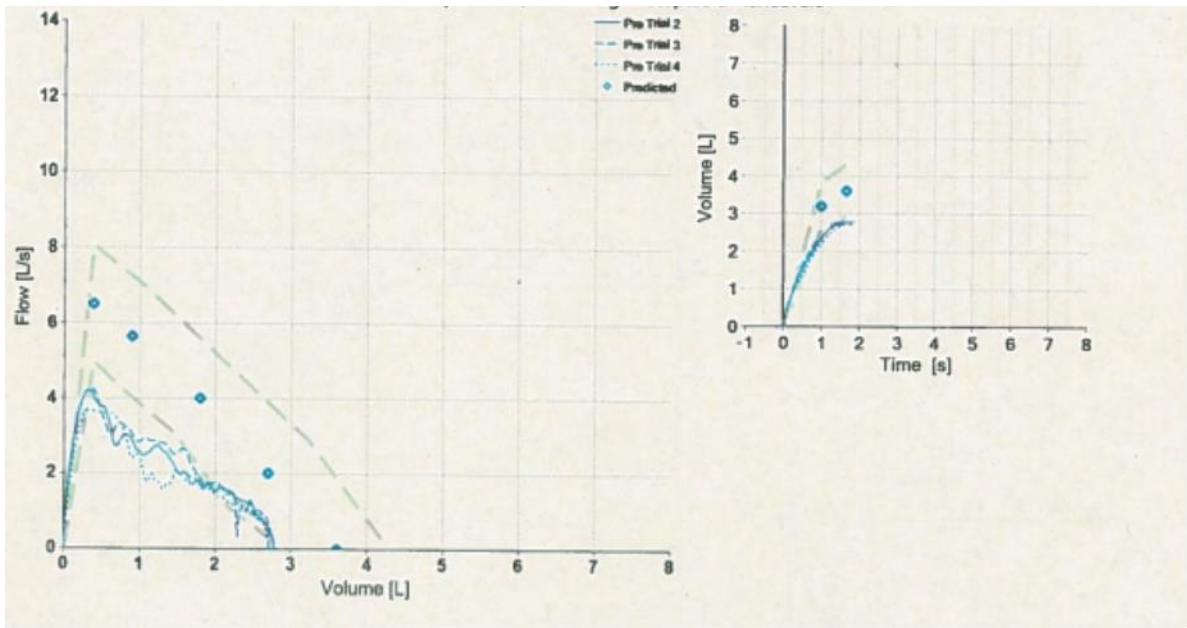
CO2- 24



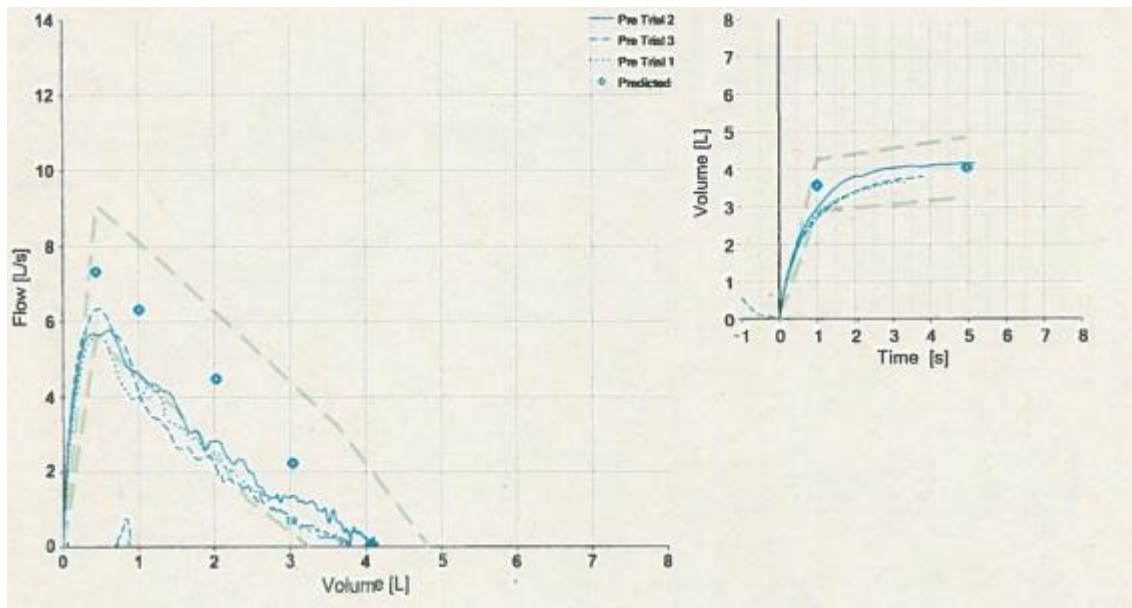
CO2- 25



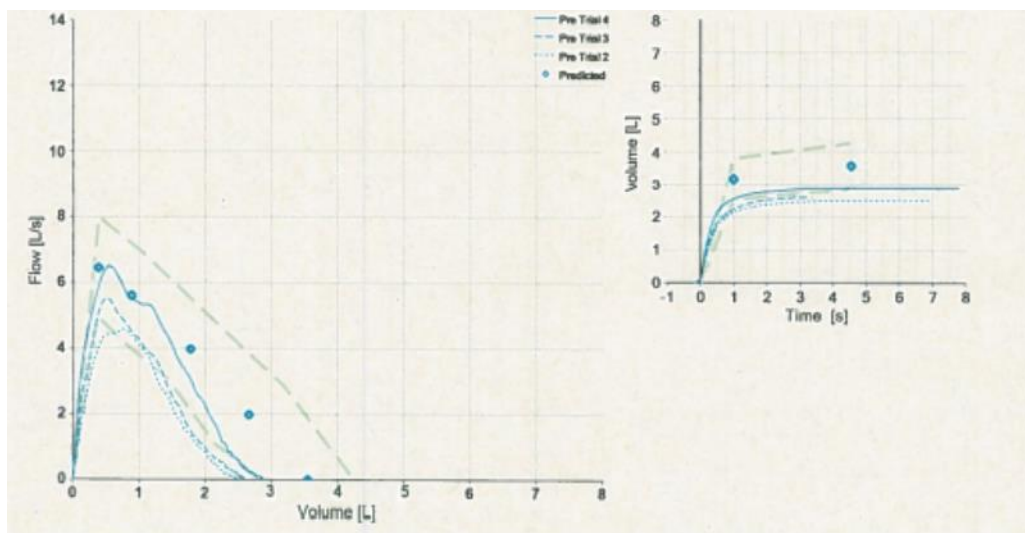
CO2- 26



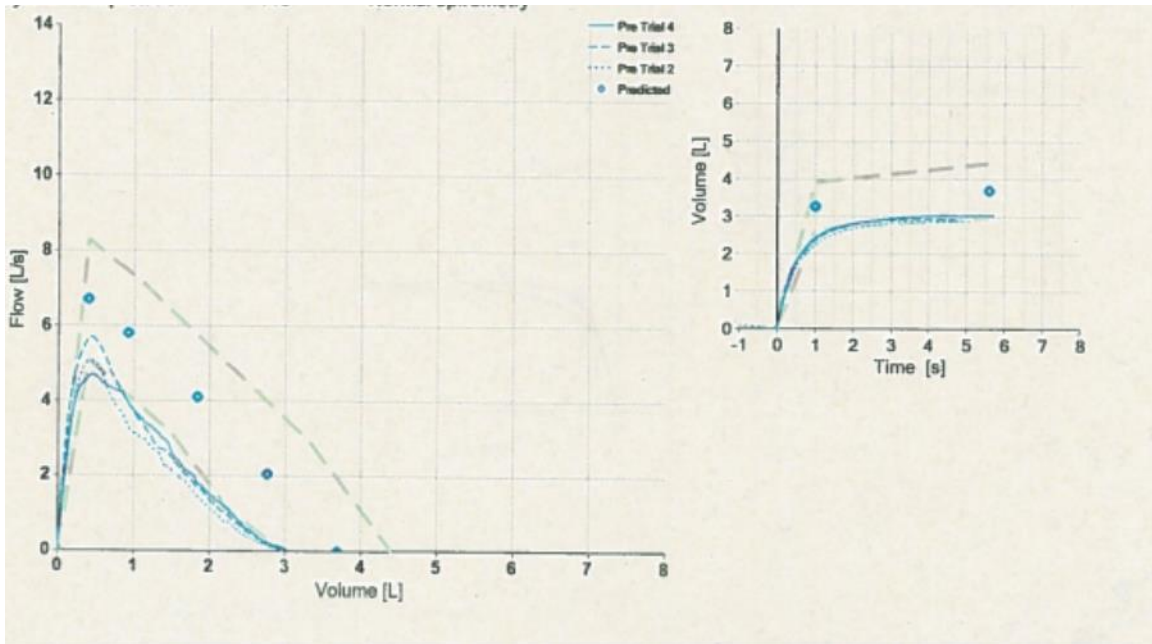
CO2- 27



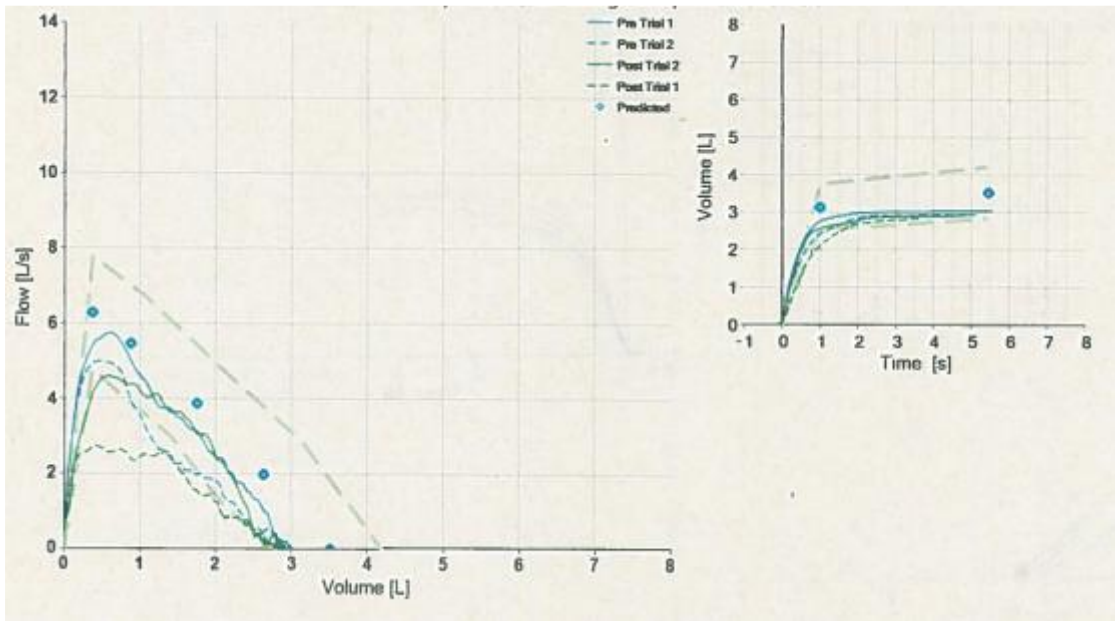
CO2- 28



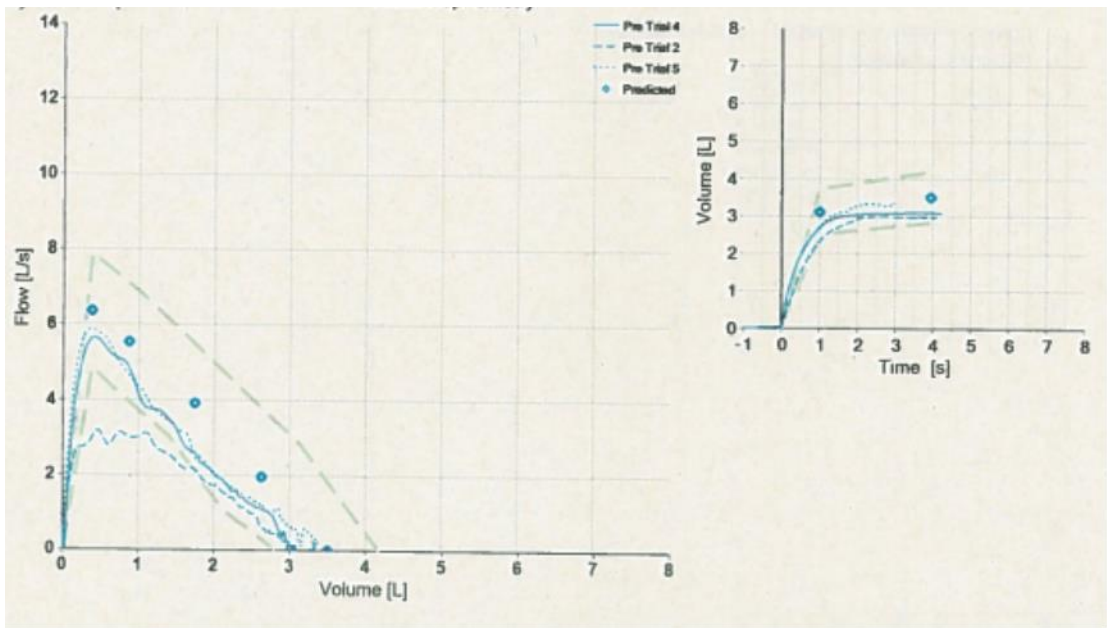
CO2- 29



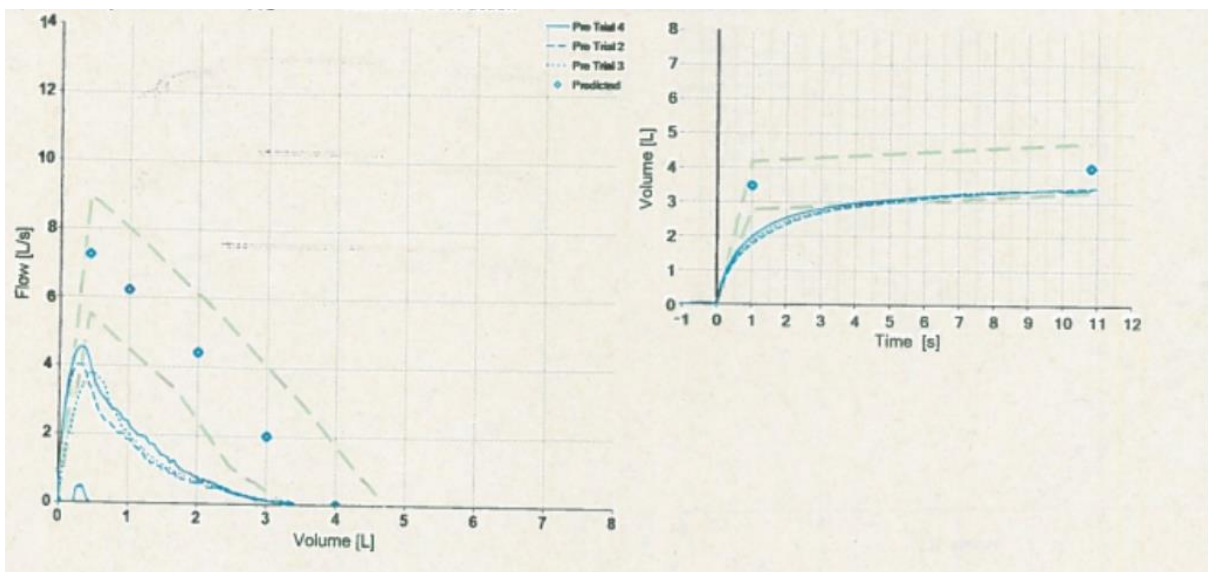
CO2- 30



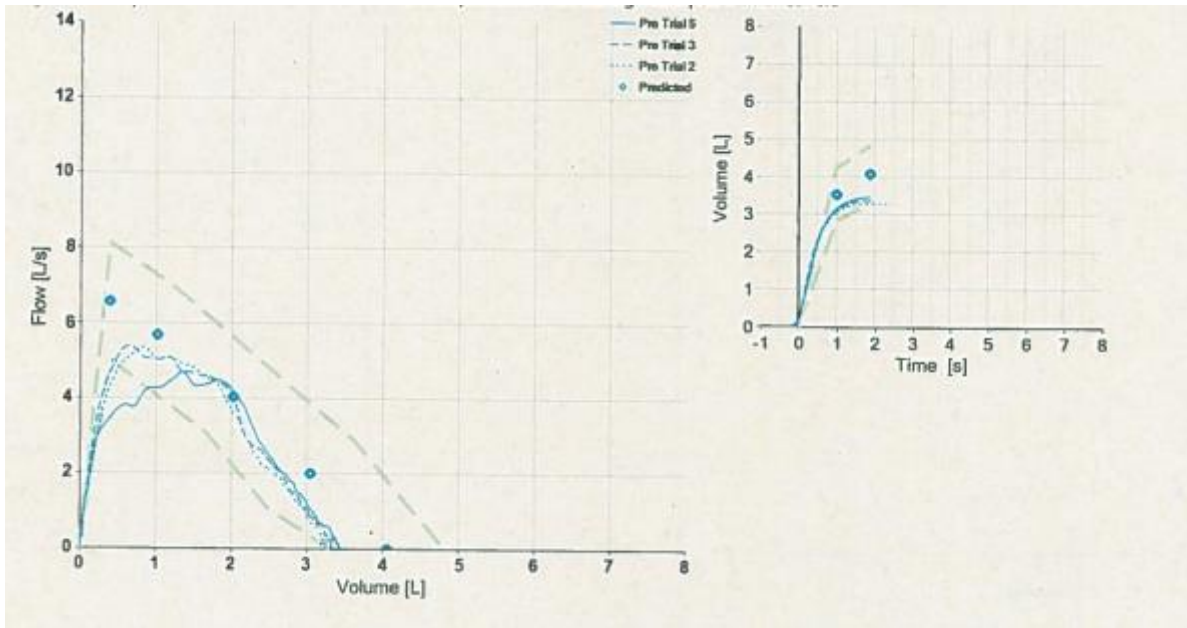
CO2- 31



CO2- 32



CO2- 33



CO2- 34

